INVESTIGATION OF PARAMETERS AFFECTING THE OPERATING CHARACTERISTICS

OF TOGGLE-SWITCHES WITH SILVER-CADMIUM-OXIDE CONTACTS

by

PETER J. WHITE

A Thesis submitted in application for the Degree of Doctor of

Philosophy of the C.N.A.A.

Plymouth Polytechnic

May 1979

DECLARATION

I hereby declare that the following thesis has been composed by me, that the work of which it is a record has been conducted by myself, and it has not been presented in any previous application for a Higher Degree.

P. J. White.

PETER JOHN WHITE

TABLE OF CONTENTS

(v)

LIST OF SYMBOLS AND ABBREVIATIONS

Symbol	Description	Units
e_t	Instantaneous arc voltage	V
i_t	Instantaneous arc current	A
T	Arc duration	s
E	Supply voltage (d.c.)	V
I	Circuit current prior to arc ignition (d.c.)	A
V_c	Cathode fall voltage	V
V_a	Anode fall voltage	V
V_p	Arc Colum voltage	V
l	Arc length	m
E_m	Minimum arc voltage	V
I_m	Minimum arc current	A
S	Contact separation	m
v	Contact opening/closing velocity	mS^{-1}
h	Contact gap with contacts at rest in open position	m
ω_s	Angular oscillation frequency of opening switch contacts	s^{-1}
τ	Time constant of exponential decay of contact oscillation	s
$\hat{E}$	Peak value of a.c. supply voltage	V
$\hat{I}$	Peak value of a.c. circuit current	A
ω	Angular frequency of a.c. supply	s^{-1}
$\dfrac{\theta}{\omega}$	Arc ignition point relative to a.c. cycle	s
ϕ	Phase angle between a.c. supply voltage and current	

SUMMARY

Experimental and theoretical studies are made of small snap-action switches designed for use in thermostatic controls operating on a.c. at 240 volts r.m.s., 50 Hz. The performance of the silver cadmium oxide contacts (Ag. CdO, 85/15%) is evaluated over a range of currents from 1 to 10 amps, for make and break operations. The arc at break is found to be the predominant factor contributing to the erosion of the contacts for the range of currents used.

Tests using a high speed camera show that the energy dissipated in the arc between the contacts can be evaluated from equations describing the arc in terms of its voltage, current and length as functions of time. Subsequently work is carried out to develop the relation between arc energy and contact erosion, with specific regard to the distribution of energy between the two contact surfaces and the arc column. This is related to the power dissipation in the two electrode fall regions, and the resulting direction of net material transfer is thought to be influenced by the length achieved by the arc before extinction. Erosion is generally in the form of anodic loss and cathodic gain and the reasons for the directional bias in this type of switch are suggested.

Ways of reducing the amount of erosion per operation by changing the switch opening characteristic are discussed and supported with experimental results.
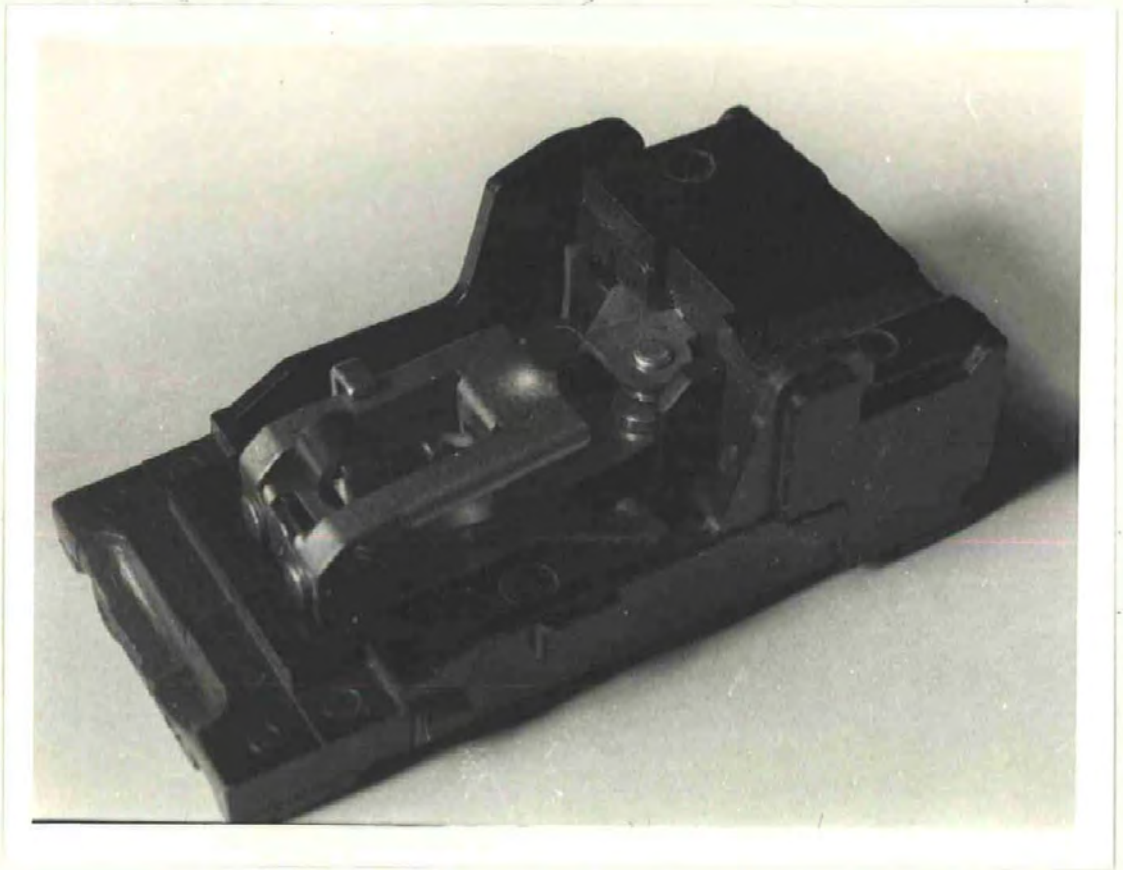
Fig. 1: Snap-Action Switch
Mechanism: Beryllium Copper Blade
Contacts: 4mm diameter, Silver Cadmium Oxide
AgCdO (85/15 %) on Copper rivets

CHAPTER ONE

INTRODUCTION

The small snap-action switch (Fig. 1) has been an integral part
of the domestic appliance industry for many years; however feedback on
its performance in the field has been difficult to acquire. Switch
failure usually precipitates appliance breakdown and this is generally
an area of concern dealt with by service engineers employed either by
the appliance manufacturer or the retail outlet. Fault rectification
is achieved by replacing any components found to have failed by new
ones. The cause and mode of failure are rarely investigated, since the
immediate concern of the service engineer is to restore the proper
functioning of the appliance as speedily as possible, to ensure
consumer satisfaction.

A succession of appliance breakdowns due to a particular component is
likely to result in the manufacturer being quickly informed. However
the frequency with which this occurs is small due to strict quality
control methods that are operated by manufacturers currently mass
producing large quantities of identical components. Also a fault or
mode of failure common to many components is generally easy to identify.
It is the infrequent premature failure, that could supply the
manufacturer with much useful data on performance and failure modes,
that usually does not find its way back to source but is discarded by
the service engineer. Alternatively the manufacturer may be completely
unaware that one of his components is capable of exceeding the required
appliance lifetime by a factor of two or three times. This information
may enable him to modify the design with a reduction in manufacturing
cost.

This background and the increasing need for the component manufacturer to produce items not only soundly engineered but also economically viable has led one company, Ranco Controls Ltd., to initiate this research project. Switches of the type illustrated in fig. (1) are made by Ranco at a rate of up to 40,000 a week for use in temperature control equipment, e.g. thermostats for domestic refrigerators. With this production rate, a small decrease in the production or material cost of each item is of considerable value overall. In particular any reduction in the amount of silver used in an electric contact has a special relevance since world consumption of silver is currently exceeding production. (1) The resulting rise in the price of silver could be offset if the amount required in each contact was reduced without adversely affecting switch reliability. Improvements using 'add on' accessories e.g. arc quenching devices, are not preferred since these constitute a significant rise in the material cost of the switch.

According to a recent report by the Electrical Research Association (2) there is unlikely to be a complete swing away from the electromechanical to the solid state in the forseeable future. In the U.K. in 1970 electromechanical switches accounted for about 80% of the market with solid state holding about 18%. By 1975 the solid state share had risen to 30%, and it is estimated this will have risen to 40% by 1980. However over the same period (1970 - 1980) the total sales are expected to rise from £100 million to £200 million, hence growth of the 'electromechanical' switch market is still assured. The report suggests that economic constraints will dictate that the solid state and electromechanical components will exist side by side. Hence even

with the growth of solid state controllers, microswitches are likely to continue as the cheaper alternative at the sensing or information input end.

The current rating and duty of the switches to be studied here are common to a very large proportion of switches. Some figures published by the U.S. Department of Commerce (3) showed that out of 408 million switches produced in one year only 42 million had a rating above 15 amps r.m.s. Of the 366 million rated at 15 amps r.m.s. or below, 228 million were rated at 10 amps r.m.s. or below. In the light of these figures it is surprising that there is not more product-orientated research on microswitches reported in recent publications.

Much literature is readily available on the high power switchgear currently in use and under development. Circuit breakers with ratings of k.V.A. e.g. vacuum breakers, SF6 breakers, have been developed as the need for larger switchgear has been required due to increased consumer demand year by year. The problems encountered in transmitting and switching increasingly higher voltages have been overcome stage by stage to keep abreast of demand.

At the other end of the scale, small reed relays used in low voltage and/or low current circuits e.g. telephone speech paths have also been the subject of much research. The reason for this may be that the fundamental contact phenomena associated with a short duration arc discharge have presented a more difficult and elusive problem to evaluate and more research effort has been applied in this direction.

The currents and voltages associated with the snap action switch have

no special handling problems, and the arc durations present have been observable by eye, or recordable on suitable measuring equipment for many years. For example, one of the first recorded observations of the electric arc was made by Sir Humphrey Davy in 1812 (4), of an arc drawn between carbon electrodes under conditions not dissimilar to those occurring when a snap action switch breaks a circuit. Towards the end of the same century Mrs. Ayrton (5) contributed to the establishment of the characteristics of this arc and more recently Holm (6) published constant arc length curves over a range of currents and voltages.

By about 1940, a.c. supplies had almost entirely replaced d.c. for industrial and domestic use. From a fundamental research standpoint the contact phenomena occurring are still the same, but the effect on the contacts in terms of the duty they have to perform is different. Nowadays most switch manufacturers ascribe an a.c. and a d.c. rating to their switches, the latter being a much lower one. The method of rating the duty of a particular switch is usually based on previous experience of requirements laid down to meet the varying standards of different national approvals boards. In the past there has been a general tendency to 'play safe' by allowing margins for underrating switch parameters. However, now that the shrinking profit margins of a competitive market are a constraining influence, this is no longer an economically viable option and it is therefore important to optimise the parameters affecting switch performance and design.

The switch to be studied here is designed to perform a specified number of operations before failure occurs. This is stated to be nominally 200,000 operations, which means an average life time in excess of 15

years for a thermostat working under normal conditions in a domestic refrigerator. Failure in this instance is constituted by one or more of the following:-

(i)   The contacts have been eroded to such an extent that they are no longer capable of making proper electrical contact.

(ii)   The strength of the weld formed between the contacts exceeds the force applied by the mechanism to break the weld, and hence the switch is no longer capable of interrupting current flow.

(iii)   Failure of the switch due to the mechanism e.g. complete fracture or fatigue effects which reduce the force the mechanism can apply to the contacts, hence effectively lowering the threshold point of a permanent weld.

The switch assembly as a whole comprises three sub-assemblies. See Fig. (1).

1.   The switch moulding or insulator.

2.   The fixed contact assembly.

3.   The moving contact assembly - integral with the switch mechanism.

This investigation is not concerned with the switch moulding, i.e. suitability of the different available materials, variation of tracking index during operations etc. This is covered by other workers in available literature, e.g. A.C. Snowden (7). The focal point of the study is the mechanism and the contacts, and the short and long term performance related to these.

The sensing equipment with which the switches are usually associated involves a slow rate of change with temperature. The switch mechanism

is the means by which this slow rate of response is converted to a movement suitable for switching electric current. Ideally the opening and closing velocities of the contacts should be completely independent of the rate of response of the temperature sensor. Traditionally the toggle or snap-action mechanism has been used as the best solution which approaches this ideal.

The initial approach to this research is one that is product orientated with a diagnostic emphasis aimed at defining the more likely areas of problem occurence. In particular controlled tests are performed using the high speed camera, to discover the degree of correlation that exists between mechanical and electrical parameters. The results from these preliminary tests indicated further areas for a more detailed investigation, including the electro-physical aspects of contact performance. The affect of varying the electrical and mechanical parameters of the switch, on the rate of contact surface degradation is therefore studied with a view to overall performance optimisation.

REFERENCES   -   Chapter One

1. H.W. Turner
    'Modern Developments in Contact Research'
    Colloquium on Electrical Contacts: I.E.E. group S3, November 1976.

2. Electrical Research Association, Leatherhead, Surrey
    'Future for Switching Components'
    A report published 1976.

3. United States, Department of Commerce, Current Industrial Reports.
    Wiring, Devices and Supplies.
    Series MA - 36K(67) - 1, 1967.

4. H. Davy.
    'Elements of Chemical Philosophy'
    (French Transl.) 1.p.187-189 (1813).

5. H. Ayrton.
    'The Electric Arc'
    The Electrician, London 1902.

6. R. Holm.
    Electric Contacts, Theory and Application.
    Fourth Edition, p.280. Springer-Verlag, 1967.

7. A.C. Snowdon,
    'Effect of Contact Material Arcing Deposits on the Surface
    Resistance of Insulating Materials'
    International Conference on Electric Contacts, Japan 1976.

CHAPTER TWO

ELECTRICAL CONTACT THEORY

2.1 Introduction

This chapter commences with a summary of classical contact theory
generally applicable to all electrical contacts. The discussion
then progresses to a study of the electric arc, including the
different ways of initiation, maintenance and extinction that exist
and the dependance on operating conditions. The ways in which
contacts are eroded by different types of arcs are surveyed and
finally contact welding is discussed. Most of the work reviewed
below has been chosen because it is considered relevant to the
particular application of switching by snap-action switches,
although few workers have previously derived or applied contact
theory in this application.

2.2 Stationary Contacts

Ideally contact is established between two perfectly clean and
smooth metallic surfaces as soon as the distance between them is
within the intermolecular range i.e. conducting electrons can move
as frequently across the interface as they can between crystallite
boundaries in the bulk metal. According to Holm (1) this occurs
since the transition resistance caused by the discontinuity of the
crystal lattice at the interface is of the same order as the resistance
between grain boundaries in a polycrystalline material. This
produces metallic bonding between the two surfaces leading to cold
welding. If the two surfaces remain at rest the welds will grow
stronger by means of rearrangement of the atoms and the development
of covalent bonds.

In practice contact surfaces are covered by surface films of varying

degrees of thickness which inhibit cold welding. These films may be

mechanically fractured when the two surfaces impact. Bresgen (2) has

reported that penetration of tarnish films up to 0.8 μm has been achieved

by frictional excursions or oscillation of the contacts immediately

after impact before reaching the rest state. Application of a voltage

across contacts in the rest state can also cause breakdown of the surface

film and allow passage of current by the tunnel effect or fritting,

as discussed by Holm (1).

The real area of the contact surfaces available to pass current is

influenced by the microtopography of the surface. Contact is established

initially at one or more of the prominent surface asperities that are

present. Current flowing between the contacts is therefore constricted

to flow through narrow channels resulting in a higher electrical

resistance at the interface. This constriction resistance is a function

of the resistivity of the contact material and the dimensions of the

conduction spot. Llewellyn-Jones (3) gives detailed calculations for

finding the constriction resistance for various shapes of conducting

spots. Since the current density at the point of contact is large

(typically up to 10^8 A/m^2 for 10 A flowing between contacts) high

temperatures can result in the immediate vicinity of the conduct area.

With symmetrical contacts the generated heat flows in the same path as

the electric currents, hence a relationship exists between voltage

(potential difference) and temperature difference. This relation is

known as the ψ, θ theorem and a detailed treatment of this is given by

Holm (4) and Llewellyn-Jones (5).

The result of this theorem in a form relating the potential ψ to the

maximum temperature θ_m is

$$\psi^2 = 2 \int_{\theta}^{\theta_m} \lambda.\rho.d\theta \text{ where } \lambda \text{ is the thermal conductivity}$$

ρ is the electrical resistivity

θ is the temperature before application of the voltage.

This is a steady state expression which holds only if there is no interchange of energy across the boundary of the contact.

To evaluate this integral requires application of the Weidemann-Franz law which states that

$$\lambda.\rho = L.\theta$$

L, the Lorenz number was assumed to be a constant until Hopkins et al (6) showed that it does vary slightly at high temperatures. Combining these two expressions and integrating gives

$$\psi^2 = L(\theta_m^2 - \theta^2)$$

For a potential difference across the contacts of $V_c = 2\psi$.

$$\theta_m = \frac{V_c}{2\sqrt{L}} \qquad \theta_m \gg \theta$$

$$\simeq 3200 \ V_c \ K.$$

Hence for a contact voltage of 1 volt, θ_m = 3200 K a temperature higher then the melting point of most metals and above the boiling point of some.

2.3 Contacts in Motion: Break

2.3.1 The Molten Metal Bridge

When the force holding two contacts together is decreased to zero and the contacts are slowly pulled apart, the final microscopic point of contact has to carry all the current.

As the voltage across this constriction rises in accordance with the relation detailed in the previous section, there is localised melting of the contact material which is drawn out into a small molten metal bridge between the separating contacts. This molten metal bridge has been the subject of extensive research by Llewellyn-Jones (7), Hopkins (8), Slade (9) and others. Detailed studies using high speed photographic and oscilloscopic techniques have been made of bridges formed between many different contact materials in defined circuit conditions, usually 6 to 12 volts d.c. with a load of 1 - 50 amps. The relation between the transient rise in voltage and the melting and boiling of contact material in the bridge has been investigated by Hopkins, Jones and Evans (10) using the high speed transient digitizers now available. Their results showed an apparent unsteadiness in the contact voltage during the molten metal bridge lifetime, and following rupture of the bridge the rate of rise of the contact voltage was found to be different for differing contact materials. The melting voltage for different silver alloys was also investigated by Sato (11), who correlated the current density in the contact area to temperature. Most workers agree that even if boiling of the molten metal bridge is not the direct cause of rupture, the temperature is certainly approaching the boiling point at rupture and at least a small part of the molten metal is vapourised. High speed photographic studies by Price and Llewellyn-Jones (12) have shown that the bridge breaks explosively and that metal vapour and droplets of molten metal are present between the contacts as they separate.

Erosion of the contacts due to rupture of the molten metal bridge has been measured after just one operation by using a radio-active tracer technique developed by Llewellyn-Jones, Hopkins and Jones (13).

Considerable scatter in the results was reported by Hopkins and Jones (14), who observed the phenomena of rebridging taking place. Rupture of the bridge resulted in the depositing of material on one or other of the electrodes without any clear preference for either. This had also been noticed by Thomas (15) using a high speed camera to record contact openings.

2.3.2 Arc Initiation

The conditions existing in the contact gap immediately after bridge rupture are :-

(i)   A cathode with an electron emitting hot spot.

(ii) Atoms of comparatively low ionisation potential provided by the metal vapour.

A potential difference across the gap establishes the essential requirements necessary for a discharge to occur. The type and duration of the discharge is dependant upon the circuit parameters and also to a lesser extent on the contact material and configuration. The discharge may evolve through several different stages before finally extinguishing. The relative significance of each stage is also dictated to some degree by the circuit parameters.

In the initial stages of opening, after bridge rupture, the contact separation is comparable to the mean free path length of electrons (10^{-3}mm). If the pressure of vapour is not too high, electrons crossing the gap from cathode to anode will make few ionising collisions and therefore will dissipate their energy in the form of heat at the anode. The current is carried almost entirely by electrons and this type of arc discharge is generally

referred to as the short arc.

As the contact gap increases, electrons crossing the gap make
more ionising collisions, producing amplification and positive
ions which drift down the electric field to the cathode creating
a cathode fall. As the arc continues to lengthen a corresponding
anode fall will develop and also a quasi-neutral column. There
is also the possibility that after rupture of the molten metal
bridge, metal vapour is present at such a high pressure that even
though the contact gap may be less than the mean free path length,
electrons cannot cross the gap without making ionising collisions.
This condition has been called a reverse short arc by Hopkins
et al (8).

2.3.3 The Short Arc

The short arc has been studied in detail by Llewellyn-Jones (7)
and Hopkins et al (17). It is the predominant feature during
current interruption of low voltage circuits (typically 6 volts)
and load currents of 1 - 50 amps. A feature of this circuit
arrangement is that the potential difference across the contacts
is dependent upon the decay of the local inductance to increase
it to value higher than the ionisation potential of the arcing
medium (and also higher than the supply voltage) and initiate an
arc. The energy dissipated in the arc for this operating
condition depends very much on the values of the local inductance
and capacitance of the contact circuit, and energy supplied to
the arc from the supply is minimal. The duration of the arc has
been shown by Slade (16) to depend directly on the product of the
local inductance and the current at bridge rupture. The energy

dissipated in the short arc has been reported by Hopkins et al (8) to be within 10% of $\frac{1}{2} L I^2$, and typically this is of the order of 25 μJ, where the local self inductance is 0.5μH and the current before bridge rupture is 10 amps. The arc duration for these conditions is in the range 1-2μs. The erosion and material transfer caused by the short arc has been studied by many workers, Hopkins et al (8), Slade (16), and Kabono et al (18) show that the amount and direction of material transfer depends on the local circuit inductance.

It is generally accepted that material transfer and erosion is the result of preferential evaporation of material from one electrode and deposition on the surface of the other, rather than by the movement of metallic ions in the arc. Spectroscopic studies by Thomas (19) have shown that the characteristics of a short arc in vacuum are not appreciably different from those produced in atmospheric air. It would seem that the arc is initiated and maintained for lengths of 1-5 x 10^{-3}mm in metal vapour, and the ambient atmosphere does not have chance to participate in the arc. As the arc lengthens ($> 10^{-2}$mm) it starts to assume the characteristics of a normal arc discharge in air i.e. with a cathode fall, anode fall and a column.

2.3.4 The Transient Showering Arc

As soon as the supply voltage has a value greater than the ionisation potential, the energy dissipated in the arc will contain an additional component drawn from the supply, providing the steady circuit current is large enough to ignite and sustain an arc. If the steady current is too small e.g. 100 mA or less but the circuit

contains inductance and capacitance an arc may still ignite. The current from the inductance charges the capacitance in the circuit such that a voltage of 300 volts or above appears across the contacts. This type of transient has been reported in detail by Mills (20) and Phamey (21). As soon as the voltage reaches 300 volts the contact gap breaks down in the form of a glow discharge and this immediately develops to an arc. This arc discharges the local capacitance of the circuit and extinguishes as a result. The inductance then charges the capacitance again until 300 volts appears across the contact gap and the discharge repeats. This process continues until the gap becomes too large for breakdown and the remaining reactive energy is dissipated as damped oscillations around the circuit. The erosion resulting from this type of arc has been correlated with the energy dissipated in the arc in a paper by Wagar (22). He expressed contact life in terms of a load energy factor which took into account the energy stored in the circuit components and the steady state circuit current. The energy dissipated by this type of arc over one operation is typically 0.5 mJ.

2.3.5 Normal Arc Characteristics

Once the circuit current is above the minimum value required to sustain an arc, and the supply voltage is above the ionisation potential, most of the energy dissipated in the arc will be drawn from the supply. For a d.c. supply Holm (23) defines this in the form of an equation :

$$\int_{o}^{T} e_c \, i_c \, dt \quad = \quad \int_{0}^{T} (E-IR) \, I.dt \quad + \tfrac{1}{2} \, LI^2$$
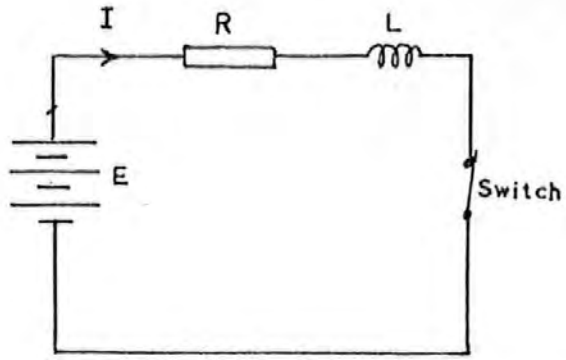
Fig. 2:   Test circuit with Inductive and Resistive
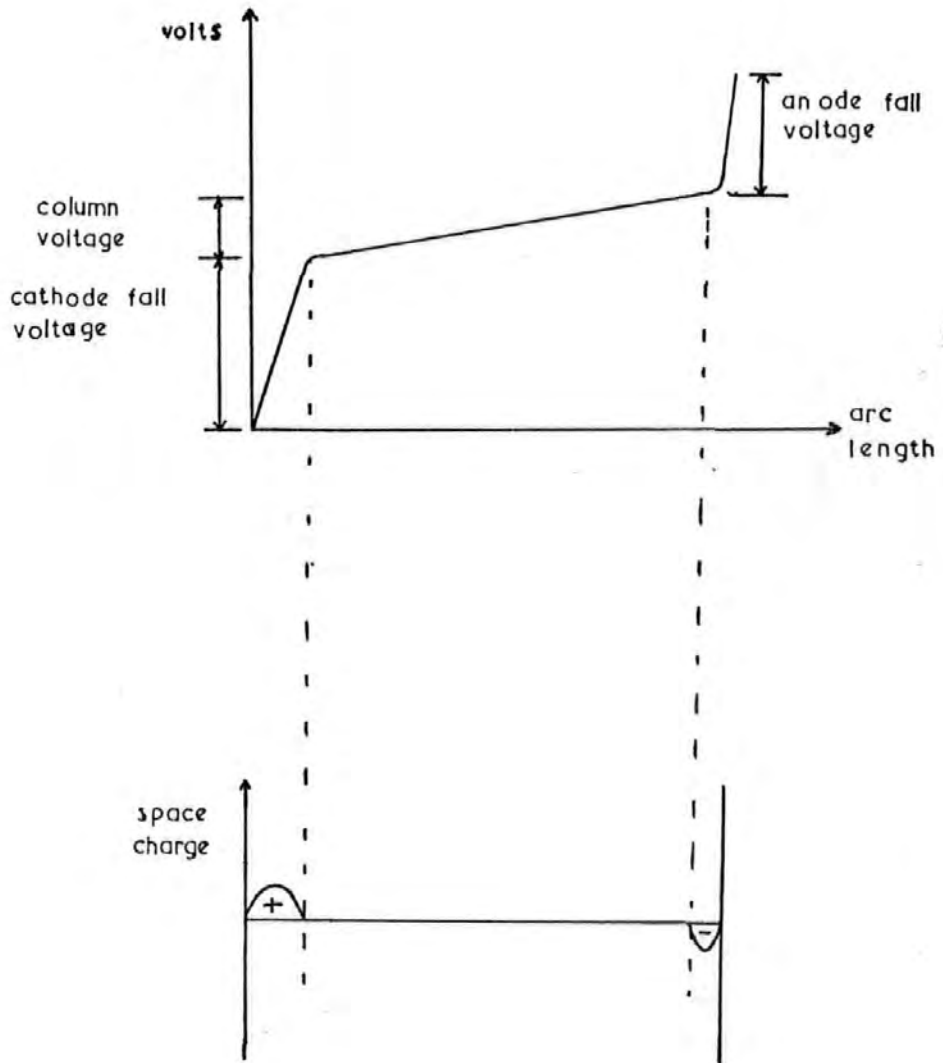   components

Fig. 3:   Potential distribution and Charge
          distribution over a normal arc

This equation refers to the circuit shown in Figure (2). $\int_o^T e_t i_t \, dt$
represents the total energy dissipated in the arc of duration T.
$\int_o^T$ (E-IR) I.dt is the energy drawn from the supply during time T and
$\frac{1}{2} LI^2$ is the inductive energy dissipated in the arc by any inductance
present in the circuit. For this operating condition the contribution
by the local self inductance and capacitance to the total energy
dissipated in the arc is very small compared to that supplied by the
source and stored in the inductive part of the circuit load. Long arcs
of this type have typical duration of milliseconds and energy contents
of 100 mJ and above, and classically have been divided into three regions
of differing voltage gradients, the cathode fall, anode fall and column.

The Arc Column

The arc column, the visible part of most arcs, represents most of the
total length of the arc. It has a potential gradient along its length,
which is usually a property of the gas in which the arc exists and varies
with the magnitude of the current, typically 1 - 2 volts/mm in air.
Figure (3) shows the location of the arc column with respect to the
potential distribution across the arc. The current density in the arc
column is usually of the order 10 - 100 Amps/mm^2 and the temperature can
reach 5000K and above. The net space charge of the stable arc column is zero
(Figure (3)), i.e. there is an equal concentration of positive ions and
electrons and hence the column satisfies the definition of a plasma.
The current through the column is carried mainly by electrons due to
their higher drift velocity in the electric field, than the more massive
positive ions. Although comprising the largest part of most long arcs,
the column is least important in terms of criterion necessary for the arc
to exist. Arcs can and do exist without a column (e.g. short arcs) at all.
The column represents a region of gaseous conduction and the current

flowing through it has to make the transition from gas to metal at both electrodes. These transition regions i.e. the anode and cathode falls are where the emission mechanisms occur so that a net current passes into the column and a stable arc is produced. The characteristics of the two fall regions are more dependant on the electrode material than the ambient gas and the type of electron emission at the cathode in particular changes for different types of material.

The Cathode Fall

There are two types of emission phenomena that can produce the necessary electrons at the cathode:

(i) Thermionic emission. This occurs for refractory cathode materials when the cathode is heated to a sufficiently high temperature that electrons are emitted thermionically. The current density in this case is given by the Richardson-Dushman equation :-

$$je = AT^2 e^{\frac{-e\phi}{kT}}$$

where A is a constant

T the temperature and ϕ the thermionic work function of the cathode surface.

e is the electron charge

k is Boltzmann's constant

The current density thus depends on the cathode surface temperature and it is only with refractory materials that thermionic emission can explain the current densities of 10 - 100 Amps/mm^2 which occur at the cathode. The thermionic emission of electrons at the cathode is sustained by the following mechanism :-

Emitted electrons are accelerated by the positive space charge present which produces a high field close to the cathode surface. Electron multiplication then occurs by collision of the electrons with gas and metal vapour atoms, and the positive ions thus produced are accelerated to the cathode. By virtue of their kinetic energy they maintain the cathode at a temperature sufficient for the required emission. As a result of this the cathode spot on refractory materials is stationary or slower moving.

(ii) Field Emission: Non refractory cathodes are unable to operate at a sufficiently high temperature for thermionic emission to be the significant contributor to the electron emission mechanism. Various theories and explanations have been put forward as to the mechanism of field emission which can extract electrons efficiently enough to produce the current densities that are known to exist. Langmuir (24) first suggested that the positive ion space at the end of the cathode fall region might produce a field sufficient to extract electrons directly from the cathode. The positive ion current density is given by the Langmuir-Child law

$$ jp = \frac{4}{9} \, \epsilon_0 \sqrt{\frac{2e}{m}} \cdot \frac{V_c^{3/2}}{d^2} $$

where   m is the positive ion mass

V_c is the cathode fall voltage

d is the distance of the positive ion space charge from the cathode surface.

According to the Fowler-Nordheim equation a current density of $10^4 - 10^5$ A /mm^2 requires a field of 10^6 volts/mm, thus d would have to be less than the mean free path length for fields this high to occur.

The possibility of field enhancement by the presence of a thin electrically charged insulating layer has been suggested by Llewellyn-Jones et al (25) and Haworth (26) as being responsible for the high field.

The current flow at the cathode is constituted either by a flow of positive ions in or the extraction of electrons from the electrode surface. The mechanism for regenerating charged particles is concentrated in the cathode fall region i.e. the cathode surface and a thin layer of electrode vapour and gas above it. The voltage drop across the cathode fall region is of the order of the excitation potential of the electrode vapour (typically 8 - 20 volts). The electric field is a result of a build up of positive space charge a few mean free path lengths thick immediately in front of the cathode surface. The electrons move through the cathode fall region much faster than the ions move in the opposite direction hence the density of positive ions is much greater than that of electrons. There is usually a high temperature gradient across the cathode fall region particularly in the space charge zone.

The arc column has a lower current density than the emitting sites within the cathode spot on the surface hence there is a contraction zone. The current density varies from that of the column at one end to much higher values at the end nearest the cathode. Similarly the electric field varies from 1 - 2 volts/mm at the column end to 10^4 - 10^5 volts/mm at the cathode end. The greatest intensity of illumination in the region of the cathode comes from a narrow region at the contraction zone end of the space charge region where some vapour atoms are excited by collision with electrons from the cathode. These excited atoms, if not undergoing further collision decay to the ground state with photon emission.

The cathode spot itself is considered to consist of several fast moving

emitting sites which increase in number with increase of the current i.e. the current/site is approximately constant. The movement of the sites appears to be random as some sites decay and others emerge Recently Itoyama (27) has shown, using high speed camera techniques that the current density of the cathode spot varies inversely with time at the initial stages of arcing, for an opening velocity of about 100 mm/sec. He also suggested that the electrons are only emitted from a few sites in the cathode spot, whereas the positive ions enter the cathode spot uniformly. Whatever the cause of changes in current distribution, they are accompanied by high frequency oscillations of the voltage with a period as short as 10^{-9} seconds. Insulating inclusions were observed by Hancox (28) to encourage the formation of new cathode spots and cathode tracks have been found to follow fine surface cracks and also seek parts of the cathode surface lying closest to the anode. It has also been shown by Meyer et al (29) that the non-thermionic arc may require for its maintenance some destruction of the cathode surface, particularly surface oxides. Arcs were found to extinguish through lack of oxide.

The large variety of factors influencing the non-thermionic cathode fall suggest that a single mechanism is unlikely to account for all of them. It is probable that several mechanisms co-exist or that there are frequent transitions e.g. non thermionic to thermionic caused by changing surface temperature as the current density changes as a result of arc root motion.

The energy balance at the cathode is complex and will include some or all of the following components.

A. Energy supplied to the Cathode

(i) Thermal energy of positive ions and the kinetic energy gained in

passing through the electric field of the cathode fall zone.

(ii) Part of the neutralisation energy of the positive ions. On reaching the cathode surface they have in addition to their kinetic energy, the potential energy eVp. Since an electron in the cathode metal must neutralise the ion, the total neutralisation energy available per ion is $e(Vp - \phi)$. Some of this may be lost owing to radiation, or as kinetic energy if the vapour atom is reflected away from the surface. If the atom remains on the surface there will be an increment of energy given to the cathode as condensation energy.

(iii) Heat conduction from the hot gas by neutral and excited atoms, and radiation from the contraction zone, column and possibly from the anode.

(iv) Joule heating of the cathode material, appreciable in the high current density regions near the emitting sites.

B. Energy lost from the Cathode

(i) Energy required for electron emission, $e\phi$ per electron.

(ii) Energy required to vapourise cathode material and release larger pieces of material i.e. globules.

(iii) Radiation from the hot spots, and heat conducted away through the bulk material and conducted or convected away to the surrounding gas.

(iv) Energy loss due to dissociation of gases at the heated surface.

The Anode Fall

The anode region has less influence on the arc than the cathode, however it performs the vital role of sustaining the arc by preserving current continuity. Unlike the cathode where the current is carried both by

- 22 -

positive ions and electrons, the current at the anode surface is carried entirely by electrons entering it. The anode fall is due to a space charge caused by the high concentration of electrons near the surface, and has a thickness usually in the range .001 - 0.1 mm. The fall voltage usually has a value of 1 - 10 volts, hence positive ions must be found very near the anode surface, and the magnitude of the fall voltage depends on the energy required for electrons to ionise the anode vapour atoms.

The anode end of the arc also has a contraction zone, however it is not so marked as the cathode since the current densities present, 10^2 - 10^3 Amps/mm^2 do not exceed the column by such a large magnitude. The positive ions formed at the anode surface by ionisation of vapour atoms drift in the electric field towards the cathode end of the contraction zone where the concentration is nearly as great as that of electrons. Hence they are almost neutralised and the electric field of the column is low compared to the field present in the fall and contraction zones; 1 - 2 volts/mm compared to 10^3 - 10^4 volts/mm.

The electrons which emerge from the anode end of the contraction zone are accelerated by the field of the anode space charge, thus their energy and the probability of making ionising collision increase as they approach the anode surface.

The energy balance at the anode comprises the following :-

A. Energy supplied to the Anode

(i)   Kinetic energy of electrons, which has a power component of IVa assuming they pass freely through the anode fall voltage.

(ii) Potential energy of the electrons, $e\phi$ per electron.

(iii)   Contribution from surface recombination of dissociated gas, and

        heat conduction and radiation from the hot gas.

(iv)   Joule heating of the anode material

B.   Energy lost from the anode

(i)   Energy required for vapourisation of metal atoms, and to release

        metal particles from the surface.

(ii)   Radiation from surface hot spots and heat conducted away through

        the bulk metal.

(iii)   Energy loss by dissociation of gas at the heated anode surface

        and heat conducted or convected away to the surrounding gas.

Voltage and Current Characteristics

Considerable information on arc structure and properties can be obtained

by the determination of voltage/current characteristics associated with

changing arc length.   Early experiments by Mrs. Ayrton (30) on relatively

short stationary arcs in air, using carbon electrodes culminated in the

familiar Ayrton equation :

$$e_t = a + b\ell + \frac{c + d\ell}{i} \quad \text{for arc voltage } e_t$$

where a =   sum of cathode and anode drops

        $b\ell$ =   voltage drop in the column

        c/i =   negative characteristic of the negative glow

        $d\ell/i$ =   negative characteristic of the column

        ℓ =   total arc length

        i =   arc current

If the total length of an arc is varied, holding the current constant,

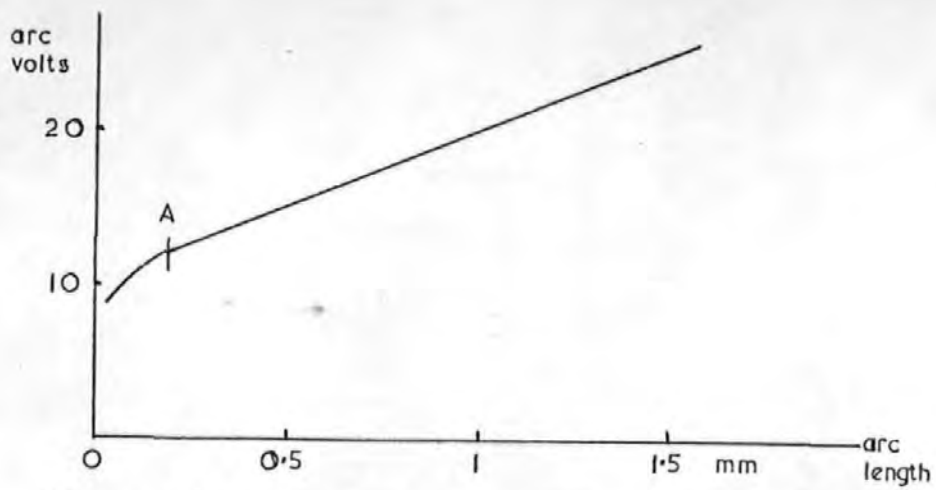and the p.d. between the electrodes is plotted as a function of arc

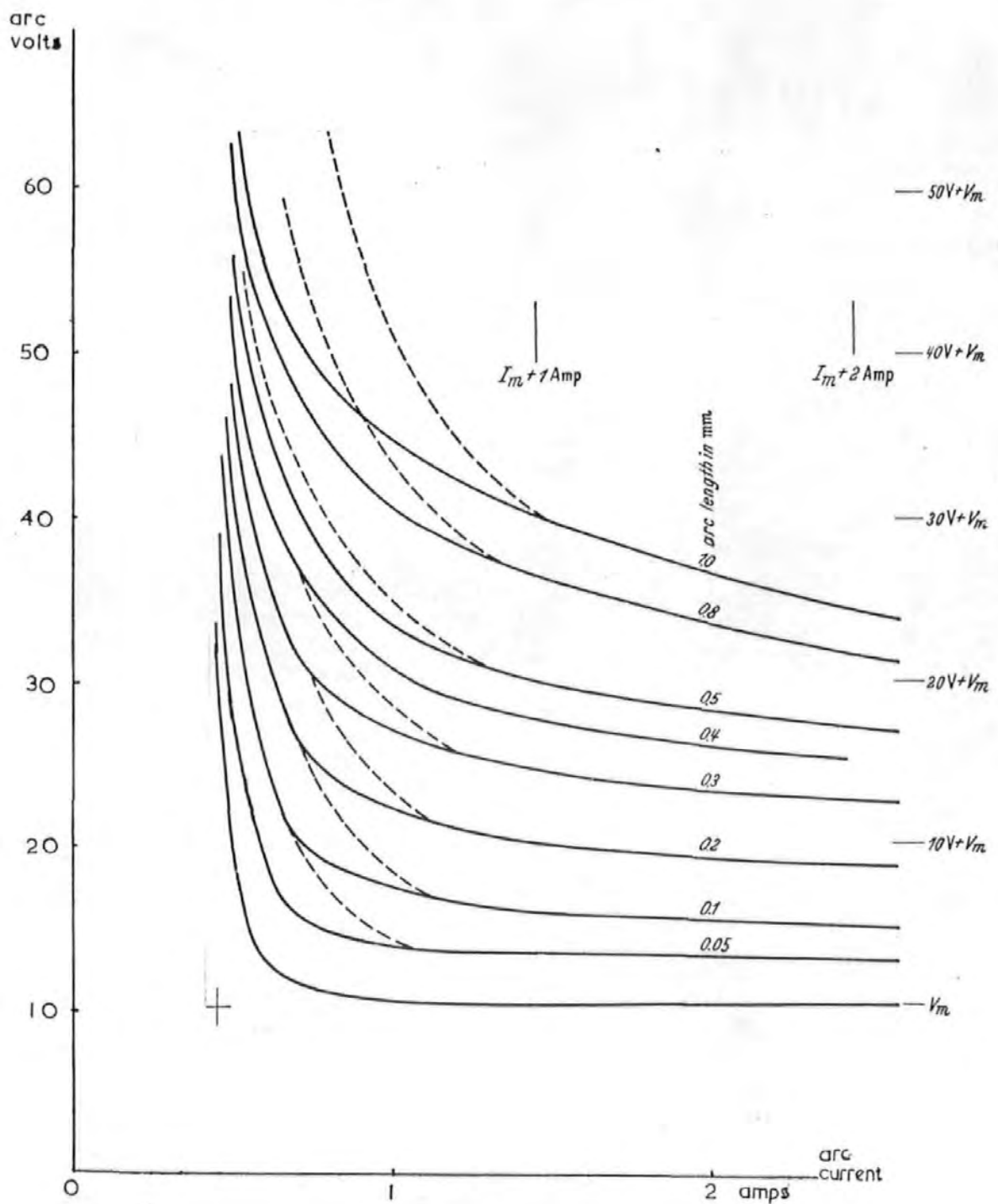Fig. 4: Variation of arc voltage with arc length.

Fig. 5: Holm's constant arc length curves

- 25 -

length, the graph shown in Figure (4) is obtained. Up to point A, the arc voltage varies non-linearly with length, due to the action and interaction of the two electrode zones. As the arc is lengthened beyond. A, a linear relationship between arc length and arc voltage develops.

Holm (31) produced a set of constant arc length curves for varying voltages and currents, using silver electrodes in air, Figure (5). He suggested that these curves could be used to determine the arc length for a given voltage and current for many different electrode materials, simply by shifting the curves with respect to the co-ordinates. This can be justified by assuming the anode and cathode fall voltages are relatively constant for a particular electrode material, even with variations in current. This was shown to be the case by Dickson and Von Engel (32) in some work performed on resolving the electrode fall spaces of electric arcs. The anode fall was found to have a constant value with the current increasing to 60 amps, the cathode fall was constant up to 30 amps, but was found to increase with current above this value.

Hence the principal changes in arc voltage appear to be a property of the arc column rather than the electrode fall regions. Nottingham (33) plotted arc voltage against current with arc length as a parameter, and proposed that his experimental data could be represented by a simple empirical equation.

$$e_t = A + \frac{B}{I^n} \quad \text{where A and B were constants}$$

dependant on the length of the arc, the electrode material and the ambient atmosphere. The index n was shown to be a constant dependant upon the boiling temperature of the anode material varying from n = .34 for zinc (B.P. 1180K) to 1.38 for tungsten (B.P. 5100K). Good agreement between

the proposed equation and experiment was found for arc lengths up to 10mm, currents up to 10 amps and voltages up to 70 volts.

Ives (34) produced similar curves to Nottingham and demonstrated the existence of a minimal arc length characteristic, or envelope curve within which the arc produced would be stable. This envelope curve can be considered to be asymptotic to the line $i = I_m$ and $e = E_m$ drawn on Holm's curves Figure (5). I_m is the minimum current at which an arc is stable, and E_m the arc voltage below which the arc will extinguish. The value of E_m is constant for a particular contact material and is related to the ionisation potential of that material. The value of I_m also varies from one contact material to another, however, the current at which the arc extinguishes has also been found to vary depending on circuit conditions. Whereas the line $e = E_m$ on Holm's curves is a clear asymptote, the line $i = I_m$ is less distinctive. Atalla (35) has shown that the minimum arc current is a function of the maximum current in the arc, and is influenced appreciably by the surface condition of the contacts. He found that activated or oxidised surfaces would support an arc at a lower current than a clean metal contact surface. Ittner and Ulsh (36) found that the arc duration for a given set of circuit parameters increased to a plateau value after about 50 operations, suggesting oxidation of the contacts produces a lower value of I_m.

Takahoshi et al (37) found that the arc termination current increased with increasing arc duration, saturating at a specific value for a particular contact material. He found this relationship to be unaffected by the load current in the range 1 - 5 amps. These saturation values were found to correspond to those listed by Holm (38) for the minimum arc current. However Holm states that the value of I_m is also influenced by such things

as cathode cross section, relative humidity of the ambient gas etc.

Farrall and Cobine (39) concluded that the arc duration, hence the minimum

arc current for a given set of conditions, is determined by the abundance

of metal vapour near the cathode and its rate of loss to the surrounding

gas. Values for minimum arc currents vary from about 0.4 amps for silver

to 1 amp for tungsten as given by Holm.

Holm's constant arc length curves were used by Aida (40) to derive

empirical formulas for the arc duration over the range covered by the curves.

The arc duration was derived in exponent form as a function of the arc

voltage, current and separating velocity. For materials like tungsten

(i.e. thermionic emission), two formulas were required to predict the arc

duration, one for the supply voltage in the range 40-70 volts, and the

other for below 40 volts. For materials where the electron emission contains

field and thermionic components, the formula was found to be valid for the

range 50 to 150 volts, however for below 50 volts a correction factor was

required.

The experimental data produced by Nottingham (33) was obtained by drawing

an arc to a specified length. The arc current was then varied using a

series resistor and the change in arc voltage noted. The arcs observed

could be justifiably assumed to be in a stable state of thermal and

electrical equilibrium.

The method used by Holm was to draw the arc at a rate considered slow

enough to represent stationary conditions at any point in time. (A velocity

of 20 cm/sec or less had been indicated by Fink et al (41) as having a

negligible effect on the arc characteristics.) Pairs of values for the arc

voltage e_t and current i_t were then read off the oscillographic records at

different points in time over the arc duration, assuming that the values
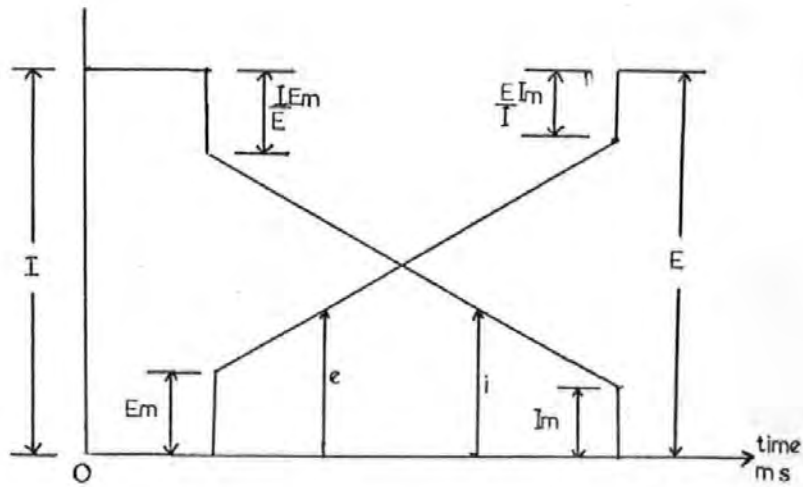
Fig. 6a: Schematic representation of the oscilloscope traces of arc voltage and current
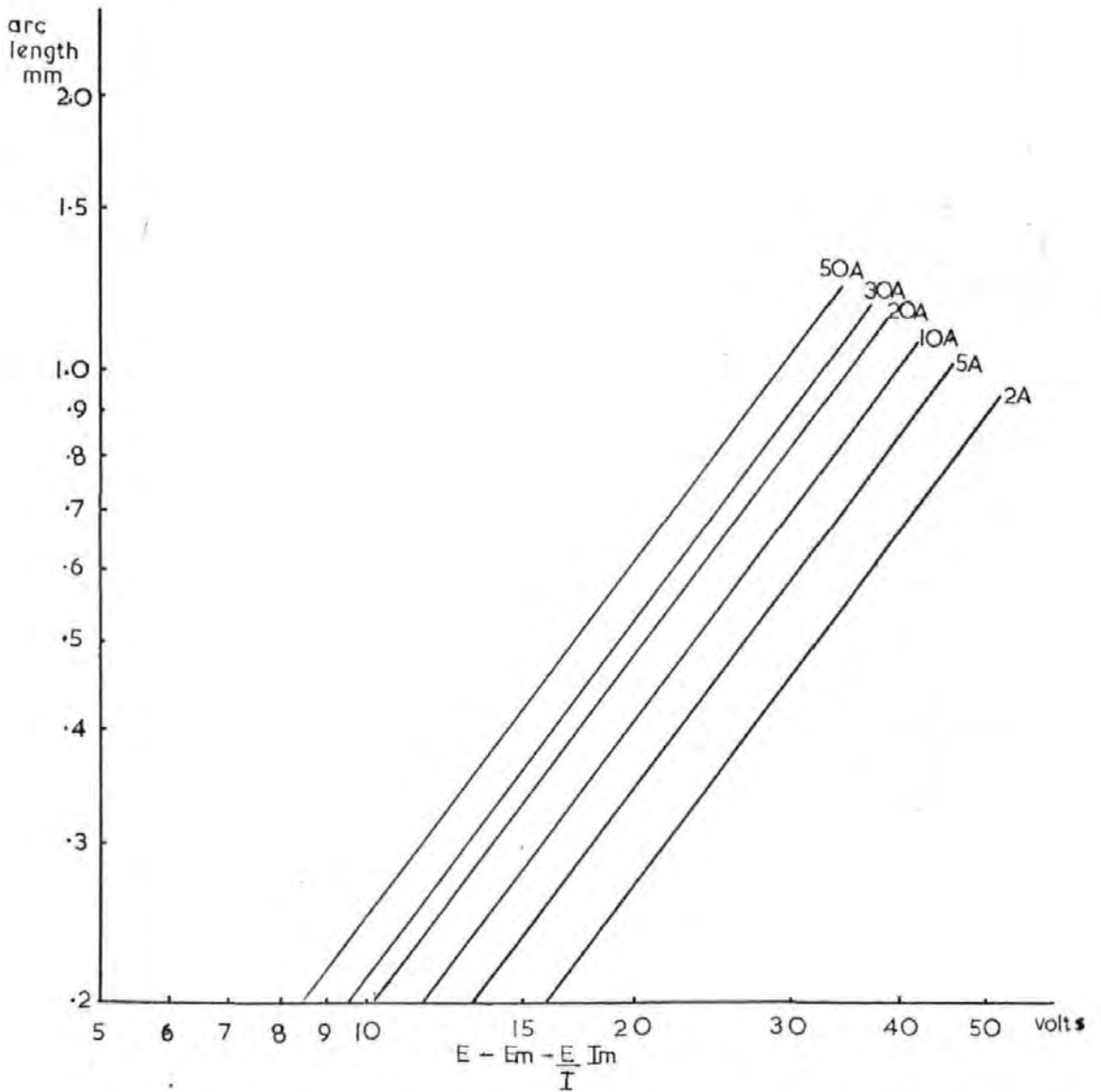

Fig. 6b: Graph of arc length at extinction against arc column voltage

represented a stationary state of the arc. The arc length corresponding to these different points was calculated assuming a constant opening velocity defined by $s = vt$, where s is the contact separation after a time t with an opening velocity v m/s.

More recently Sato et al (42) have produced some equations defining the arc voltage and current in terms of circuit parameters and a constant opening velocity. These equations were obtained from measurements of the oscilloscope recordings of arc voltage and current as shown in Fig. 6a. The arc length at extinction was defined as the length of an arc column in which the voltage difference was given by $E - Em - \left(^E/I\right).Im$. Using silver contacts breaking a resistive load in air an equation was deduced giving the arc length at extinction in terms of this column voltage and the circuit current immediately prior to ignition. This was stated as

$$\text{Arc length} \quad \ell = K(E - Em - \left(^E/I\right).Im)^{\frac{3}{2}} \quad . \quad I^{\frac{1}{2}}$$

where K is a constant and has a value of 1.5×10^{-3} for arc length in mm.

The experimental data verifying this equation for silver contacts is shown in Fig. 6b. This data was obtained by measuring the value of $E - Em - \left(^E/I\right)Im$ from the oscilloscope trace and also noting the arc duration. The arc length was then obtained assuming a constant opening characteristic of $s = vt$. By varying the open circuit voltage E and the load current I, a whole family of curves could be built up as shown in Fig. 6b. The above equation for the arc length was stated as being applicable only up to supply voltages of 70 volts and arc lengths of 2mm, i.e. the range covered by Holm's curves. Using this equation and measurements from the oscilloscope the equations for arc voltage and current were obtained as

$$e_t = Em + \frac{v}{K}(E - Em - \frac{E}{I}.Im)^{-\frac{1}{2}}.I^{-\frac{1}{2}} t.$$

$$i_t = I - \frac{I}{E}.Em - \frac{v}{K}(E - Em - \frac{E}{I}.Im)^{-\frac{1}{2}}.I^{-\frac{1}{2}}.\frac{I}{E}.t$$

This type of approach was then applied to the same circuit using an a.c. supply not exceeding the range covered on d.c. i.e. 70 volts. The method assumed that every point on the a.c. half cycle represented a stationary condition which could be treated as a d.c. increment for the instant of time under consideration. Discrete values of $\hat{E} \sin \omega t$ and $\hat{I} \sin \omega t$ could then be inserted into the above equations for different points in time across the a.c. half cycle, to enable calculation of values for the a.c. voltage and a.c. current. Hence in the equation E becomes $\hat{E} \sin \omega t$ and I becomes $\hat{I} \sin \omega t$. The values calculated for e_t and i_t were found to agree well with those measured from the oscilloscope traces. These equations provide one way of calculating the arc energy using the expression $\int_{o}^{T} e_t.i_t.$ dt to represent the area under the power curve obtained by plotting the instantaneous values of the product $e_t.i_t$ against time.

Methods of obtaining values for the energy dissipated in arcs have occupied a place in the research of electrical contact phenomena for many years, since it was realised that there was direct correlation between arc energy and contact erosion for long arcs. Eskin (43) made measurements of arc energy for a.c. arcs using a ballistic wattmeter, which effectively integrated the expression $\int e_t.i_t.$ dt to give readings directly in Joules. More recently Tibolla (44) using data from Holm's curves produced values for the arc energy by utilising a computer program to integrate the expression $\int e_t.i_t$ dt. Lesinski et al (45) recently reported a new electronic instrument capable of giving a direct digital display of the

energy dissipated in an arc.

The next section is devoted to a review of the literature covering the field of contact erosion as applicable to the snap action switch.

2.4 Contact Erosion by the Break Arc

Contact erosion is influenced by many different factors. Both the direction (anode to cathode or cathode to anode), and the rate at which it occurs depend on items such as contact configuration, surface profile, contact material, circuit parameters, switch mechanism parameters (velocity etc.), ambient atmosphere (low pressure/high pressure/vacuum/humidity/inert/oxidising). Hence most workers have concentrated their erosion studies in a particular area e.g. measurements with a particular material for a specific range of circuit parameters. Thus the conclusions from one set of experimental conditions may be completely reversed for a different operating duty.

2.4.1 Bridge and Short Arc Transfer

The molten metal bridge has been shown by Llewellyn-Jones et al (7) to make a significant contribution to the erosion of contacts switching low voltage (< 12 volts) low inductive ($<10^{-6}$ H) circuits . It has been observed by Thomas (15) and Cowburn (46) that the bridge can be directly responsible for displacing contact material when it boils and breaks, and for low inductive circuits ($<10^{-6}$H) this can be the main contributing factor to the contact erosion. The molten metal bridge effectively sets up a micro-plasma in which the micro-arc discharges when the bridge ruptures. The duration of the micro-arc has been shown by Hopkins et al (8) to be closely dependant on the local self inductance of the contact circuit,

however no region of inductance was found where bridge transfer was the only erosion effect. Price (47) reports that the micro-arc appears to occur even with inductances as low as 10^{-8}H.

Studies of the micro-arc by Hopkins and Jones (8) have related the erosion which occurs to the local circuit inductance. The scatter in their results was attributed to the bridge transfer also taking place. The whole sequence of events after bridge rupture between platinum contact switching a 10 amp load was suggested as follows:-

The short arc which follows after the explosive rupture of the bridge, produces metal vapour in the gap at pressures up to 40 atmospheres for a current of 10 amps. A reverse short arc then occurs, which is regarded as being less effective in producing vapourisation of metal, hence the pressure falls and a second short arc can occur. Pressure produced by the second short arc is estimated at 6 to 8 atmospheres. As this pressure diffuses out of the gap the long arc sets in and the ambient gas atoms are able to participate in the arc column. For these low voltage circuits (6 - 12 volts supply) cathode gain is usually a feature of the transfer mechanism. Slade (16) gives the following explanation for this.

After rupture of the molten metal bridge a dense cloud of metal vapour is released. The metal droplets which make up the vapour produce much thermionic emission and become positively charged, hence they are attracted to the cathode resulting in cathode gain. The contact gap at this stage can be of the order of the mean free path length, therefore most of the electrons crossing the gap will either recombine with the positively charged metal droplets hence reducing the net cathode gain, or ionise the metal vapour, or go straight to the anode without collision. In this last case the electrons will dissipate the energy they have gained

from the electric field at the anode thus causing evaporation and transfer from anode to cathode.

As the duration of the arc increases there is sufficient time for the more massive and slower moving positive ions to drift across the electrode gap under the influence of the field, producing a cathode fall and eventually a column. The high field produced near the cathode accelerates some positive ions which dissipate their energy as heat on collision with the cathode. This is a characteristic of long arc or normal arc transfer, and the erosion mechanisms for this condition are discussed below.

2.4.2 Erosion due to the Long Arc

Ittner and Ulsh (36) investigated the erosion of contacts made of several different materials by an arc they refer to as a normal arc. This they define as an arc where most of the energy is dissipated in the arc plasma and the cathode fall. They assume that there is no appreciable anode fall and that the arc plasma tends to cushion the anode from direct electron bombardment.

The operating conditions were 50 volts, 1-5 amps d.c. resistive and inductive loads, producing arc durations in the range 1-11 milli-seconds with contact gaps over a range of 0.1-2mm. Controlled measurements of arc transfer carried out over this range of operating conditions showed that the principal mode of transfer consisted of material loss at the cathode, some of which was subsequently deposited on the anode. They expressed their measure-ments as cathode loss per coulomb of arc current and this was found to be essentially constant over the range investigated independent of the circuit load and e/i_t charactistics of the arc. This

substantiated a relationship previously proposed by Holm (48) for this type of arc, that the material transfer is proportional to the total charge passed in the arc. The anode gain, on the other hand they found to be much less consistent, ranging from 3 to 80% of the cathode loss. In general they found that the fractional anode gain decreased with increasing arc duration and current.

The measurements by Ittner & Ulsh of cathode loss were found to be in agreement, to a first approximation with a formula proposed by Llewellyn-Jones (7) for the cathode transfer coefficient k, in cubic centimetres per coulomb.

$$k = \frac{\alpha - \beta T^4 - \delta \lambda T}{\rho (c + \frac{21}{A}) T}$$

where   α, β & δ are constants

λ is the thermal conductivity

T the material boiling temperature

ρ the density

C the specific heat

A the atomic weight of the material.

This formula assumes that the heat available for vapourisation at the cathode is equal to the total heat supplied to the cathode by the arc less the heat which is conducted and radiated away from the cathode spot. This is accommodated by the three constants α, β, δ which are related respectively to the fraction of the total energy available for evaporation at the cathode, the fraction of energy lost by radiation, and the fraction lost by conduction.

El Koshairy et al (49) have investigated the dependancy of contact erosion

on arc charge for higher current values (200 amps and above). They also
explored the effect of current amplitude and waveshape, and arc length.
They found the electrode erosion to be sensitive to contact separation,
with a reduction in separation producing a net reduction in loss
particularly from the cathode. This they ascribed to increased metal
vapour condensing back on the contact surface. For the purpose of
calculating an energy balance they assumed that the anode and cathode
fall voltages were constant, but for the arc lengths tested (up to 1mm)
the cathode suffered the greater erosion due to the higher value of the
fall voltage compared to the anode.

Capp (50) has investigated how the amount of energy absorbed by the
electrodes is related to the total energy dissipated in the arc. Operating
conditions were typically 50 volts, 5 amps d.c., and arcs were drawn up
to a length of 2mm. The contact diameter was 8mm so it was assumed that
all the energy dissipated in the arc would find its way to one or both
electrodes. This was confirmed by experiment when the power absorbed by
the electrodes was measured by measuring the temperature rise of the
contacts due to arcing. It was found that an increasing proportion of the
arc power developed at the anode as the arc length increased. The power devel-
oped at the cathode increased more slowly with arc length compared to
the anode. He inferred from this that the anode fall voltage increased
with arc length and arc voltage, but that conditions in the cathode fall
region did not vary much as the arc length changed. He concluded that the
increase in power at the cathode as the separation increased was caused
by the increased power dissipation in the column and the consequent
increase in heat thermally conducted to the cathode. At larger separations
i.e. where the arc length approached the contact diameter, the increase
levelled off due to the heat from the column not going to the electrodes

but being lost to the surroundings.

Capp   performed no cumulative measurements on the erosion of the
contacts due to arcing. However, in the initial stages of arcing it is
likely that the erosion from the cathode will result since the bulk of
the arc energy is dissipated here. During later stages of arcing when
the anode is receiving more energy than the cathode, it is possible that
the erosion from the anode will dominate. This is not analogous to the
concepts of 'anode dominated arc' and 'cathode dominated arc' described
by Holm (48). The 'anode dominated arc' referred to here is analogous
to the short arc defined by Hopkins et al (8). A critical length is also
described by Holm as marking a transition point at which the erosion
characteristic changes from one of anode loss (short arc) to cathode loss.

Sato (51) in an investigation of the erosion of silver based electrical
contacts also defines a transition region in which the transfer
characteristic changes from one of cathode loss to anode loss. Operating
conditions were a supply voltage of 40 volts and currents in the range
1 - 50 amps d.c. The transition region was defined in terms of the
current and for silver cadmium oxide contacts was stated as occuring at
around 6.5 amps. For currents below this, material transfer was measured
as being cathode to anode, and for values above this markedly anode to
cathode. From a study of erosion due to a.c. operating conditions, it
was shown that the direction of transfer could be related to the value
of the peak current of the a.c. wave.

Slade and Holmes (52) investigated the erosion characteristics of silver
contacts switching a.c., with particular regard to pip and crater formation.
Operating conditions were different to those used by Sato (51) in that
both make and break operations were performed by the test contacts as

opposed to break only. The velocity of the contacts used by Slade et al was also very much lower, 0.4 mm/sec. as compared to 63mm/sec used by Sato, hence the arc durations were much longer. Over the range of currents tested (5 - 12 amps) Slade et al, found that transfer was predominantly cathode to anode for full wave rectified a.c. with a pip built up on the anode and a crater formation on the cathode. For a.c. operation they observed pip and crater formations on both electrodes. This was attributed to the arc roots holding the same position on the contact surface as at previous operations with the same polarity arrangement. The build up of the anode pip was expressed in terms of charge transfer/ operation, no account was taken of the arc voltage for this type of switching operation. In a later paper (53) they showed that it was possible to lessen the formation of pip and crater effects by adding to the contacts a small percentage of Tungsten (10%). This was considered to promote greater arc root motion over the electrode surface reducing the possibility of the arc roots always forming in the same position. It was also observed that the volume of material transferred was dependent to some degree on the temperature of the contact. The actuating mechanism used involved a bimetallic heater, and it was found that greater erosion occured when the anode was the hotter contact.

Kubono (54) also investigated the relation between erosion and contact temperature, for copper electrodes. He calculated the cathode loss using a relation between evaporation rate and contact temperature and showed how the temperature and radius of the cathode spot were a function of arc current and cathode fall voltage.

Burkhard (55) in his work on the power balance at the anode, using silver cadmium oxide contacts, suggested that movement of the cathode spot

and the type of cathode emission are related. He went on to show that the energy dissipated at the anode surface, and hence the anode erosion was also dependant on the cathode electron emission.

Kume et al (56) in his work at higher currents (above 1000 amps), on a model circuit breaker showed that the erosion from both contacts varies in proportion to the arc energy.

This review of previous research work identifies the mechanisms that occur when contacts break an electric circuit and demonstrates the diversity of results that can be obtained for different operating conditions.

The main influences which appear to affect the direction and rate of erosion of the contacts in this application are listed below in three groupings :-

1.	Arc Parameters:	Arc Charge
		Arc Energy
		Arc Voltage
		Arc Current
		Arc Length
2.	Circuit Parameters:	Supply Voltage (a.c. or d.c.)
		Load Current
		Resistive or Reactive
3.	Switch Parameters:	Contact Velocity
		Contact Gap
		Contact Material
		Contact Size

To study the performance of snap action switches not only involves consideration of each of the above independently, but perhaps more importantly requires an understanding of how these parameters inter-relate.

The erosion of the contacts has been identified by most workers as being either in the category of anode loss and cathode gain or cathode loss and anode gain. A transition region between these two has also been suggested and related to the magnitude of the circuit current. Since the snap action switch does not fall exactly into any one of the operating conditions reported in the literature, the type of erosion occuring due to the break arc will need to be ascertained by experiment before the main factors influencing it can be studied.

2.5 Contacts in Motion: Make

The preceding sections have dealt with contacts at rest in the 'made' position with conduction established across the interface, and the results of interrupting the current flow. The section below covers the research carried out on the processes involved and resulting from establishing current conduction between two initially open contacts.

2.5.1 Breakdown prior to Contact

The electrical breakdown of a gas between electrodes is described by Paschen's law, which expresses the breakdown potential as a function of the product of electrode gap and gas pressure. Classically this shows the minimum voltage at which breakdown can occur to be in the region of 300 volts. However, for very small gaps (10^{-4}mm) breakdown and arc ignition have been observed with voltages as small as 50 volts by Germer (57) et al, who suggested that the arc is initiated and maintained by field emission current from the cathode. For this to occur fields of $10^5 - 10^6$ volts/mm are needed to give cold extraction of electrons from pure metals according

to Fowler-Nordheim theory. At 50 volts the electrodes would have to approach within 10^{-5} mm, less than the mean free path length of electrons, hence ionisation is unlikely to occur to the extent required to cause breakdown. Germer (57) also noticed that arc ignition appeared more readily for activated contacts, and Llewellyn-Jones (58) has suggested that a layer of organic or oxide film is responsible for some secondary ionisation process which occurs at the cathode surface enabling breakdown at fields of 10^4 volts/mm.

Another suggestion proposed has been the intensification of the local field at surface asperities or by particles on the surface. Holm (59) introduces the concept of 'whiskers' on the contact surface. As the contacts approach and the whisker is contacted, it is immediately heated to explosion point with the ignition of an arc in the vapour. Contact at a whisker differs from contact between two surface asperities which may also be heated by the current to vapourisation leading to an arc discharge. In the case of the former, since the whisker has a much smaller cross section and hence a higher resistance, the transient current which flows before vapourisation is less than that which flows between two asperities in contact. This larger current is usually sufficient to cause a transient lowering of the contact voltage to zero before vapourisation.

Pharney (60) distinguishes between three types of closure phenomena from his observations using a high speed oscilloscope.

    i.   Arc discharge without any initial metallic continuity, due to field enhancement effects.

    ii.   Initial metallic contact, either whisker or asperity, followed by vapourisation to an arc.

    iii.   Closure with no arcing.

Phamey observed that the size of the anode crater thrown up by the arc before contact increased with increasing arc energy, and that metallic contact after the arc had extinguished usually occured at the anode crater rim. Germer and Haworth (61) related the height of this crater rim to the energy dissipated in the arc using the expression:

$$\text{height } h \; \alpha \quad \sqrt[3]{\text{energy}}$$

From measurements of closing velocity and rim height Pharney calculated the local breakdown field as $2 - 3 \times 10^5$ volts/mm which is still too low for appreciable cold extraction.

Germer (57) classified two types of arc discharge prior to contact, the 'anode arc' and the 'cathode arc'. He identified a critical distance below which an anode arc occured with loss of material from the anode, and above which material loss from the cathode dominated. For silver he states the critical distance as being 3 to 4×10^{-3} mm which means for a closing velocity of 100mm/sec, an arc duration of 50 μ seconds.

When arc ignition occurs before contact a process can occur described by Holm (59) as floating. This results from the contacts being held apart by high vapour pressure produced as a consequence of the initial metallic constriction or asperity being heated to boiling. It can also occur when the contacts are made and at rest, as a result of a high current surge. If the contact area is not able to increase to accomodate the extra current flow, floating results.

Whether floating occurs, or an arc discharge, as a result of asperity vapourisation the contacts will close together with the likelihood of at least a small amount of molten metal between them. Also, since current conduction is established at asperities first, these will soften and

possiblly melt due to the high initial current density, and hence they will yield to increase the contact area until equilibrium is reached. Effectively the contacts weld together even though the weld strength may be small. Sato (51) has expressed the softening and welding temperature either as a function of contact voltage or of current and contact force. He ascribed light welding or sticking to softening of the contact material, and heavy welding to melting of the contact material. Static welding of contacts due to transient high current pulses has also been studied by Turner et al (62), who measured the weld strength which results when contacts are in series with a fuse blown on short circuit.

2.5.2 Contact Bounce

Usually the process of bringing together two contacts and establishing current flow, does not finish at the first impact. For most electromechanical devices bouncing occurs as the kinetic energy of the moving contact member is dissipated. A bounce means in effect that the contacts go through another complete switching operation i.e. a break and make, although the conditions prevailing are not the same as for a break and make in isolation. Erk and Finke (83) studied bouncing contacts at length both from a mechanical standpoint and from electrical considerations. They found that the amplitude of the first bounce was not always the longest duration, nor did it always achieve the largest gap. The reason for this was attributed to high frequency oscillations of the fixed contact after first impact. This would then add to or detract from the kinetic energy of the moving contact at subsequent bounces.

Bouncing involves drawing a molten metal bridge, rupture, arcing, followed by closure onto molten contact material which subsequently solidifies as the heat is conducted away through the bulk of the contact. The occurrence of more than one bounce depends on the energy in the mechanism still to be dissipated and the strength of the weld after the first bounce. Shaw (64) found that the weld produced by the first bounce usually prevented any further bouncing. Erk and Finke found the strength of the weld to be very eratic, depending on the distribution of the contact material from a particular operation and also varying for different types of contact material. Materials of a lower arc voltage were inclined to produce smaller weld strengths. Of the materials they tested Silver Cadmium Oxide 85/15% was found to have the lowest energy dissipated in the bouncing arc, due to its low arcing voltages of 10 - 12 volts.

Turner et al (65) of the Electrical Research Association investigated weld strengths after bouncing, and also the effect of contact size on the weld strength for silver based contacts. They found for a given current a minimum size of contact could be determined at which the weld strength jumped from around 10N to 100N and more. The point at which this occured for silver cadmium oxide contacts was found to be slightly dependent on the percentage of CdO present. The limit for Ag/CdO.85/15% was found to be 65 Amps/mm^2 of cross section and this was related to the absolute minimum fusing current of silver wire.

Koepke and George (66) investigated the strengths of welds produced at break, by applying the test current after the contacts had come together. They defined weak welds (1 - 3 grms) as cold welding of the contact surfaces followed by localised resistance welding upon application of the current. Strong welds (5 - 9 grms) they suggested were either due to

- 44 -

contact being re-established after the boiling voltage had been reached, or due to molten droplets or vapour redeposited back onto the contact surfaces while they were in close proximity. This is analogous to re-bridging as described by Hopkins et al (8). Koepke et al also studied the effect of the ambient atmosphere on the tendency for contacts to weld at break. For silver based contacts particularly, they found the weld strength to decrease with increasing oxygen content of the environment. This they suggested was due to the fact that silver in the molten state absorbs oxygen (also confirmed by Hewett 87), and can sustain a surface oxide layer up to $200^{O}C$, which would impair welding resulting from the condensation of the molten metal bridge.

The significance of the make operation related to snap action switches, and the weld strengths which may occur is not explicit from this literature review. Initial experimental work on the switch will attempt to establish the relative importance of the make operation when compared to the break operation.

REFERENCES   -   Chapter Two

1.   R. Holm
     Electric Contacts, Theory and Application.
     Fourth Edition, P.8 et seq. Springer-Verlag, 1967.

2.   H. Bresgen.
     'Reducing the Contact Resistance of Tarnish Layers on Silver by
     means of an Oscillating Load.'
     International Conference on Electric Contacts, Japan 1976.

3.   F. Llewellyn-Jones.
     Physics of Electrical Contacts.
     P.12 et seq. Oxford, Clarendon Press 1957.

4.   R. Holm.
     Electric Contacts, Theory and Application.
     Fourth Edition. P.60 et seq. Springer-Verlag 1967.

5.   F. Llewellyn-Jones.
     Physics of Electrical Contacts.
     P.17 et seq. Oxford, Clarendon Press 1957.

6.   M.R. Hopkins and D.I. Jones.
     'The Lorenz Number for Iron and Nickel at High Temperatures.'
     Phys. Stat. sol. (9) 15, 151 (1973).

7.   F. Llewellyn Jones.
     'Matter Transfer in Contacts and the Microscopic Molten Metal Bridge.'
     Proc. of the Relay Conference, Stillwater, Oklahoma 1964.

8.   M.R. Hopkins and R.H. Jones.
     'Transients, Bridges, Micro-Arcs and Metal Transfer.'
     Holm Seminar on Electric Contact Phenomena, Chicago, Illinois, 1972.

9.   P.E. Slade, P.P. Koren, M.D. Nahemow.
     'Molten Metal Bridge stage of Opening Electric Contacts.'
     Holm Seminar on Electric Contact Phenomena, Chicago, Illinois, 1974.

10. M.R. Hopkins, R.H. Jones and J.A. Evans.
     'Short Time Transients in Electrical Contacts.'
     International Conference on Electric Contacts, Japan 1976.

11. M. Sato.
    'Studies on Silver Base Electrical Contact Materials.'
    Trans. Nat. Res. Inst. for Metals Japan. Vol. 18. No. 2.   1976.

12. M.J. Price and F. Llewellyn Jones.
    Brit. J. Appl. Physics, 2, 589. 1969.

13. F. Llewellyn Jones, M.R. Hopkins and C.R. Jones.
    Brit. J. Appl. Physics 12, 485, 1961.

14. M.R. Hopkins and R.H. Jones.
    'Transients and Transfer in a Single Contact Operation.'
    Int. Conf. on Electric Contact Phenomena. Japan 1976.

15. B.R. Thomas.
    Ph.D. Thesis. University of Wales. 1967.

16. P.G. Slade.
    'Current Interruption in Low Voltage Circuits.'
    Holm Seminar on Electric Contact Phenomena, Chicago, Illinois, 1968.

17. M.R. Hopkins, R.H. Jones and A. Davies.
    'Voltage Variation and Arcing between the Electrodes of Opening
    Low Voltage Contacts.'
    Int. Conf. on Electric Contact Phenomena, Paris 1974.

18. Takayoshi Kuborro and Kunio Mano.
    'Material Transfer by a Short Arc on Opening Switch Contacts.'
    Electronics and Communication in Japan, Vol. 56-C, No. 3 1973.

19. T.H. Thomas.
    Ph.D. Thesis. University of Wales 1970.

20. G.W. Mills.
    'The Mechanisms of the Showering Arc.'
    Holm Seminar on Electric Contact Phenomena, Chicago, Illinois,
    November, 1968.

21. J.R. Pharney.
    'Closed Form Solutions for the Various Energy Factors in a 'B'
    Type Transient.'
    Proc. of the 6th Int. Conf. on Electric Contact Phenomena.
    June 1972.

22. H.N. Wagar.
    'Predicting the Erosion of Switching Contacts that break Inductive
    Loads.'
    Proc. of the Holm Seminar on Electric Contact Phenomena.
    November 1968.

23. R. Holm.
    Electric Contacts, Theory and Application.
    Fourth Edition. P.323 et seq. Springer-Verlag 1967.

24. I. Langmuir.
    'Positive Ion Currents in Positive Columns of a Mercury Arc.'
    General Electric Review, P.731, 26, 1923.

25. F. Llewellyn-Jones and E.T. de la Perelle.
    'Field Emission of Electrons in Discharges.'
    Proc. of the Royal Society. A216, P.267. 1933.

26. F.E. Haworth.
    'Experiments on the Initiation of Electric Arcs.'
    Physical Review, 80 P.223. 1950.

27. K. Itoyama.
    'The Current Density Change of Anode Spot at Breaking Arc.'
    Int. Conf. on Electric Contact Phenomena, Paris 1974.

28. R. Hancox.
    'Importance of insulating inclusions in arc initiation.'
    British Journal Applied Physics. 10, p.468-471, 1960.

29. J.L. Meyer and G.E. Doan.
    'Arc Discharge not obtained in Pure Argon Gas.'
    Physics Review. 40, p.36-39, 1932.

30. Mrs. H. Ayrton.
    'The Electric Arc.'
    The Electrician, London 1902.

31. R. Holm.
    Electric Contacts, Theory and Application.
    Fourth Edition, P.280 & 441. Springer-Verlag 1967.

32. D.J. Dickson and A. Von Engel.
    'Resolving the Electrode Fall Spaces of Electric Arcs.'
    Proc. of the Royal Society A. vol. 300. 1966.

33. W.B. Nottingham.
'Normal Arc Characteristic Curves.'
Physical Review. Vol. 28, P.764, October 1926.

34. H.E. Ives.
'Minimal length Arc Characteristics.'
Journal of the Franklin Institute. Vol. 198, No. 4. October 1924.

35. M.M. Atalla.
Bell System Technical Journal, 32, p.6. 1953.

36. W.B. Ittner and H.B. Ulsh.
'Erosion of Electrical Contacts by the Normal Arc.'
Proc. I.E.E. No. 104, p.63. 1957.

37. A. Takahochi and K. Miyachi.
'Arc Termination Current on Breaking Contacts.'
Holm Seminar on Electric Contact Phenomena, Chicago, Illinois 1975.

38. R. Holm.
Electric Contacts, Theory and Application.
Fourth Edition, P.440. Springer-Verlag 1967.

39. G.A. Farrall and J.D. Cobine.
'Stability of Arcs in Gases.'
J. Appl. Physics Vol. 36 p.53-56, January 1965.

40. T. Aida.
'General Formulas for Arc Duration in Air.'
Elec. Eng. Japan. Vol. 90, No. 6, 1970.

41. H.P. Fink.
'Understanding the Operation of Moving Contacts.'
Wiss. Veröff. Siemens-Werk 17. 1938.

42. M. Sato, M. Hijikata and I. Morimoto.
'Characteristics of the Arc breaking a Non inductive Circuit in Air.'
Trans. Japan Inst. Metals. No. 2. March 1974.

43. S.G. Eskin.
'Arc Energy in a.c. Switching.'
General Electrics Review, Vo. 42. No. 2, P.81. 1939.

44. J.F. Tibolla.
    'Average Arc Energy for Random Opening A.C. Electrical Contacts.'
    M.Sc. Thesis. University of Pensylvania. May 1970.

45. S. Lesinski and M. Glaba.
    'Electric Arc Energy Measuring Device.'
    Int. Conf. on Electric Contact Phenomena. Japan. 1976.

46. M.C. Cowburn.
    Ph.D. Thesis. University of Wales, 1969.

47. M.J. Price.
    'The Microscopic Molten Metal Bridge and the Erosion of Contacts.'
    Proc. of the 13th Relay Conf. Stillwater, Oklahoma, 1965.

48. R. Holm.
    'Electric Contacts, Theory and Application.'
    Fourth Edition, P.304 et seq. Springer-Verlag 1967.

49. M.A.B. El-Koshairy, M. Khalife, F. Aboul-Makarem.
    'Erosion of Contacts by Arcing.'
    Proc. I.E.E. February 1961.

50. B. Capp.
    'Power Balance in Electrode Dominated Arcs.'
    J. Physics. D. Appl. Phys. Vol. 5, 1972.

51. M. Sato.
    'Studies on the Silver Base Electrical Contact Materials.'
    Trans. Nat. Res. Inst. for Metals. Vol. 18, No. 2. 1976.

52. P.G. Slade and F.A. Holmes.
    'Erosion Characteristics of Silver Contacts.'
    I.E.E.E. Trans. Parts, Hybrids and Packaging Vol. PHP13,
    No. 1, March 1977.

53. P.G. Slade and F.A. Holmes.
    'Pip and Crater Formation during Interuption of Alternating Current.'
    Int. Conf. on Electric Contact Phenomena. Japan 1976.

54. T. Kubono.
    'Theory of Cathode Erosion in the Arc Discharge.'
    Int. Conf. on Electric Contact Phenomena, Japan 1976.

55. G. Burkhard.
'Power Balance at the Anode.'
Int. Conf. on Electric Contact Phenomena, Japan 1976.

56. M. Kume and A. Fukui.
'Current Interruption Characteristics in A.C. Low Voltage High
Current Circuits.'
Int. Conf. on Electric Contact Phenomena, Japan 1976.

57. L.H. Germer.
'Physical Processes in Contact Erosion.'
Journal of Appl. Physics. Vol. 29, No. 7, July 1958.

58. F. Llewellyn-Jones.
Ionisation and Breakdown in Gases.
Science Paperbacks, Chapman and Hall Ltd. 1966.

59. R. Holm.
Electrical Contacts, Theory and Application.
Fourth Edition, P.277 et seq. Springer-Verlag, 1967.

60. J.R. Pharney.
'Clarifications of Arc Initiation Phenomena for Closing Contacts.'
Holm Seminar on Electric Contact Phenomena, Chicago, Illinois, 1969.

61. L.H. Germer and F.E. Haworth.
'Erosion of Electrical Contacts on Make.'
Jour. Appl. Phys. Vol. 20. November 1949.

62. C.A. Turner.
'Contact Behaviour in Power Circuits.'
Colloquium on Electrical Contacts. I.E.E. November 1976.

63. A. Erk and H. Finke.
'The Mechanical Processes of Bouncing Contacts.' Heft 5, 129.
'The Behaviour of Different Contact Materials for Bouncing Contacts'
Heft 9, 297,
E.T.Z - A (1965).

64. N.C. Shaw.
'Investigations of Contact Bounce and Contact Welding.'
Symposium on Electric Contact Phenomena. Graz. Austria (1964).

65. C. Turner and H.W. Turner.
     'Minimum Size of Silver based Contacts prone to Dynamic Welding.'
     Int. Conf. on Electric Contact Phenomena. Paris, 1974.

66. B.G. Koepke and R.I. George.
     'Welding of Medium Energy Electric Contacts.'
     Holm Seminar on Electric Contact Phenomena, Chicago, Illinois 1972.

67. B.L. Hewett.
     'Erosion of Silver - Palladium alloys in different gases.'
     Thesis: University of London, May 1974.

CHAPTER THREE

EQUIPMENT AND EXPERIMENTAL APPARATUS

3.1 The High Speed Camera

High speed photography has been for many years a much used tool for
research and development in switchgear applications. It is a direct
method of expanding the time scales of short duration events to
allow observation and measurement of rapidly changing quantities.
The different types of high speed camera available and their
particular applications have been reviewed in a recent publication
by Bagshaw and Kelsey (1).

The high speed camera selected for use in this research is a
'Hyspeed' rotating prism camera manufactured by John Hadland U.K.
This camera uses 16mm. film perforated down both edges, and the
principle of operation is to move the image derived from the lens
system in synchronism with the film during the instant of exposure.
This is achieved by mounting an 8 sided prism between the lens and
the film plane, on a shaft which is rotated by the film passing
over sprocket wheels. This ensures that there is no relative move-
ment between the image and the film. Figure (7) shows details of
the camera and its working mechanism.

This particular camera has a maximum speed of 11,000 frames/second
using a full 16mm. frame size. To attain this speed requires an
acceleration time of 1.5 seconds, using 60m. of film. Since the
films used in this work were readily and economically available in
30m. lengths it was not possible to achieve this maximum frame rate.
Instead 6000 frames/second was chosen as a working velocity since
this could be achieved after passage of 20m. of film in about
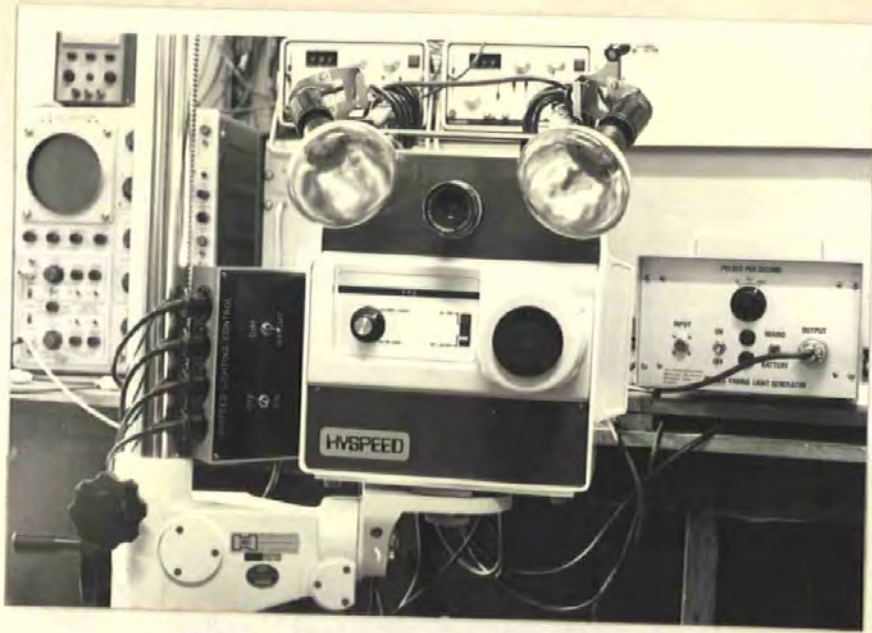
Fig. 7a.   Rotating Prism High Speed Camera.

OPTICAL HEAD

SHUTTER PULSE ASSEMBLY

CONNECTOR OPTICAL HEAD ELECTRICS

PRISM, SPROCKET & SHUTTER ASSEMBLY

SHIMS

TAIL CUT-OFF MICROSWITCH

LENS MOUNT SHIM

APERTURE MASK

LENS 'C' MOUNT SEE NOTE

SPEED SENSOR ASSEMBLY

'O' RING

GLASS WINDOW OR RETICLE

'C' MOUNT COVER
DUST COVER
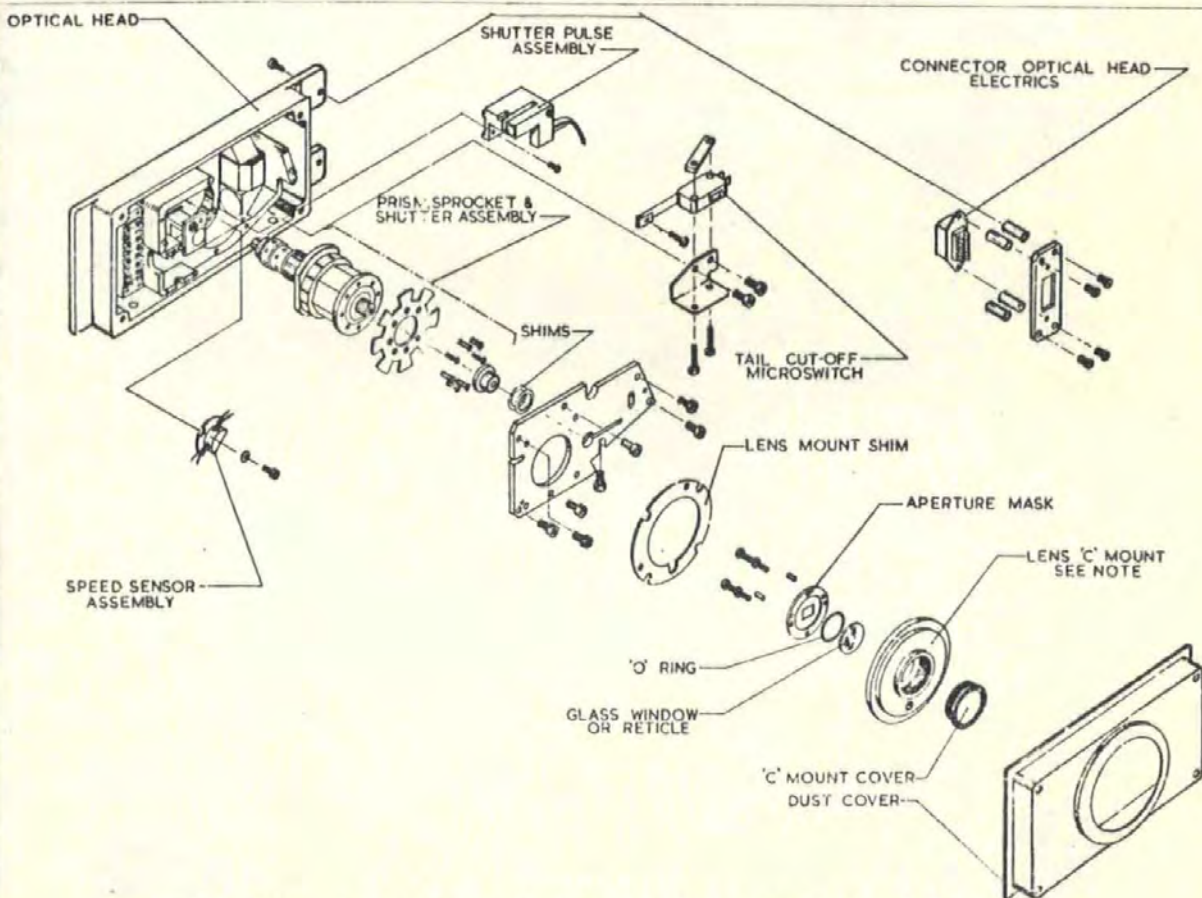
Fig. 7b.   Rotating Prism Mechanism and Optical Head.

0.8 seconds. This then left 10m. of film available to record the event. Synchronisation of the event onto this last 10m. of film was achieved using the trigger facility fitted to the camera. This enabled a relay to close a circuit at any point during film passage, and this could be preset to 20m. before starting the camera. The exact speed of the film at any instant could be found from the time base superimposed on the film edge by the camera. This was achieved by a small timing light inside the camera, which could be preset to flash with a frequency of 10, 100 or 1000 Hz. Hence at 6000 frames/second a timing spot could be positioned once every 6 frames.

The films used for the experimental work were Kodak 4-X, 400 A.S.A. negative film (monochrome) and Ektachrome E.F. 7240 125 A.S.A. colour reversal film. The former was used where a positive monochrome print of an operating sequence was required, whilst the colour film was suitable for direct projection.

This camera has an effective aperature limit of f3.2 and a shutter exposure ratio of 1 : 2.5. Hence for a film speed of 6000 frames/second the exposure time for each frame is 1/15000 of a second. This necessitates very high light levels to obtain a clear photographic record. Using four 500 watt photoflood spotlights it was found necessary to uprate both film types to 800 A.S.A., so that a sufficient depth of field could be obtained by stopping the lens aperature down to f5.6.

The lens used for most of the photographic work was a standard 50mm. Pentax Takumar lens, positioned on 120mm. extension tube, producing a field of view 10mm x 7mm with a field depth of 2mm. The resolution of the lens at the centre is stated to be 80 lines/mm. However, using it at such a long distance from the film plane in conjunction with an uprated

and rather grainy film, the smallest dimension change which could be detected was .03mm. This is sufficiently accurate for the arc lengths and contact seperations to be photographed where the magnitudes are of the order of 1 - 2 mm.

The measurements obtained from the high speed films are subject to certain limitations imposed by the camera shutter mechanism. Since the exposure ratio is 1 : 2.5, at 6000 frames/second there is a time interval between each frame of 100μs when the camera is effectively blind to any changes in the event being recorded. Hence the information on the film is comprised of discrete 'packets' of data with 150μs duration, taken at a sampling rate of once every 100μs.

3.2 The Transient Recorder

The high speed film gives an easily accessible visual record of a switch making and breaking a circuit. The electrical transients which also occur need to be stored in some convenient and accessible form for study and analysis. Previously this has been achieved using some type of analogue storage device, e.g. storage oscilloscope, u.v. recorder. However recent advances in large scale circuit integration and digital techniques have meant that electrical transients can now be recorded as a series of discrete points using high speed sampling techniques. Although not producing a true continuous record, digital storage of transients has several important advantages over analogue methods, see Trachslin (2). The principle of operation involves recording and storing a signal as a number of equally spaced points representing the amplitude of the waveform at discrete moments in time. During recording, each sample of the signal is converted into digital form and stored in the

- 56 -
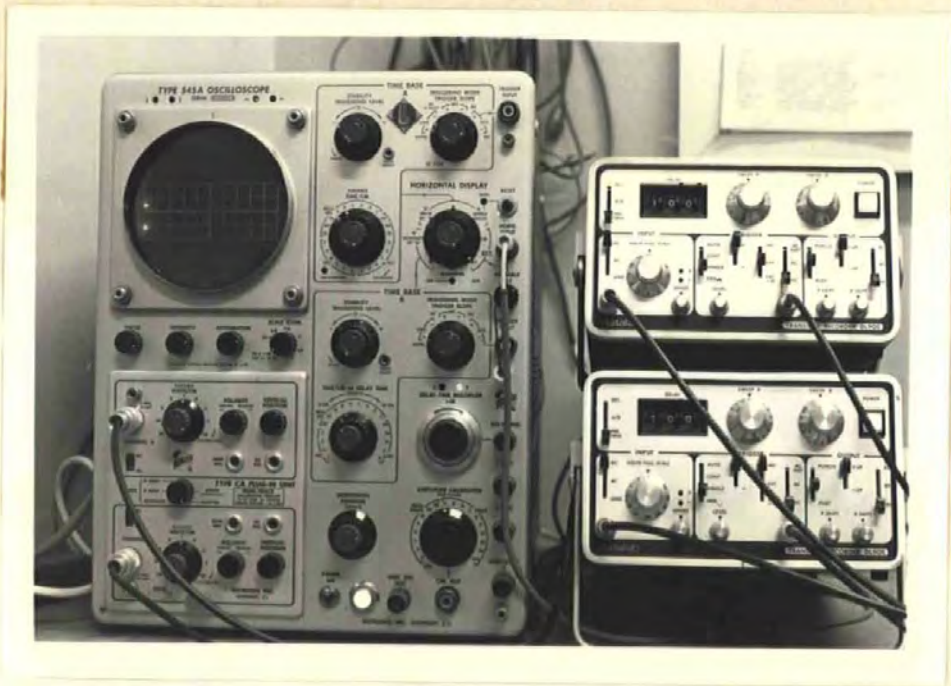
Fig. 8   Transient Recorders with Oscilloscope display.
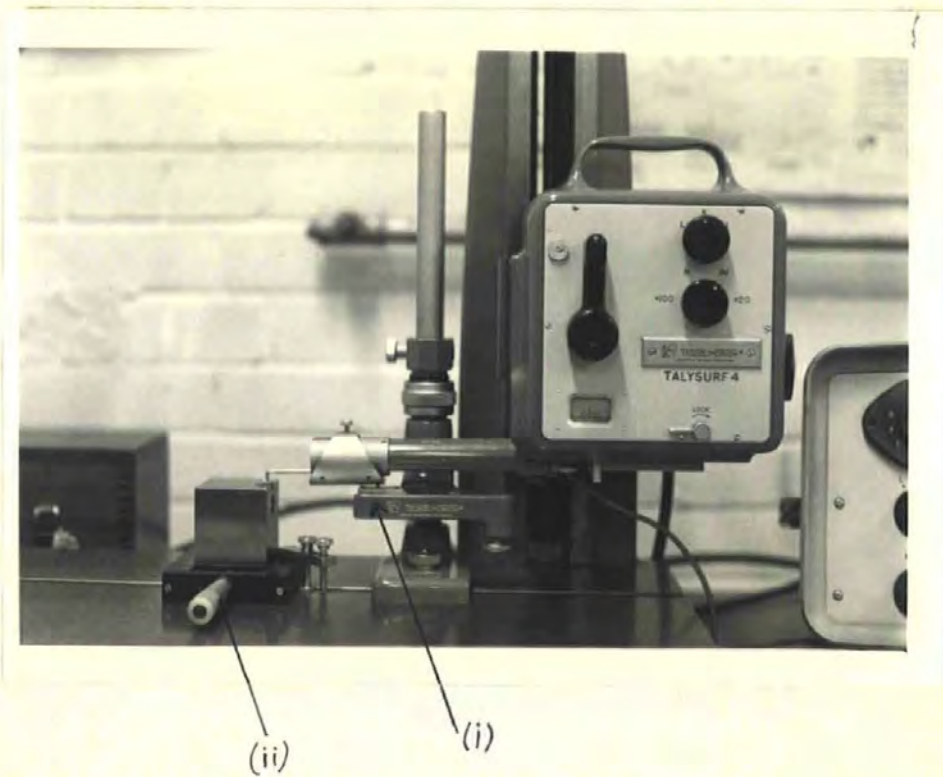
Fig. 9.   Talysurf, showing the external reference datum(i) and
the contact positioning device(ii).

memory. The two transient recorders used in this investigation were both Datalab D.L. 905's, which have a 1000 words of memory and an amplitude resolution with 8 bit accuracy. The fastest sampling rate obtainable with this type of recorder is 5 MHz and the smallest amplitude change detectable is 4 mV.

The waveform stored in the digital memory is reconstructed via a digital to analogue converter as a repeating sequence of 1000 analogue values. This can then be displayed on a conventional C.R.O. This digital method of data storage and retrieval has one particularly useful advantage over other methods. The memory is continuously recycling, i.e. it accepts new information at one end and discards the oldest information at the other. This principle allows information to be retained prior to the trigger impulse which causes the memory to 'freeze' its contents. Hence the leading edge and the baseline information before the onset of the transient is retained.

Alternative ways of retrieving and displaying the data stored in the recorder, other than the C.R.O. are also available. The recorder can be made to output the contents of the memory in analogue form at a rate suitable for plotting on an X - Y recorder, thus producing a permanent copy. Alternatively the stored data can be retrieved as a binary code, suitable for paper tape storage or interfacing directly to a computer for immediate analysis.

The two recorders in this investigation were coupled to a common time base to prevent drift occuring, and were used to store the arc voltage and current transients. A permanent copy was obtained using the output connected to an X - Y recorder.

3.3 The Talysurf

Damage to the contact surfaces, as a result of opening or closing an electrical circuit, can be conveniently assessed using the Talysurf. This instrument produces a magnified contour plot of the surface, and from this a quantitative evaluation of the volume of contact material displaced from the original surface profile can be carried out.

The method entails scanning the contact surface profile at equally spaced intervals using an optically flat glass strip as a reference datum. The volume of material displaced is obtained by summation, after measuring the cross sectional areas represented by the profile traces and multiplying by the spacing interval. Typical magnification factors used were 2 000X in the vertical direction and 100x along the horizontal axis, with a spacing interval between traces of 0.1mm. The horizontal magnification factor depends directly on the relative speed of the Talysurf pick up as it moves across the contact surface and the chart recorder, which gives a permanent record of the surface profile.

The Talysurf used in this study is a Taylor-Hobson mark 4 (Fig. 9). The residual magnification error of this instrument when properly set up is stated to not exceed 2%. The repeatability of this method, calculating the volume of material displaced, was checked by obtaining four different sets of data from one contact surface by rotating the contact through 90° after each set of measurements. The repeatability of the measurements worked out to be within $\pm$ 5% of the mean of the values calculated for the volume of material displaced.
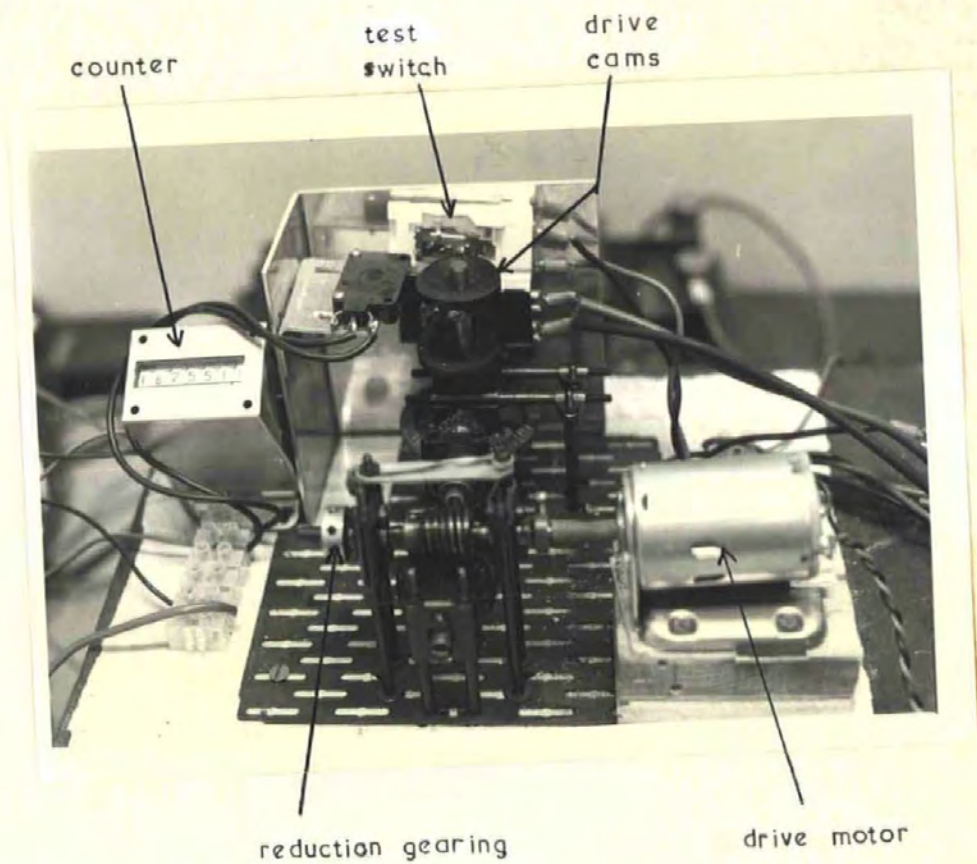
Fig. 10 Apparatus for life testing of Switches

The advantages of the Talysurf method of surface evaluation over other methods is that not only does it produce quantitative data on how much material is redistributed or lost but also gives an exact description of the pattern location of the redistributed material.

3.4 The Scanning Electron Microscope (S.E.M.)

This instrument has been increasingly used over the past few years to study contact surfaces. The three dimensional appearance imparted to photographs taken on the S.E.M. is due to the large depth of field which can be achieved even at large magnifications. The high quality of results obtainable has been demonstrated by Hopkins et al (3) and Vasile et al (4). Used in conjunction with the Talysurf it is particularly useful for producing a visual representation of a set of surface profiles.

The S.E.M. used in this research is a Cambridge Stereoscan type S4-10, linked to a television display unit. This facility is very useful for contact surface work since the specific region of interest can easily be identified then suitably magnified for photographing.

3.5 The Switch Re-cycling Apparatus

Since part of this research is to study the effect of many operations both on the switch mechanism and the contacts, some form of automated repetitive actuator is needed which can be set to perform a predetermined number of operations. A photograph of the apparatus constructed to do this is shown in fig. (10). It consists of a 6 volt d.c. motor driving two shaft mounted cams through a worm drive and reduction gears. The cams act as the

switch actuators and by rotationally displacing them with respect to each other, one switch can be made to perform all the circuit closing operations whilst the other performs all the break operations. By varying the supply voltage to the motor the speed of operation can be varied between 2 and 20 operations per minute. A microswitch mounted to the side of the test switches and driven by one of the cams is used to drive an electromechanical counter to register the number of operations performed. Using this operational rig, it was possible to life test a switch i.e. 200,000 operations in about 1 week. While being tested the switches were connected to the transient recorders so that the arc voltage and current waveforms could be checked at intervals during the life test.

REFERENCES -   CHAPTER THREE

1. J.R. Bagshaw and T. Kelsey
    'High Speed Photography in Switchgear Development.'
    Reyrolle Parsons Review, (GB) 1972-3, (1), pp. 15-20.

2. W. Trüchslin
    'Recording of Events occuring while switching an Electrical
    Circuit.'
    Paris Symposium on Electrical Contact Phenomena, 1974.

3. M.R. Hopkins and D.H. Watkins.
    'Experimental Study of the Geometry of Erosion Patterns.'
    Holm Seminar on Electric Contact Phenomena, Chicago, Illinois,
    1972.

4. M.J. Vasile and G.W. Kammlott.
    'Electric Contact Phenomena using the Scanning Electron Microscope.'
    Holm Seminar on Electric Contact Phenomena, Chicago, 1971.

CHAPTER FOUR

EXPERIMENTAL RESULTS AND DISCUSSION

4.1 Introduction

This study of electrical contact phenomena in relation to the small

snap-action switch can be considered to comprise three distinct areas

for investigation.

1. Mechanical Characteristics : Contact separation, velocity, force

2. Electrical Characteristics : Current, voltage, transient

values, arc durations.

3. Physical Characteristics   : Contact surface deterioration,

erosion, welding.

However, to obtain a more complete understanding of switch operation with

a view to being able to predict more accurately the life of a switch, it

is not only important to investigate these three areas in isolation, but

also to understand the way in which they are interdependent.

A photograph of the switch around which this investigation is centred is

shown in Fig. (1). A schematic diagram of the mechanism is shown in

Fig. (11). It is essentially a mechanical bistable device employing an

omega over-centre spring to supply the toggle or snap action effect.

The mechanics of this arrangement produce instability in the neutral

plane, hence the mechanism will not remain in a position where the force

holding the contacts together is zero.

To construct an operational rig to simulate the forces and velocities

occurring in the toggle action would have been difficult and in the final

analysis may have proved to introduce variables not present in the

actual switch, e.g. different thermal capacities, masses, spring stiffness.

The alternative, to perform all experimental measurements using actual

CONTACTS CLOSED
STABLE
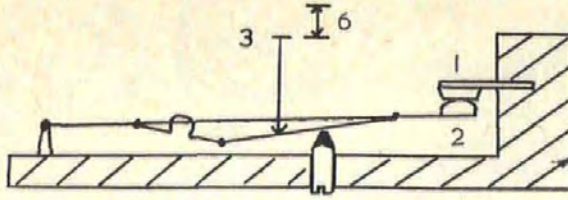
1. Fixed Contact
2. Moving Contact
3. Actuator
4. Omega Spring
5. Differential Screw
6. Operating Stroke
7. Switch Moulding

CONTACTS OPEN
STABLE
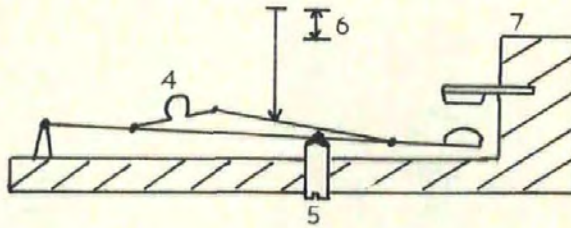
NEUTRAL PLANE
POSITION
UNSTABLE

Fig. (11) Schematic diagram of the toggle switch mechanism showing unstable neutral plane position.
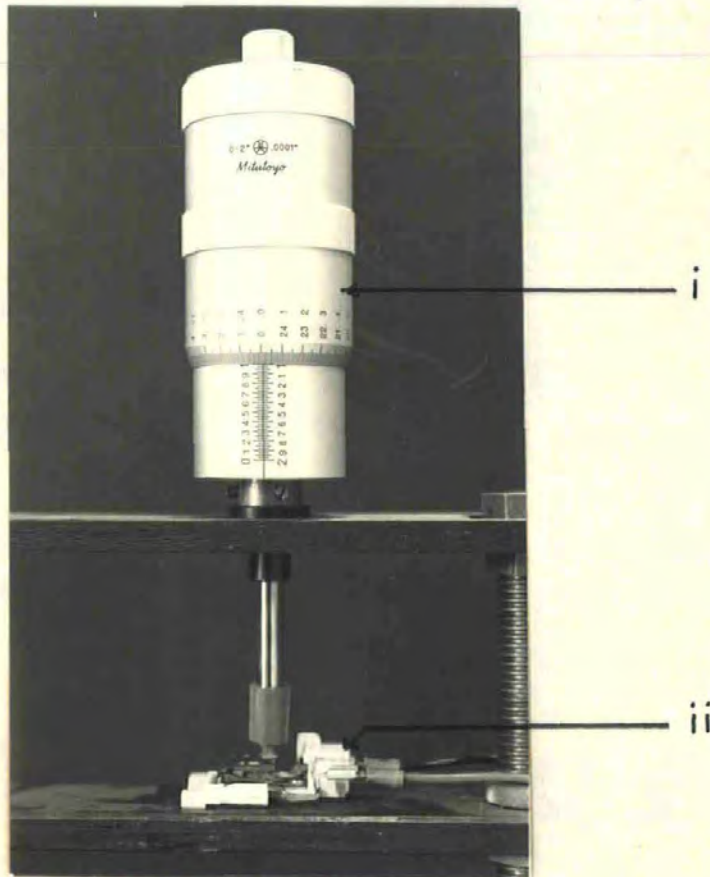
Fig. (12)   i. Micrometer Actuator

        ii. Switch with moulding cut away to enable filming of contact motion.

production switches has the limitation that the contacts are not
easily removed or replaced. In fact, it was necessary to destroy the
switch to enable the contacts to be examined under a microscope or on
the Talysurf. However, since the switches are a readily available item,
being cheaply produced in large quantities, it was decided to base all
experimental measurements on the actual switches. This will also enable
the repeatability of the mechanical characteristics of a sample of
switches to be assessed, which may in itself be an important factor
influencing switch performance.

4.2 The Switch Mechanism

A report by Harris, Riley and Brunel of the Battelle Laboratories (1)
to Ranco Inc. (U.S.A.) emphasized the following as being the most desirable
characteristics of the switch mechanism to produce the greatest overall
switch reliability.

1.   Availability of high contact separating forces to break welds.
2.   Maintenance of the contact force right up until the separation
      point of the break cycle.
3.   High relative acceleration of the contacts on break.
4.   Low contact closing velocity.
5.   Minimum contact gap of 0.25 mm.

Other workers, e.g. Eskin (2), Tibolla (3), have stated for certain a.c.
operating conditions the opposite of points (3) and (4) is required for
optimum performance.

The toggle switches investigated here have certain inherent mechanical
characteristics by virtue of their construction. The initial experimental
work undertaken was to isolate and define the mechanical characteristics
of the toggle switches with a view to assessing their suitability for the
electrical duty required.

separation
±·03mm

0·8

0·6

0·4

0·2

key: fig 17
⊙ distance CD
⊡ " at centre ₵
× " A B

point
of
contact

oscillations
after first
impact

0   1   2   3   4
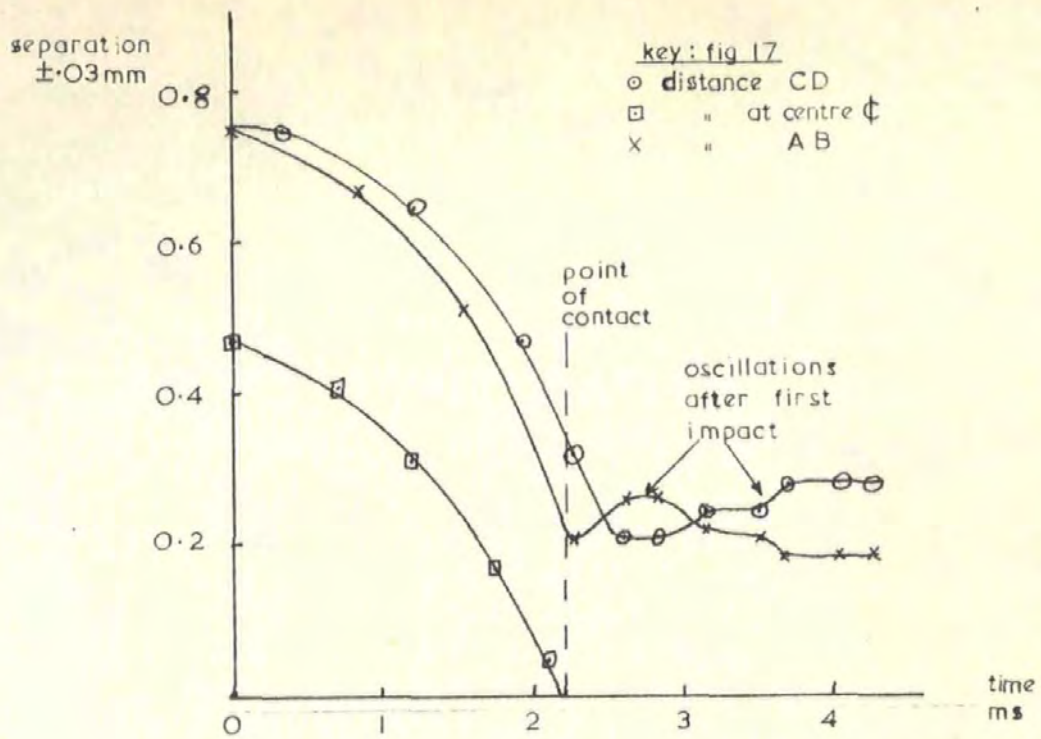
time
ms

Fig. (13a) Separation/time plot of switch contacts closing
Operating stroke 0.53 mm.

impact

1 ms
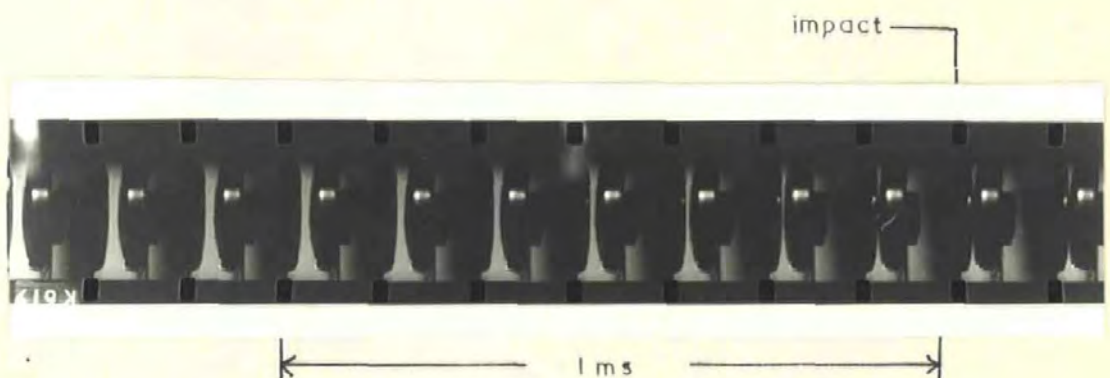
Fig. (13b) High speed film of contacts closing
Operating stroke of switch 0.53 mm.
Film speed 6670 frames/second

- 67 -

key: fig 17
⊘ distance CD
▣   "   at centre ₵
✕   "   AB
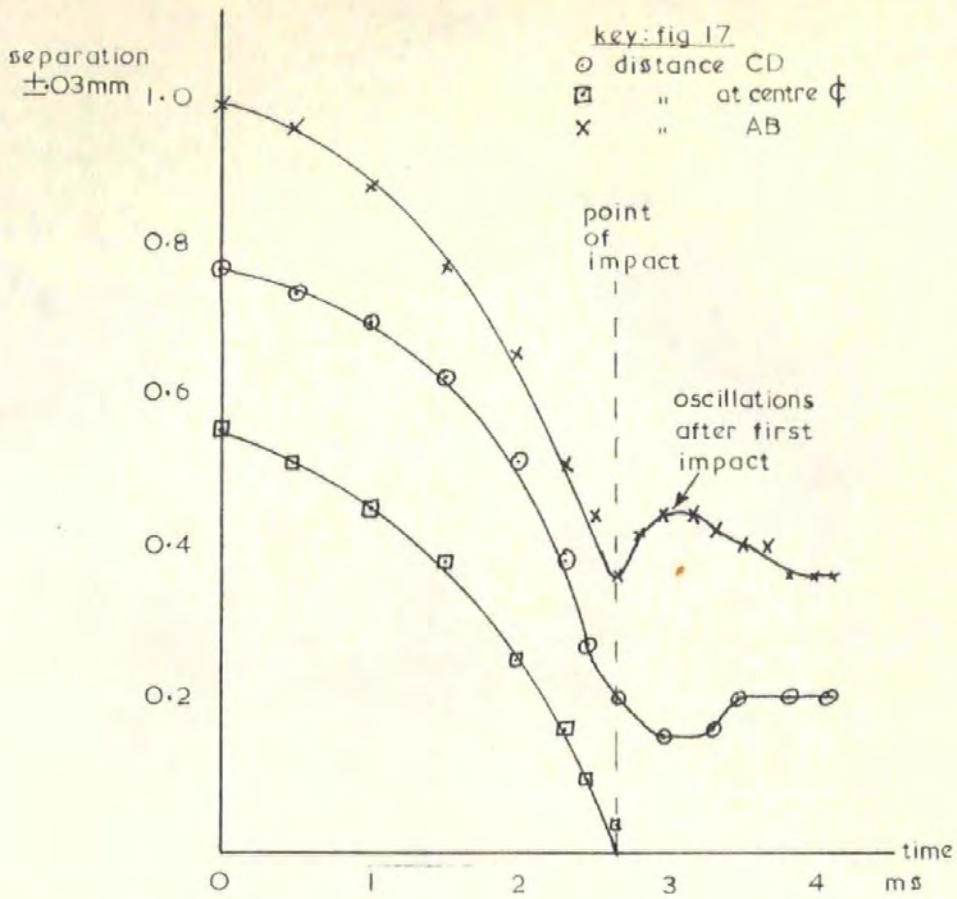
Fig. (14a)   Separation/time plot of contacts closing
Operating stroke 0.64 mm.
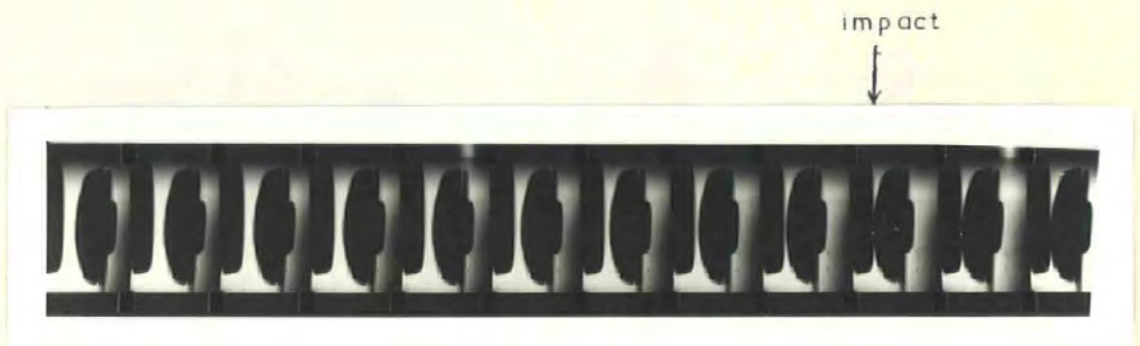
Fig. (14b)   High speed film of contacts closing
Operating stroke of switch 0.64mm.
Film speed 6670 frames/second

- 68 -
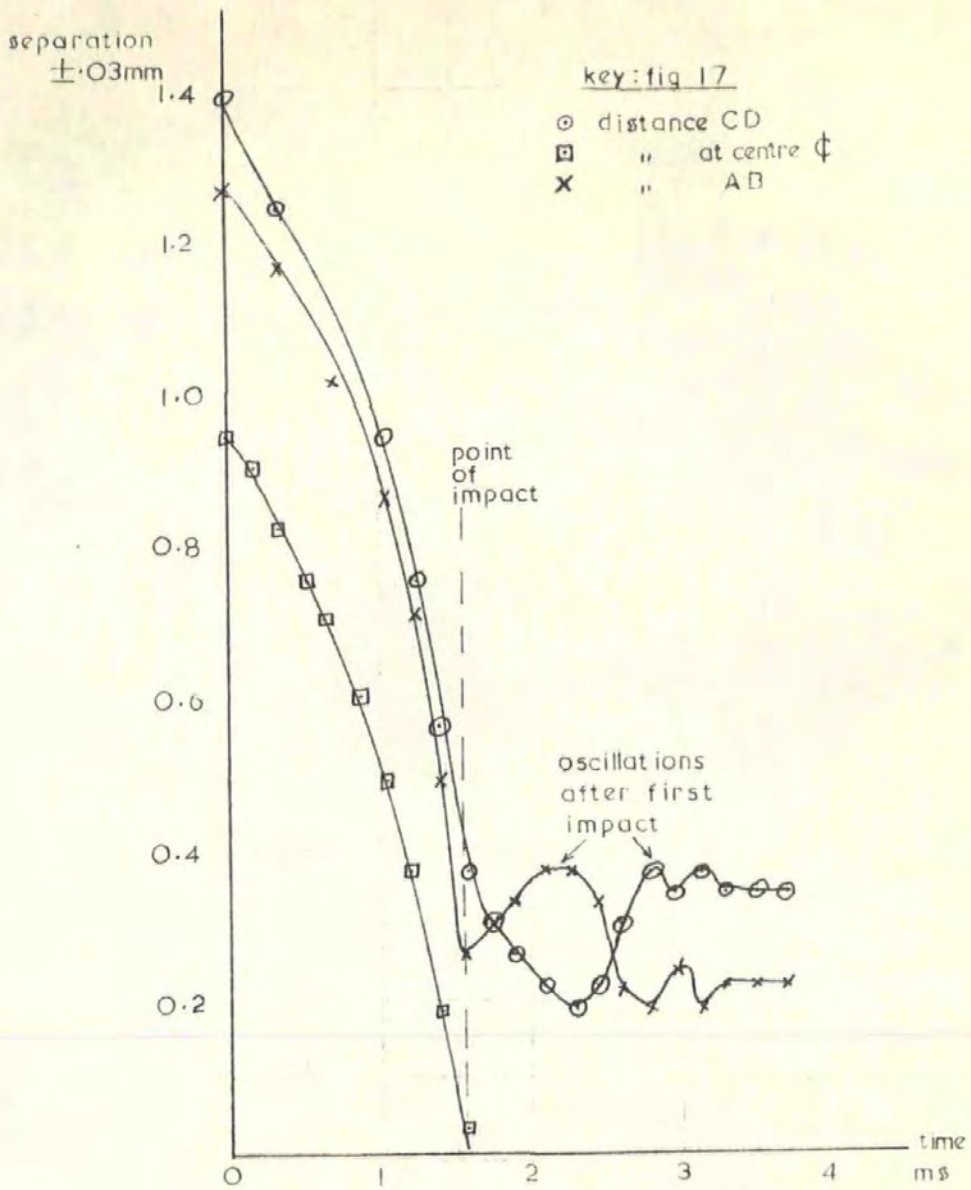
Fig. (15a)   Separation/time plot of contacts closing
Operating stroke 0.86 mm.

Fig. (15b)   High speed film of contacts closing
Operating stroke 0.86mm.
Film speed 6670 frames/second

- 69 -

The switch mechanism incorporates one adjustable component called the differential screw, (5) in Fig. (11). This allows variation of the static contact gap and also sets the operating stroke of the switch. This is the distance through which the actuator moves to open the contacts after they have just closed and for this switch is usually set in the range 0.5 mm to 0.75 mm.

4.3 Experimental Method

The opening and closing characteristics of the switch were observed using the high speed camera. To enable the operating stroke to be accurately set a micrometer barrel was used, with graduations accurate to .0001" (.0025 mm). This was also used as the actuator of the switch during all the experimental work, Fig. (12). By turning the micrometer slowly to toggle the switch, minimal velocity was imparted to the switch mechanism hence the opening or closing velocity was a result of forces due to the mechanism only. This is a reasonable representation of the working situation of the switch where the toggle point is approached slowly.

To enable the contact to be filmed a small portion of the switch moulding was cut away so that the contacts were visible from the profile position, Fig. (12). The information on the high speed film was presented graphically in the form of separation/time plots of the contacts opening and closing, making use of the time base superimposed on the film edge by the camera.

4.3.1 Results from High Speed Films of Make Operations

Typical separation/time graphs for make operations are shown in Figs. (13) to Figs. (15) together with clips from the corresponding high speed films for operating strokes of 0.53 mm, 0.64 mm and 0.86 mm respectively.
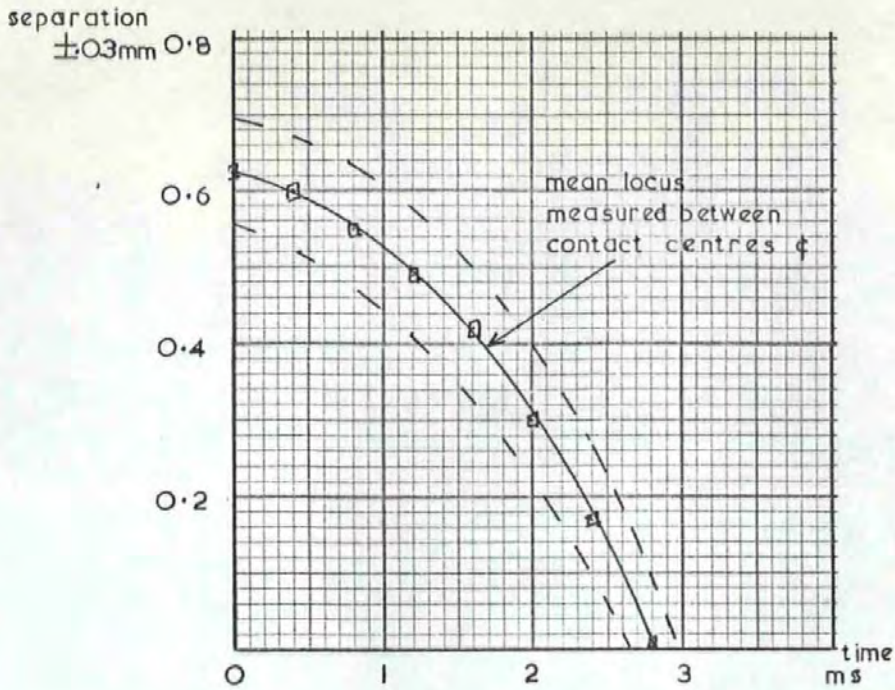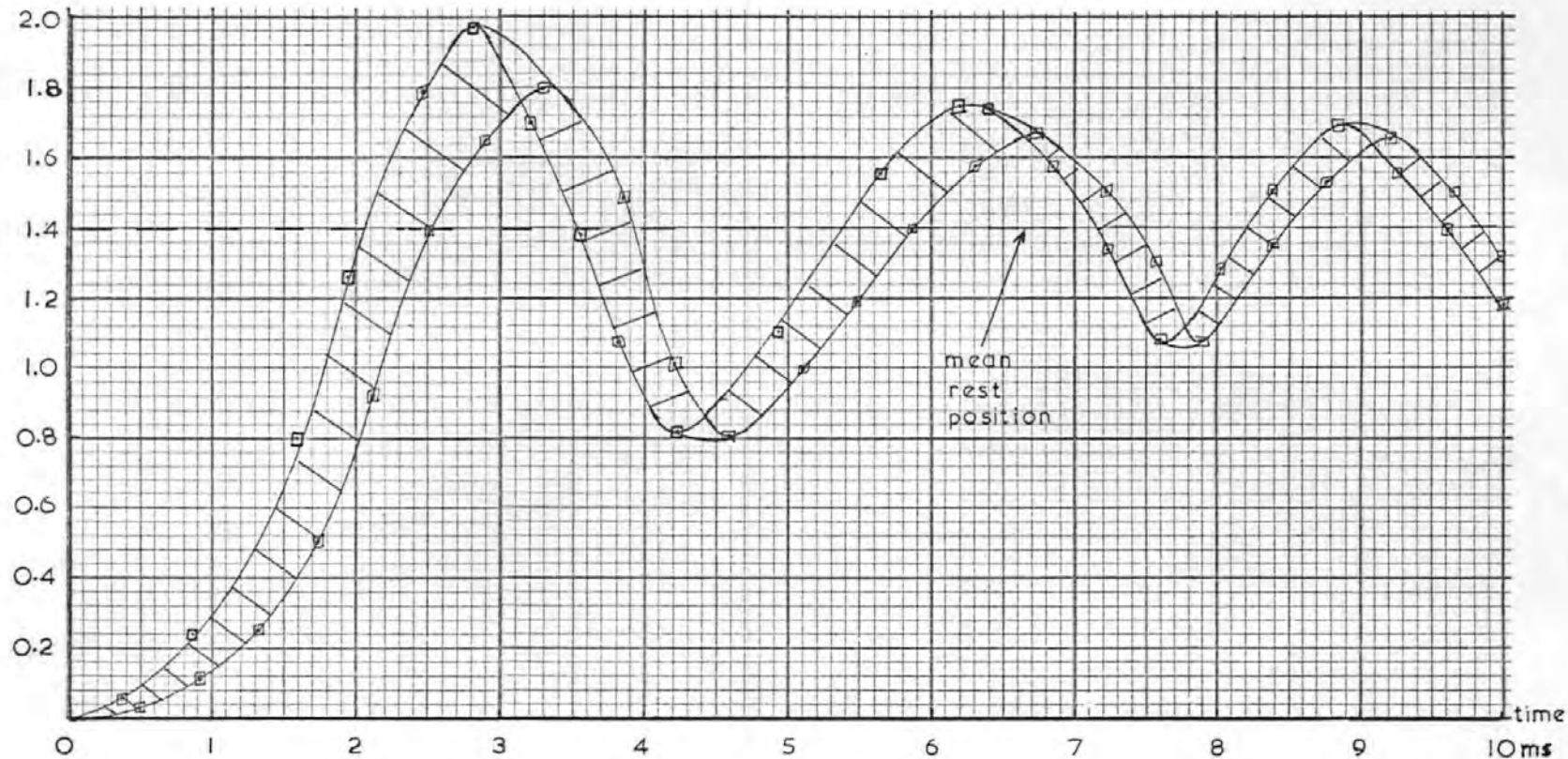
Fig. (16)   Separation/time plots from a sample of 20 switches
with operating strokes set to 0.64 mm. The dotted
lines indicate the spread in the results of the
above sample.
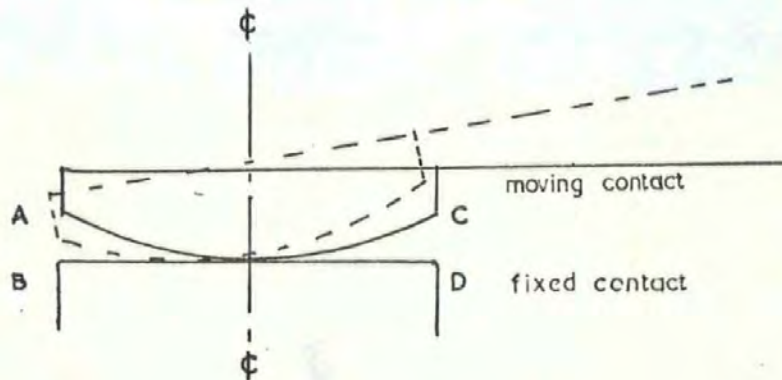
Fig. (17)   Key to separation/time graphs; showing
oscillations of the moving contact after
first impact.

- 71 -

Three measurements were made of contact separation from each film frame as detailed in Fig. (17), enabling a complete description of the contact motion to be obtained. The results are summarized in Table (1).

Operating Stroke mm	Contact Gap mm	Maximum Closing Velocity m/s
0.53	.45	.35
0.64	.70	.47
0.86	1.00	0.90

Table (1)

The graphs show that there was a continuous acceleration period of the moving contact, which finally impacted on the fixed contact after 2 to 3 ms. attaining its maximum velocity just prior to impact. The moving contact continued to roll or oscillate about its final rest position for up to 1 - 2 ms. after first impact. No separation of the contacts due to bounce was detectable from the high speed films other than this rolling motion.

The results above were all obtained using the same switch. To obtain an idea of the consistency of operation between different switches a sample of 20 was selected at random and filmed when performing a make operation for an operating stroke of .53 ± .03 mm. Fig. (16) shows the results in graphical form. For clarity, only the locus of the centre of the contact is shown for each case. The degree to which the closing characteristics are similar is clearly demonstrated, with a maximum departure from the 'mean' closing time (2.8 ms) of no more than 7%. The periods of oscillation after impact are all within ± 0.2 ms of 1.5 msecs.
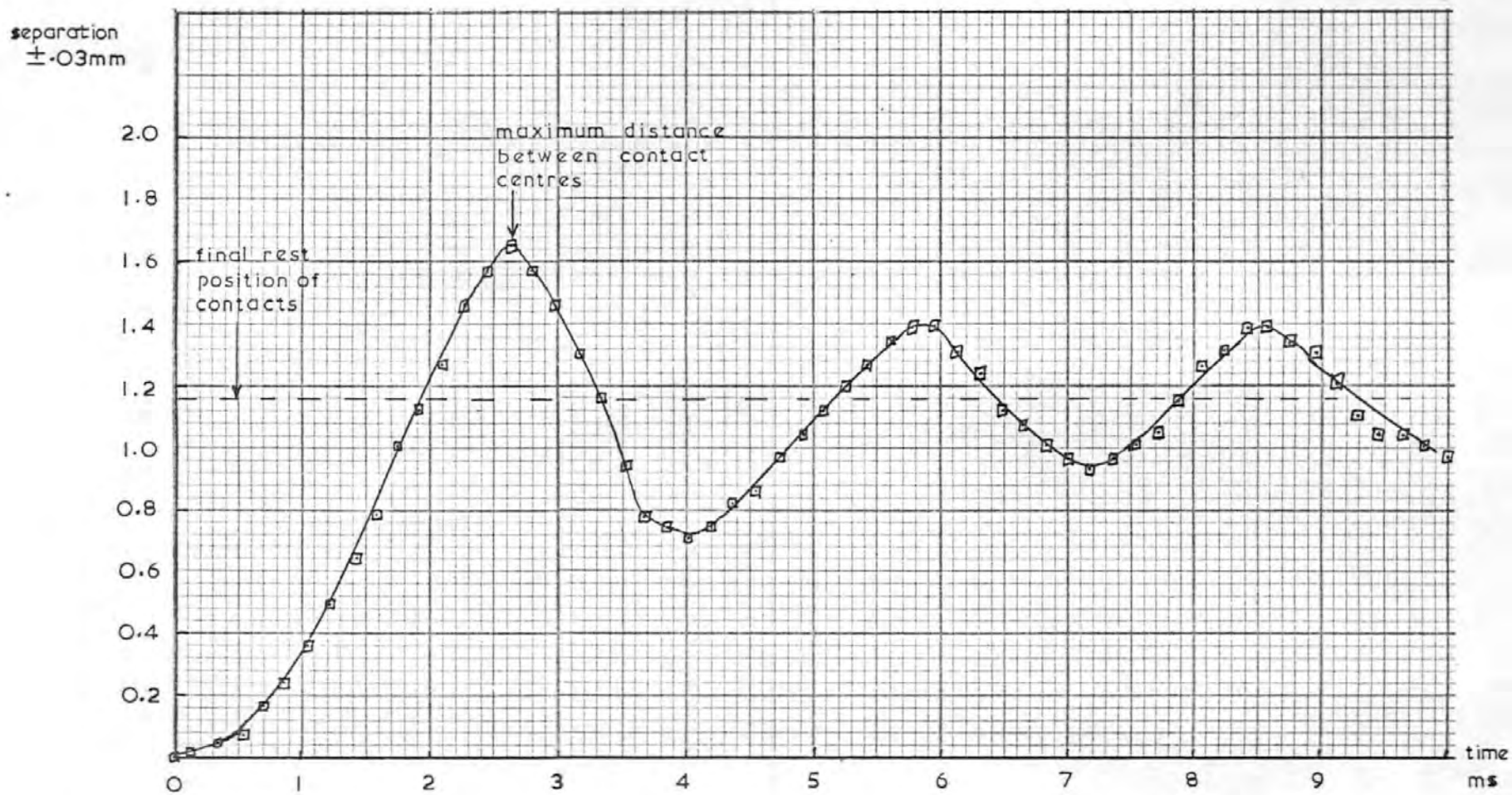
Fig. (18) Separation/time plot of contacts opening.
Operating stroke of switch 0.53 mm.
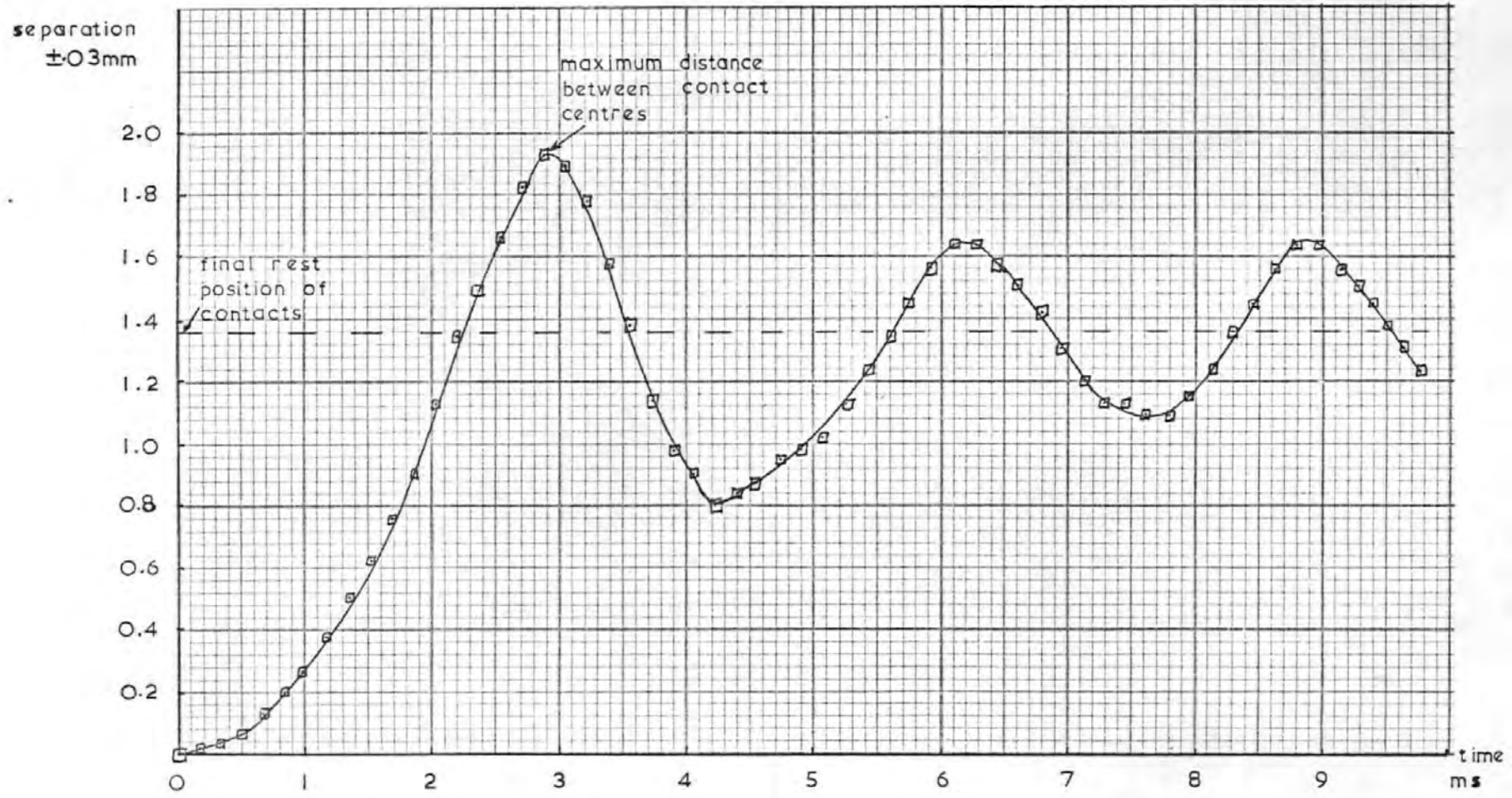
Fig. (19) Separation/time plot of contacts opening.
Operating stroke 0.64 mm.
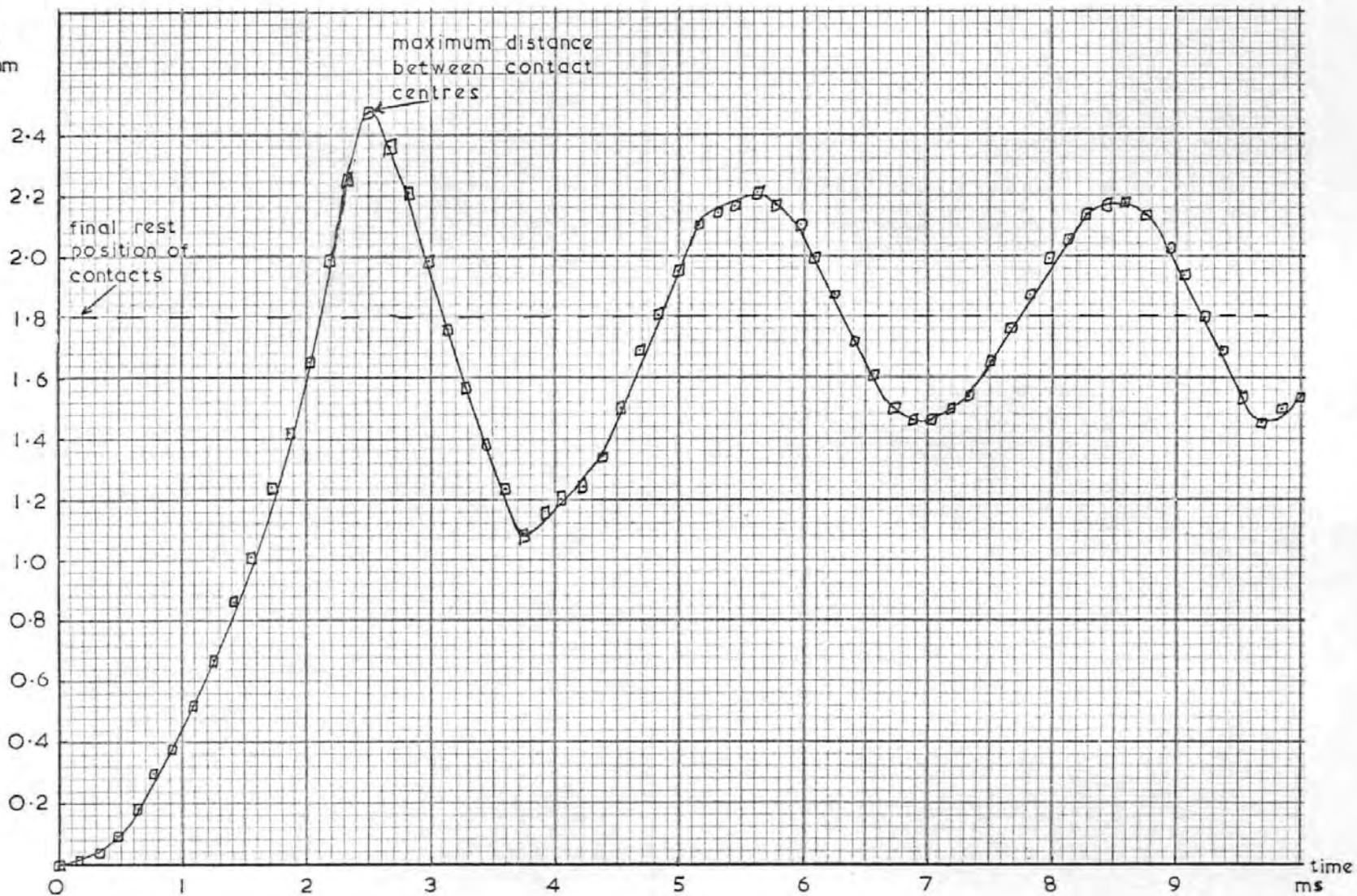
Fig. (20)   Separation/time plot of contacts opening.
            Operating stroke 0.86 mm.

4.3.2 Results from High Speed Films of Break Operation

Typical separation/time graphs for break operations are shown in Figs. (18) to (20) for switches with the same operating strokes as above. The results are summarized in Table (2).

Operating Stroke mm	Final Separation mm	Maximum Opening Velocity m/s
0.53	1.1	0.9
0.64	1.4	1.1
0.86	1.8	1.8

Table (2)

The graphs show that there was an initial acceleration period of the moving contact which reached the maximum separation point after 2 - 3 ms, and then continued to oscillate about the final rest position. Generally the results show the larger the operating stroke the larger the acceleration and the final distance between the contacts when they come to rest.

To compare the opening characteristics of different switches a sample of 20 switches was used again with the same operating stroke of 0.64 mm. Fig. (21) shows the spread of results obtained. The final rest position deviates by ± 7% from a mean value of 1.4 mm.

To observe the variation of the closing and opening characteristics of the switch while operating over the specified lifetime (nominally 200 000 operations), high speed film were taken every 25 000 operations. Fig. (22) shows the spread in the closing characteristics and Fig. (23) that obtained for the opening characteristics. The results from just five of the high

Fig. (21)   Separation/time plots from a sample of 20 switches with operating strokes set to 0.64 mm.
            The spread in the results is indicated by the shaded area.
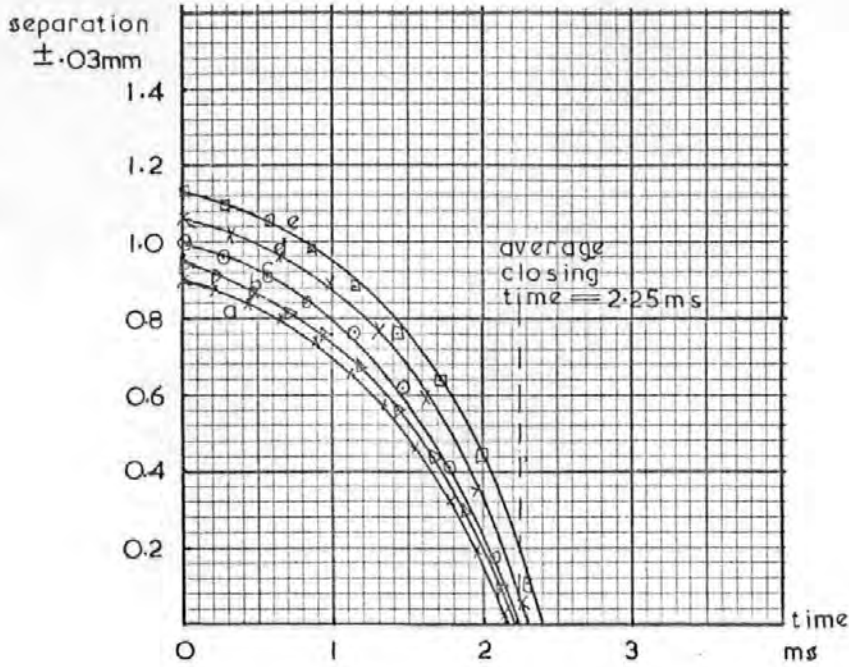
Fig. (22)   Selected separation/time plots of contacts closing for a switch
            performing a life test (200,000 operation). Data from 5 high
            speed films is shown.

            (a) New unused switch - contacts closing

            (b) Contacts closing after 50 000 operations

            (c)   "   "   "   100 000   "

            (d)   "   "   "   150 000   "

            (e)   "   "   "   200 000   "

      Note: The difference between the largest and shortest
            closing times measured from the film is 0.25ms.
            Since the point at which the contact starts moving
            is only determined to an accuracy of 1 film frame,
            the accuracy of the time scale is limited to ± 0.12ms
            at a film speed of 5000 frames/second (See section 3.1).
            The results shown here are the worst case ones, hence
            the differences between the closing loci are more
            marked.
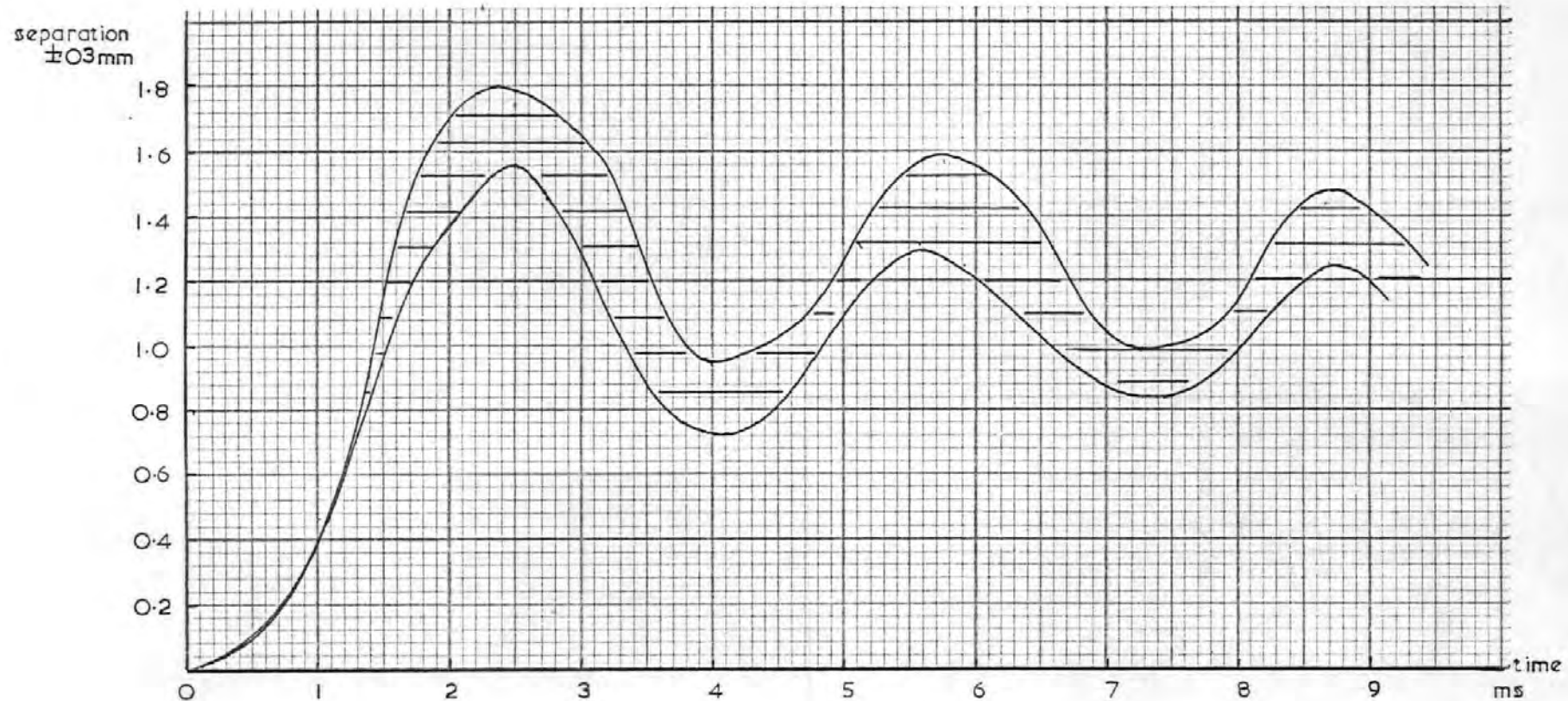
Fig. (23)   Selected separation/time plots of contacts opening for a switch performing a life test.
The shaded area contains all results obtained at intervals of 50,000 operations up to
200 000 operations.

speed films are plotted in Fig. (22) for clarity, the curves 'a' to 'e' represent the closing locus as obtained from the film at every 50 000 operations. The shaded area in Fig. (23) represents the band within which all the opening loci were found to be, when filmed at intervals of 25 000 operations. Both sets of graphs indicate that the variation in the opening and closing loci is not large, being about 12 - 15% after 200 000 operations. This 12 - 15% is likely to have two main sources:

(i) 'Ageing' of the spring mechanism resulting in different spring stiffnesses and hence different applied forces

(ii) Erosion of the contacts hence changing their effective separation

Figs. (22) and (23) are the worst case conditions, i.e. of the 4 switches tested in this way 3 switches were within a 8% variation over 200 000 operations. Mechanical inconsistencies in the switch mechanism over its prescribed lifetime are not sufficient in themselves to constitute a major problem. The effect of mechanical variation on the electrical performance of a switch, in particular, the contacts will be investigated later.

4.3.3 Static Contact Force

The experimental work detailed above revealed mechanism characteristics in terms of

(i)   opening velocity

(ii)   closing velocity

(iii) contact gap

It did not quantify the force holding the contacts together in the closed position, or reveal how this force varied as the toggle point was approached. To facilitate measurement of this force a small hole was drilled in the switch moulding directly under the moving contact. A
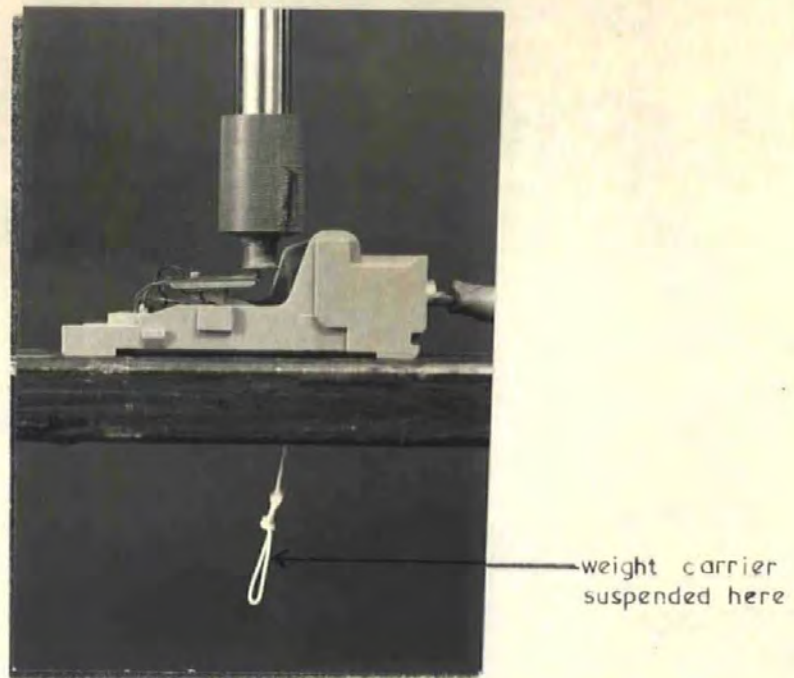
Fig. (24)   Method of measuring the static contact force.

Fig. (25)   Variation of contact force as the switch mechanism approaches the toggle point.

- 81 -
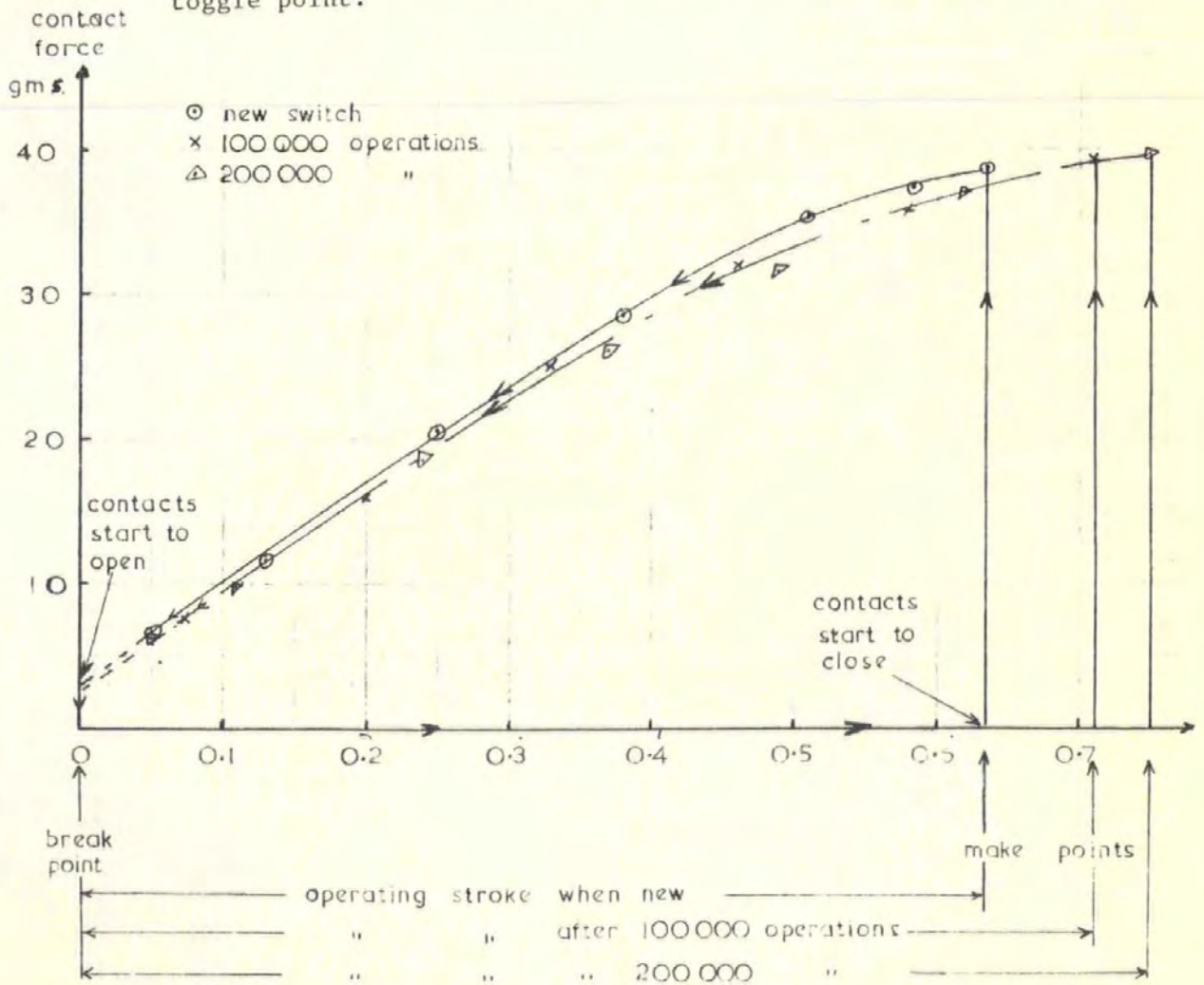
short length of nylon drive cord was bonded to the back of the contact, Fig. (24) and an avometer on the ohms range was connected across the switch. This effectively passed 0.25 mA across the contacts in the closed position. By hanging weights from the nylon cord the contact force would be relieved and the total force was equal to the total weight (including the cord and bonding adhesive) which would just cause the avometer to read a high resistance (>10kΩ). To obtain consistent results it was necessary to –

1. Clean the contacts with Isopropyl-alcohol

2. Add the weights to the contact at a very small
   incremental rate to avoid imparting momentum to the
   mechanism

This latter requirement was achieved by dropping water drops into a small container attached to the nylon cord. The dropper was an ordinary disposable syringe and the drop size would be varied by using needles with different bore sizes. A 25G needle was found to produce a drop of mass 25 mg, which gave the measurements sufficient accuracy.

Values of the contact force were obtained at regular intervals over the range of the operating stroke until the mechanism was within .05 mm of the toggle position. At this point it was found that the mechanism became too unstable for measurements to be made. The results are shown graphically in Fig. (25) as a plot of contact force (grammes) against distance of the actuator from the toggle point. Extrapolating the graph beyond the .05 mm point to zero (the break point) shows that the mechanism sustains a force on the contacts approaching 2 grammes until the toggle point is reached. This has also been confirmed in an internal report by Ranco (5).
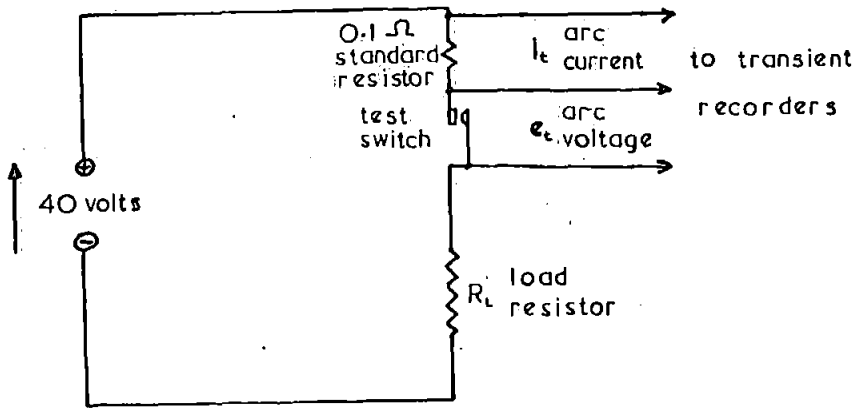
Fig. (26)   Test circuit for single make and break operation.
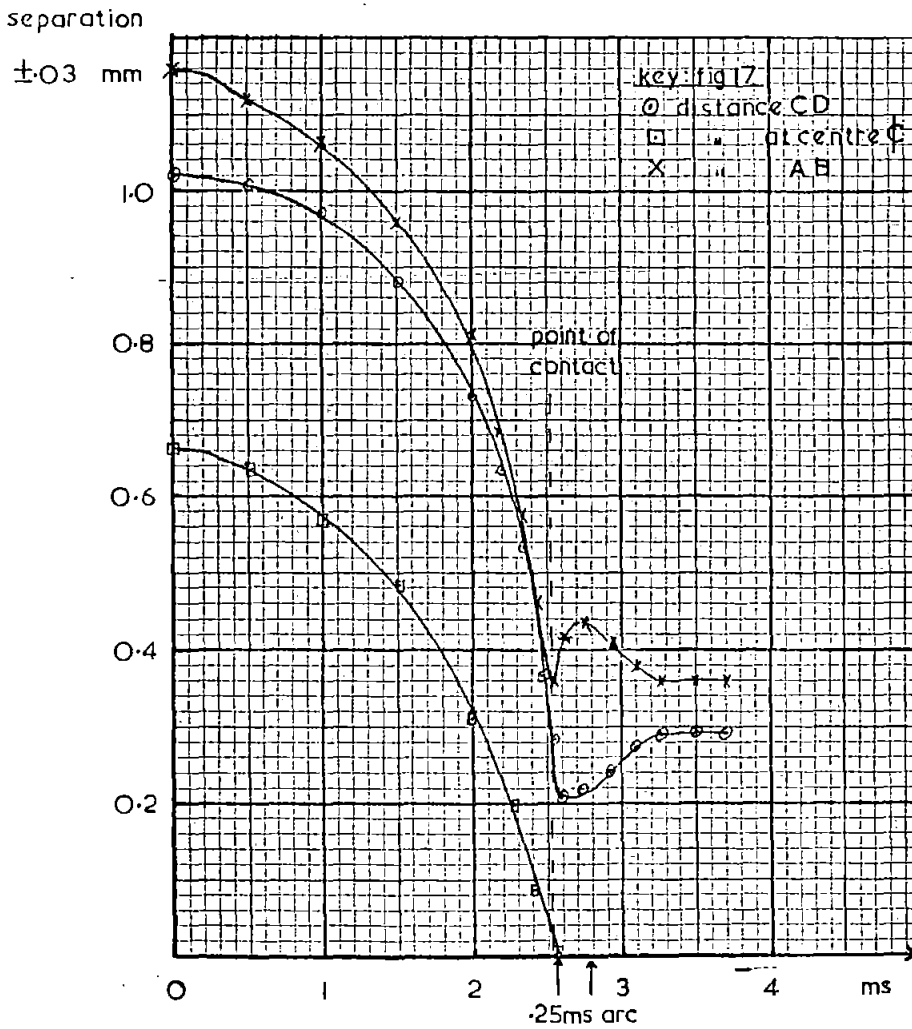
Fig. (27a) Separation/time plot for contacts closing on electrical circuit.

This measurement procedure was also applied at regular intervals to switches on life test to determine the variation in the applied force. Results for one switch are shown in Fig. (25), where there is a measurable decrease in the force of about 7% after 200 000 operations. There is also an increase in the operating stroke of the switch, 10% after 100 000 operations and a further 5% after 200 000 operations total. The reasons for this have already been suggested in section 4.3.2.

This preliminary examination of the mechanical characteristics of the switch shows that the repeatability of performance between switches lies within acceptable limits for a mass produced item. (± 7% ref. Hanka (4)). The switches have been observed to perform consistently over the required life (nominally 200 000 operations) and the variations that are present are not sufficient in themselves to make mechanical unreliability the probable cause for failure. Separation of the contacts due to bouncing was not seen on the high speed films. However, a rolling motion of the contacts after impact may be significant when electric current is flowing.

4.4 Single Operations using a d.c. supply and resistive load

4.4.1 Operating Conditions

A simple test circuit was constructed, Fig. (26) using a 40 volt stabilised d.c. supply and non-inductive resistors for the load. Circuit current was set to 8 amps and then high speed films were made of switches opening and closing this load. Simultaneous recordings were made of voltage across the contacts and current flowing in the circuit by measuring the voltage change across a 0.1Ω shunt. The information was stored by the transient recorders and plotted out onto an X-Y recorder and displayed on an oscilloscope.
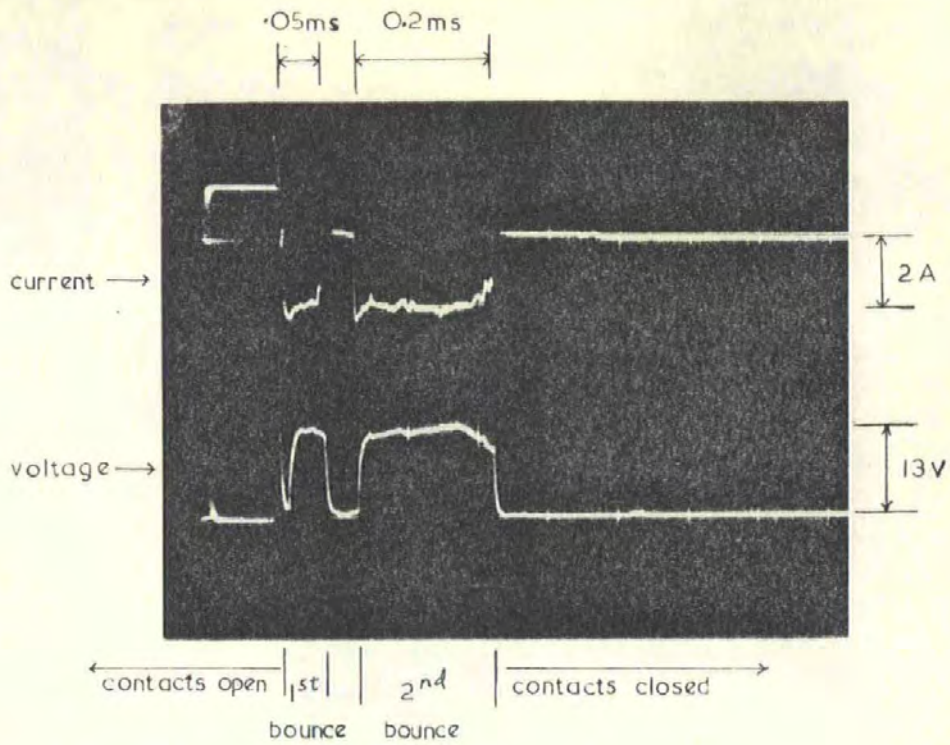
Fig. (27c)   Voltage and current transients corresponding to the arcing
             recorded on the high speed film.
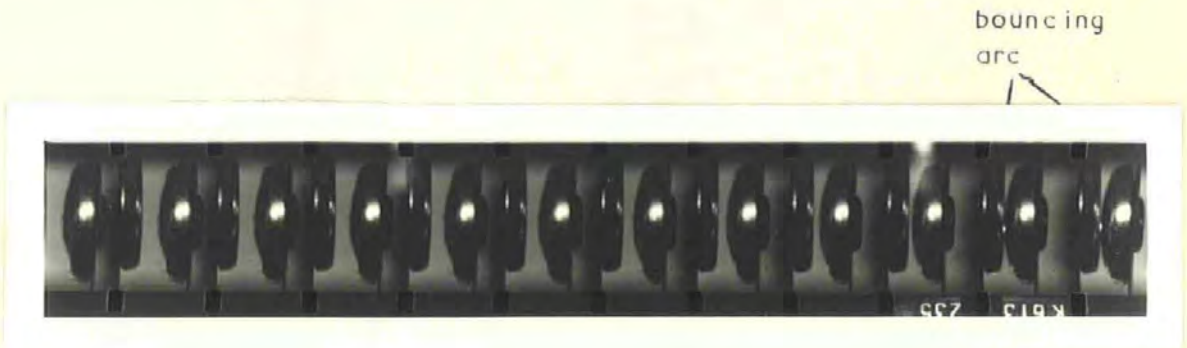
Fig. (27b)   High speed film used to produce the graph of Fig. (27a)
             Film speed is 5400 frames/second
             Arc duration is 0.25 ms.
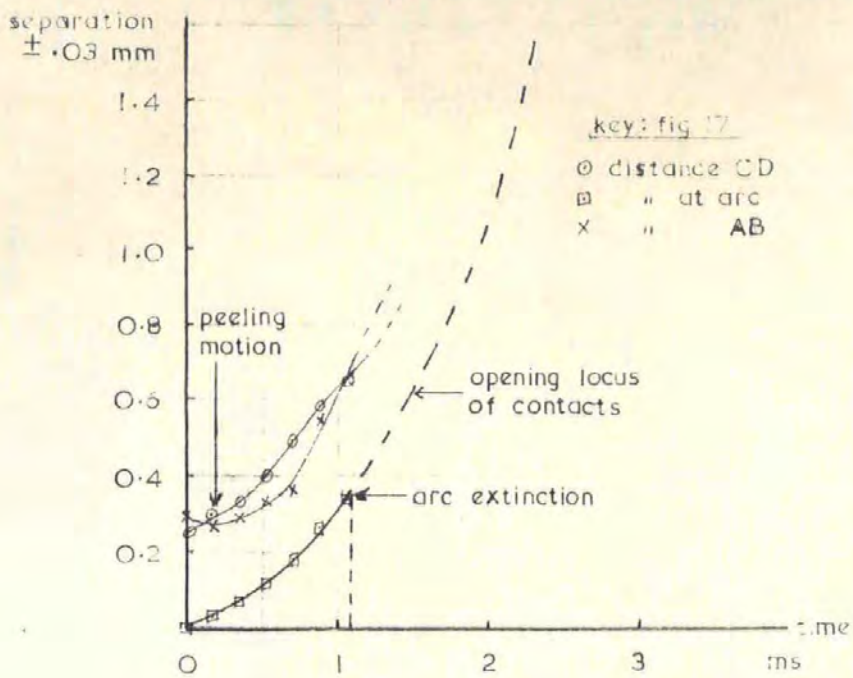
Fig. (28a)   Graph of arc length/time for switch contacts breaking
             d.c. with a resistive load (40 volts 8 amps)
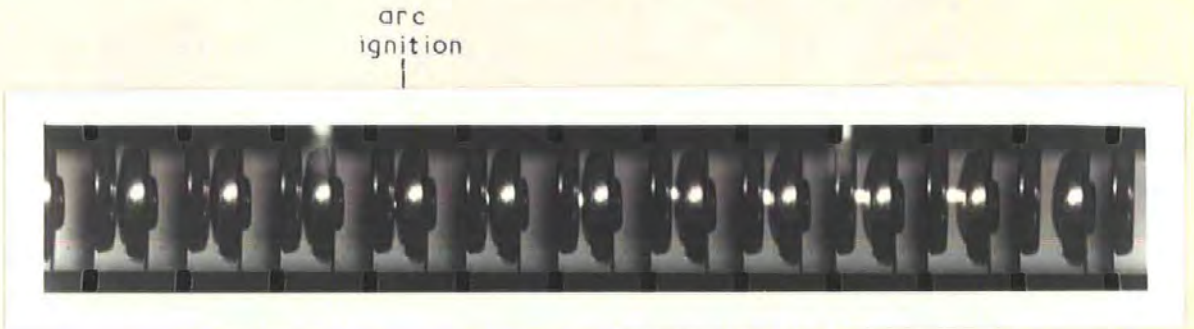
Fig. (28b)   High speed film from which the data for Fig. (28a) was
             obtained. Film speed was 5650 frames/second.
             Arc duration 1.1 ms, arc length at extinction 0.35 mm.
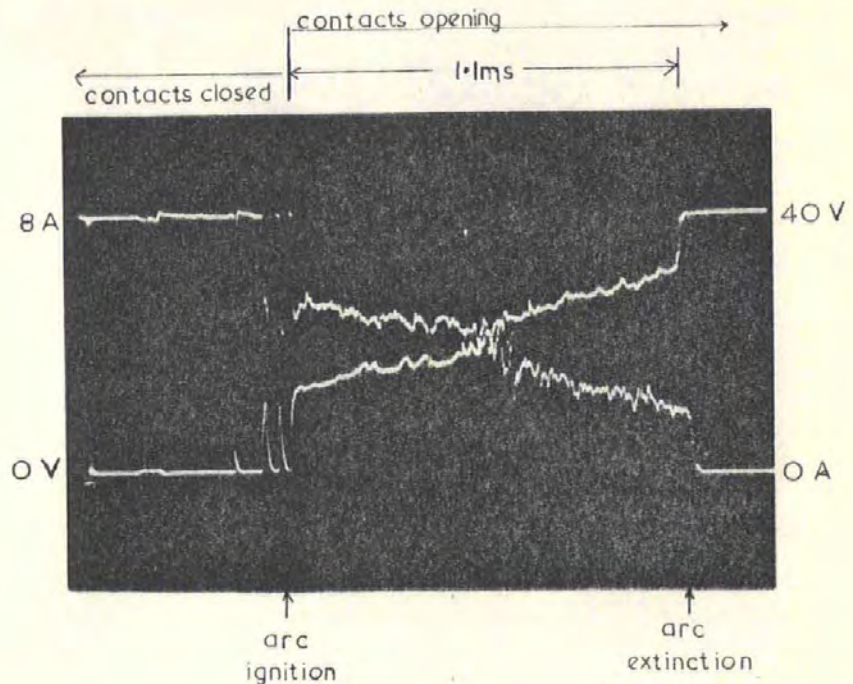
Fig. (28c)   Voltage and current transients corresponding to the above
             film record.

- 86 -

4.4.2   The Make and Break Arcs

The high speed film of Fig. 27b shows a small arc of 2 frames duration, which corresponds to a time of 0.1 ms to 0.35 ms depending on the relative position of the film shutter when the arc ignited.   The exact arcing time is shown on the oscilloscope record (Fig. 27c), viz 0.25 ms. The presence of an arc after impact indicates that the contacts are bouncing apart although the amplitude of the separation is outside the resolving capability of the film and lens system (.03 mm).   Alternatively it is possible that the voltage and current interruptions are due to asperity vapourisation as the contact rolls after impact and the site of current conduction is changed.

The high speed film in Fig. 28b shows the growth of the arc as the contacts separate.   The arc duration, measured from the oscilloscope trace is 1.1 ms and this corresponds to an arc length measured from the film of 0.35 mm.   By measuring the contact separation not only at the centre, (i.e. the arcing point), but also at the contact edges, (as in the case of the make operation), it is seen that initial separation of the contacts occurs as a rolling or peeling action.   This was found to be the case on all the high speed films made of this switch performing a break operation.   It is suggested that this may account for the initial multiple interruptions that occur immediately prior to complete separation and arc ignition.   As the moving contact rolls over the fixed contact, the actual point of current conduction is changed.   Molten bridges and short duration arcs may occur as the contact point is moved giving rise to the short transient rises in voltage just before the contacts separate.   This is clearly visible on Fig. 28c.   It was also noticed after many tests had been performed on many switches that these multiple short duration voltage transients occurred more readily on a switch with new contacts.   After the switch had performed about 10 operations the switch generally accomplished the ignition of the break arc with fewer

MAGN: 185x

Fig. 29a.　　Scanning Electron Microscope (S.E.M.) photograph
of the anode surface after 1 make operation.
Erosion is parallel to the axis of roll.

MAGN: 185x

Fig. 29b.　　S.E.M. photograph of the cathode surface after 1
make operation.　　Erosion is the mirror image of
that on the anode.

- 88 -

or none of these multiple interruptions. This suggests that surface films, destroyed by arcing, may account for some of the multiple interruption characteristic as the contact rolls before separation.

For both make and break arcs the short arc process dominates for the first few microseconds of arc life, see Hopkins et al (5). The relative abilities of the different types of arc to produce erosion has been reviewed in section 2.4. For the operating conditions being considered here the short arc dominates for a larger proportion of time in the make arc compared to the break arc. Any material evaporated by the arc will be redeposited on the electrodes since the arc length, (i.e. the contact gap), is small (< 0.03mm) compared to the contact diameter (4 mm).

4.4.3 Erosion due to the Make and Break Arc

S.E.M. Photographs of the anode and cathode surfaces after one make operation are shown in Figs. (29). The distribution of erosion on the contact surface lies parallel to the axis of roll and the cathode surface is the mirror image of the anode surface. Both electrodes have the appearance of localised melting of contact material, with the anode having a predominance of small overlapping crater formations. The cathode is characterised by smaller pits and protuberances with some finely divided condensed vapour sprayed around the eroded area.

Photographs of the arc electrode surfaces after one break operation are shown in Figs. 30. The anode surface is characterised by one larger crater (diameter $\approx$ 0.2 mm) surrounded by overlapping smaller craters. The cathode comprises many small pits and protuberances spread over an area which appears to have been sprayed by finely divided metal vapour. There is also evidence of some larger deposits of resolidified molten metal which has been thrown up from the anode crater.

MAGN : 130x

MAGN : 315x

Fig. 30a.   S.E.M. photograph of the anode surface after 1 break
             operation.   The large central crater is surrounded
             by smaller overlapping craters in a 'roof tile' effect.

MAGN: 130x

MAGN: 700x

Fig. 30b.   S.E.M. photograph of the cathode surface after 1 break
             operation.   Small pits are present in the surface due
             to positive ion bombardment, with some resolidified molten
             metal possibly thrown up from the anode crater.

A single make operation appeared to inflict less damage on the contact surface than a single break operation, predictably since the duration of the break arc in this case exceeded that of the arc due to 'bounce'. The cumulative effect of multiple make operation was investigated first, since this represented a simpler set of operating conditions about which the following assumptions could be made,

1. There is negligible loss of energy or contact material to the surroundings due to the short times involved and also due to the very small contact gap compared to the contact diameter.

2. Arc voltage and current are constant for the duration of the arc.

3. The energy dissipated by the make arc between the contact is proportional to the total charge passed in the arc (since the arc voltage is a constant for a given contact material).

    i.e.   Energy $= e_t . i_t . t$ joules

    $= e_e q$

    $\propto q$

This is not the case for the break arc where the arc voltage increases with length. Also it would appear that it is not sufficient to assess the erosion just in terms of arc charge. Erk & Finke (6) found that materials with lower arcing voltages produced weaker welds. The implication of this is that the amount of metal melted and vapourised by the arc is in some way proportional to the arc energy.

4.5   Multiple Make Operation

A test circuit was constructed using a 50 Hz full wave rectified mains supply i.e. 340v peak and a resistive load of 10 amps peak.

0.34 ms
multiple interruptions
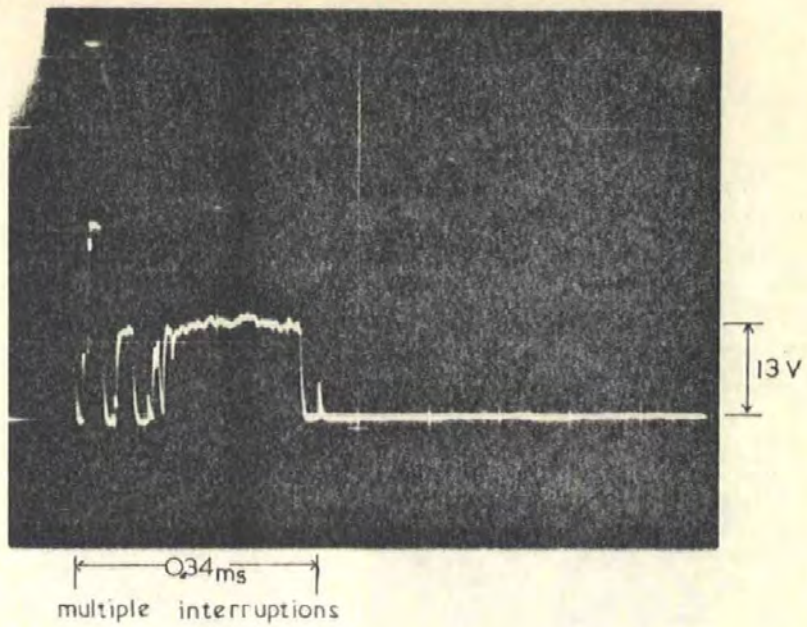
Fig. 31a. Voltage transient occuring across previously unused contacts of a switch closing on electric circuit. Operating Conditions: 340 volts peak, 10 amp peak, full wave rectified, 50 Hz.

0.19ms
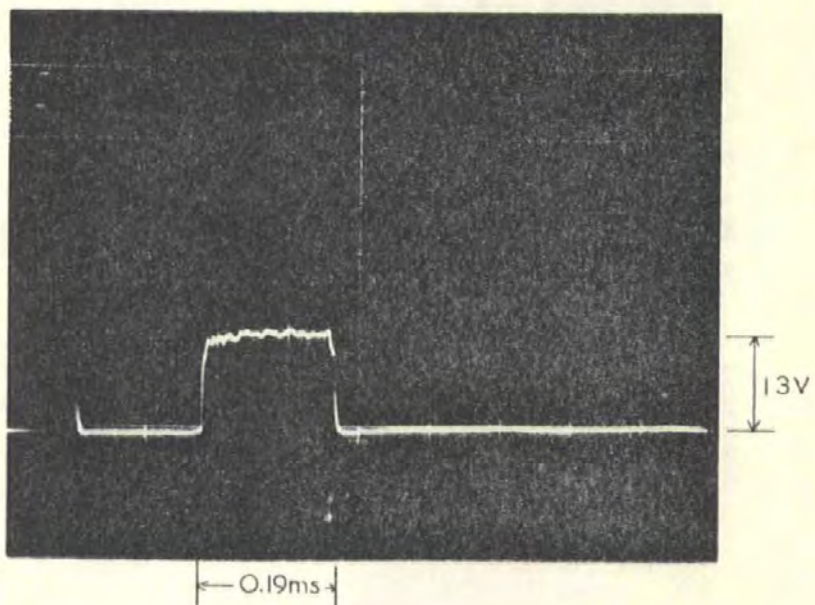
Fig. 31b. Regular voltage transient occuring after the switch has performed 10 operations.

This would simulate the periodic zeros of a.c. but allow the effect of polarity of the contacts to be observed. Using the apparatus described in section 3.5 for life testing, a batch of switches was cycled over 500, 1000, 1500 and 2000 operations respectively, performing 'make only' operations. The break operation was performed by a switch in series with the test switch. Although this sort of repetitive duty would not normally occur, each repeat make operation is representative of the usual operating conditions, and the cumulative effect of multiple operation enabled the rate and direction of material transfer to be assessed.

The electrical interruptions corresponding to each make operation were recorded regularly at 50 operation intervals. This was so that an average value for the energy/operation could be deduced at the end of the test run. It was observed that a regular shape to the electrical transient (Fig. 31b) established itself after 10 to 15 operations with little deviation from it as the test continued. The discrepancies occuring in the first few operations Fig. 31a were attributed to surface films which were gradually destroyed in the vicinity of the contact area, by the arc. After the initial impact force it would seem that the rolling action of the contact did not always break the surface film, or it was thick enough to resist conduction by fritting or tunnel effect allowing the voltage to rise for short intervals ($< 20\mu s$) to the open circuit value.

The energy dissipated at any one make operation varied according to the point on the a.c. cycle at which the contacts first impact. For a number of operations of 500 or more, it was assumed that the average value of the current $\hat{I} \sin wt$ could be used without introducing significant error into the value of the arc energy calculated by

$$\text{Energy} = E_m \frac{2}{\pi} . \hat{I} \sin wt . \tau \quad \text{joules}$$
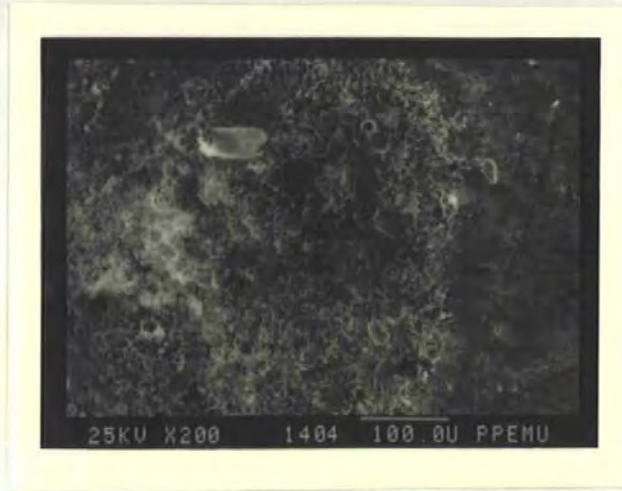
Fig. 32a.   Anode Surface after 500 operation closing a load of
            10 amps peak, resistive.   Supply voltage was 340 volts
            peak, 50 Hz, full wave rectified.
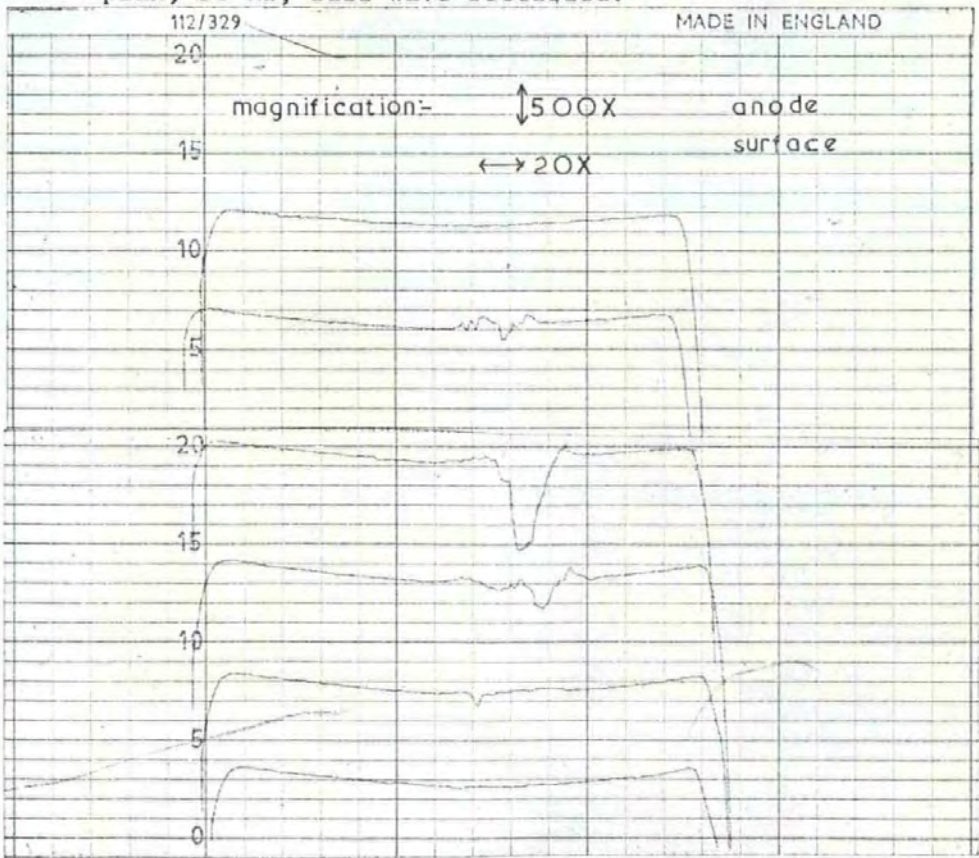
Fig. 32b.   Talysurf contour plot of the surface shown above.
            The profile traces are recorded at 0.2 mm intervals
            across the surface.
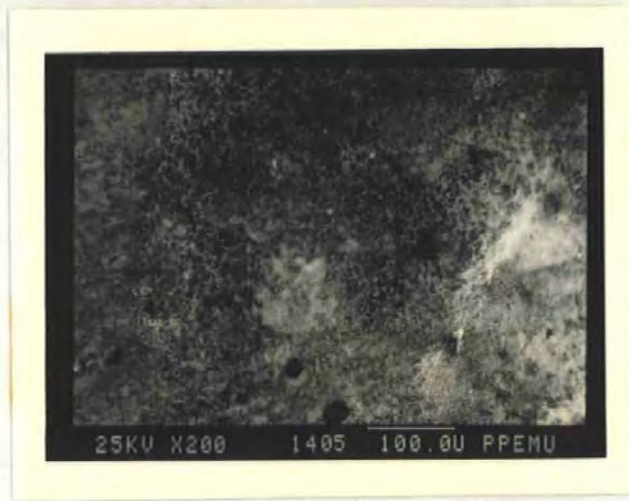
Fig. 33a.   Cathode surface after 500 operations closing a resistive
             load.   Operating conditions as Fig. 32a.
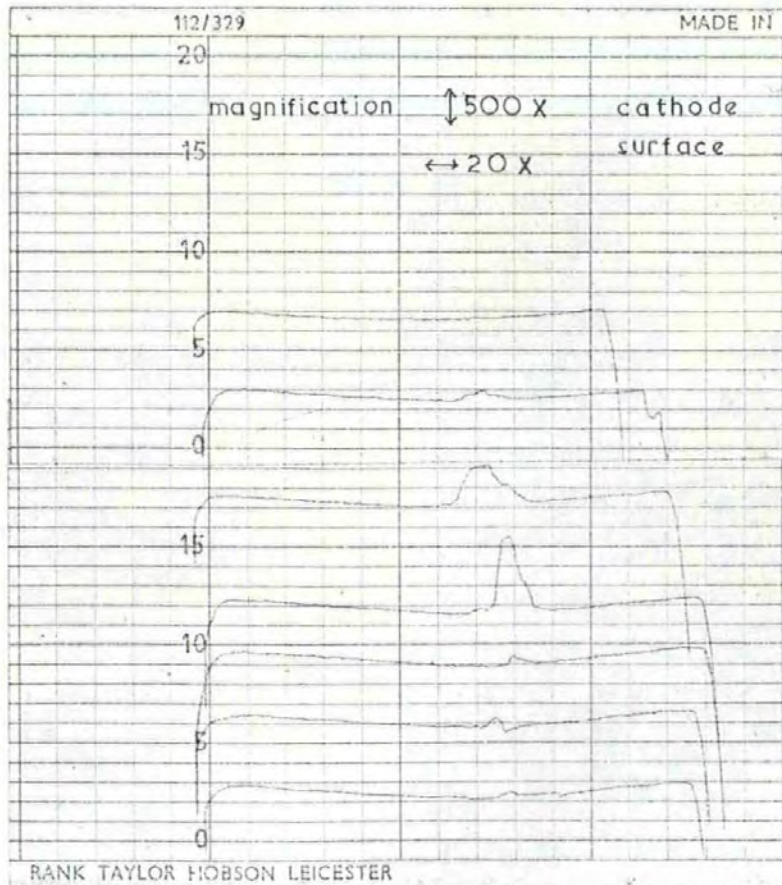
Fig. 33 b.   Talysurf countour plot of the surface shown above.
              The profile traces are recorded at 0.2 mm intervals
              across the surface.

where T is the total arc duration for one operation.

In section 4.4.3 it was assumed that the current was constant during a given make operation. For a.c. this can still be assumed since for bounce time of 0.1 ms, $\hat{I} \sin(\omega t)$ changes by less than 10% on the steepest part of the sine wave. Two thousand operations was specifically chosen as the upper circuit for this series of tests. To perform any more make only operations than this may have distorted the true picture of events since normally make operations alternate with break operations.

Photographs and Talysurf profiles of the contact surfaces after 500 operations are shown in Figs. 32 and 33. The anode is characterised by a large dominant crater with some material deposited around the crater rim. The cathode has a pronounced pip formation of similar volume to the anode crater. The respective volumes are plotted against total energy, i.e. average energy/operation x number of operations, in Fig. 34. The graph demonstrates that the volume of the anode crater is equal to the sum of the material deposited around the crater rim and the volume of the cathode pip. The erosion mechanism is one of material transfer from anode to cathode. As already defined in section 4.4.2, the short arc process is clearly the one which dominates for most of the arc duration, and is responsible for most of the transfer of material. Rupture of the molten metal bridge will also contribute to the erosion process, however as already demonstrated by Slade (7), for arcs of this duration the effect of the molten metal bridge is negligible.

To summarize, the amount of transfer varies in proportion to the energy dissipated by the arc between bouncing contacts Fig. 34, i.e. a decrease in bounce time will result in a decrease in erosion. The inter-relation

- 96 -
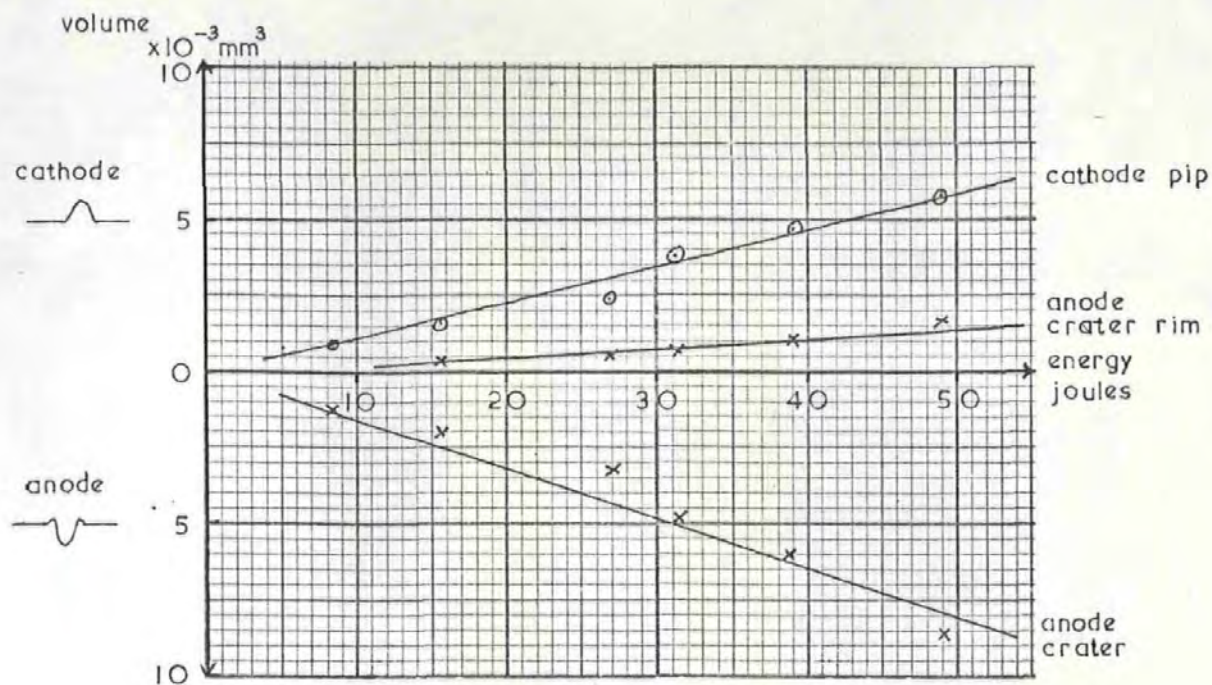
Fig. 34.   Graphs of volume of material transferred from the anode to
the cathode against total energy dissipated in the arc
as the contacts bounce after impact.
Operating Conditions: 340 volts peak, full wave rectified
50 Hz a.c.   Resistive load of 10 amps peak.

between make and break operations has been ignored for the purposes
of investigating the effect of bounce, however section 4.4.3 shows that
the break arc has the potential to inflict more damage due to its longer
duration.

4.6   The Break Arc

4.6.1.   Voltage - Current Characteristics

It has already been shown that there exists a relationship between
erosion of the contacts and energy dissipated in the arc.   The arc
energy depends on the arc voltage, arc current and duration, hence the
arc length and opening velocity are also significant.   The relation
between arc voltage, current and length has been published by several
workers.   Holm (9) appears to have obtained his constant arc length
curves by recording the arc voltage and current at different time
instants and then assuming a constant opening velocity obtained the
corresponding arc length from the relationship $l = vt$.   Sato (9)
obtained his data by varying the values of the supply voltage and
current to produce different arc durations, and again obtained the
corresponding arc length by assuming a constant opening velocity charac-
teristic.   Since the toggle switch under investigation here does not
have a linear opening characteristic, no such assumption can be made
about the opening velocity.   The high speed films however, allow the
arc length at any given time instant to be known, so by making simul-
taneous records of the arc voltage and current on the transient recorders
a complete set of results can be obtained.   This is equivalent to Holms'
method.

To collect the data in the form that Sato obtained it i.e. maximum arc
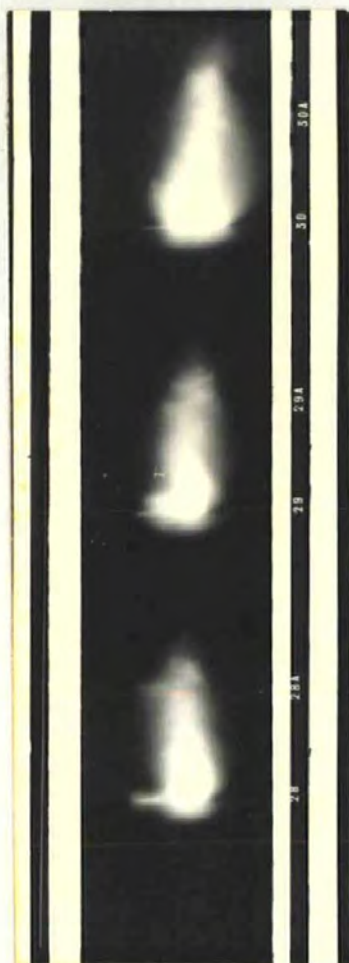
Fig. 35. Arc length measurements using a 35 mm camera
and triggering the arc in front of an open
shutter.
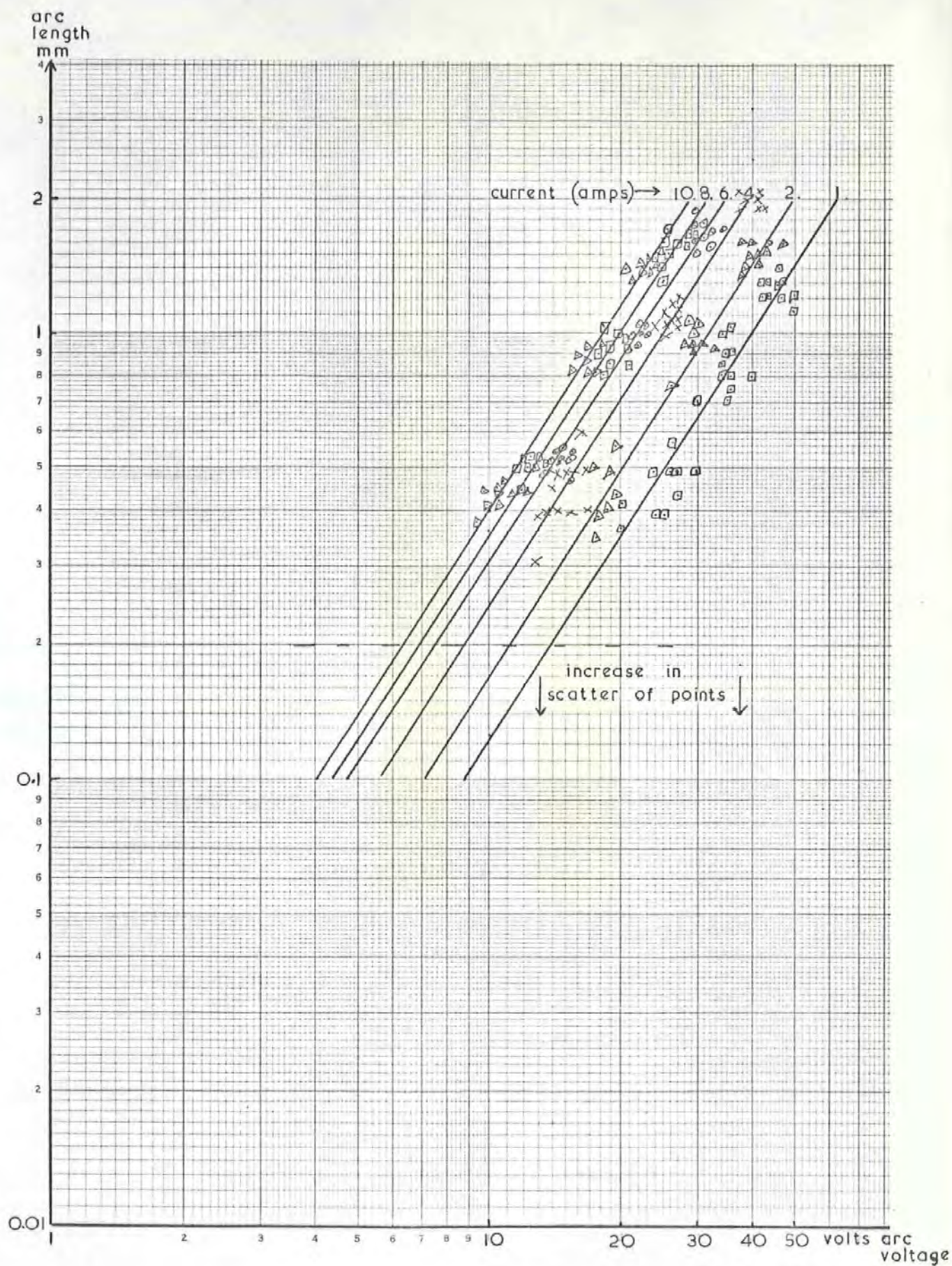
Fig. 36. Graph of arc length against arc voltage $(e_t - E_m)$ plotted with current as a paramter. Data was obtained using high speed films and the static 35 mm film technique.

length achieved for a given supply voltage and current, a method was devised whereby the arc occuring between the opening contacts was recorded directly onto 35 mm film. To do this the switch was surrounded by a light - tight enclosure with two close fitting openings to accommodate the camera lens and the switch actuator. With the camera shutter open the switch was made to open the circuit and thus an image of the arc was recorded on the film. By up-rating the film during the developing process the intensity difference at the extremities of the arc was reduced to a minimum. Typical arcs are shown in Fig. 35, up to 12 recordings were made at each supply voltage and current setting, and the mean calculated. For a mean length of 1.6 mm, the standard deviation was .075 mm over 12 measurements.

Two complete sets of experimental data were obtained. One, using Holms' 'dynamic' method where the rate of growth of the arc is assumed to be sufficiently slow to simulate stationary conditions, the other using Sato's approach and recording the maximum arc length achieved prior to extinction. Plotting both sets of results on log-graph paper with current as a parameter gives a family of straight lines Fig. 36, as previously shown by Sato (9). The two sets of experimental data are indistinguishable when plotted in this form. The reason for this is demonstrated below.

Four arc voltage/current transients are shown in Fig. 37. Transient (a) was obtained by actuating a switch to break a d.c. resistive load of 40 volts, 10 amps, and a high speed film record was also made of this switching operation. Three points with co-ordinates e_t, i_t are shown on transient (a) as being typical of the experimental data as obtained by Holm. The co-ordinates are detailed in table 3.
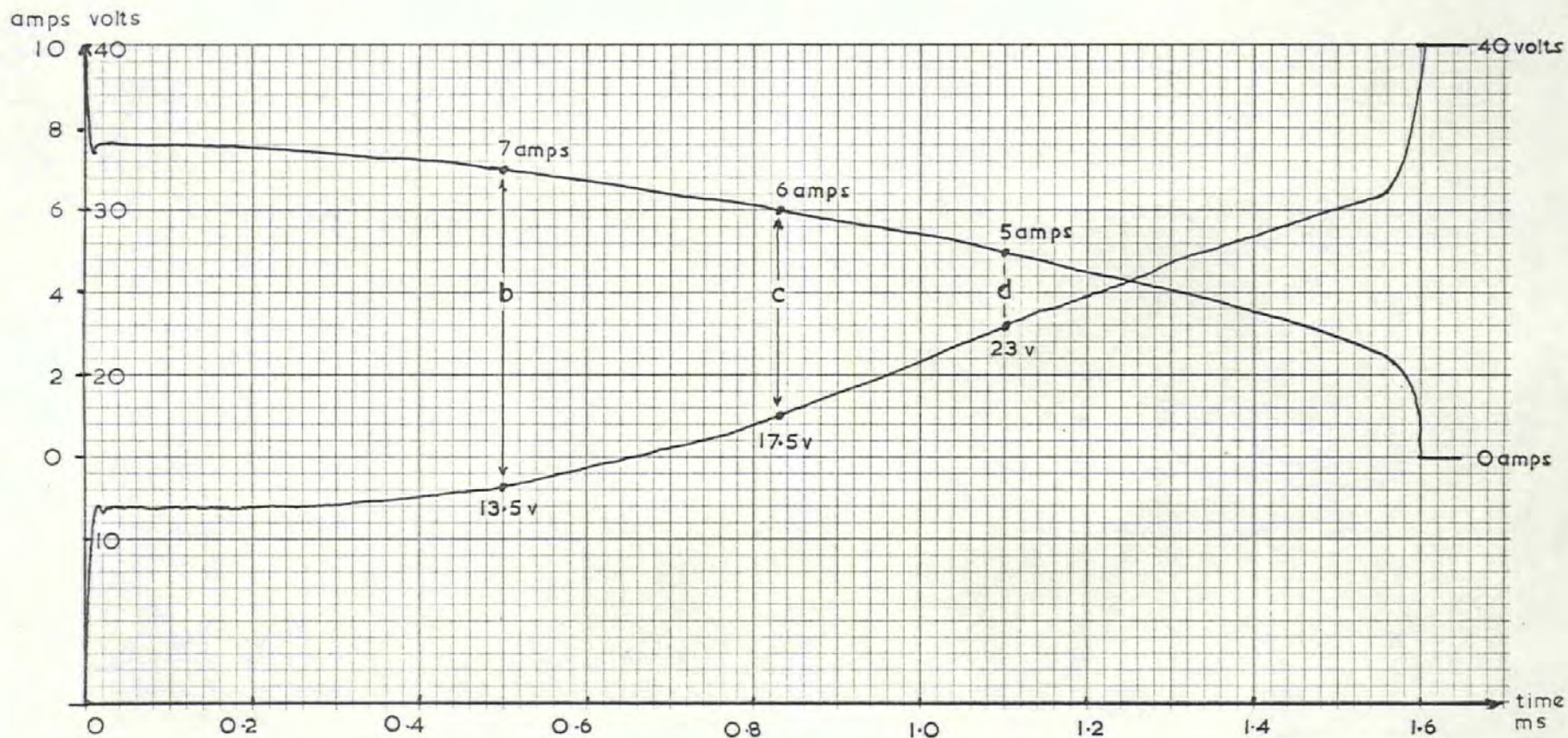
Fig. 37a.   Arc voltage/current transient recorded on the graph plotter when the switch contacts break a resistive load of 10 amps, with a supply voltage of 40 volts d.c.
Arc duration = 1.6 ms.   Three co-ordinate points for e_t and i_t are marked (13.5 v, 7A), (17.5v, 6A) (23 v, 5A).

Coordinate Point	Arc Voltage e_t volts	Arc Current i_t amps	Time ms t	Arc Length mm	$e_t - E_m$ volts
b	13.5	7	0.5	0.03	1.5
c	17.5	6	0.33	0.13	5.5
d	23.0	5	1.1	0.3	11.0

Table 3

These three sets of data could also be produced by three different circuits if $e_t - E_m$ was equal to the column voltage defined by Sato as

$$E - E_m - \frac{E}{I} \cdot I_m$$

i.e. $e_t - E_m = E - E_m - \frac{E}{I} \cdot I_m$

$$E\left(1 - \frac{I_m}{I}\right) = e_t$$

$$\therefore \quad E = \frac{e_t \cdot I}{I - I_m}$$

From table 3 substituting values into this expression of e_t and $I_m(=1.6A)$ and putting I equal to the values of i_t in each case, gives values of E as 17.5V, 25V and 36V for points b,c and d respectively. The arc transients obtained for these 3 sets of operating conditions are summarized in table 4, and shown in fig. 37b,c and d respectively.

Corresponding point on fig. 37a	Supply Voltage E volts	Load Current I amps	Arc Duration T ms	Arc length at extinction mm	$E - E_m - \frac{E}{I} \cdot I_m$ volts
b	17.5	7	0.51	0.03	1.5
c	25.0	6	0.33	0.13	5.5
d	36.0	5	1.1	0.3	11.0

Table 4

Comparing table 3 and table 4, the arc lengths at extinction in table 4 are the same as the instantaneous lengths of the arc corresponding to the coordinate points detailed in table 3. Also in each case $e_t - E_m$ is equal to $E - E_m - \left[\frac{E}{I}\right] \cdot I_m$, hence the abscissa in fig.36 can be defined by either expression.
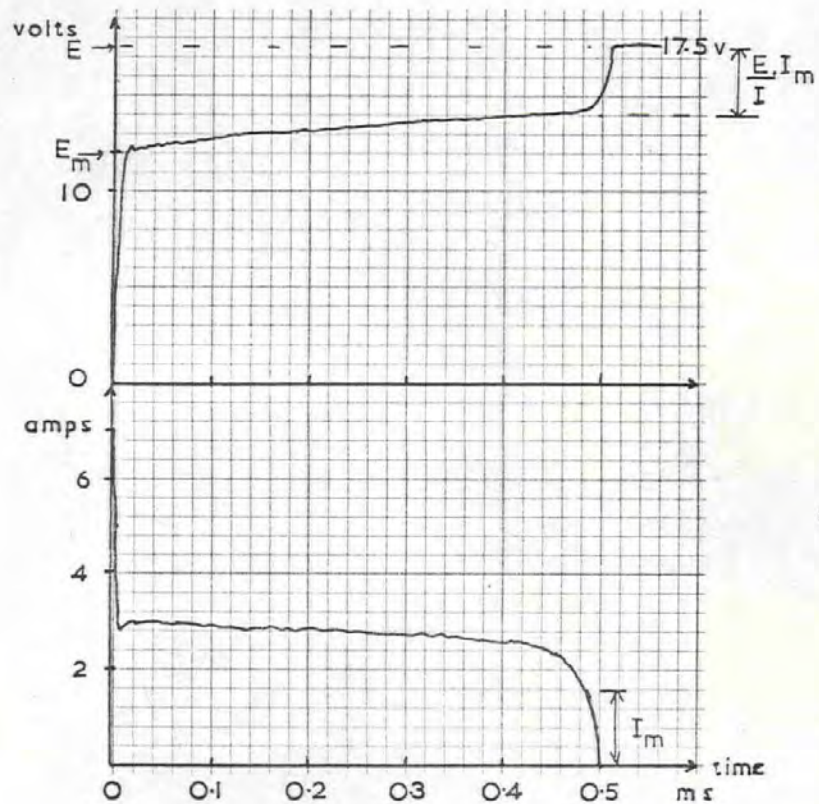
Fig. 37b.   Arc voltage/current transient
recorded on the graph plotter when
the switch contacts break a resistive
load of 7 amp, with a supply voltage
of 17.5 volts d.c. Arc duration =
0.51 ms.
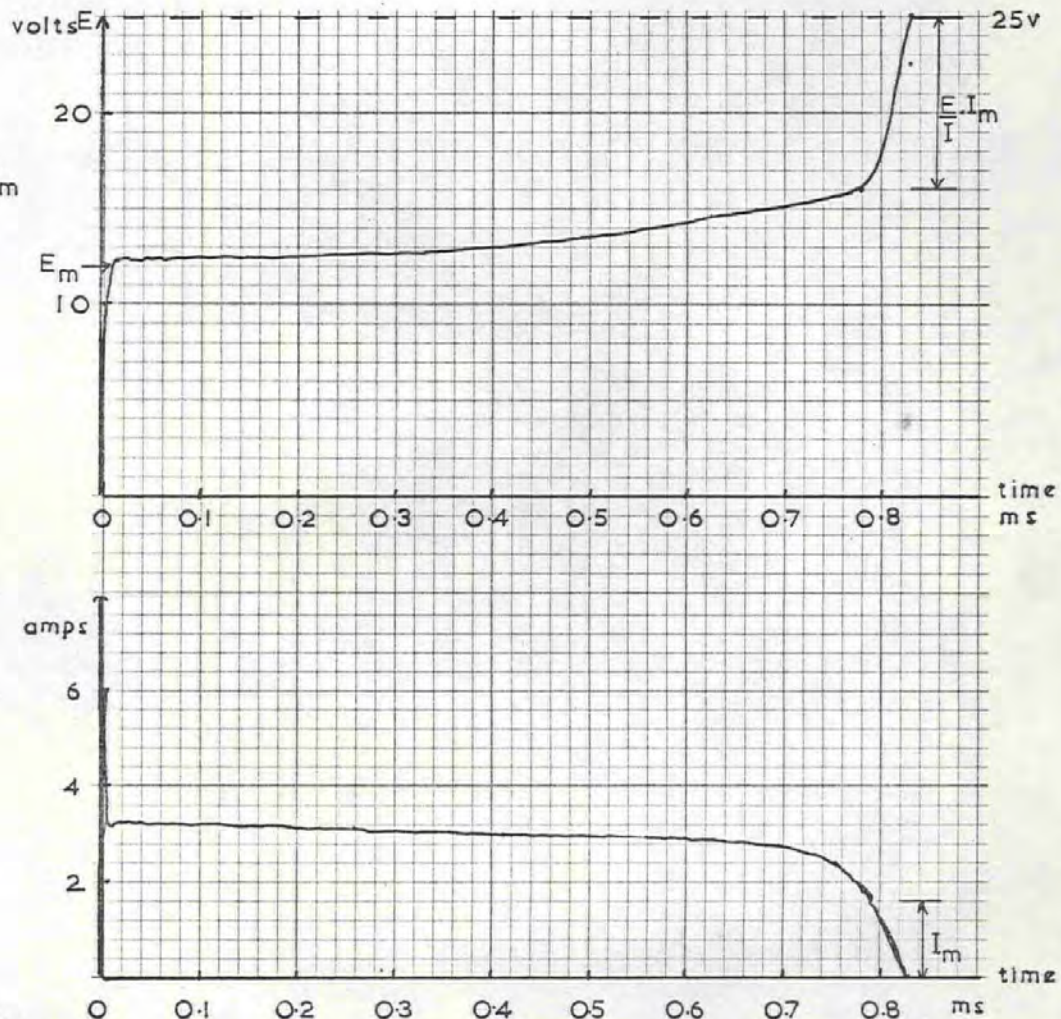
Fig. 37c.   Arc voltage/current transient recorded on the graph
plotter when the switch contacts break a resistive
load of 6 amps, with a supply voltage of 25 volts d.c.
Arc duration = 0.83 ms.
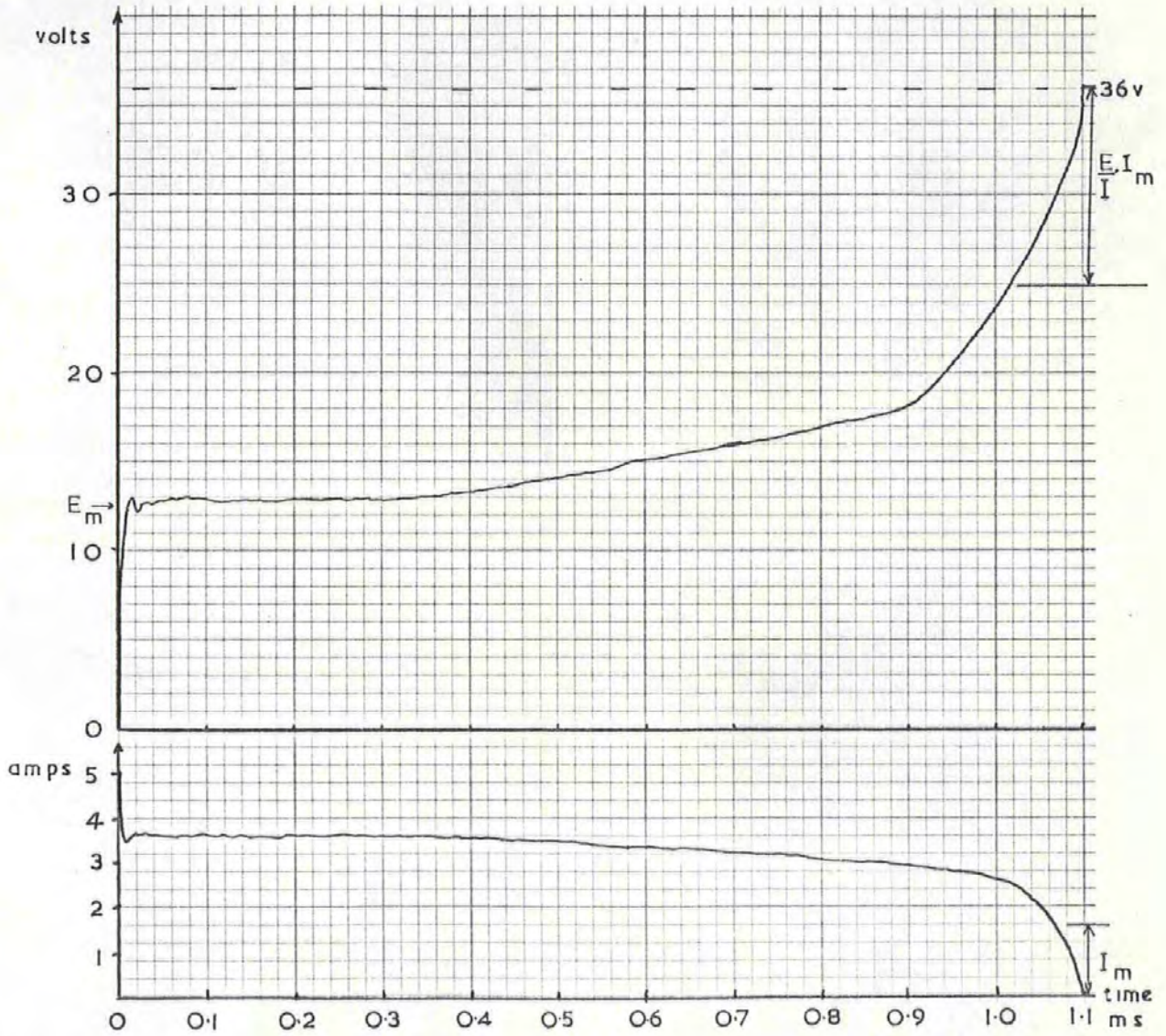
Fig. 37d.   Arc voltage/current transient recorded on the graph plotter
             when the switch contacts break a resistive load of 5 amps,
             with a supply voltage of 36 volts d.c.   Arc duration = 1.1 ms.

The data represented graphically in fig. 36 gives the relationship between arc voltage, current and arc length. Defining the axis by $(E - E_m - \frac{E}{I} . I_m)$ enables the arc length to be expressed as

$$\ell = K.(E - E_m - \frac{E}{I} . I_m)^{3/2} . I^{\frac{1}{2}} \qquad (1)$$

where K is a constant with a value 4×10^{-6} for AgCdo (85/15), with ℓ in m. Equations defining the arc voltage e_t, and arc current i_t, in terms of the arc length can now be expressed as

$$e_t = Em + (E - Em - \left[^E/_I \right].Im).^{-\frac{1}{2}}I.^{-\frac{1}{2}} \frac{\ell}{K} \qquad (2)$$

$$i_t = I - \frac{I}{E}. E_m - (E - Em - \left[^E/_I \right]Im).^{-\frac{1}{2}}I.^{-\frac{1}{2}}\frac{I}{E}.\frac{\ell}{K} \qquad (3)$$

For known operating conditions i.e. supply voltage and load current the arc voltage and arc current can be predicted using these equations providing the arc length is known.

4.6.2 Definition of Opening Characteristic

The arc length occuring between opening contacts is determined by the rate at which the contacts separate. Hence if a time dependent function $f(t)$ can be obtained which mathematically defines the motion of the contacts, this can be substituted for ℓ in equations (2) and (3). This assumes that the contact gap and the arc length are always the same and although the arc is subject to some lateral movement over the surface during its life, the difference this makes to the arc length is negligible. The graph in Fig. 38 shows a plot of the contact gap measured at the centre for the first 10ms of opening.

There are two obvious features of this separation locus:

1. Contact performs oscillations of sinusoidal form.

2. Amplitude decay of these oscillations appears as exponential.

- 106 -

A general equation to define this sort of response is

$$\ell = h\left[1 - e^{-\alpha t} \cdot (\cos\omega_s t)\right]$$

where h is the final steady state separation,

$\alpha = \dfrac{1}{T}$ where T is the time constant of the exponential decay ω_s is

the angular frequency of the oscillation.

A computer program was compiled to obtain a 'best fit' of this equation

by comparing the computed values with those measured from the films. The

assumed experimental values of ω_s indicated that the period of the

sinusoidal oscillation itself decreased as time increased. By raising

$(\omega_s t)$ to a power it was found this decrease could be accommodated in

the equation which now becomes

$$\ell = h(1 - e^{-\alpha t} \cdot \cos(\omega_s t)^n) \qquad (4)$$

The values of h, α, ω_s and n are given in Fig.38 for that particular

locus. Strictly these values only define the particular switch

characteristic used to deduce them. However it has already been

demonstrated in section 4.5.2 that switches set to the same working

stroke produce a consistency of operation, so the equation can be

realistically applied to all the toggle switches of the same type.

A plot of the calculated locus and the experimental one is shown in

Fig. 38 for comparison.

Substituting equation (4) into equations (2) and (3) produces

$$e_t = Em + (E - Em - \left[E/_I\right].Im).^{-\frac{1}{2}}I^{-\frac{1}{2}}\frac{h}{K}.\left[1 - e^{-\alpha t}\cos(\omega_s t)^n\right] \qquad (5)$$

$$i_t = I - \left[I/_E\right].Em - (E - Em - \left[E/_I\right].Im).^{-\frac{1}{2}}\frac{I}{E}.\frac{h}{K}.\left[1 - e^{-\alpha t}\cos(\omega_s t)^n\right] \qquad (6)$$

For a given operating condition all the terms in these equations are

known, hence the values of arc voltage and arc current can be

calculated as functions of time.
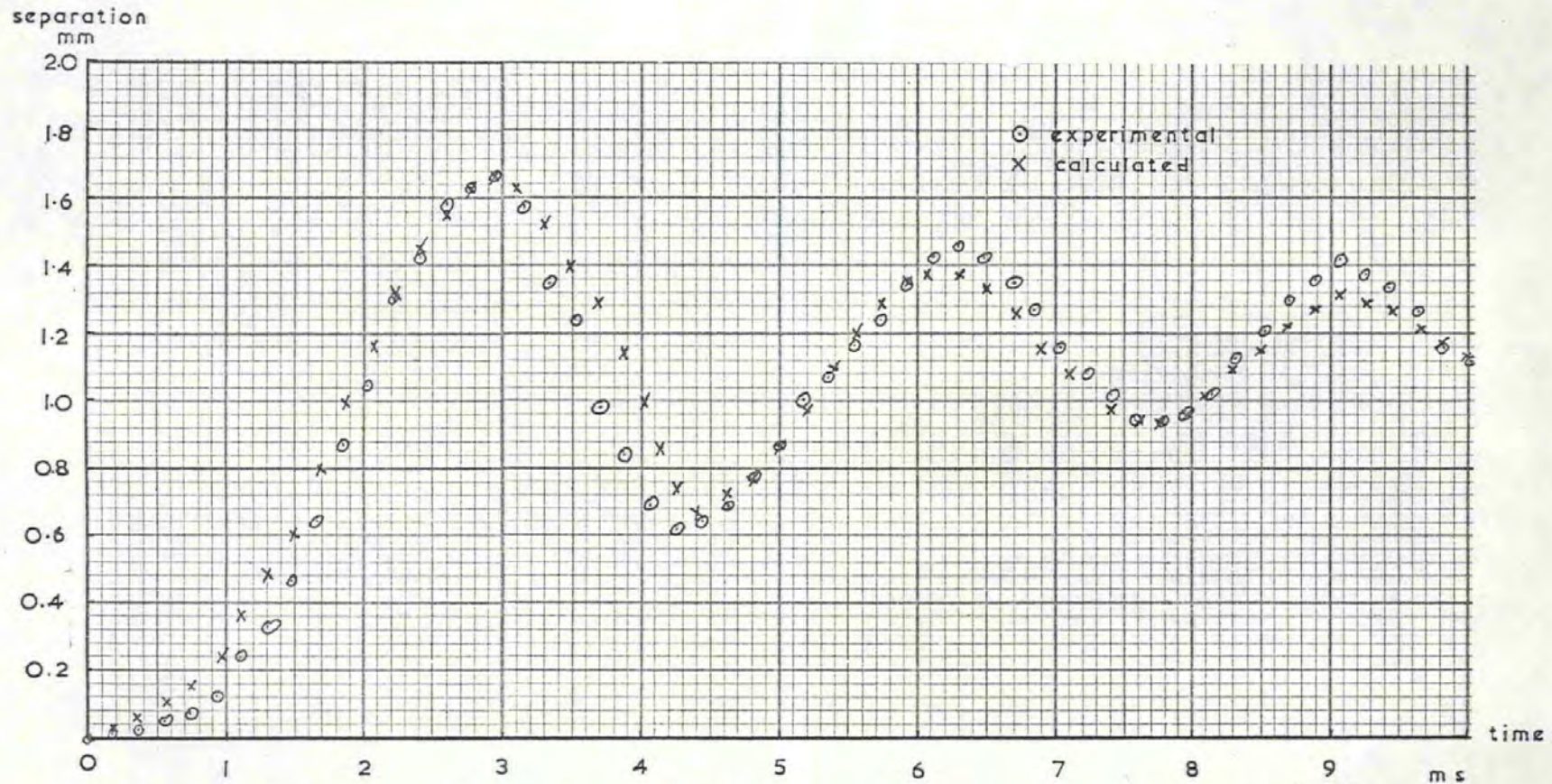
Fig. 38. Opening characteristic of a toggle switch. Points plotted - ⊙ - were experimentally measured from the high speed film. Points plotted - × - were calculated using the equation

Separation $\ell = h(1 - e^{-\alpha t}\cos(\omega_s t)^n$

where $h = 1.1 \times 10^{-3}$ m,

$\alpha = \dfrac{1}{\gamma}$ where $\gamma = 4.8 \times 10^{-3}$ s, $\omega_s = \dfrac{2\pi}{.009}$, $n = 1.45$

4.6.3 Arc Power and Arc Energy

The usefulness of equations (5) and (6) is manifested when considering the arc power and arc energy. From a knowledge of the supply voltage and load current the instantaneous arc power can be calculated. The area under the graph of arc power against arc duration gives the total energy dissipated in the arc. Mathematically the arc energy is

$$\int_0^T e_t \cdot i_t \cdot dt \qquad \text{where T is the arc duration.}$$

This can easily be evaluated numerically with a computer using Simpson's rule or other numerical methods for finding the area under curves.

To check the validity of the equation, a set of experimental data was obtained for a switch operating over voltages and currents in the range covered by the graph in Fig.36. The arc voltage and arc current in each case were recorded onto graph paper by the transient recorders. From these the product $e_t \, i_t$ was obtained and plotted against the arc duration (Fig..39). Fig. 36 was used to ensure that the arc extinguishing capability of the switch was not exceeded, i.e. the value of $E - Em - E/I$ Im and I would not produce an arc length ℓ, according to equation (1) such that ℓ was greater than h. This is the reason that the current was restricted to lower values for the higher supply voltages.

The values of the arc power obtained from the product of equation (5) and (6) are also plotted in Fig.39 for comparisons, and it was seen that there is close agreement between the experimental and calculated results.

The arc energy was calculated using the computer to find the area under each arc power curve. Fig.40 shows the graph of arc energy against load current with supply voltage as a parameter. These curves can be
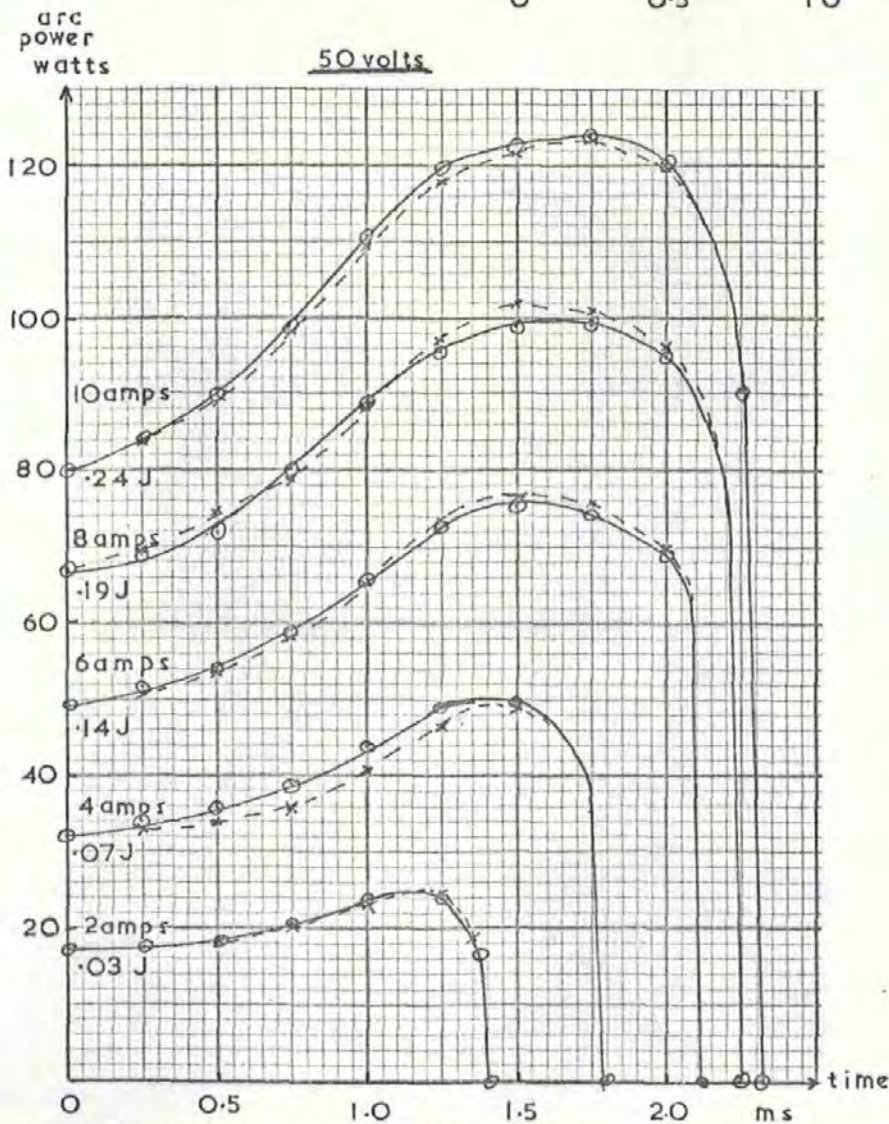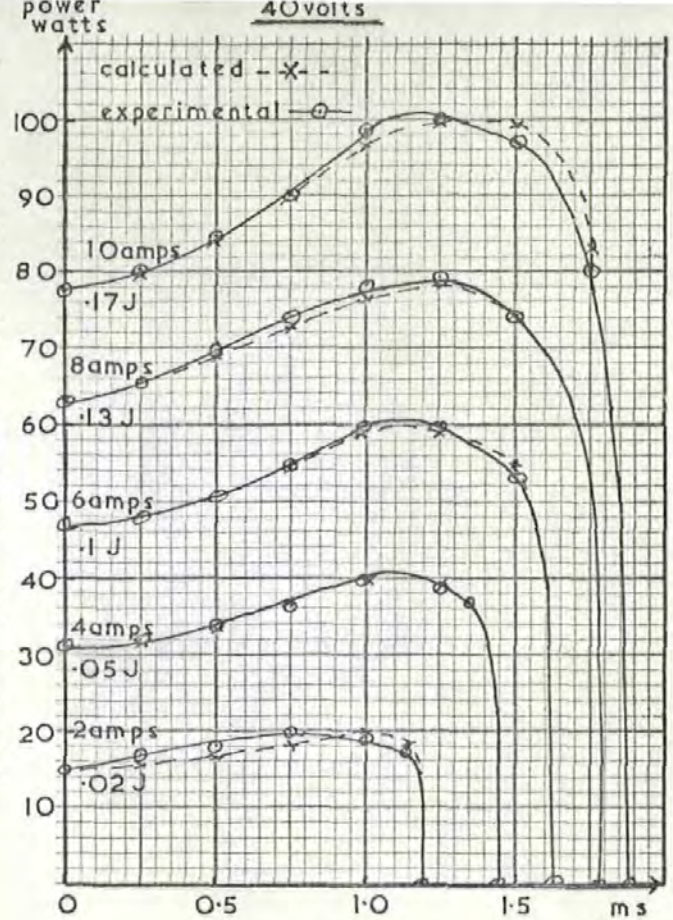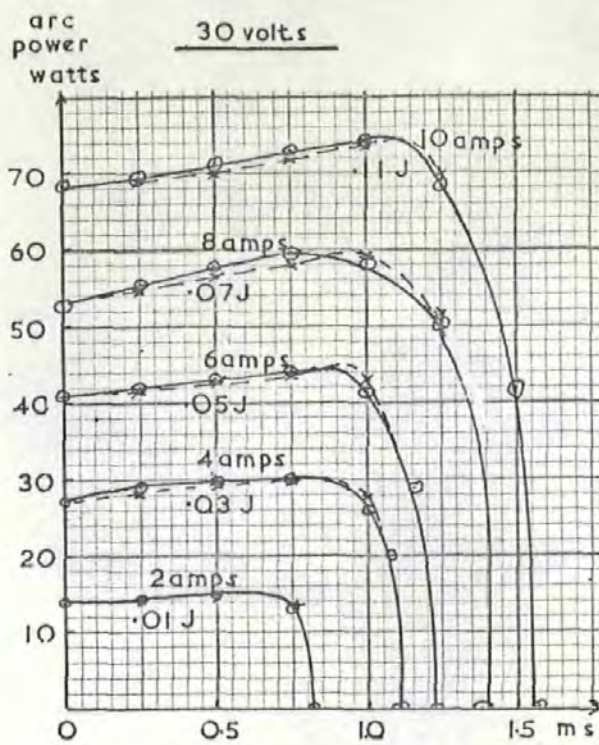
Fig. 39a. Graphs of arc power/arc duration for resistive loads of 2 - 10 amps Supply voltages arc 30v, 40v, 50v d.c.   Total arc energy is given by the area under each curve. Point plotted - ⊙ - were experimentally measured. Points plotted - X - were calculated using the product of equation (5) and (6).
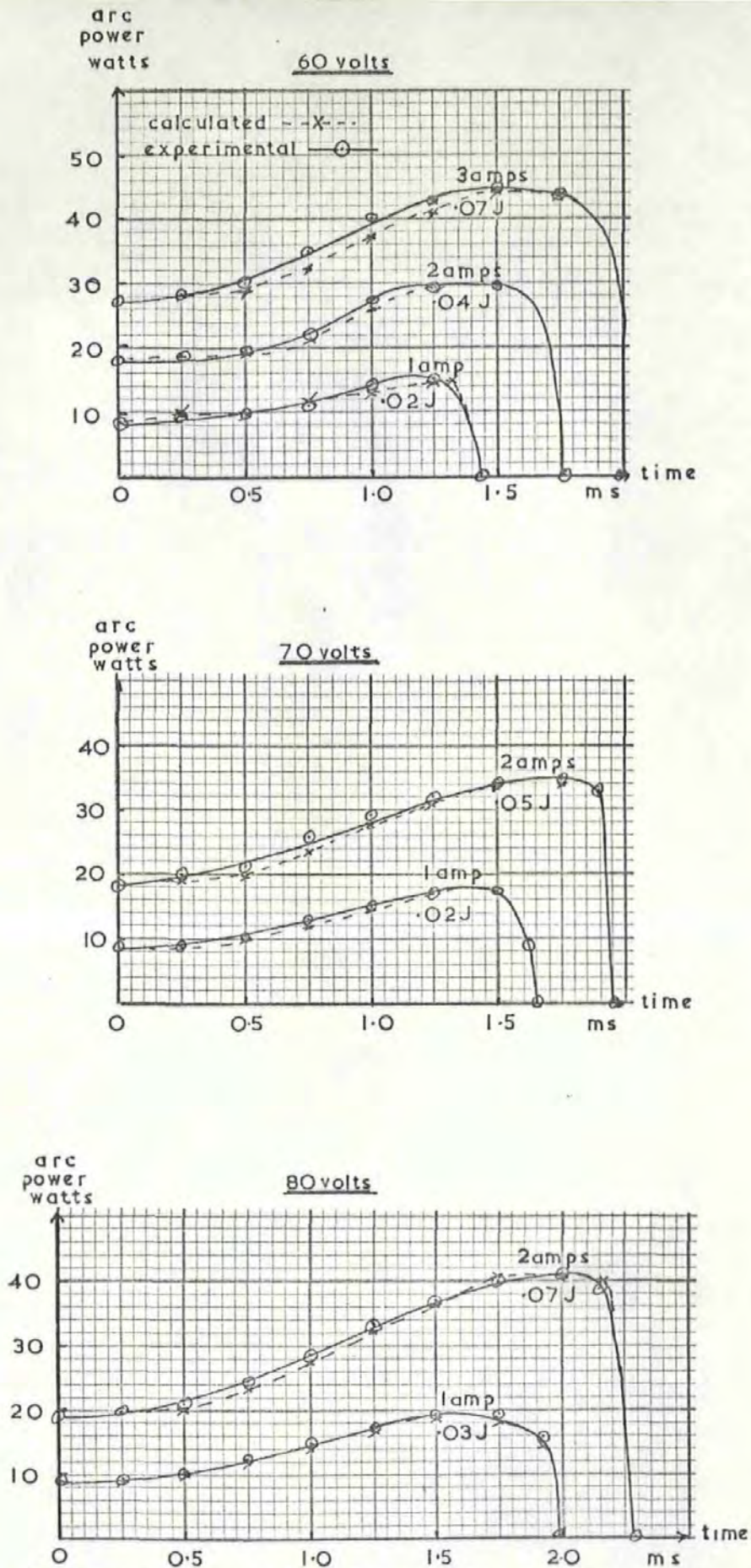
Fig. 39b   Graphs of arc power/arc duration for resistive loads of 1, 2 and
3 amps.   Supply voltages are 60v, 70v, 80v, 80v d.c. Total arc
energy is given by the area under each curve.   Points plotted
- O - were experimentally measured. Points plotted - x - were
calculated using the product of equation (5) and (6).
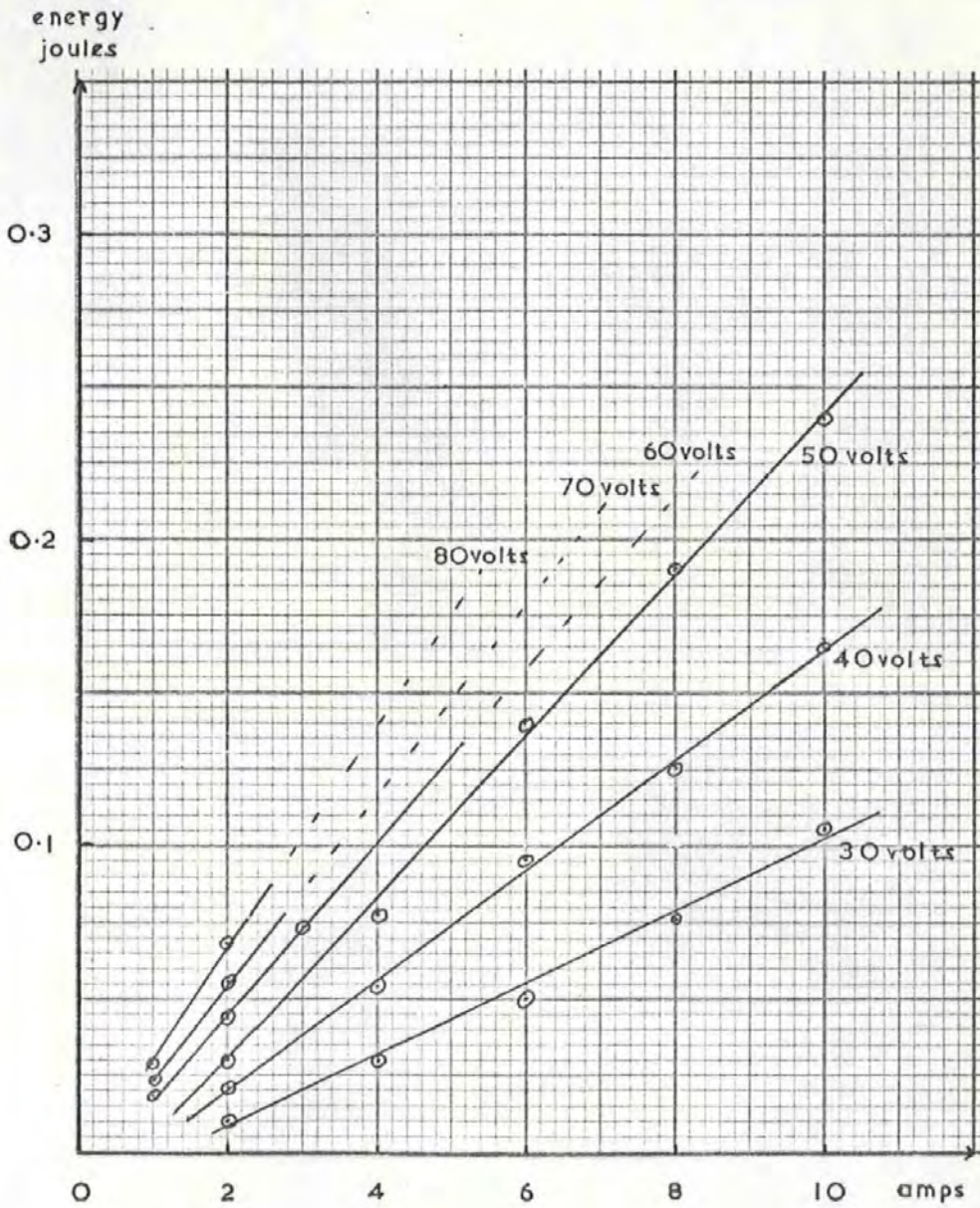
Fig. 40.   Graphs of arc energy/load current for the range of supply
voltages shown in Fig. 39.   For a   given load current
and supply voltage the arc energy can be predicted using
this graph.   Dotted lines indicate that these d.c. operating
conditions are outside the range over which the switch is
capable of extinguishing the arc.

easily used to predict the energy/operation from a knowledge of the supply voltage and load current. They are directly applicable to the toggle-switches with operating strokes of 0.64mm i.e. the same as the test switches used to obtain the data. For switches with a shorter stroke i.e. slower opening velocity, the curves will be rotated anti-clockwise, for a faster opening velocity i.e. larger stroke, clockwise rotation. If the operational limits for a given application of the switch are known they can be drawn onto this graph and hence it can be generally applied to predict the energy dissipation for switch lifetime.

In Chapter 2, Section 2.3.5 remarks were made concerning the variability of Im, the minimum arc current, which depended to some degree on the circuit parameters and the arc duration. This seems to be confirmed by the graphs of Fig.40. If the lines of constant voltage are projected down until they intercept the current axis, it is seen that for increasing voltage the value of the current at intersection decreases. Since the higher voltages correspond to larger arc durations this is in agreement with previous reasoning on this. A similar graph to Fig.40 has been published by Takahachi (10) who evaluates the relationship between arc energy and arc termination current.

4.7 Operation on A.C. Supply

The equations to calculate the arc power and energy have been verified for a switch breaking a resistive load with a d.c. supply. The information obtained from this investigation can be used to guide the experimental-observations of the same switches operating on an a.c. resistive load.

The usual application of the toggle switch in the United Kingdom involves breaking 240V.r.m.s. at 50 Hz. Referring back to Fig. 36
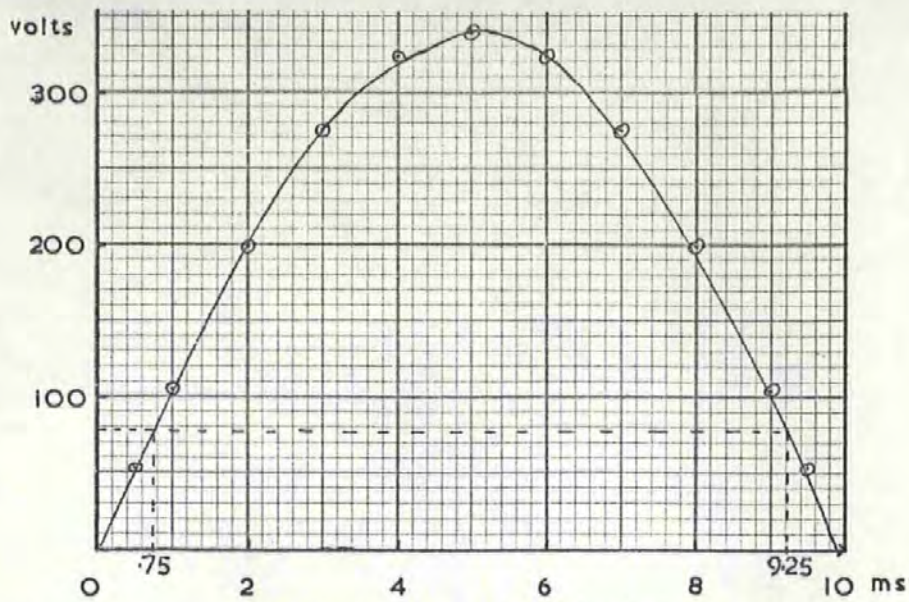
Fig. 41a.   A.C. supply voltage wave 340 sin (2π50t) volts
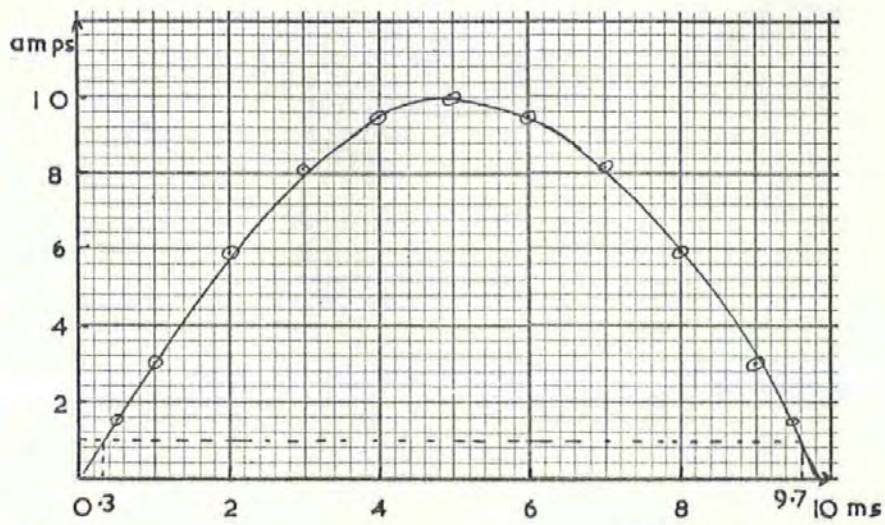
Fig. 41b.   Current wave defined by 10 sin (2π50t) amps.
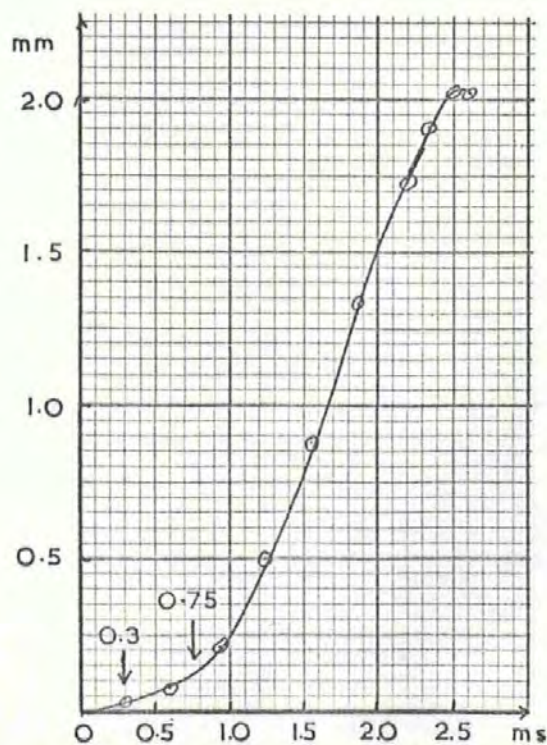
Fig. 41c.   Typical separation/time characteric of opening contacts.

- 114 -

the graph here shows that for a nominal contact separation of 2mm, an arc drawn at a current of 1 amp with a supply voltage of 80 - 90 volts, will be just extinguishable. If the voltage wave on a.c. is given by

$$V = 340 \sin \omega t$$

the instantaneous value of the voltage is only within this range of 80 - 90 volts for the first and last 0.75 ms of each half cycle Fig.41c. Similarly if the current wave is defined by

$$I = 10 \sin \omega t$$

the instantaneous value of current does not fall to the value of 1 amp except for the first and last 0.33 ms of a half cycle Fig.41b. Referring to the separation characteristic Fig.41c, the switch requires at least 2 ms to attain a separation of 2mm, hence it is unlikely for the switch to extinguish an arc which ignites at the beginning of a half cycle. Hence the arc will persist until some point in time within the last 0.75 ms, depending on the rate at which the arc current approaches the particular value of Im for these a.c. operating conditions.

By considering the last 0.75 ms of the half cycle to consist of small steady state d.c. increments the arc voltage and current can be calculated using equations (5) and (6) in Section 4.8.2 by substituting E.sin($\omega t + \theta$) for E and I.sin ($\omega t + \theta$) for I:-

$$e_t = Em + \left[E.\sin(\omega t+\theta) - Em - \frac{E}{I}.Im\right]^{-\frac{1}{2}\frac{h}{K}}\left[1 - e^{-\alpha t}\cos(\omega_s t)^n\right] \quad (7)$$

$$i_t = \hat{I}\sin(\omega t+\theta) - \frac{I}{E}.Em - \left[E.\sin(\omega t+\theta)-Em-\frac{E}{I}Im\right]^{-\frac{1}{2}\frac{I}{E}\frac{h}{K}}.\left[1-e^{-\alpha t}\cos(\omega_s t)^n\right](8)$$

θ is the point on the a.c. cycle at which the arc ignites. By putting $\frac{\theta}{\omega}$ = 9.25 ms values of e_t and i_t can be calculated at suitable time increments. This was done using a computer program and the results are plotted in Fig. 42a. Results from an experimental oscillograph
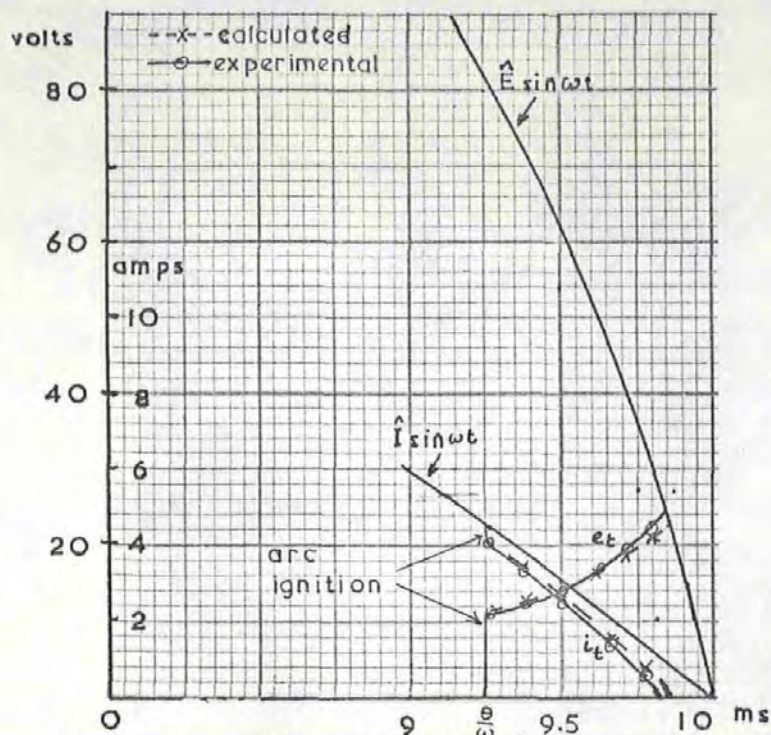
Fig. 42a.   Arc voltage and current transients occuring when the
             switch contacts open 9.25 ms after a zero.
             Operating conditions: 240V rms, 50 Hz, resistive load
             of 10 amps peak.
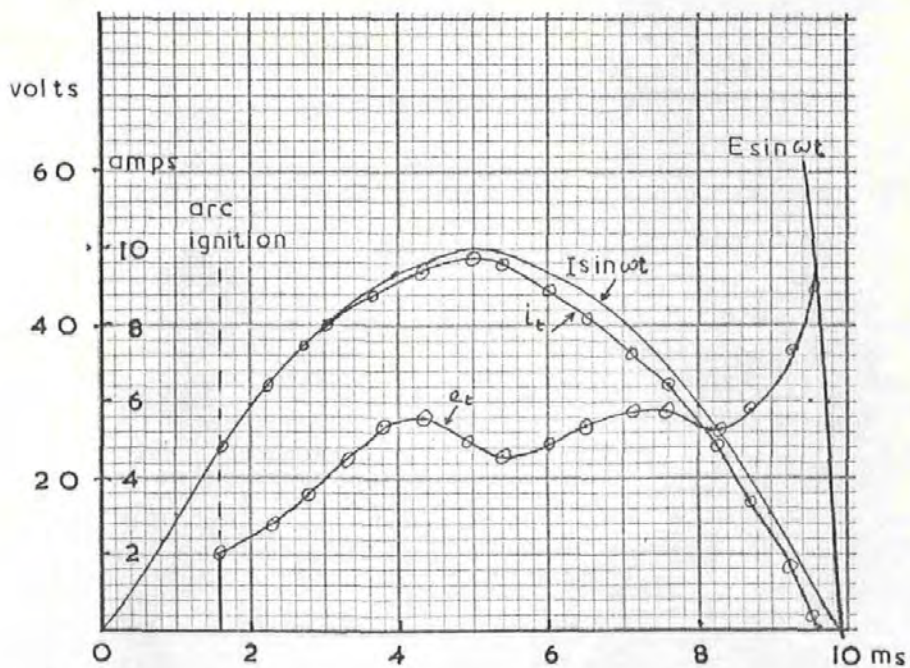
Fig. 42b.   Arc voltage and current transients occuring when the
             switch contacts separate 1.6 ms after a zero.
             Operating conditions: 240V rms, 50 Hz, resistive load of
             10 amps peak.

- 116 -

are also plotted for comparison verifying that the equations are
valid for this particular point on the cycle.

Since it is not possible to use point on wave triggering with normally
operated switches, the instant in time that the switch opens relative
to the a.c. wave is not controllable, therefore to obtain the experi-
mental data for Fig. 42a the switch was operated many times.   By doing
this a complete set of oscillographic data was acquired with arc ignition
points distributed uniformly across the half cycle.   One set with
ignition point early on in the cycle ($\frac{\theta}{\omega}$ = 1.6 ms) is shown in Fig. 42b.

To enable the arc power and arc energy to be calculated for any ignition
point, equations are required that will give values of e_t and i_t for
the whole arc duration, as with the d.c. operating conditions.

Looking closely at the experimental oscillographs in Fig. 43 three
things are immediately apparent.
1.   The arc voltage changes 'in phase' with the contact motion,
      i.e. change in arc length.
2.   The arc current does not deviate by more than 0.5A   from $\hat{I} \sin \omega t$.
3.   The values of e_t and i_t and l (arc length), do not lie outside
      the range covered by the graph in Fig. 36, at any time during the
      arc duration.

In section 4.6.1 it was shown that the voltages defined by e_t − Em
and E − Em −$\left(\frac{E}{I}\right)$.Im were for the purposes of Fig. 36 the same.   Hence
the equation for arc length, equation (1) section 4.6.1 can be rewritten
as:

$$l = K(e_t - Em)^{\frac{3}{2}} (i_t)^{\frac{1}{2}} - (9) \text{ since } i_t \equiv I \text{ for this representation,}$$

re-arranging gives $e_t = Em + \left(\dfrac{l}{K.i_t^{\frac{1}{2}}} \right)^{\frac{2}{3}}$ — (10)

i.e. an equation for e_t in terms of i_t with l the only other variable

l has previously been shown to be defined by the contact separation locus.

Equation 8, for i_t can be re-written as

$$i_t = \hat{I} \sin(\omega t + \theta) - \frac{I}{\hat{E}} \left[Em + (\hat{E} \sin[\omega t + \theta] - Em - \frac{E}{I} - Im)^{-\frac{1}{2}} (\hat{I} \sin \omega t + \theta)^{-\frac{1}{2}} \right.$$

$$\left. \frac{h}{K} \left\{ 1 - e^{-\alpha t} \cos(\omega_s t)^n \right\} \right]$$

The terms inside the square brackets in this equation equal e_t (equation 7).

Hence this simplifies to:

$$i_t = \hat{I} \sin(\omega t + \theta) - \left[\frac{I}{E} \right].e_t$$

$\frac{E}{I}$ defines the load resistance of the circuit say R_L

$$\therefore i_t = \hat{I} \sin(\omega t + \theta) - \frac{e_t}{R_L}$$

$$= \frac{\hat{E} \sin(\omega t + \theta) - e_t}{R_L}$$

It has already been noted that i_t does not appear to deviate much from

$\hat{I} \sin \omega t$. The reason is now seen to be that for most of the a.c. cycle

$e_t \ll \hat{E} \sin \omega t$.

Hence $i_t \approx \dfrac{\hat{E} \sin(\omega t + \theta)}{R_L} = \hat{I} \sin(\omega t + \theta)$

Equation (10) now becomes $e_t = Em + \left(\dfrac{l}{K(\hat{I} \sin \omega t + \theta)^{\frac{1}{2}}} \right)^{\frac{2}{3}}$ — (11)

Substituting the expression of the separation locus for 1 gives

$$e_t = Em + \left[\frac{h(1 - e^{-\alpha t} \cos(\omega_s t)^n)}{K(\hat{I} \sin \omega t + \theta)^{\frac{1}{2}}} \right]^{\frac{2}{3}}$$

This equation enables the arc voltage e_t to be calculated for any ignition

point on the a.c. cycle. The error caused by approximating i_t to $\hat{I} \sin(\omega t + \theta)$
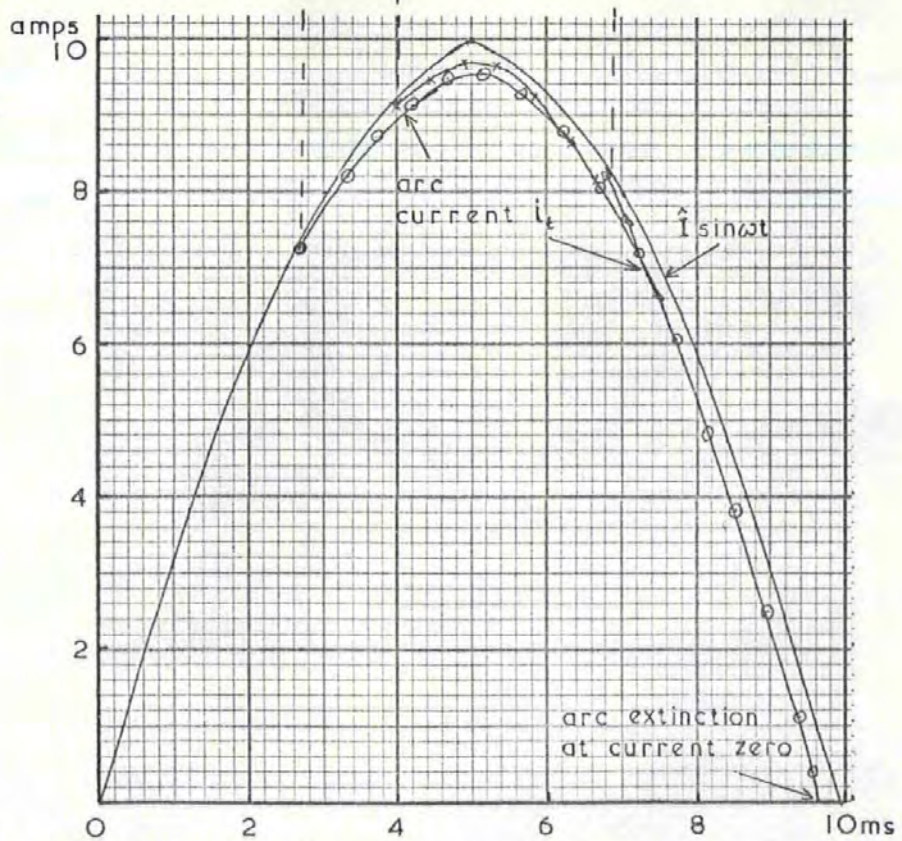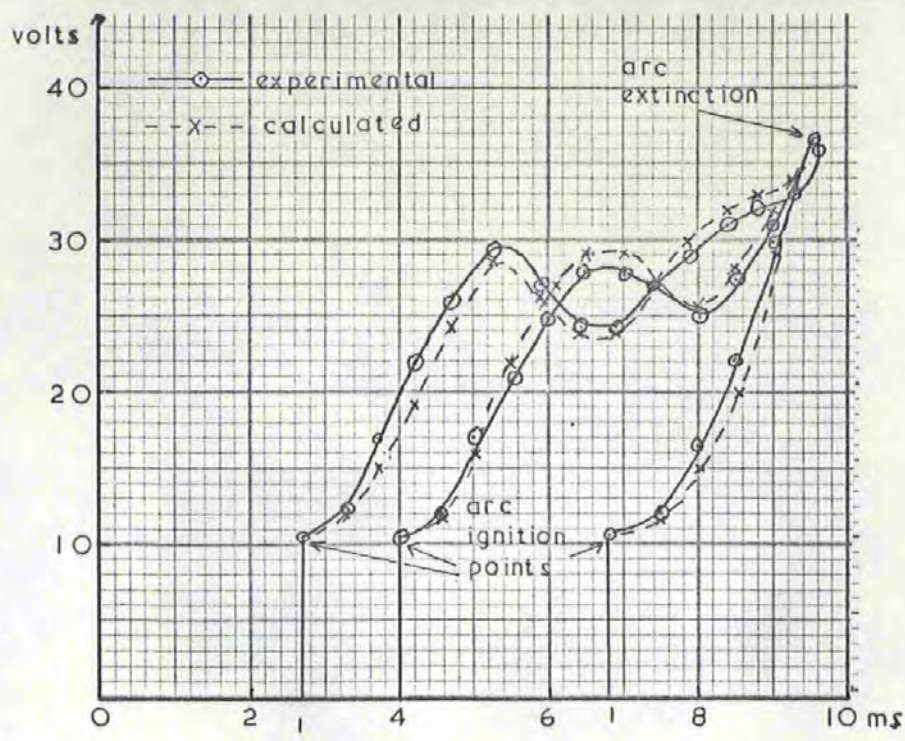
Fig. 43.   Arc voltage and current transients occuring for 3 arc ignition
            points on the a.c. cycle.
            The arc voltage changes in 'phase' with the separation of the
            contacts.
            The arc current follows the form of $\hat{I} \sin \omega t$ with a maximum
            deviation of $0.5A$ at any point.

is not significant apart from the last 0.75 ms of each half cycle, when the resistance of the arc approaches, and exceeds in the last few μs, the resistance of the circuit. To maintain accuracy, equations (7) and (8) could be used to calculate values for i_t and e_t over this last 0.75 ms as shown in Fig. 42. However as the following section shows, from an engineering standpoint, in calculating values for the arc energy the error introduced by assuming the arc current is $\hat{I} \sin(\omega t + \theta)$ is generally less than 10%.

4.7.1 Arc Power and Arc Energy for A.C. Loads

Using the transient recorders 7 sets of e_t and i_t transients were obtained at approximately $1.0 \rightarrow 1.5$ ms intervals across the a.c. half cycle, for a peak current of 10 amps. For clarity, only three sets are shown in Fig. 43. Using equation (12) values of e_t were calculated, and these are plotted in Fig. 43 for comparison with the experimentally measured ones. $\hat{I} \sin \omega t$ has been drawn in Fig. 43 for comparison with the experimental values of i_t.

The expression for arc power is obtained by multiplying equation (11) by $\hat{I} \sin(\omega t + \theta)$ giving

$$e_t \cdot i_t = Em.\left[\hat{I} \sin(\omega t + \theta)\right] + \left[\frac{\ell . \hat{I} \sin(\omega t + \theta)}{K}\right]^{\frac{2}{3}} \quad - (13)$$

The arc power curves corresponding to the data of Fig. 43 are shown in Fig. 44(a), both for the experimentally measured e_t and i_t and the calculated values. The arc energy $\int_o^T e_t \cdot i_t \, dt$ is evaluated by calculating the area under the arc power curve as in the dc case, however for a.c. the arc energy is also dependant upon the ignition point. Fig. 44b shows how the arc energy varies with the instant
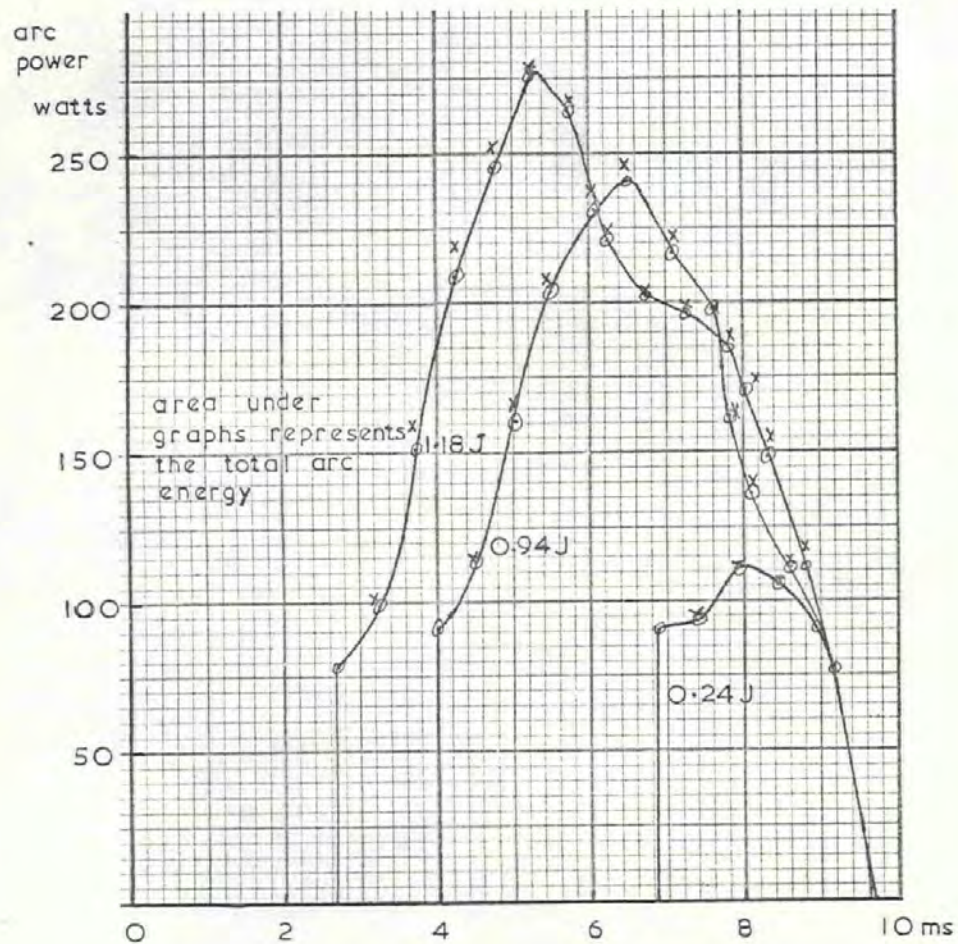
Fig. 44a. Arc power curves for 3 ignition points on the a.c. half cycle. Operating conditions: 240 vrms, 50Hz, 10 amps peak, resistive load. Experimentally measured points plotted - ⊖ - Calculated values plotted - X -
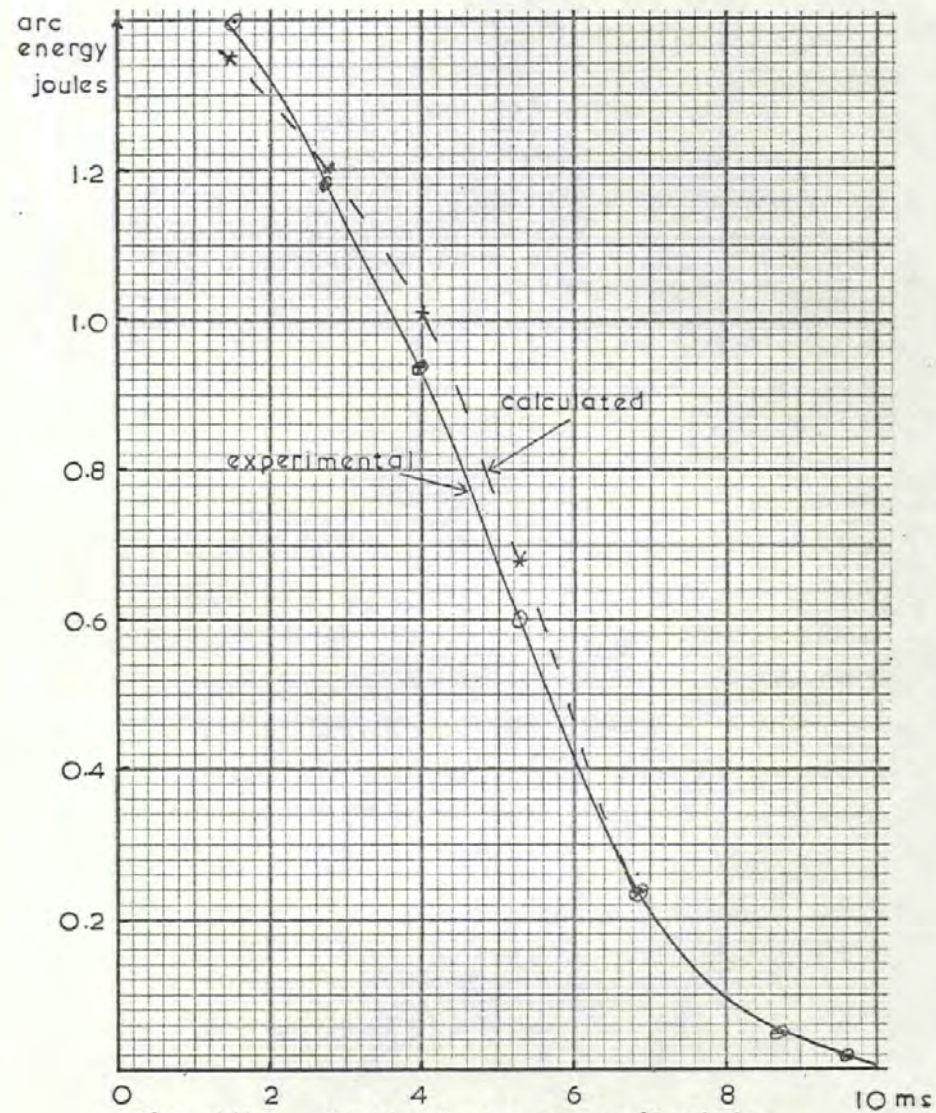
Fig. 44b. Graph of arc energy/ignition, corresponding to the area under the arc power curves. 7 ignition points were used to plot the graph.
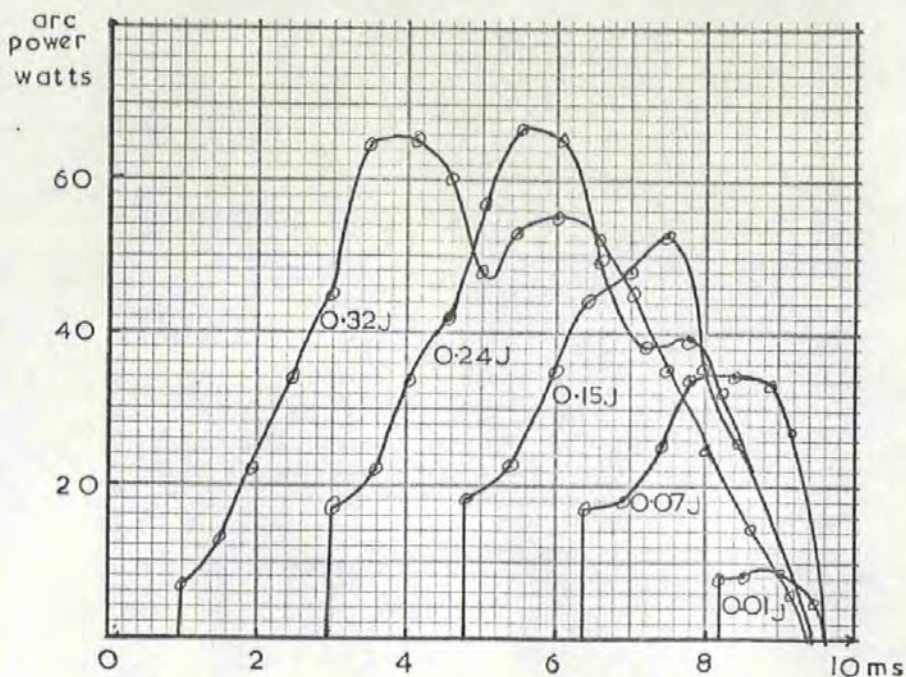
Fig. 45a. Graph of arc power/ignition point for a resistive load of 2 amps peak. Supply voltage was 240 Vrms, 50 Hz. The area under each curve represents the total arc energy,
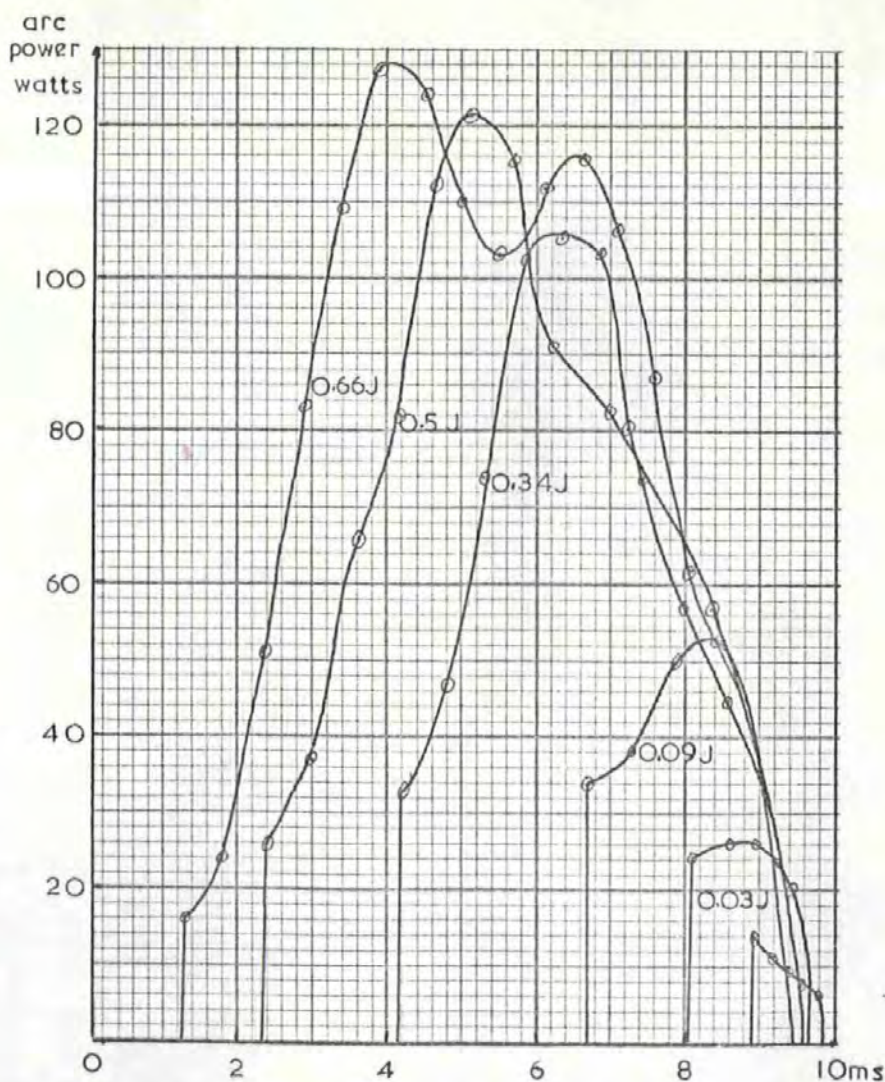
Fig. 45b. Graph of arc power/ignition point for a resistive load of 4 amps peak. Supply voltage in 240 Vrms, 50Hz. The area under each curve represents the total arc energy.
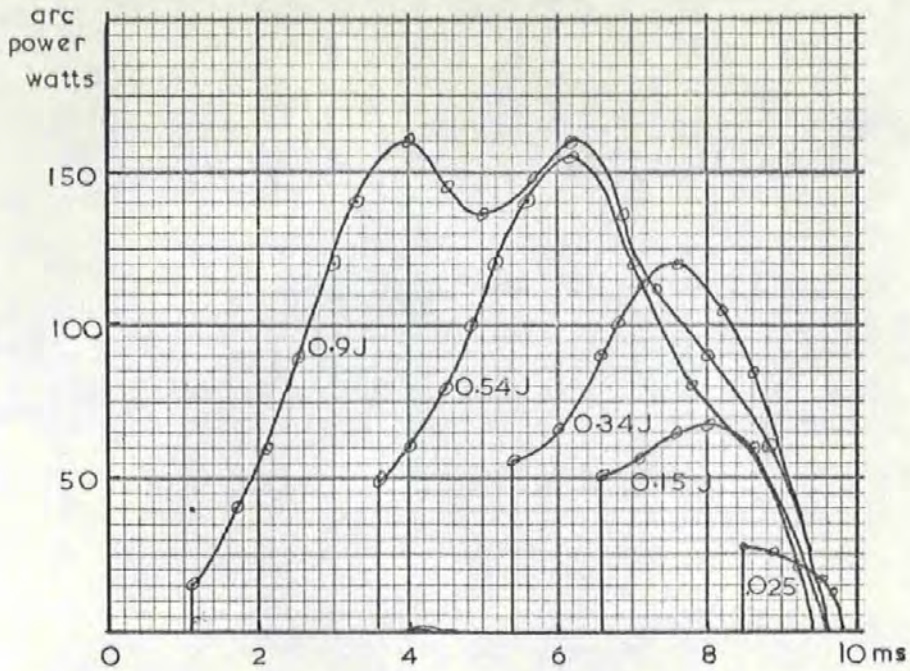
Fig. 45c.   Graph of arc power/ignition point for a resistive
             load of 6 amps peak.   Supply voltage was 240 Vrms,
             50 Hz. The area under each curve represents the
             total arc energy.
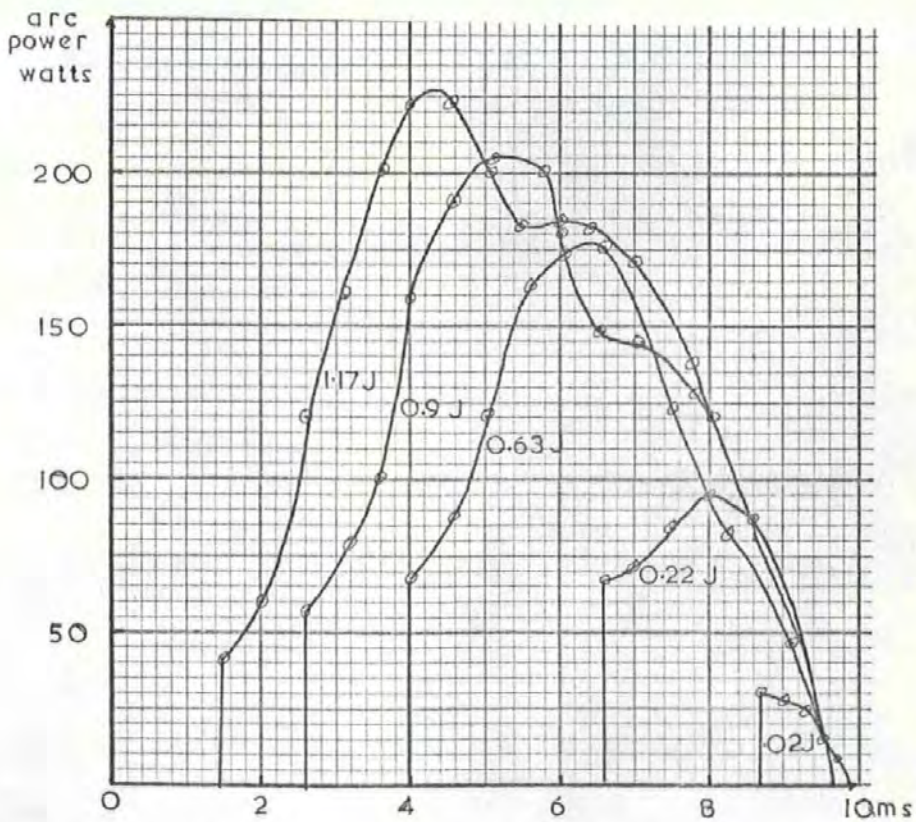
Fig. 45d.   Graph of arc power/ignition point for a resistive
             load of 8 amps peak.   Supply voltage was 240 Vrms, 50Hz.
             The area under each curve represents the total arc
             energy.
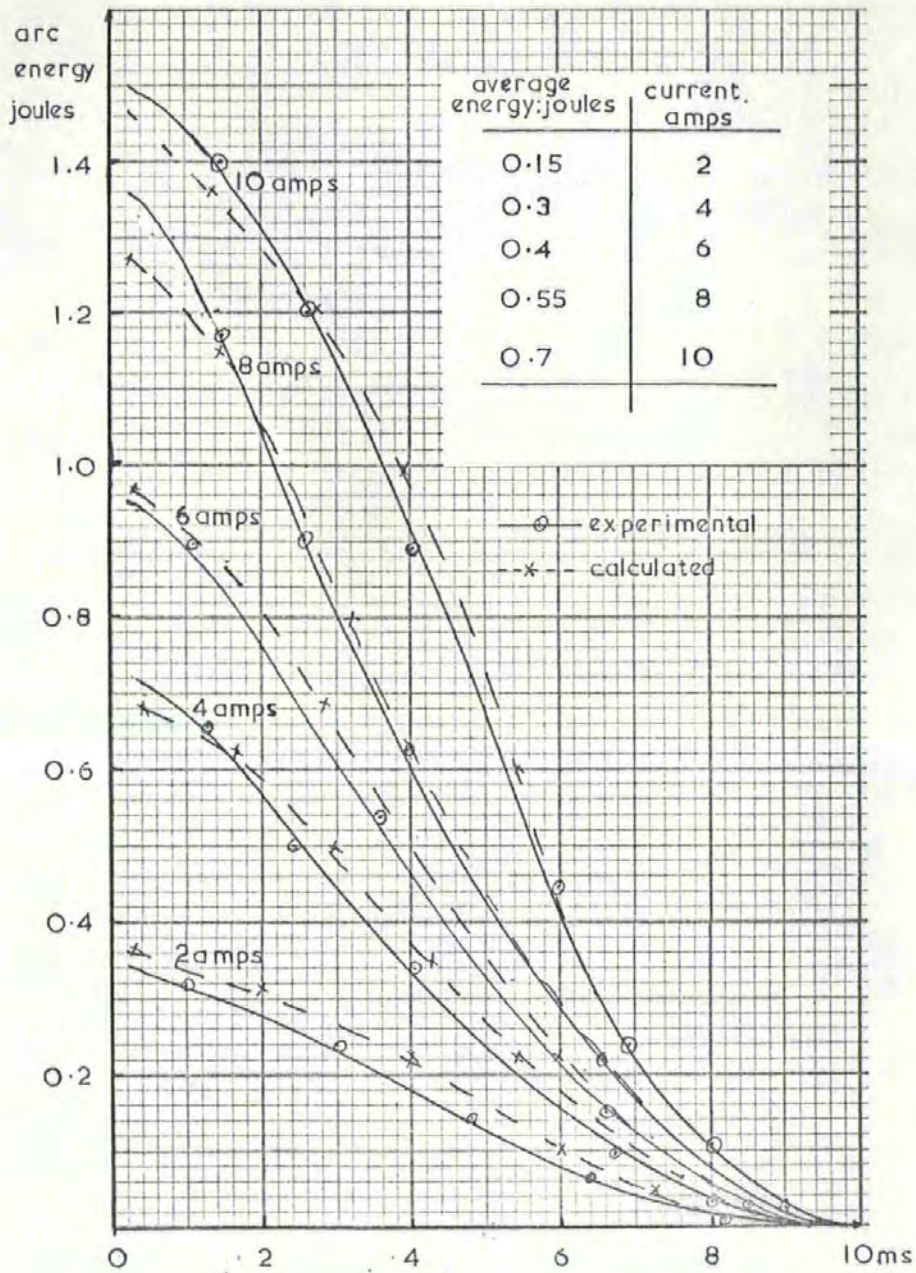
Fig. 46. Arc energy/ignition point for peak currents of 2 - 10 amps. The experimental results were obtained by evaluating the area under the arc power curves of Fig. 45.

at which the arc ignites, seven ignition points were used to produce this curve for the 10 amp case, and the calculated values are again plotted for comparison with the values obtained from the experimental measurements.

A range of results are shown in Fig. 45a - d, representing the arc power produced at different ignition points on the half cycle for load currents of 2, 4, 6, 8 amps peak. From these the arc energy is calculated and in Fig. 46 it is plotted against ignition point with load current as a parameter. This graph enables the energy dissipated between the contacts to be found for a known load current. Since for these switches the point in time when the contacts open is random when referred to the a.c. half cycle, for many operations (Switch life = 200,000) the arc will ignite an equal number of times at every point on the cycle. Hence to determine the total energy dissipated over the life of the switch it is permissible to multiply the number of operations by a value which represents the 'average energy' per operation. The values for this are listed in Fig. 46, as calculated on the computer for each curve.

The work completed thus far enables the arc energy to be calculated from a knowledge of the load current and the switch opening characteristic. All the experimental measurements have been made using a resistive load. Since toggle switches are frequently used on inductive loads, the effect this has on the arc energy at break will next be considered.
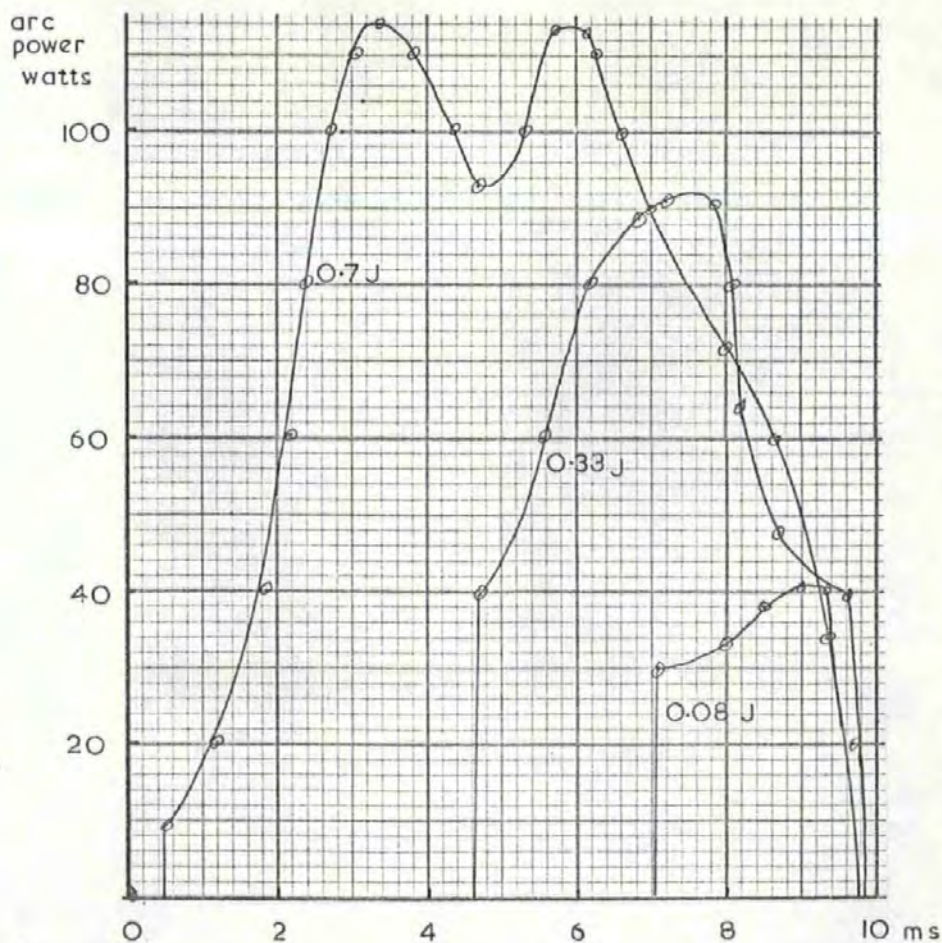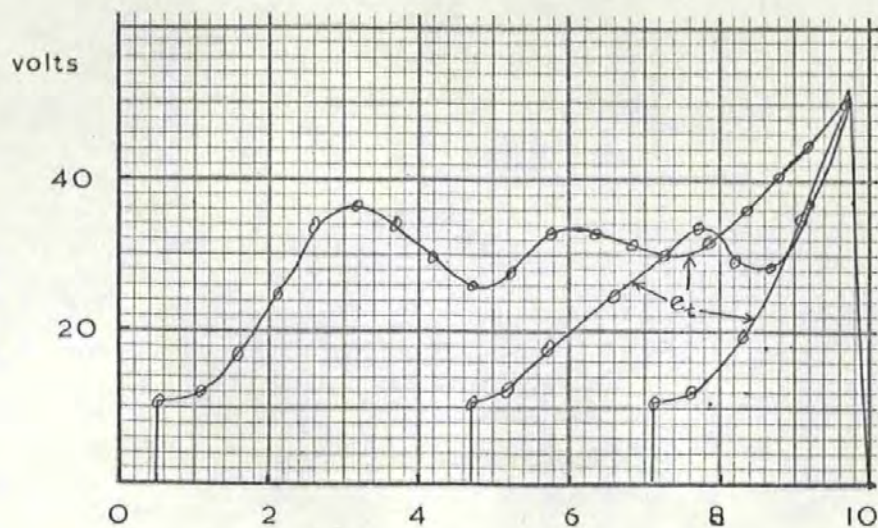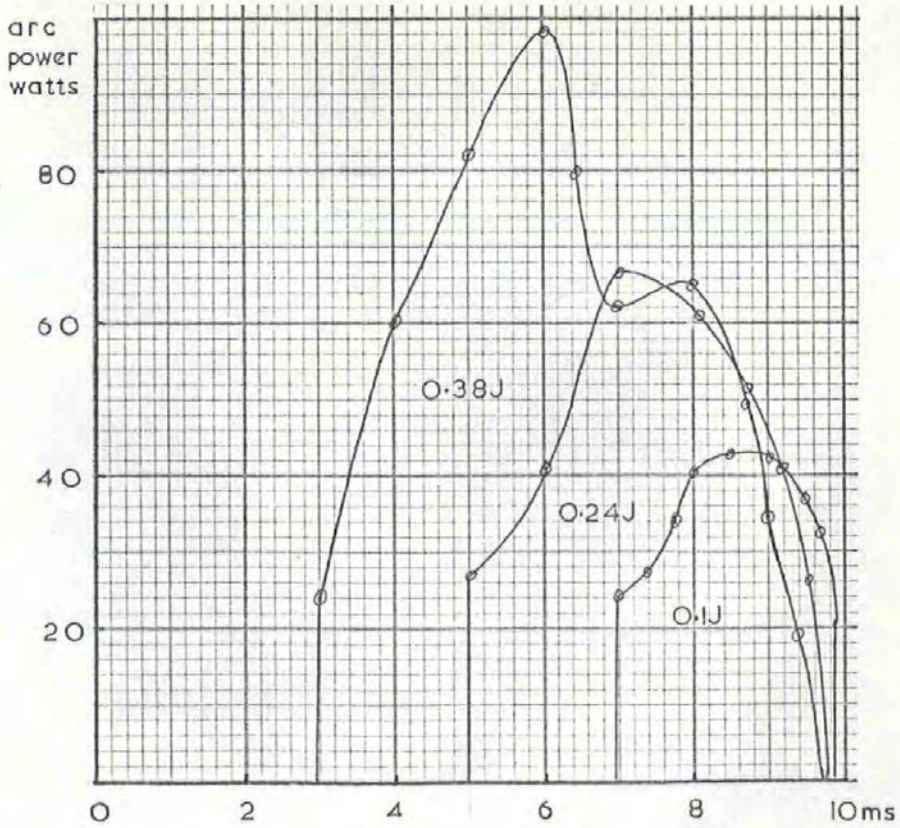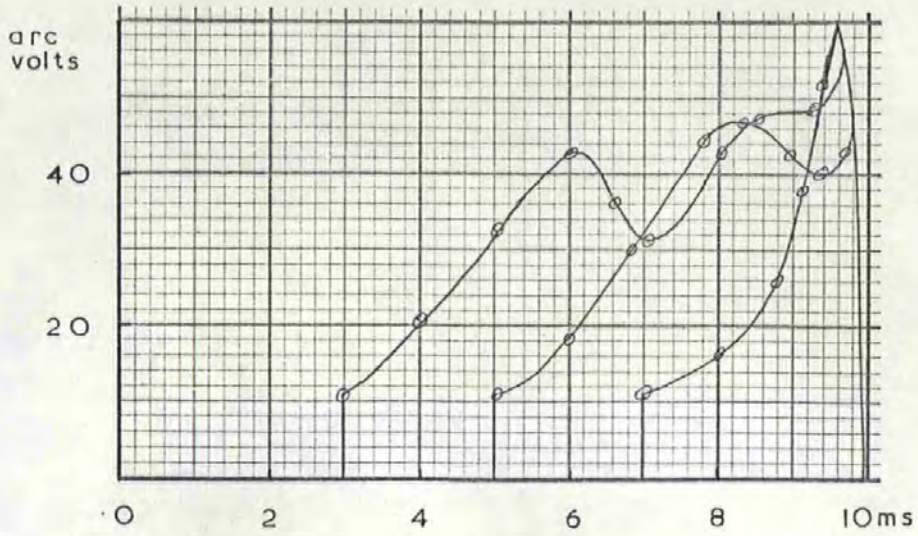
Fig.47. Arc voltage and power curves for 3 ignition points on the a.c. half cycle. The area under the arc power curves represents the total arc energy.
Operating conditions: 240 V.rms, 50Hz, 4A peak.
Inductive load, cos $\emptyset$ = 0.58
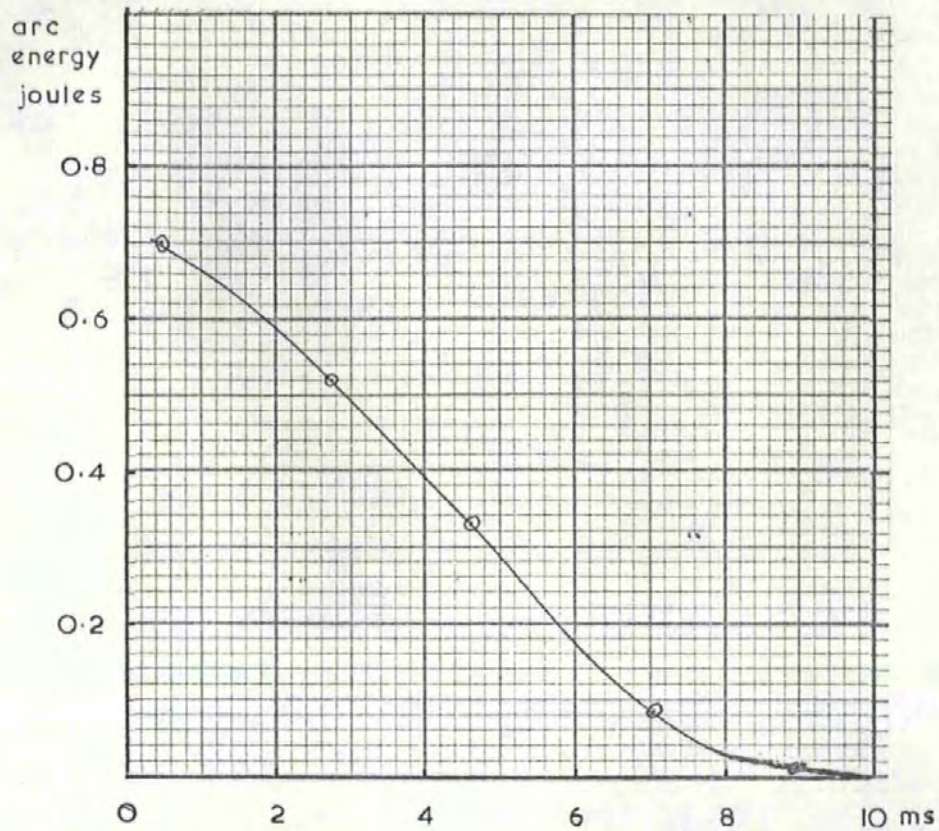
Fig. 48.   Arc energy/ignition point for an inductive load
            with cos ∅ = 0.58.

            This curve is of similar form to the one obtained
            for a 4 amp resistive load (Fig. 46).

Fig. 47 shows three of the arc voltage and current graphs obtained
with the switch contacts breaking an inductive load power factor of
cos $\emptyset$ = 0.5, the load current was 4 amps peak. The arc power graphs
shown in Fig. 47 and the arc energy in Fig. 48, appear similar in shape
and magnitude to those obtained using a resistive load, (Fig. 45 & 46).

In equation (13) the arc power is given as a function of the load
current of the circuit, no term for the supply voltage appears in this
equation. Hence although the current (i.e. arc current) is lagging the
supply voltage by some angle ϕ, the arc voltage is unaffected and is
in phase with the arc current, despite the fact that the supply voltage
will go through zero before the current. The arc extinguishes as on
resistive load, when the current decreases below I_m. The voltage across
the contacts after extinction will not be zero but some magnitude
depending on the power factor of the circuit, and of opposite polarity
to the arc voltage. For the current magnitudes and contact gaps
being dealt with here, the rate of rise of the dielectric strength of
the gap is sufficient to remove the possibility of restrike.

To complete this section of work a set of measurements was made with
the switch controlling a compressor motor, one of the normal applications
of the switch. The arc voltage and current waveforms, and the arc power
for three ignition points are shown in Fig. 49. The power factor of
this load was 0.5 at a current of ' 2.6 amps peak. Since the motor
contains magnetic material with a non-linear B/H curve it is likely
some harmonic content will be reflected in the current waveform
distorting it from a true sinusoidal shape. However this was not
visible in the results obtained and there was no observable effect
on the arc power or arc energy curves, Fig. 50.

Fig.49. Arc voltage and power curves for 3 ignition points on the a.c. half cycle. The area under the arc power curves represents the total arc energy.
Operating conditions : 240 V.rms, 50Hz, 2.6 A peak. Electrical load was a compressor motor, power factor cos ∅ = 0.5.
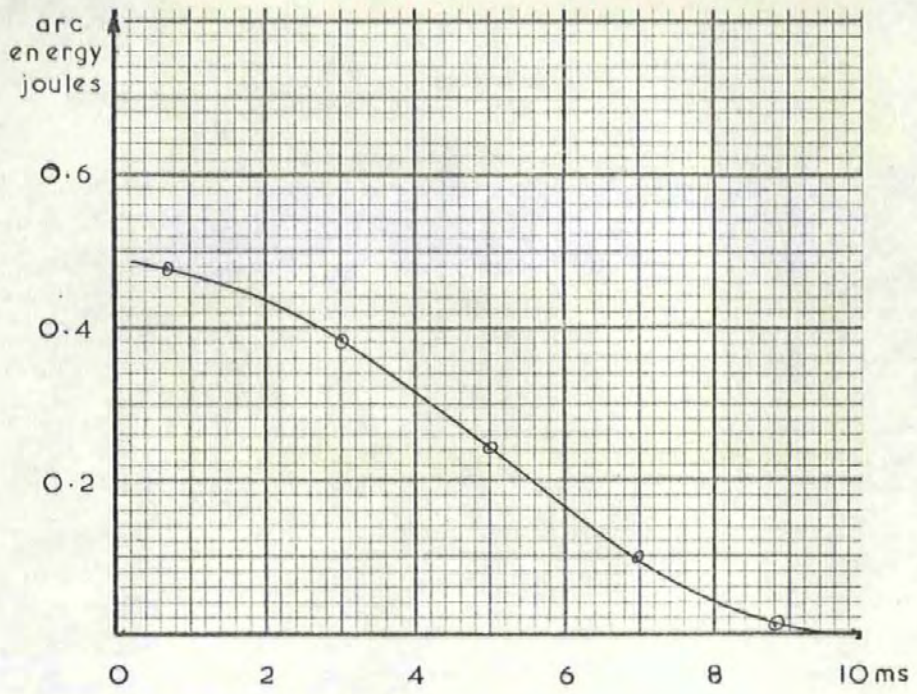
Fig. 50.   Arc energy/ignition point for switch contacts breaking
an electrical load comprising a compressor motor
with a power factor cos $\emptyset$ = 0.5.
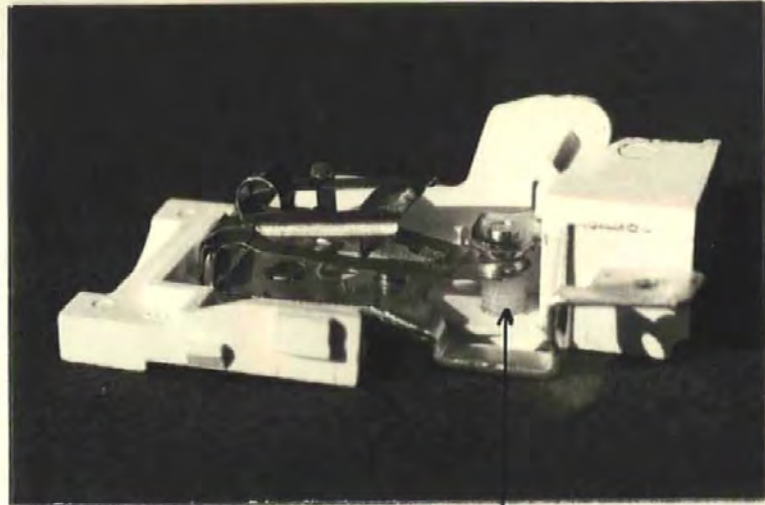
backstop

Fig. 51a. Switch with adjustable backstop inserted to limit contact travel.
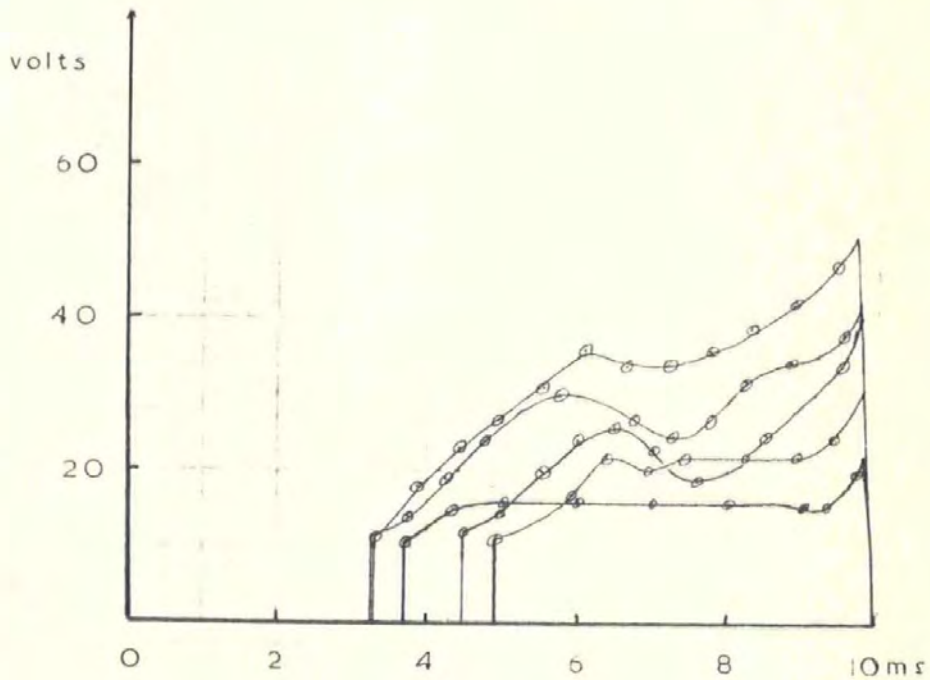
Fig. 51b. Arc voltage levels obtained for differing contact gaps. Operating conditions 240Vrms, 50Hz, 10 amps peak, resistive load.

arc
ignition
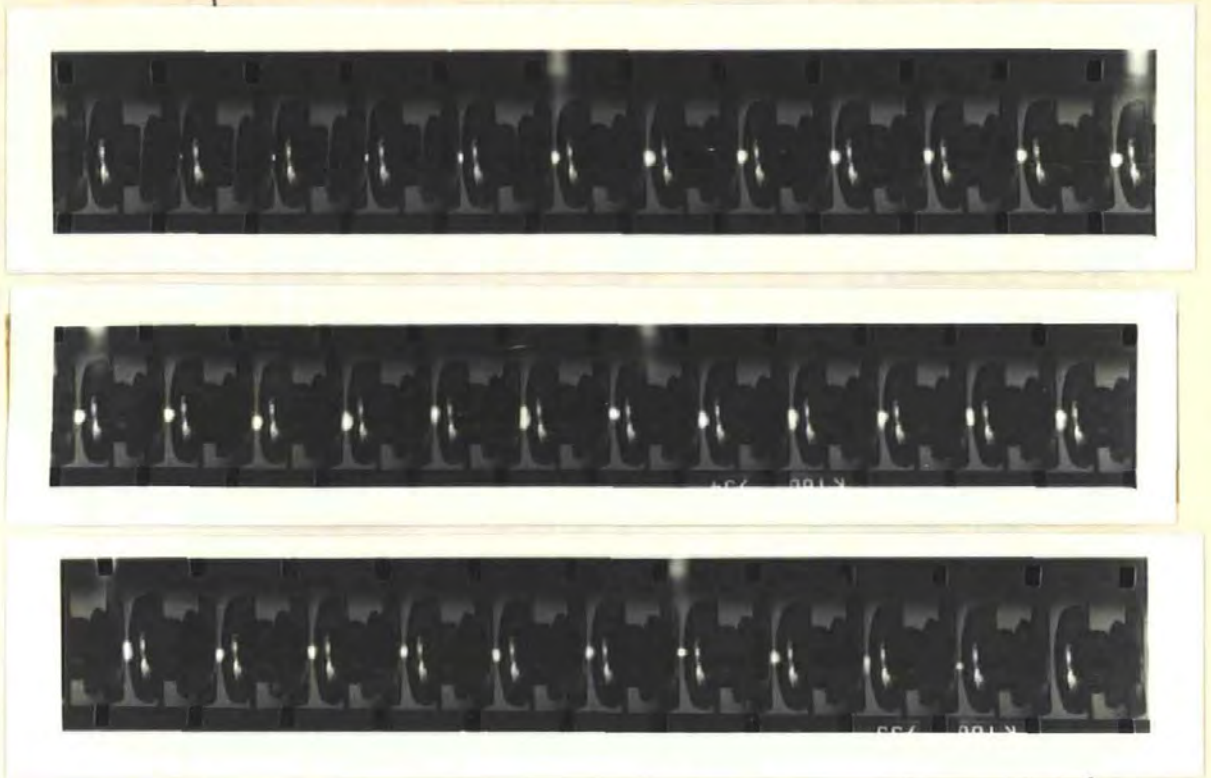
arc
extinction

Fig. 52a.   High speed film of switch contacts breaking on a.c.
            resistive load of 10 amp peak.   Switch contacts were
            limited to a travel of 0.15 mm by a backstop.   Arc duration
            is 6.4 ms.   Film speed was 6,200 frames/second.
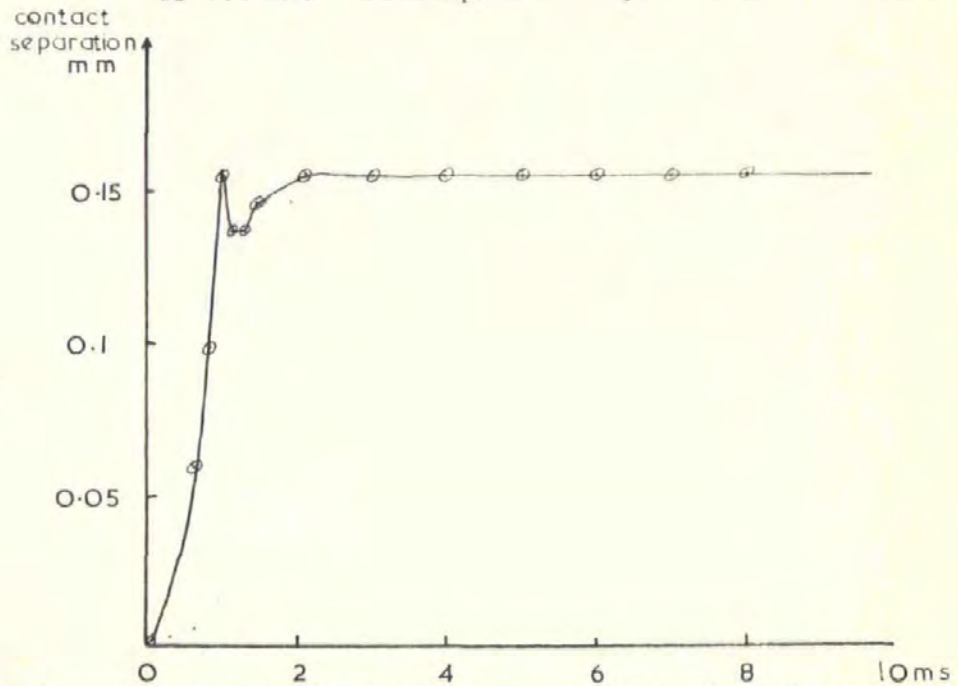
Fig. 52b.   Separation/time characteristic obtained from the
            high speed film shown above.   Contact bounces after
            first impact with backstop, before coming to rest.

- 132 -
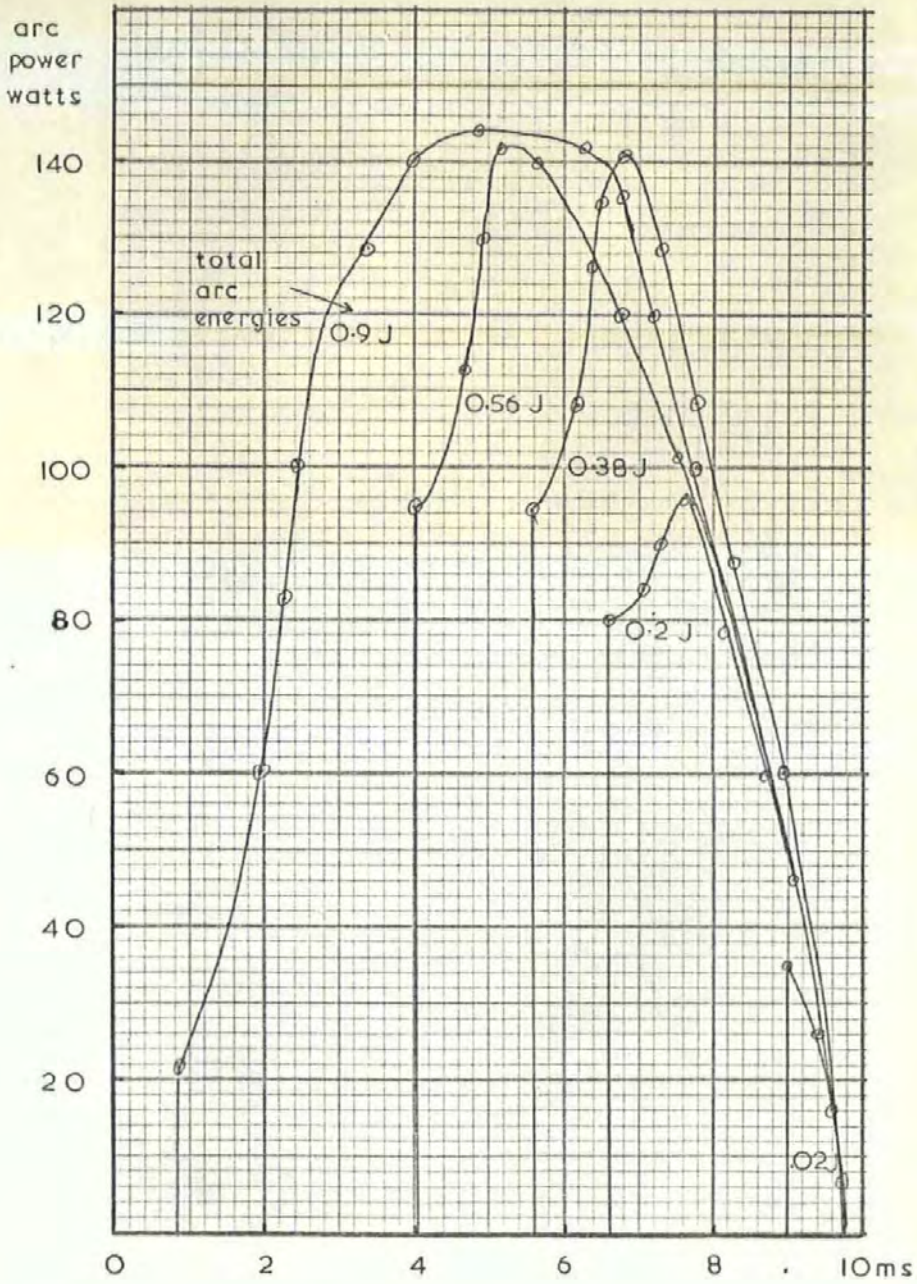
Fig. 53.   Arc power/ignition point for switch with contact
travel limited to 0.15 mm by the backstop.
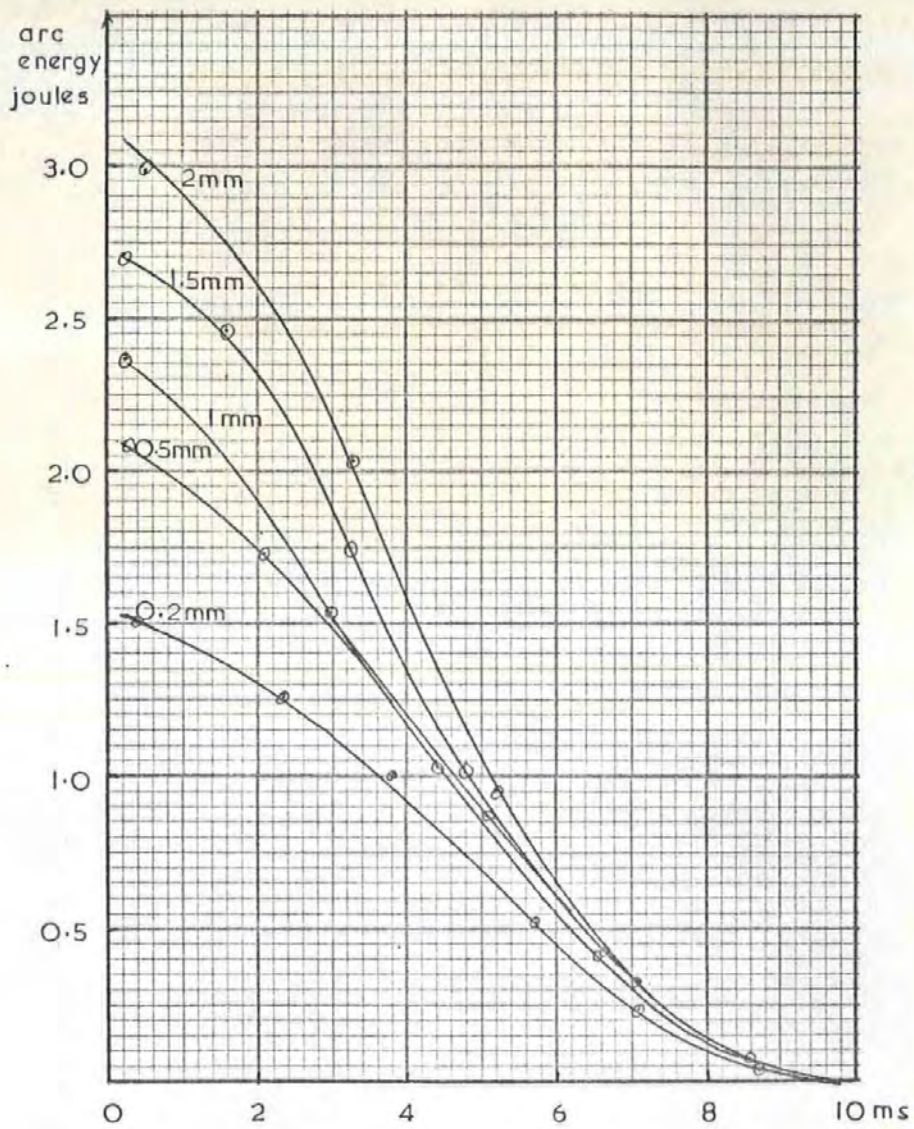
Fig. 54. Arc energy/ignition point. The effect of progressively decreasing the contact travel is a decrease in the energy dissipated in the arc.

Operating conditions 240Vrms, 50Hz, 15 amps peak, resistive load.

A non-sinusoidal current would not invalidate equations (11) or
(13) providing the function defining the current with harmonic content
was substituted for $\hat{I} \sin (\omega t + \theta)$. The arc power and arc energy
could then be calculated as usual.

The equation for arc power (equation 13) consists of the sum of
two terms:-

    i. $Em (\hat{I} \sin (\omega t + \theta))$

    ii. $\left(\dfrac{\lambda . \hat{I} \sin (\omega t + \theta)}{K} \right)^{\frac{2}{3}}$

The magnitude of term i. depends on:

    (a) $\hat{I} \sin (\omega t + \theta)$, which is a function of the electrical
           load being controlled and therefore pre-determined.

    (b) Em which is a function of the ionisation potential of
           the particular contact material. Hence a contact
           material with a lower value of Em would result in a lower
           value for the instantaneous arc power and therefore
           less energy dissipated in the arc.

However, Erk and Finke (6) in their studies of contact materials found
that silver cadmium oxide had one of the lowest minimum arc voltages
(10 - 12 volts) of the materials they tested, hence there appears to
be little room for improvement of this parameter.

The magnitude of term ii. depends on ℓ & K. K is a constant dependent
on contact material and the ambient gas hence in this situation is

predetermined. ℓ is determined by the mechanism of the switch and is a parameter which can be controlled by design. A reduction of 50% in ℓ will produce a decrease in the instantaneous arc power at any point, of about 40%, with a consequential reduction in arc energy.

4.7.2 Reduction of Arc Energy by limitation of the Contact gap

This then offers a way of using the mechanical performance of the switch to tailor the electrical characteristics for a minimum energy solution. To test this, some switches were modified as shown in Fig. 51a. by inserting an adjustable backstop underneath the moving contact. The switches were then arranged to switch the same a.c. load (10 amps peak) with each switch set to have a different contact gap. The differing arc voltage levels are shown in Fig. 51b. The high speed film of a switch with the backstop is shown in Fig. 52 together with a plot from the film. This shows that after the initial acceleration the contact impacts against the backstop and after a small amount of instability due to 'bounce'comes to rest with a contact gap in this case of 0.2 mm. This was the smallest contact gap selected and hence shows the greatest reduction in the arc voltage, which was constant for most of the arc duration at 15 - 16 volts, Fig. 41(b). The arc power graphs for this 0.2 mm gap are shown in Fig. 53, and Fig. 54, and compare: the arc energy at different ignition points for the differing contact gaps. It is seen that there is about a 40% decrease in the energy dissipated in the arc by reducing the contact gap from 2 mm for the unmodified switch to 0.2 mm for the switch with the backstop.

For the purposes of calculating the arc voltages and the arc power, equations (11) and (13) are still applicable. ℓ is now defined by

the contact gap to which the switch has been designed to open. To
take into account the first 1 m s of time during which the contact
is in motion, it was found by measurements from the high speed films
that, assuming a constant opening velocity of 0.15 m/s gave values
for the separation within 5% of the actual distance.

In section 4.9 the arc current i_t was stated as approximately equal
to $\hat{I} \sin (\omega t + \theta)$ by assuming $e_t << \hat{E} \sin (\omega t + \theta)$. This still
applies, in fact it is more valid to assume this here since e_t for
a switch with backstop is 50% less than the normal unmodified switch.
This is because the reduced arc length offers even less resistance
to the passage of current through the circuit.

4.8 Erosion due to the Break Arc

Introduction

The result of material being eroded by the arc from the contact surface is either:-

i. Transfer, i.e. material preferentially evaporated from one electrode and deposited on the other.

ii. Loss, i.e. material irrecoverably lost to the surroundings.

Transfer is clearly less damaging in the long term for switches operating on a.c. since the direction of transfer will alternate with the polarity of the contacts.

It has been stated by Hopkins et al (5) that material transfer due to the arc is generally the result of evaporation of material from one contact surface and deposition on the other as opposed to movement of metallic ions down the arc channel. In the light of this it is important to know how much energy is dissipated at the contact surfaces and how much is lost to the surroundings. The previous section has enabled the total energy in the arc discharge to be calculated from a knowledge of circuit and switch mechanism parameters. To continue this study, the possibility of identifying component energy parts absorbed by the anode and cathode which together comprise the total arc energy, will be considered.

As previously, this work will commence with the simple d.c. operating condition, followed by full wave rectified a.c., and then sinusoidal a.c. Finally the effect of reducing the contact travel on the erosion characteristics of the contact will be considered.

4.8.1 Erosion at break, using a d.c. resistive load

Photographs taken using the Scanning Electron Microscope of the anode and cathode surfaces have previously been shown in Figure 30. The photographs show a large crater on the anode surface 0.1 - 0.2 mm diameter, and many small pits on the cathode of diameter $1 - 5 \times 10^{-3}$ mm.

The various arcing processes were reviewed in section 2.4, so to define the arcing mechanisms here the erosion patterns must be matched to the known results of the different types of arcs. The high speed films give the arc length as about 1 mm at extinction with a duration of 2.0 m s. Hopkins et al have stated that the short arc is more efficient at removing material than the long arc, and is effective in producing crater-like erosion patterns on the anode. During the first few microseconds of arcing when the short arc only is present, the arc current is highest and all the current is carried by electrons which will liberate much heat at the anode. The crater observed here appears to be the result of just such concentrated heating of the surface. As the arc lengthens and the arc column and anode fall develop, some of the current is carried by positive ions which impact on the cathode and liberate some heat. Since the positive ions are more massive and hence slower moving than electrons they liberate less heat, also by the time they are contributing a significant part of the current flow there is much less current flowing through the arc. The small pits observed here on the cathode would result from ion bombardment of the surface.
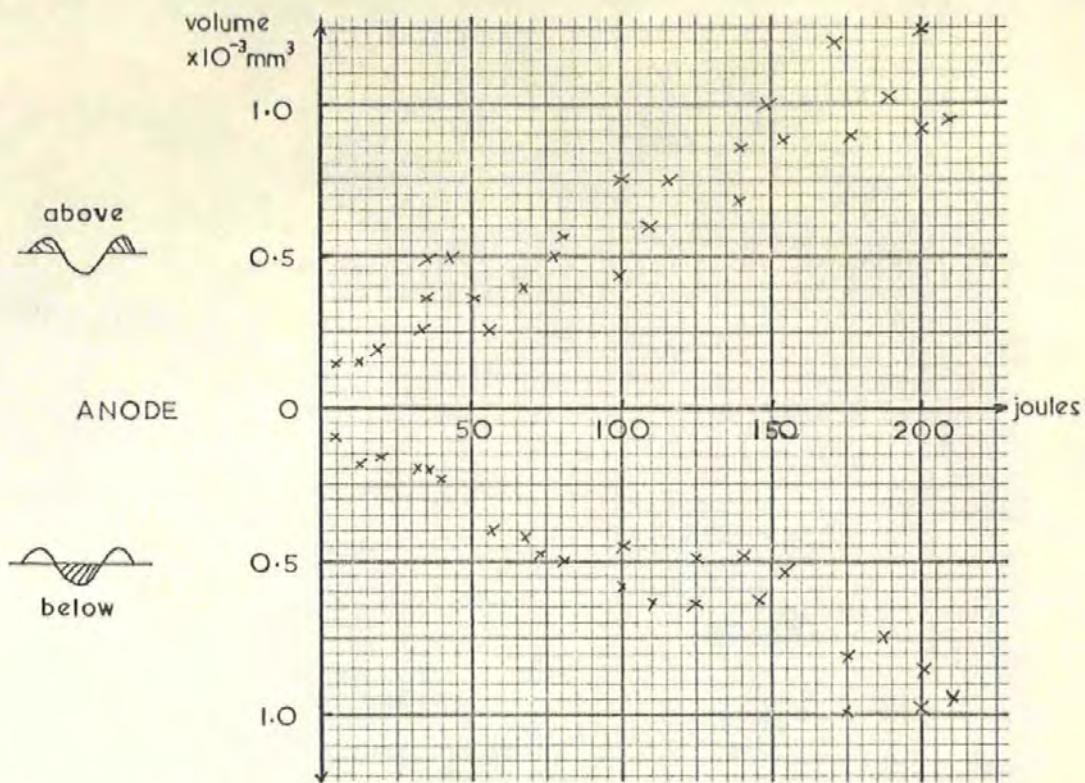
Fig. 55 . Graph of material displaced above and below the original surface
profile for the anode contact. The total arc energy was obtained
by sampling the transient recorders as the test proceeded.
Operating conditions: 40 volts, 8 amps d.c. resistive load,
break only operation.
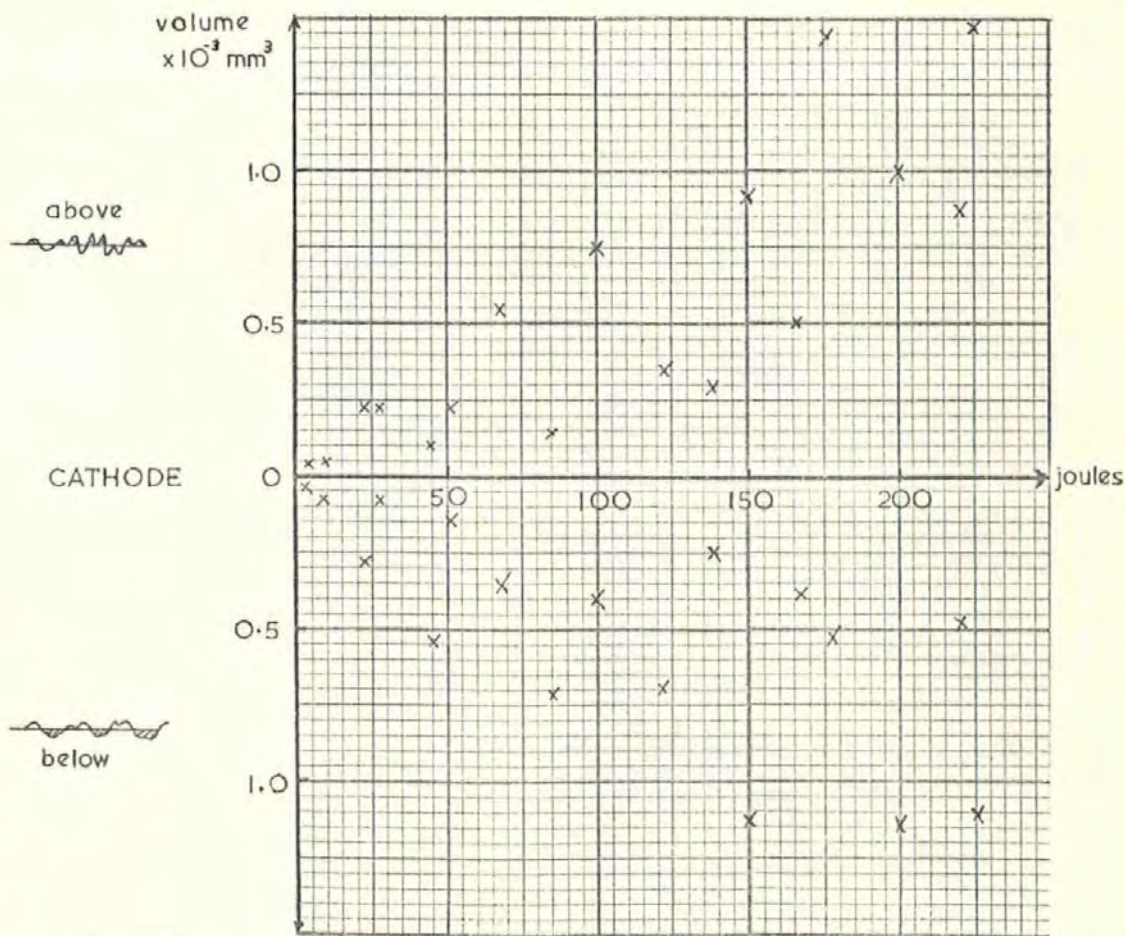
Fig. 56 . Graph of material displaced above and below the original surface
profile for the cathode contact. The electrode surface is
characterised by many small pits and protrusions.
Operating conditions as above.

Quantifying the results using the Talysurf plots gives the volumes of the anode craters in the range .015 to .025 x 10^{-3}mm^3 and to a first approximation the volume of material around the crater rim is of similar magnitude. There is no net measurable material movement after one operation from the cathode surface, just an even distribution of pits and spikes.

After one break operation it was difficult to quantitatively evaluate the erosion in terms of directional transfer so it was decided to perform more tests using the same circuit and investigate the erosion after predetermined numbers of multiple break operations. The duration of the tests were chosen as 50, 100, 250, 500, 1000, 2000 operations, after which the contacts were removed for examination on the S.E.M. and Talysurf.

An attempt was then made to present graphically the data obtained from the Talysurf as a representation of material redistribution on the electrode surfaces over multiple operations. Fig. 55 . shows the volume of material above and below the original surfaces profile plotted against total arc energy (or No. of operations) for the anode. The data obtained from measurements of the cathode surface recorded a greater degree of scatter, with the material above and below the surface profile much less clearly defined. The surface was characterised by an area of small pits and protrusions with larger pits in some places and larger build up of material in others. Since the effect of using the surface profile as a reference was less reliable it was difficult to categorise the material displacement, however, there appeared to be no preferential trend of material removal or material deposit.
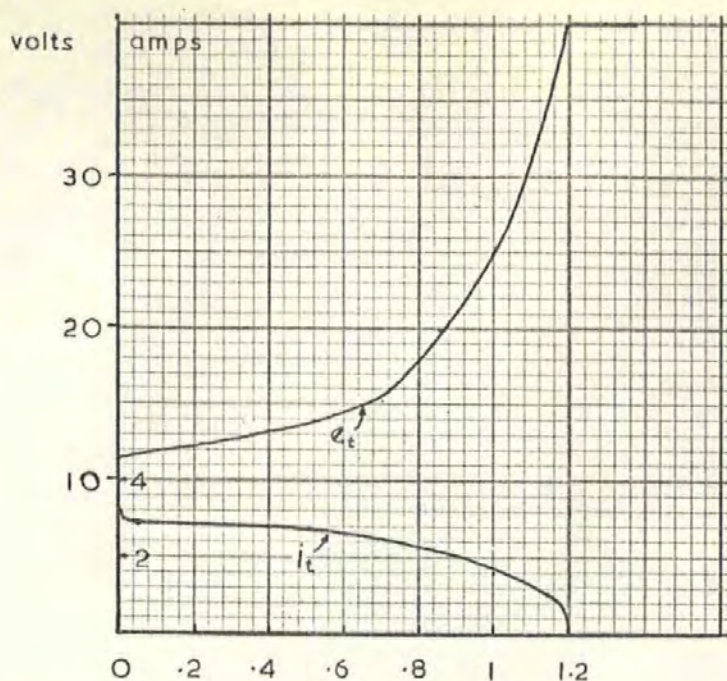
Fig. 57a.   Arc voltage and current transients occurring for switch contacts breaking a resistive load of 4 amps, dc, with a supply voltage of 40 volts.
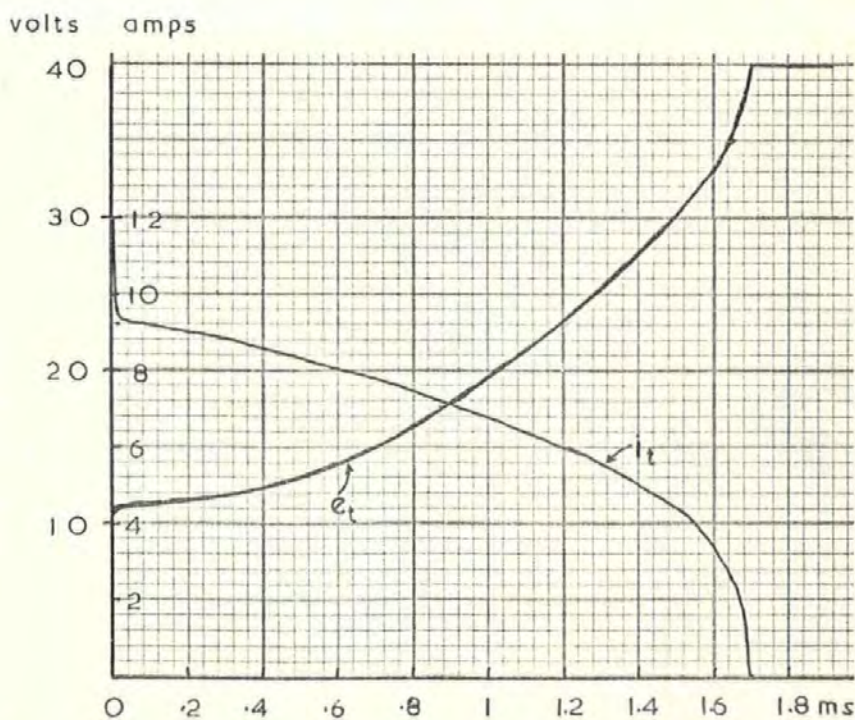
Fig 57b.   Arc voltage and current transients occurring for switch contacts breaking a resistive load of 12 amps, dc, with a supply voltage of 40 volts.

The current of 8 amps, d.c. was defined by Sato (11) as the region of transition current at which according to his results no net directional transfer of material occurred. He demonstrated that for silver cadium oxide contacts the direction of transfer of material was cathode to anode below 6 amps, and anode to cathode in the region of 10 amps. The applied voltage used by Sato was 40 V i.e. the same as used here, however, the opening velocity of his contacts was 63 mm/sec which gave an arc duration of about 15 m s, i.e. 7 x the duration using these toggle switches. Hence the energy dissipated in the arcs he was measuring would be considerably more than obtained here.

At first appearance the results of erosion obtained so far agree with Hopkins et al (5), who state that the initial stages of opening are dominated by the short a.c., i.e. anode loss by electron bombardment, followed by cathode loss due to ion bombardment as the arc length increases, and that the short arc is more efficient in removing material.

To try and clarify the erosion mechanisms taking place it was decided to perform some tests on the switch with the current magnitude well away from this transition region as defined by Sato. Keeping the supply voltage at 40 V, 4 amps. and 12 amps were chosen as the test currents. Five hundred operations were performed by a sample of switches breaking 4 amps or 12 amps, typical arc voltages and current transients are shown in Fig. 57(a) and (b). Examination of the surfaces on the Talysurf revealed the following :- (Figs. 58 and 59).

4 amp load

The cathode surface had a well defined area where material had been removed, i.e. volume of material removed from below original surface profile was much in excess of material deposited above it.

The anode had more material deposited above the surface profile than eroded from below it.

12 amp load

The cathode surface displayed a prominent build-up of material, there was no evidence of erosion of material below the original surface profile.

The anode surface had an area of material eroded from below the original profile which exceeded in volume the material deposited on the surface.

This is summarized and quantified in Fig. 58 and 59 using the Talysurf plots.

The deductions from these tests are:-

    i. At 40 V, 4 amps load, net material transfer is cathode to anode.

    ii. At 40 V, 12 amps load, net material transfer is anode to cathode.

    iii. At 40 V, 8 amps load, this is the transitional region and there is no net movement of material.

These results agree with Sato's reasoning and give an explanation why the first batch of measurements made at 8 amps were inconclusive.

Increasing the current from 4 amps to 12 amps means that:

    i. Arc length achieved before extinction will be increased.

    ii. Arc duration will be increased.

    iii. Total energy dissipated in the arc will be increased.
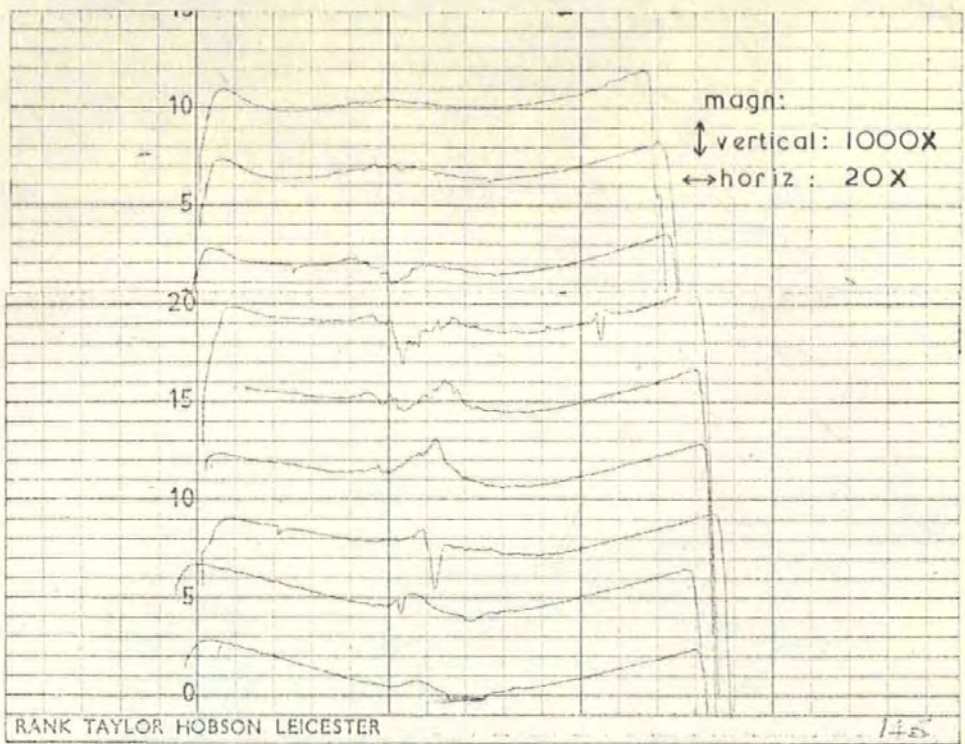
anode :   0.1 mm between traces
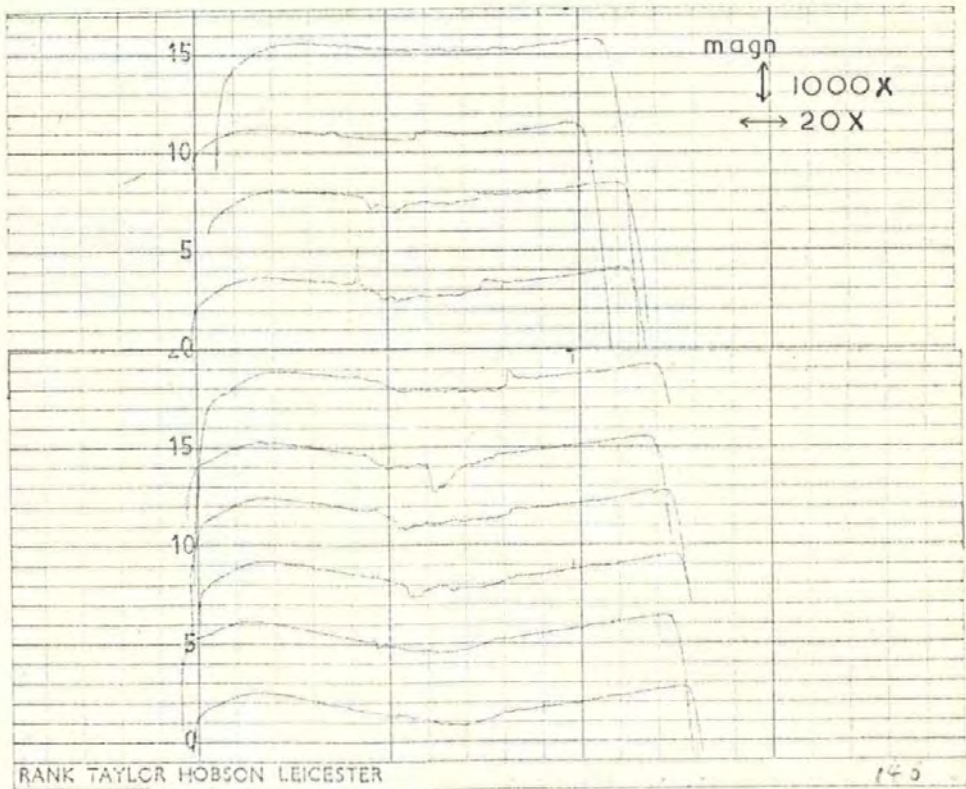
cathode: 0.1mm between traces

Fig. 58.   Talysurf profile traces of the anode and cathode contact
surfaces after performing 500 break only operations.
Operating conditions 40 volts, 4 amps, d.c. resistive load.

RANK TAYLOR HOBSON LEICESTER

magn: ↕1000x, ←→20x, 0.1mm between traces

anode

cathode

112/329   112/329

LOR HOBSON LEICESTER   LOR HOBSON LEICESTER
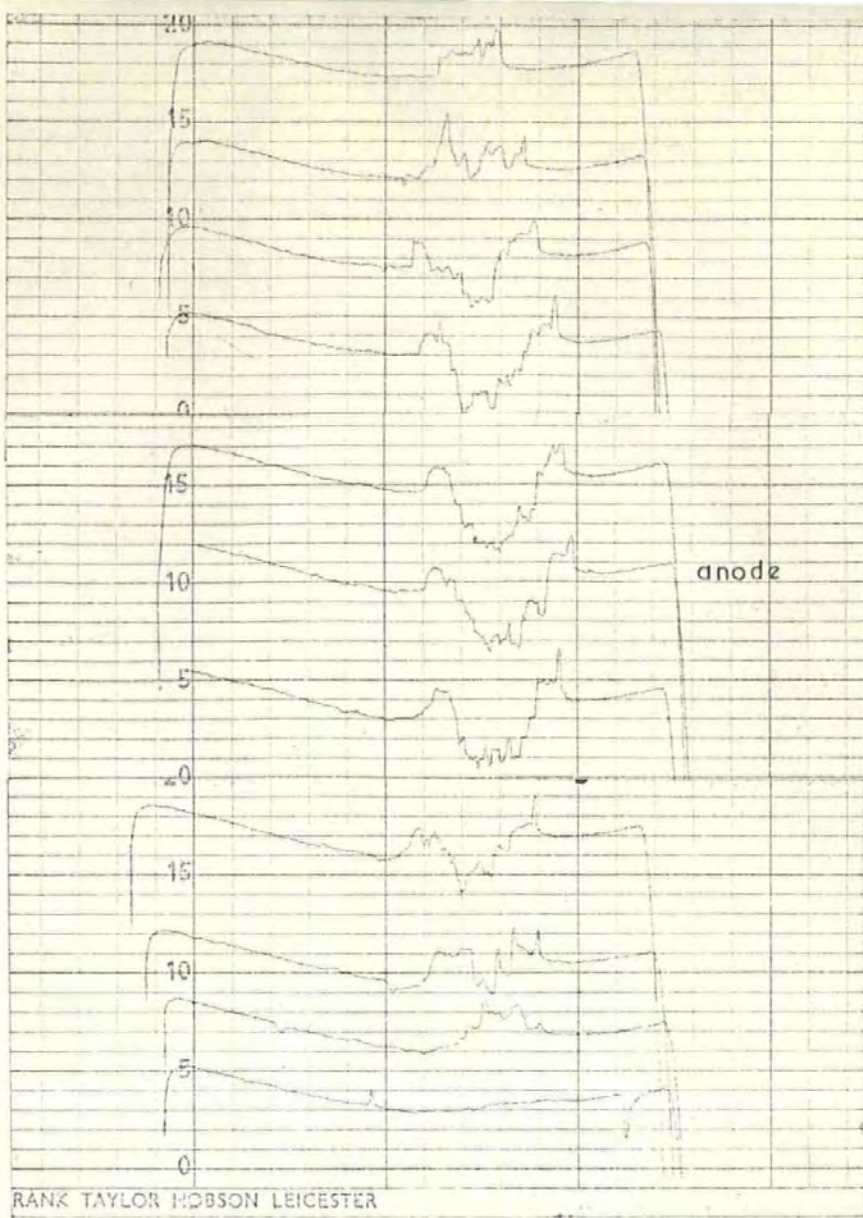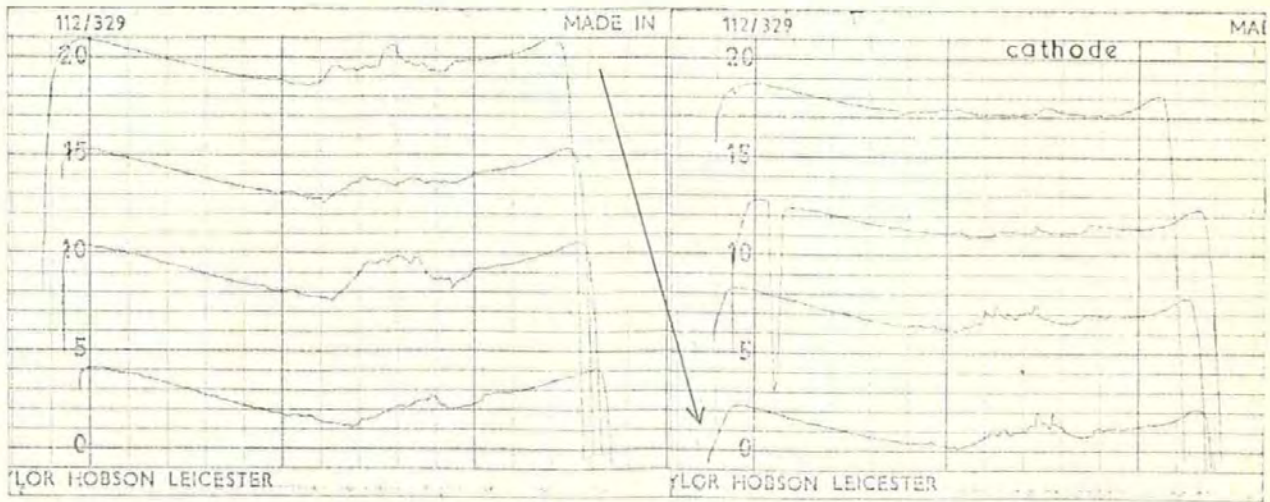
Fig. 59. Talysurf profile traces of the anode and cathode contact surfaces after performing 500 break only operations: operating conditions, 40 volts, 12 amps, d.c., resistive load.

- 146 -

The inference from these is that a greater volume of material will be involved in the displacement process which Figs. 58 and 59 show, due to the increase in energy and greater arc duration. However, this does not explain the directional change in the transfer of electrode material. The only other difference between the two operating conditions is the length the arc achieves before extinguishing.

In a paper by Capp (12), experimental evidence was produced to demonstrate that as the arc length increases the power conducted into the anode increases at a greater rate than the corresponding increase into the cathode. He concludes that the reason for this is that the anode fall voltage increases with length at a greater rate than the cathode fall. For the purpose of calculation he assumed that the cathode fall remains constant with increase of arc length and that any increase in the power conducted into the cathode was a result of increased power dissipation in the arc column, as it lengthened, being thermally conducted to the cathode.

This proposition offers an explanation of the so-called transition region observed by Sato. When the contact separation exceeds the mean free path length of electron ($\sim 10^{-3}$mm) i.e. they are no longer crossing the gap and bombarding the anode directly, most of the voltage of the arc constitutes the cathode fall. In this case for silver cadmium oxide the minimum arc voltage is about 11 volts and 8 volts of this is dropped across the cathode fall, i.e. within a distance of 4×10^{-5} mm, according to von Engel (13). Hence while the arc is of short length, most of the power dissipated in the arc is dissipated very near to the cathode surface which will therefore receive more energy than the anode. It is more likely therefore

short
arc

mean
free $\left(10^{-3}\,mm\right)$
path

motion

i

---

40 volts
4 amps

0.5 mm

$$\int_0^T V_A . i_t\,dt \; < \; \int_0^T V_c . i_t\,dt$$

motion

ii

---

40 volts
8 amps

0.9 mm

$$\int_0^T V_A . i_t\,dt \; = \; \int_0^T V_c . i_t\,dt$$

iii

---

40 volts
12 amps

>1 mm

$$\int_0^T V_A . i_t\,dt \; > \; \int_0^T V_c . i_t\,dt$$

iv
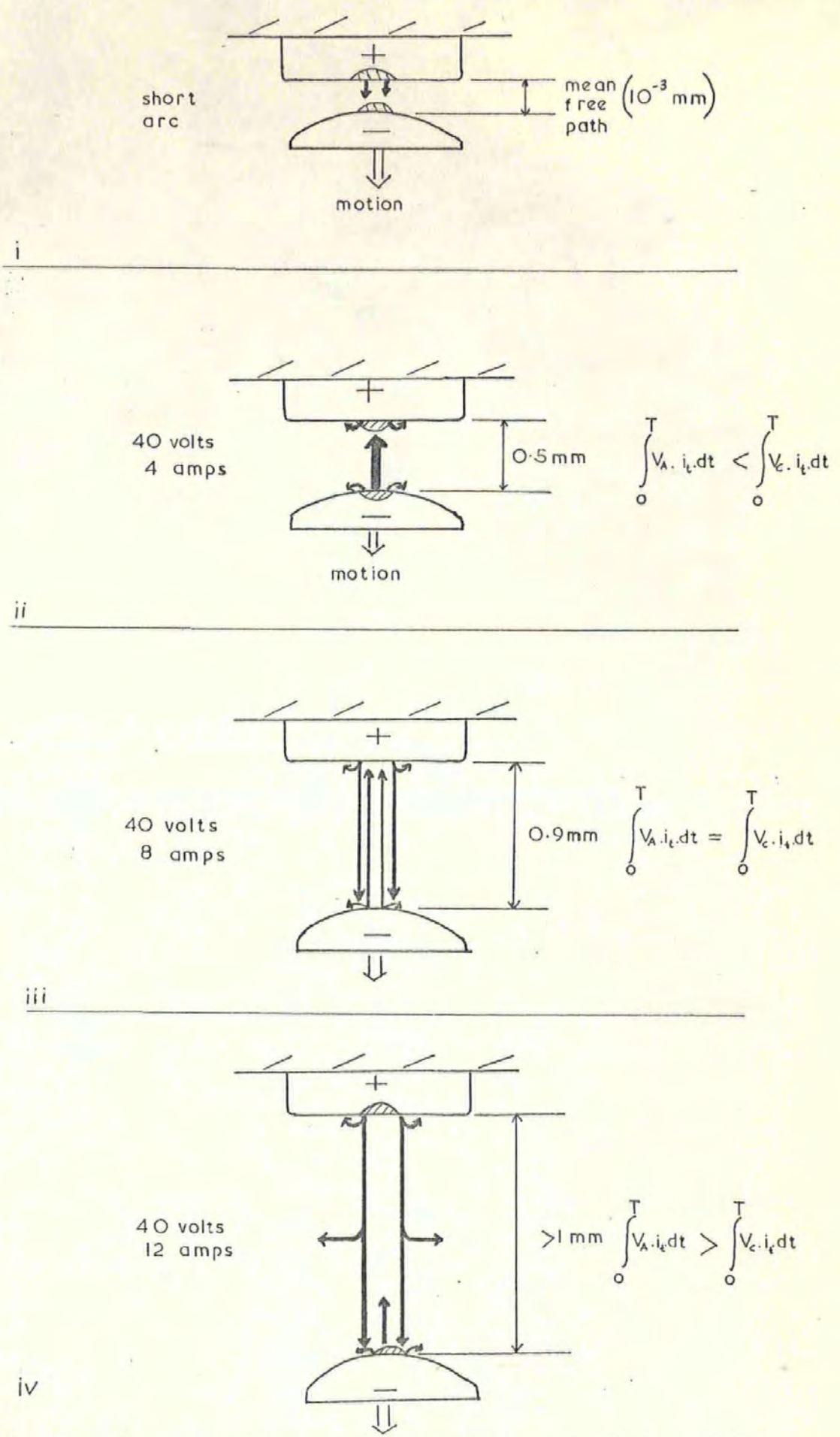
Fig. 60.   Dependence of the transfer direction on operating conditions.
   i.   Short arc transfer   :   Anode to Cathode.
   ii.   40 volts 4 amps   :   Cathode to Anode
   iii. 40 volts 8 amps: Transition region: Material movement
         in both directions.   No net transfer.
   iv.   40 volts 12 amps   :   Anode to Cathode.

- 148 -
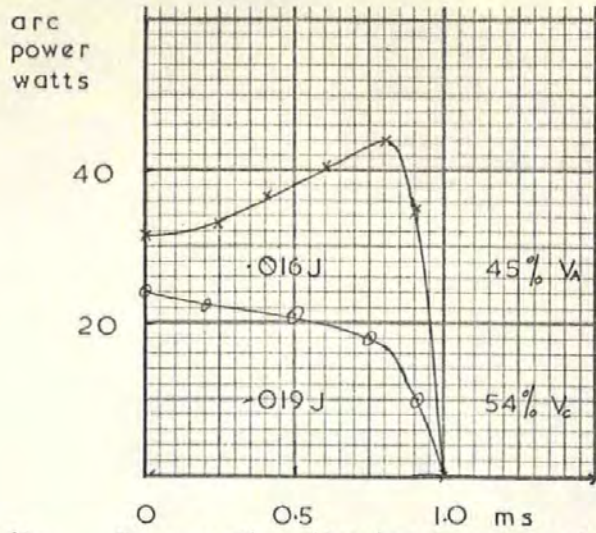
Fig. 61a.   Energy distribution between the anode and
cathode for operating conditions of 40 volts
d.c. 4 amp resistive load.
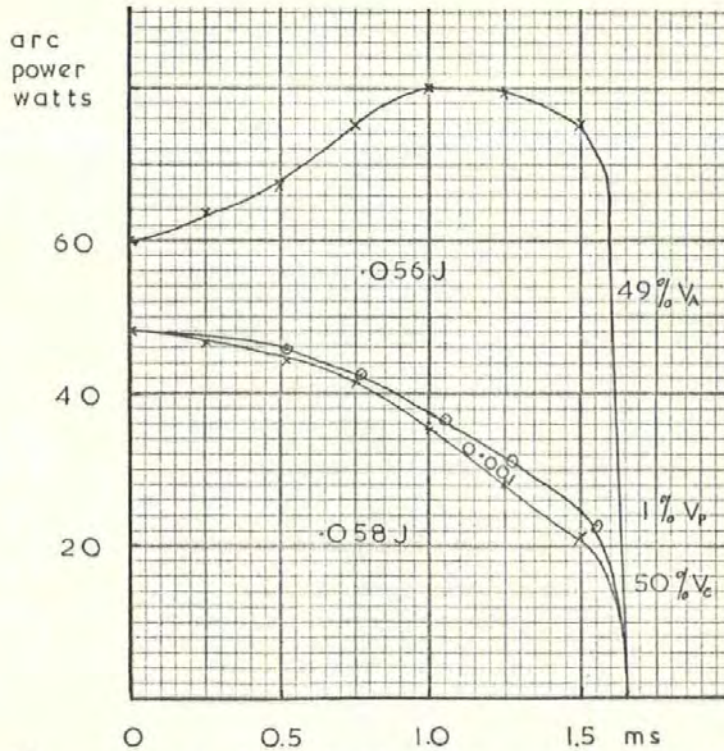
Fig. 61b.   Energy distribution between anode and cathode
and column, for operating conditions of 40 volts
d.c., 8 amps resistive load.
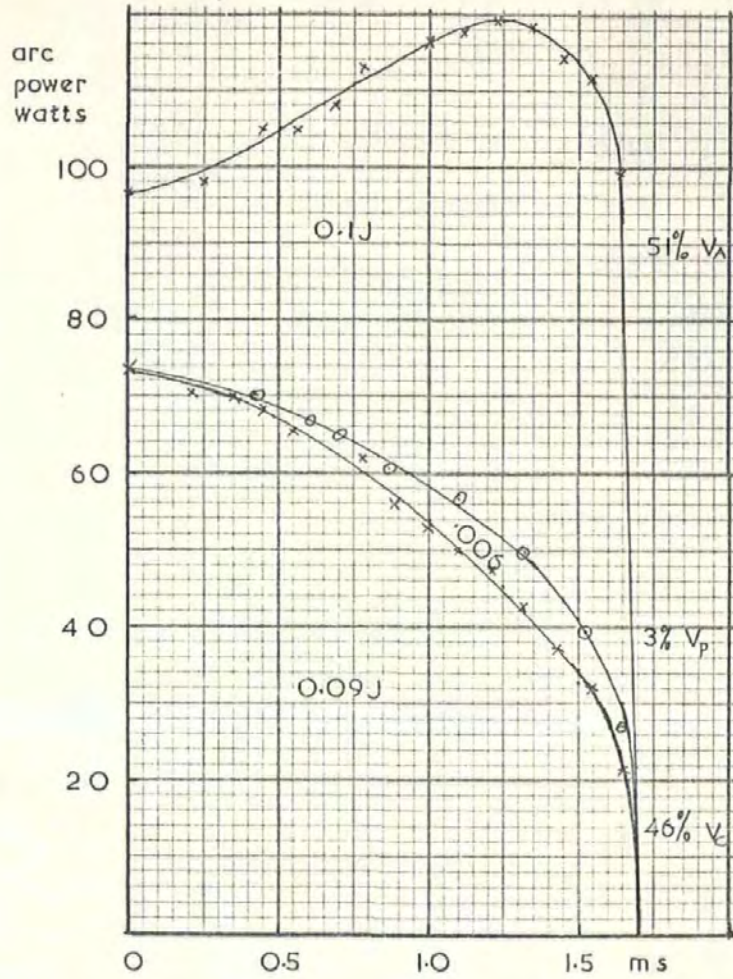
Fig. 61c. Energy distribution between anode, cathode and column for operating conditions of 40 volts d.c., 12 amps resistive load.

that material will be evaporated from the cathode and deposited on the anode at this stage of arc growth.

As the arc lengthens the column develops with a voltage gradient across it dependent upon the gas in which the arc exists. For air at atmospheric pressure this gradient is about 20 V/cm at a current of 10 amps (Farrell, 14). The remainder of the voltage is dropped across the anode fall, and it is this voltage according to Capp which increases at a greater rate than the column voltage and the cathode fall voltage.

Hence the arc will eventually reach a length where there is as much power dissipated in the anode fall as in the cathode fall. This is the transition region as defined by Sato, and for a 40 volts supply, occurs when the load current is around 6 - 8 amps. Since the energy received by both electrodes is about the same, and the contacts are both made of the same material, the erosion from each contact will be of similar magnitude, with the likelihood of material transfer in both directions but at different times during the arc life.

As the arc continues to lengthen, it reaches a point where the anode fall exceeds the cathode fall and more energy is directed into the anode than the cathode. Depending on the time duration while the arc is in this state there will be more material eroded from the anode than from the cathode and the net transfer will be anode to cathode.

Fig. 60 shows schematically the various phases that the arc passes through before extinction. After the initial short arc the condition for cathode loss to be predominant is:

$$\int_0^T V_{a_t} \, i_t \, dt < \int_0^T V_c \, i_t \, dt$$

where V_a is the anode fall at time t.
where V_c is the cathode fall (assumed constant)
i_t is the arc current
T is the arc duration.

For there to be no net transfer in a particular direction

$$\int_0^T V_{a_t} \, i_t \, dt = \int_0^T V_c \, i_t \, dt$$

For anode loss to predominate

$$\int_0^T V_{a_t} \, i_t \, dt > V_c \int_0^T i_t \, dt$$

To complete the analysis, the energy dissipated in the arc column must be taken into account, although for the operating conditions examined so far this is small due to the small voltage drop across the column compared to the fall voltages.

For the results measured to date the values of the integrals detailed above have been calculated and are shown in Fig. 60. For the 40 V, 4 amp operating conditions (Fig. 61a) it is seen that the cathode fall has 9% more energy dissipated in it than the anode fall. The voltage drop across the column is small for this case and has not been plotted.

Fig. 61b shows the energy distribution for the arc obtained when breaking a 40 V, 8 amp load, i.e. the transition region. As predicted the values of energy dissipated in the electrode fall regions are about equal, 49% for the anode, 50% for the cathode with about 1% dissipated in the column.
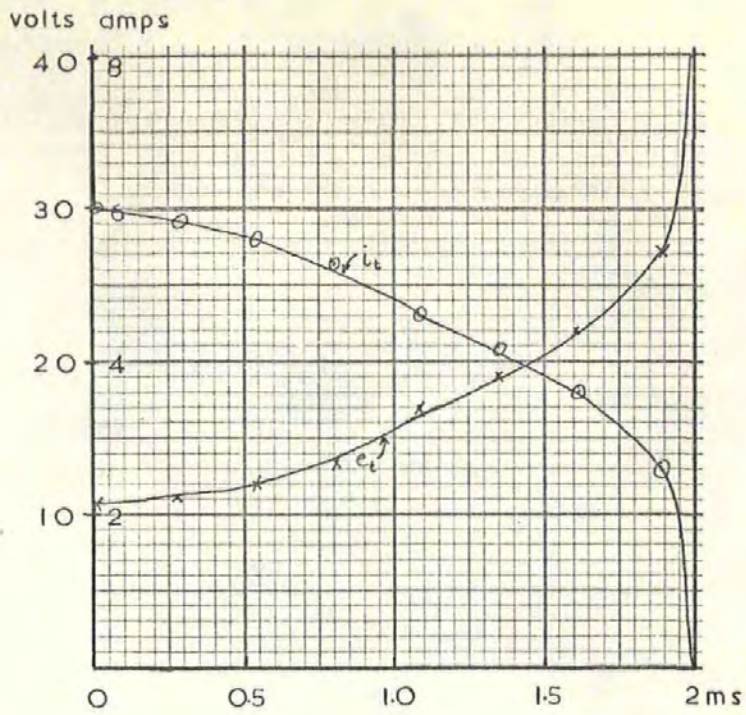
Fig. 62a.   Arc voltage and current transient occurring
for contacts breaking an 8 amp resistive load
with a supply voltage of 40 volts dc.
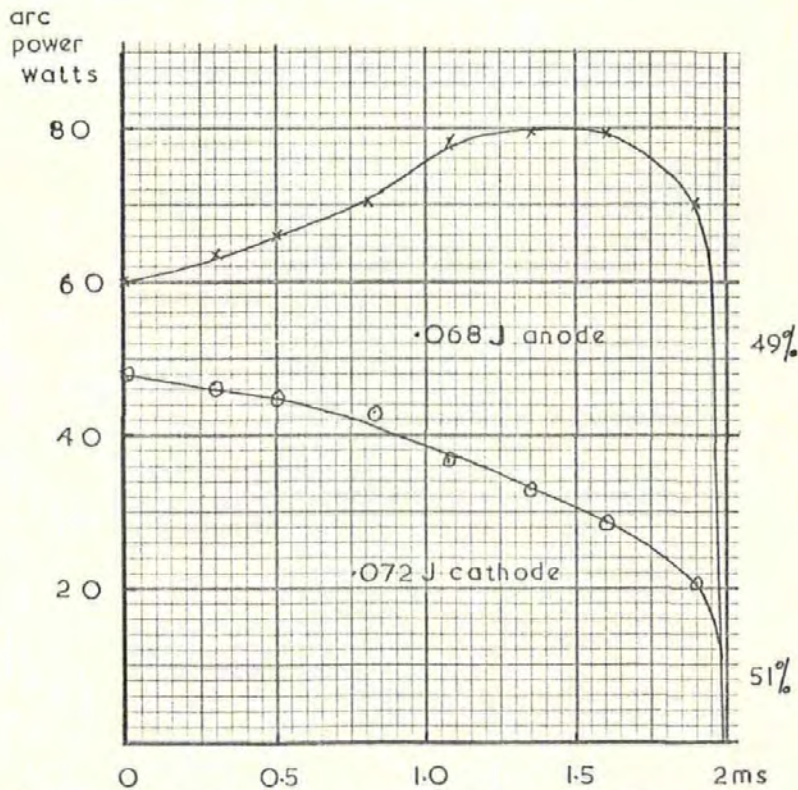
Fig. 62b.   Arc power curve showing how the arc energy
is divided between the two electrodes.
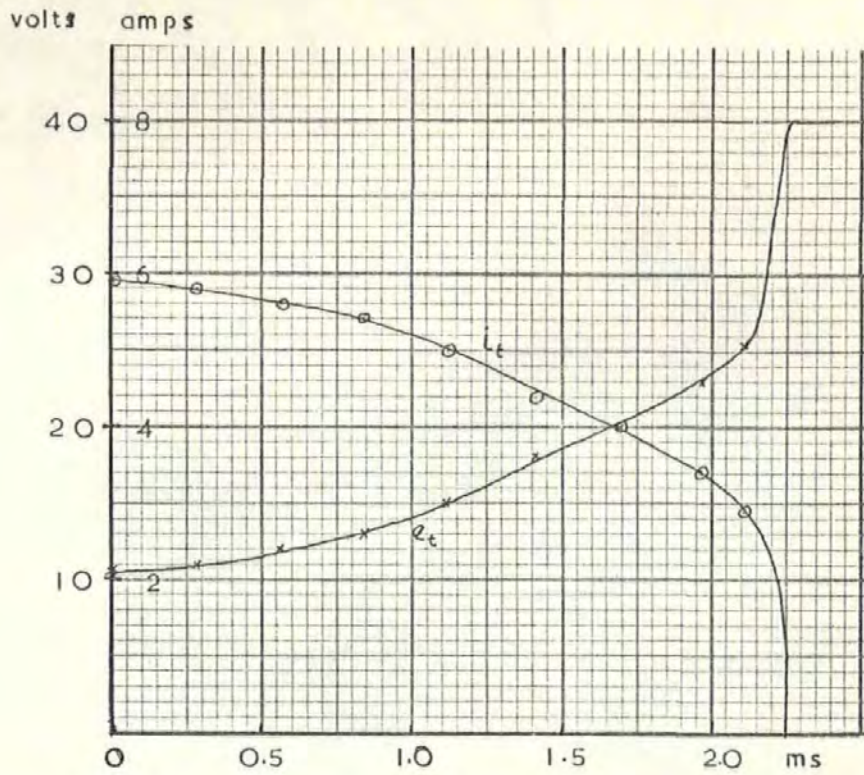Cathode 51%
Anode 49%
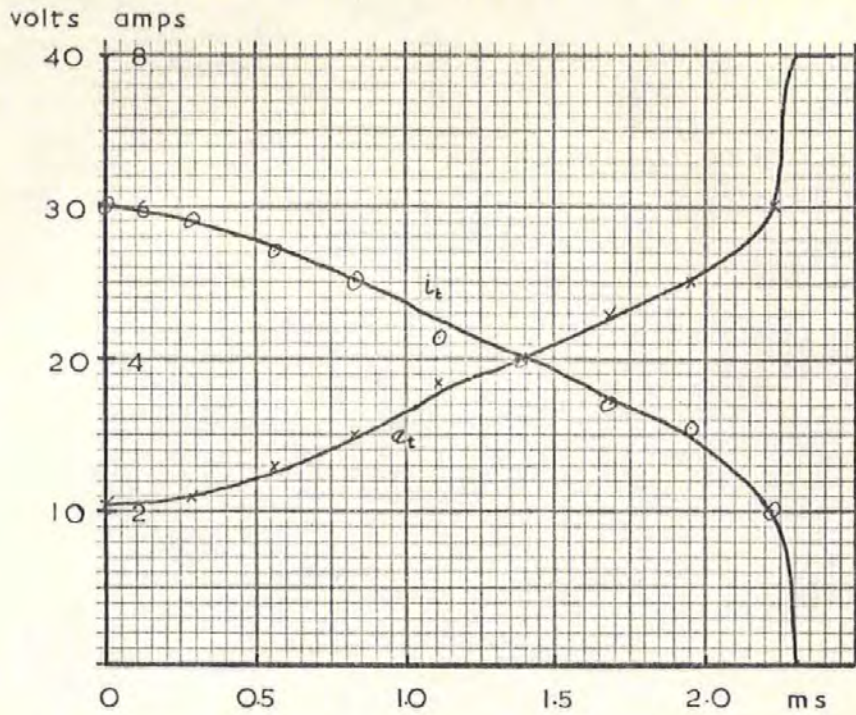
Fig. 63a.   Arc voltage and current transients:
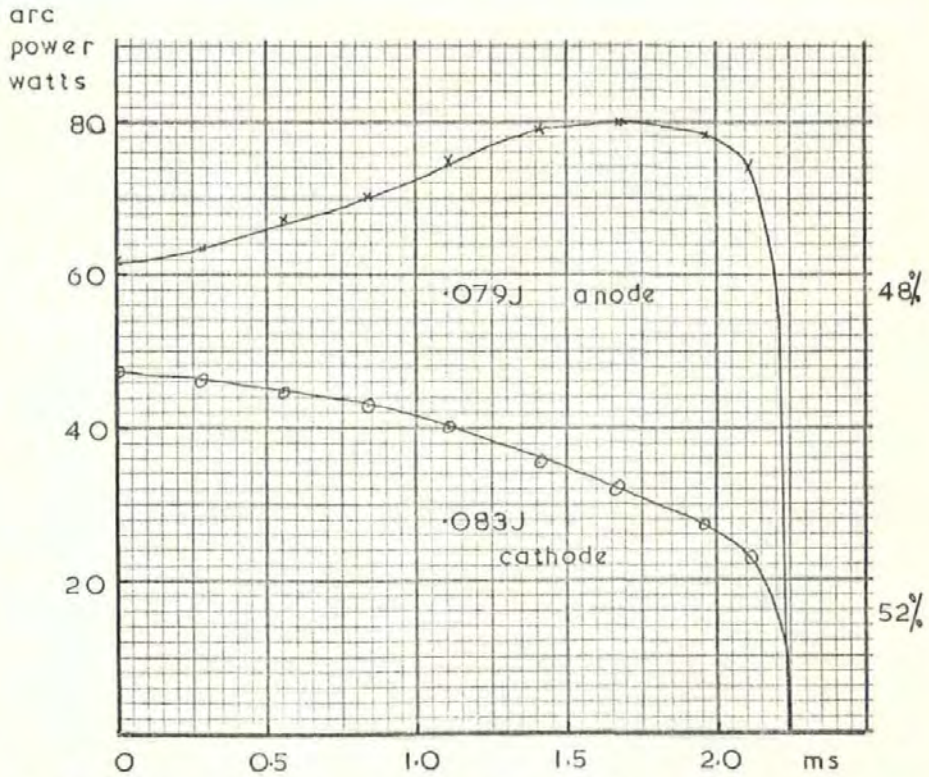   Operating conditions as Fig. 62.
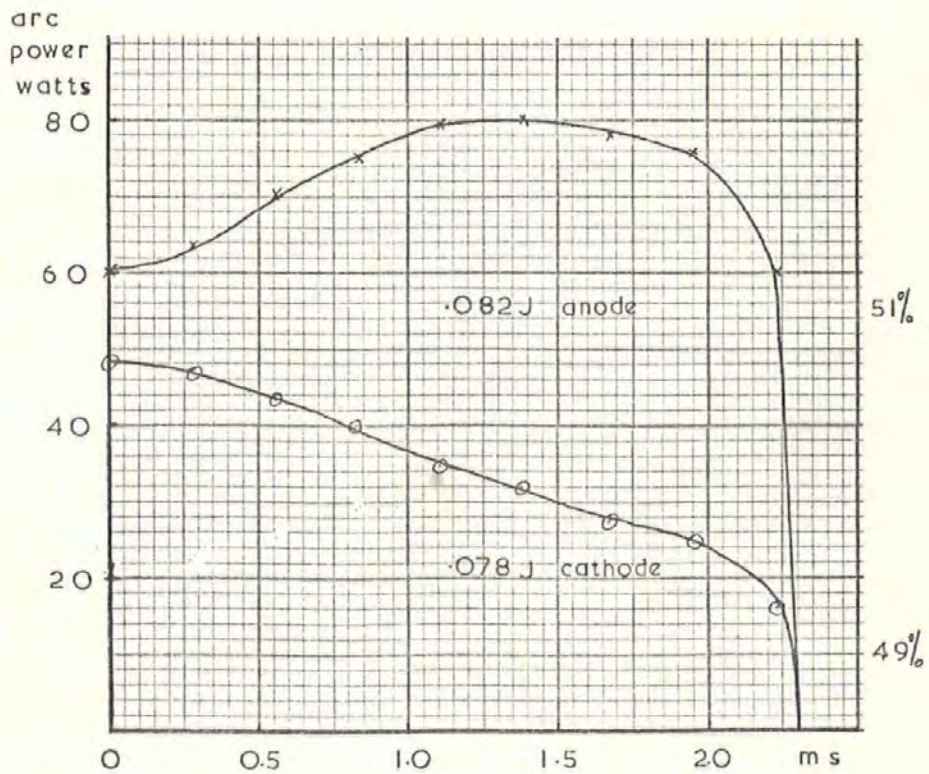
Fig. 63b.   Arc Power curve showing how the arc energy is
             divided between the two electrodes.
             Cathode 49%
             Anode 51%

Fig. 64a.   Arc voltage and current transients:
Operating conditions as Fig. 62.

Fig. 64b.   Arc Power curves showing how the arc energy is
divided between the two electrodes.

The curves for the 40 V, 12 amp operating conditions are shown in Fig. 61c. Here the arc has sufficient duration for the length to increase to a point where the anode fall exceeds the cathode fall with the result that the anode receives more energy than the cathode. Since the arc length is still small compared to the contact diameter the energy dissipated in the arc column can be assumed to be absorbed by the electrode in equal quantities so for this latter case the anode receives 52% of the total arc energy and the cathode 48%.

It is clear from these measurements that the transition region depends not only on whether the arc exceeds a certain length, but also on the velocity at which the length of the arc is increasing. For example, for the 40 volt, 12 amp operating conditions the energy dissipated in the anode fall only just exceeds that of the cathode fall (4% more). This is due to the fact that the opening velocity of these switches is not constant, and initially is of the order of 0.1 m/s. Since by the time the anode fall voltage has exceeded the cathode fall, the opening velocity has risen to 1 m/s. the arc will exist (for this operating condition) with $V_a > V_c$ for less time than when $V_c > V_a$. Hence it would be expected that the transfer of material from anode to cathode per operation would be small. From the Talysurf traces shown in Fig. 59. which were taken after 500 operations at 40V 12 amps the transfer rate is calculated as 3.4×10^{-6} mm^3/operation, (+ or - 10%).

Now that the erosion mechanism has been clarified the results contributing to the graphs of erosion/energy (or number of operations) Fig. 56. can be more meaningfully interpreted. Figs. 62-64 show three sets of arc voltage/current oscillograph traces and arc power

- 156 -

curves selected from those recorded. All the switches (except the three dealt with later) had total arc energies in the range 0.14 - 0.16 joules/operation, so these three are typical sets of results. The distribution of the energy with regards to the anode and cathode arcs:- 49% anode, 51% cathode for Fig. 62b., 51% anode, 49% cathode for Fig. 63b., 48% anode, 52 cathode for Fig. 64B., i.e. all grouped around the 50% division mark. The resulting erosion trend, which was sometimes anode loss slightly the greater, other times cathode loss, for the 8 amp operating condition is thought to be the result of this equilibrium distribution of energy.

Of the sample of fifty switches used to obtain the data at 40 V 8 amps for Fig. 56, there were three which gave consistently different results when compared to the rest. These three had dominant anode gain and cathode loss erosion characteristic which was significantly differently from all the other results. A typical Talysurf trace of one of the anode electrodes is shown in Fig. 65. When compiling the graph of Fig. 56 these three sets of data were ignored as being spurious, however, closer inspection of their voltage and current oscillograph, and opening characteristics reveals that they have a similarity. All three have a slower initial acceleration than the rest of the switches tested. The result of this can be seen in the voltage and current oscillographs, Fig. 66. The arc voltage is held at a low value for a large proportion of the arc duration, i.e. for a 3.5 ms arc the arc voltage doesn't rise significantly until 2.5 ms have elapsed; correspondingly the arc current stays at a higher value. The result of this is seen in Fig. 66. More energy, (16% more), is dissipated at the cathode than at the anode, so the erosion characteristic would be predicted as being cathode to anode.

magn: ↕ 1000x , ↔ 20x , 0.1mm between traces
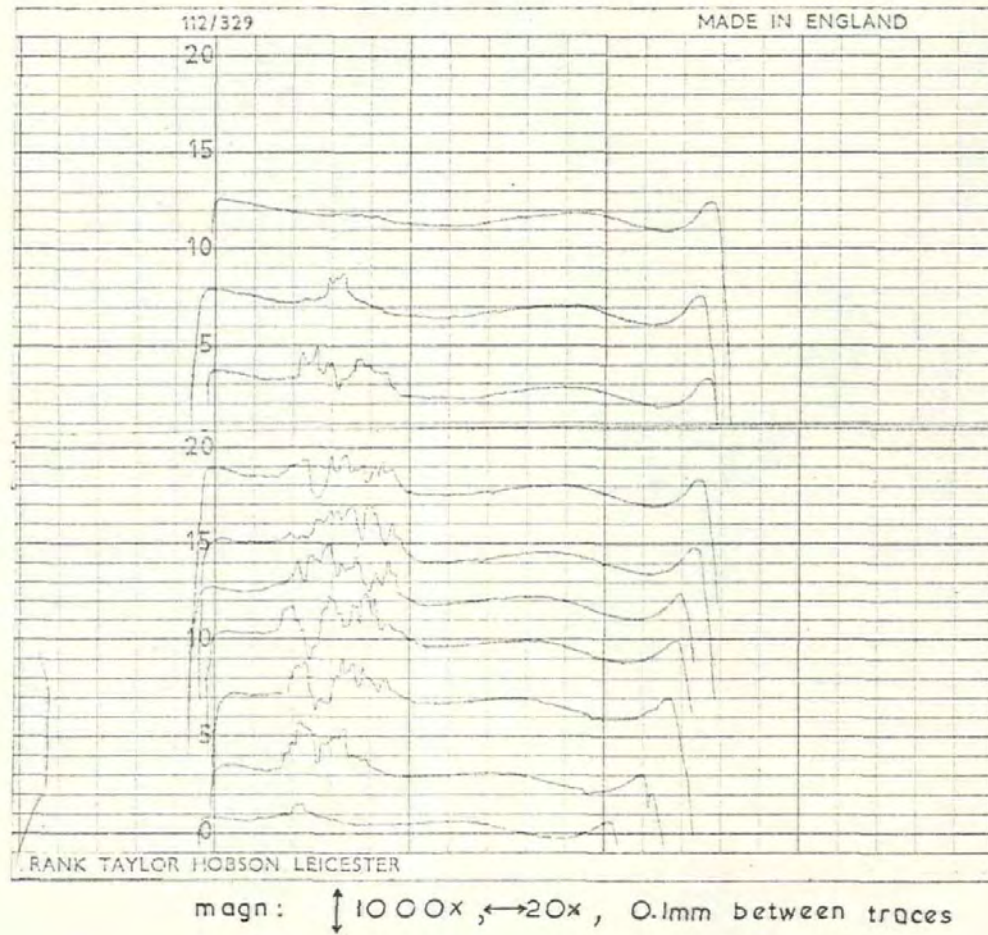
Fig. 65.   Talysurf profile trace of the anode contact of a slower operating switch after 250 operations breaking a load of 8 amps resistive, supply voltage 40 volts d.c.
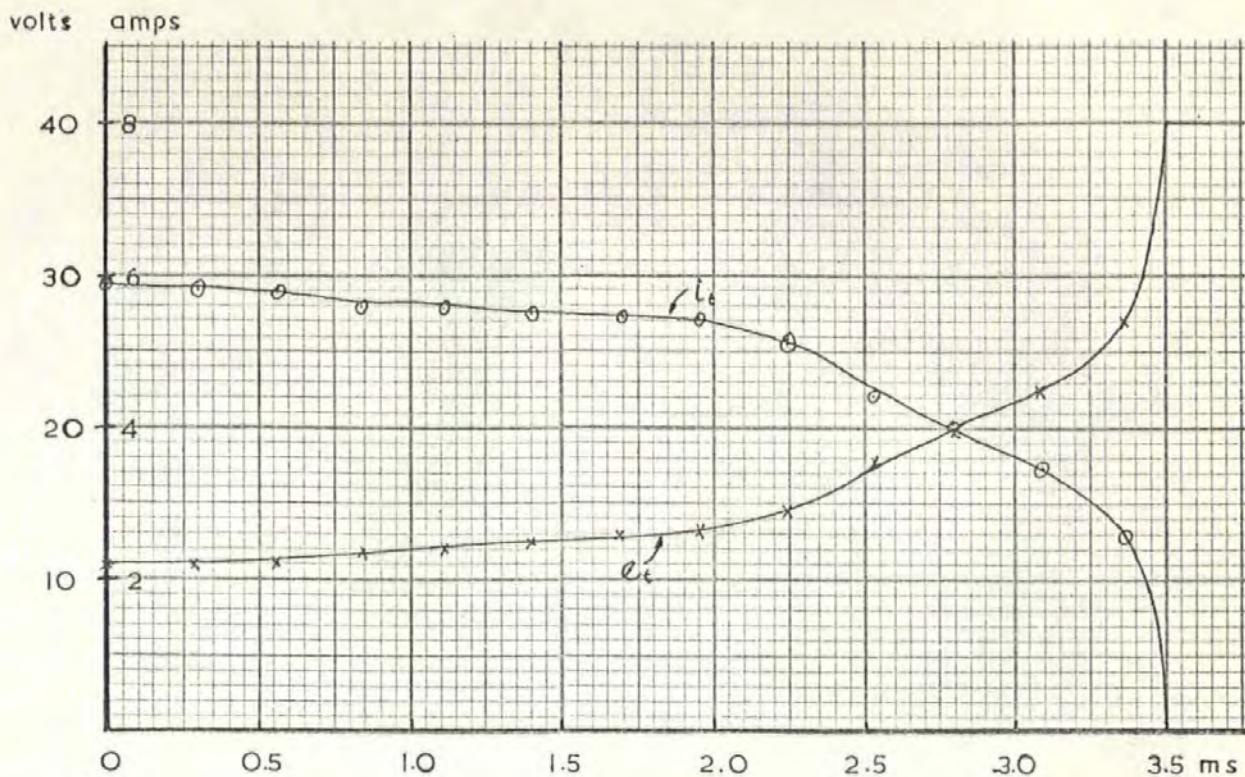
Fig. 66a. Arc voltage and current trace for a slower opening switch.
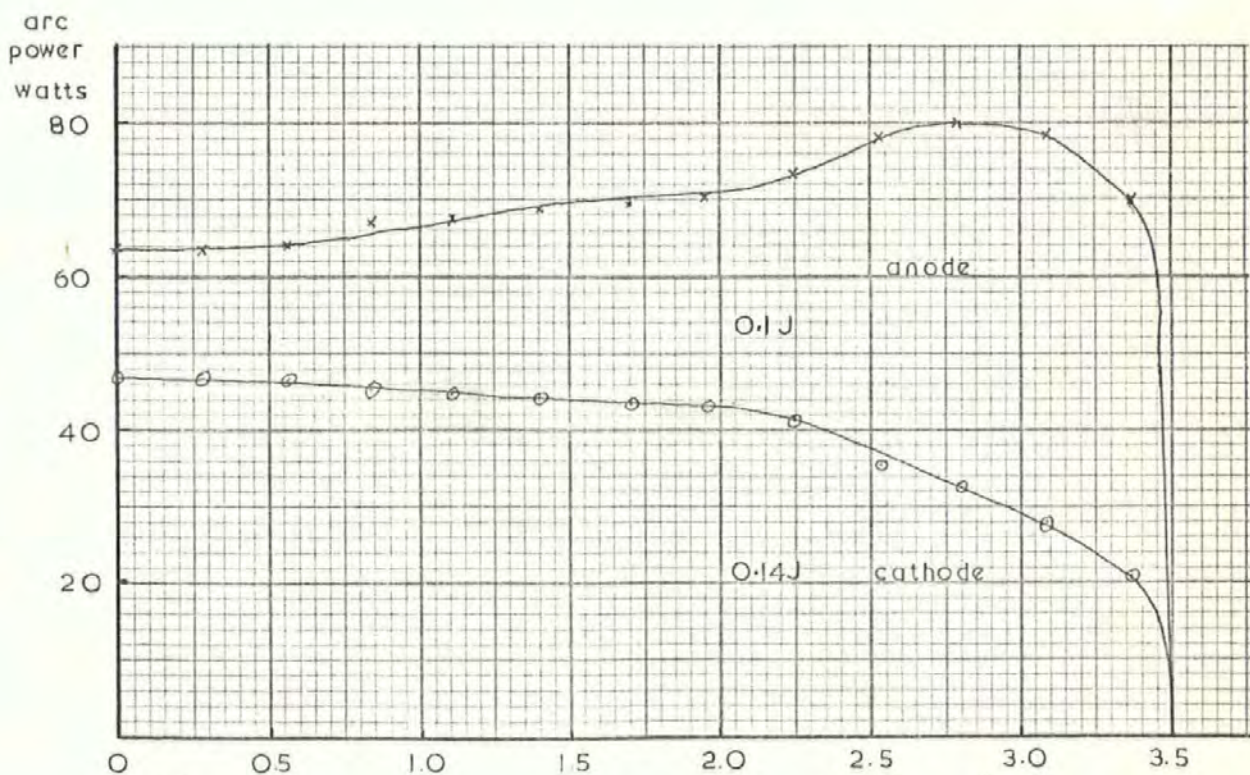Operating conditions, 40 volts dc, 8 amp resistive load.

Fig. 66b. Arc power curves for a slower opening switch. More energy
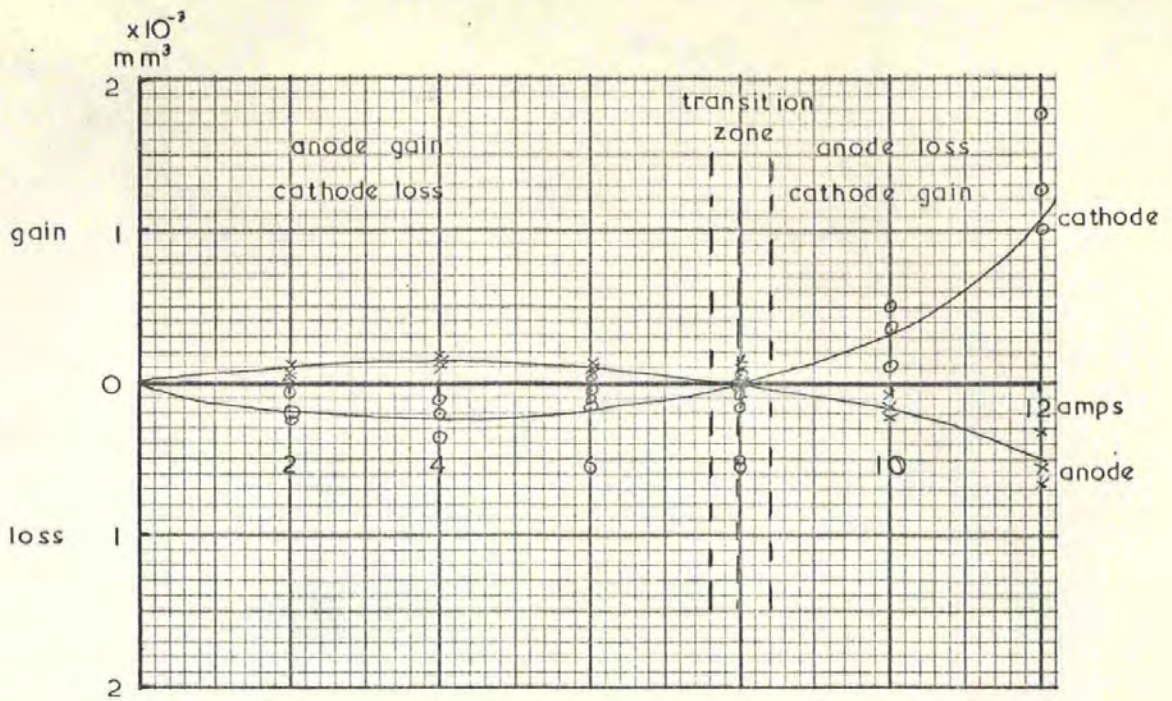is dissipated in the cathode fall than the anode fall.

Fig. 67. Graph showing the net material transfer after 500 operations.
Operation condition 40 volts dc, resistive load.
Load currents 2 - 12 amps in 2 amp steps
Transfer direction changes from one of anode gain and cathode
loss below 8 amps to cathode gain and anode loss above 8 amps.
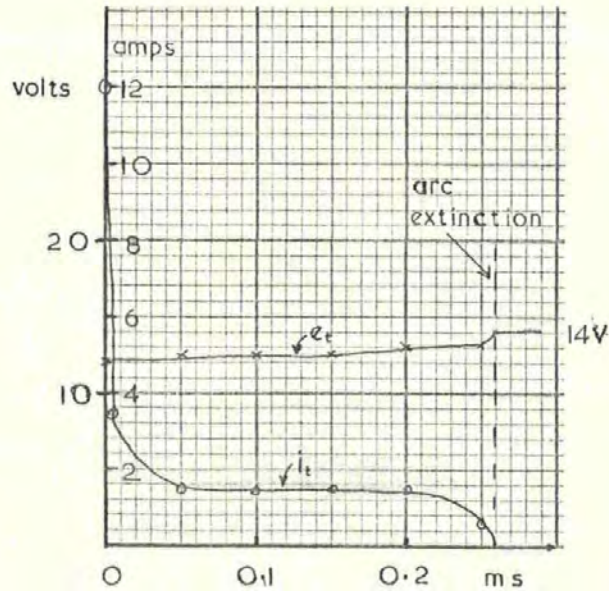
Fig. 68a. Arc voltage and current trace for switch contacts breaking
a 12 amp dc resistive load, with a supply voltage of 14 V.

- 160 -

This example indicates the effect that the mechanical parameters, (the velocity in particular), can have on the electrical and erosion characteristics of a switch and why it is important to specify completely the experimental conditions used to obtain a particular set of results.

To state then that a transition current occurs at a particular magnitude for a given contact material is not a sufficient definition. The characteristics of the mechanism in the form of opening velocity need to be stated to complete the definition.

Sato states that the transition current occurs at 6.4 amps for silver cadmium oxide. The opening velocity used was 63 mm/sec. The opening velocity of the switch being tested here is in the order of 1.5 m/sec. To locate the transition current a sample of switches was put through 500 operations at currents or the range 2 - 12 amps in 2 amp increments for d.c. supply. The net material gain or loss to the electrode was then plotted against current as shown in Fig. 57. This shows a crossover point of between 7.5 to 8.5 amps, i.e. higher than that specified by Sato. This would be expected due to the fact that initially when the arc is short, i.e. cathode erosion is dominant the contacts are moving more slowly than when the arc is larger and anode erosion is dominant. Hence for more energy to be dissipated when anode erosion prevails the circuit must be capable of supporting an arc of length such that the duration when the anode fall is greater can exceed the duration of when the cathode fall is larger.

This discussion on the mechanism of transfer has ignored the presence of the short arc during the initial stages of separation. This is justified by the fact that at these larger durations (1 - 2 ms), the effect of the short arc is not distinguishable due to the dominating effect of the long arc mechanism. However, if circuit operating conditions were such that the long arc was not the dominant feature of current interruption , attention would need to be given to the erosion capability of the short arc.

For a circuit with a supply voltage of 14 V and current of 12 amps the arc length capable of being supported is in the order of .02 - .03 mm (Fig. 36), and the duration is recorded as 0.26 m/s (Fig. 68a). Since a larger proportion of the arc duration is now constituted by the short arc discharge and also, according to Hopkins et al (5), this is more efficient than the long arc in producing erosion, short arc transfer dominates and there is a characteristic pip (cathode) and crater (anode) formation. The Talysurf plots (Fig. 68b) clearly show this.

This type of erosion is similar to that which occurs at make due to contact bounce. The only difference between the arcing is the way in which the extinction of arc occurs. After bounce, contact is re-established thus extinguishing the arc, at break the arc extinguishes due to there being insufficient voltage available to support its increase in length. In terms of the energy dissipated the erosion rates for these two curves are:

i. Make operation $0.175 \times 10^{-3} mm^3$/Joule,transferred from anode to cathode.

ii. Break operation $.38 \times 10^{-3} mm^3$/Joule,transferred from anode to cathode.
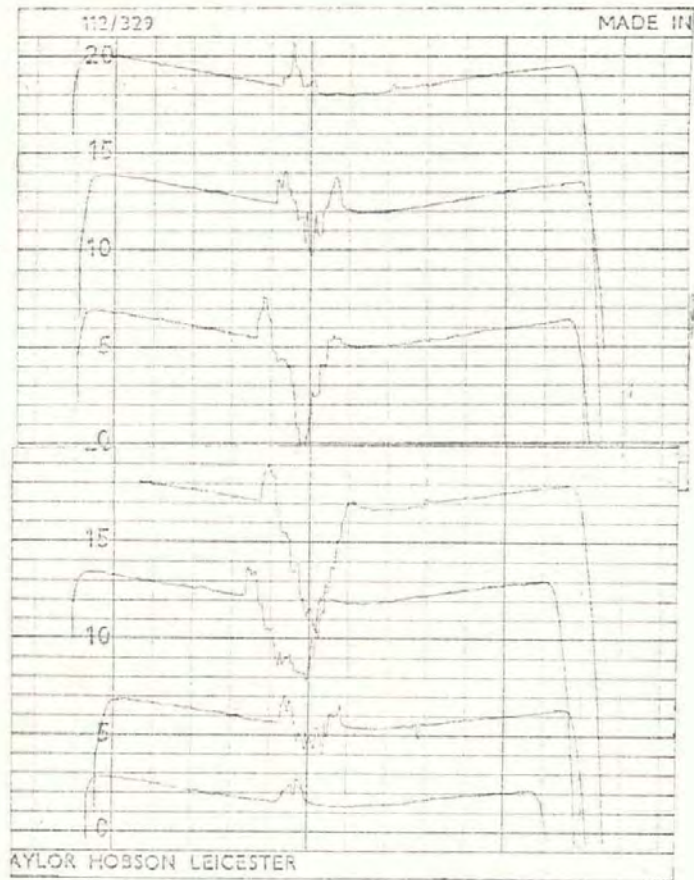
anode
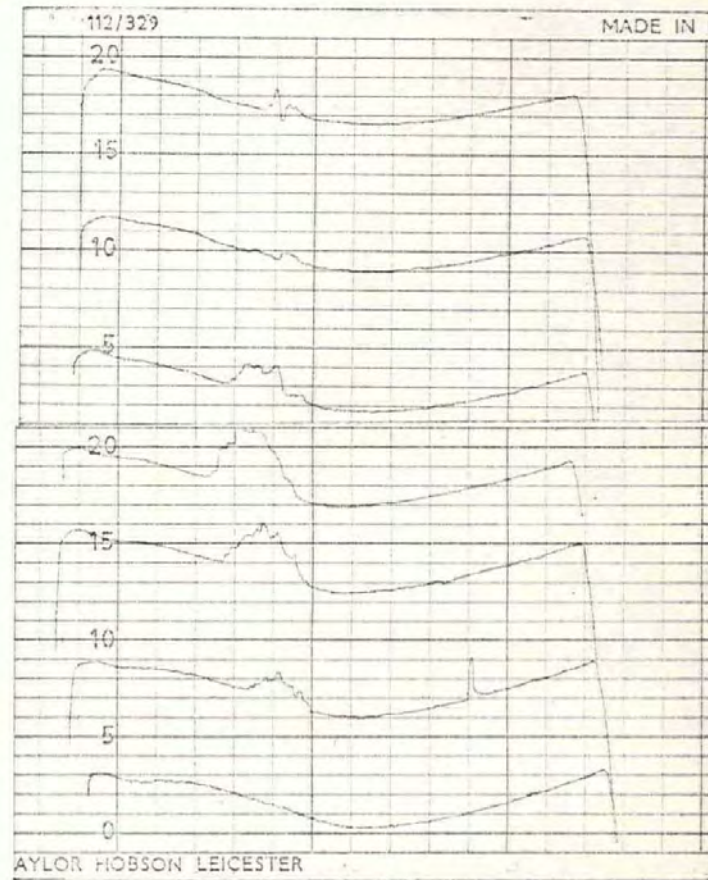
cathode

magn: $\updownarrow$ 1000, $\longleftrightarrow$ 20, 0.1mm between traces

Fig. 68b. Talysurf traces obtained from the anode and cathode contacts of a switch which has performed 500 break operations, switching a 12 amp load with a supply voltage of 14 V d.c.
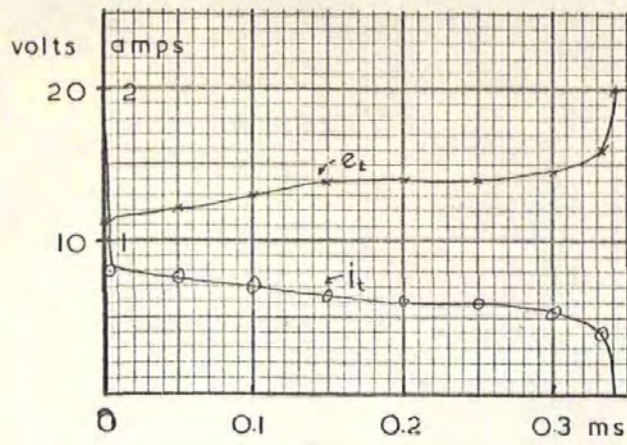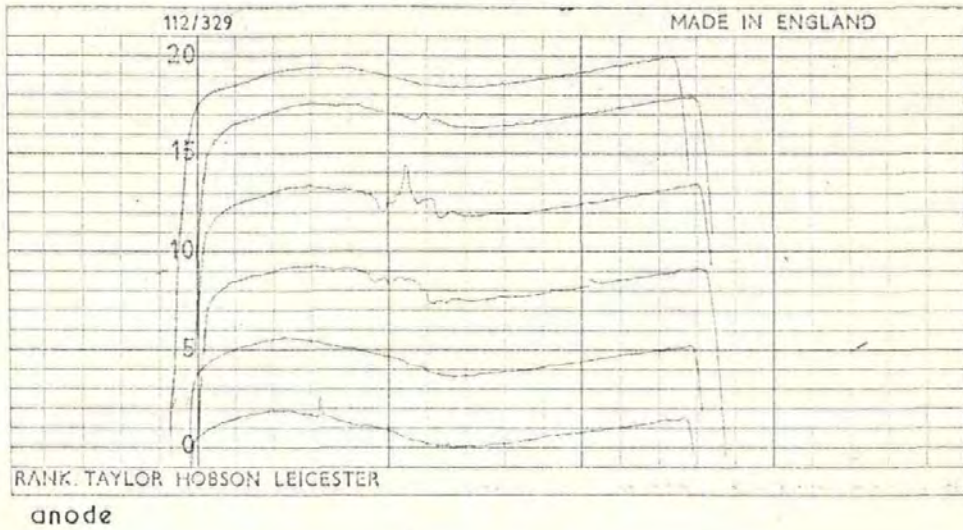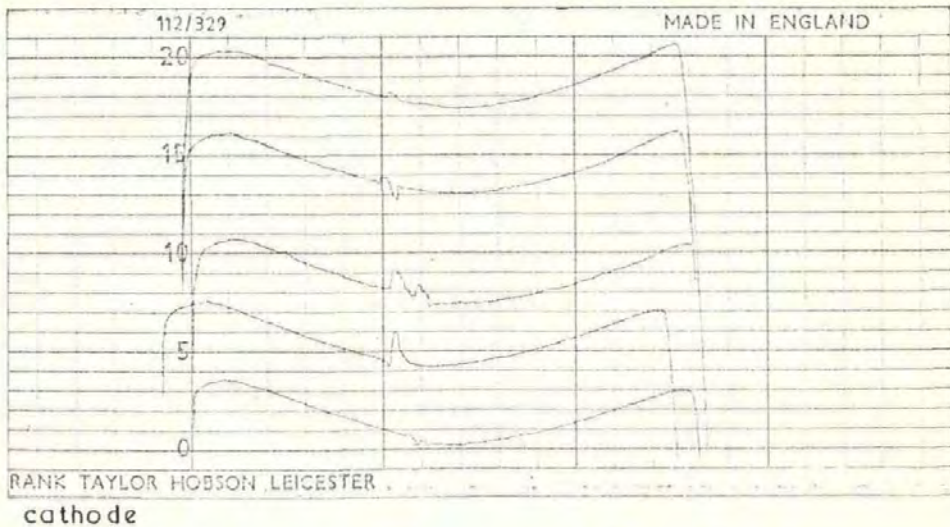
Fig.69a. Arc voltage and current for switch contacts breaking a 2 amp resistive load, supply voltage 20 volts d.c.

anode

cathode

magn: ↕1000x, ↔20x , 0.1 mm between traces

Fig.69b. Talysurf profile traces of anode and cathode contacts which have performed 500 break operations, switching a 2amp resistive load, supply voltage 20 volts d.c.

- 164 -

The apparent large difference in the rate of transfer which occurs may be due to the likelihood of material re-adhering to the anode surface, in the case of the bouncing contacts, when they re-close.

Fig. 69 shows the set of results obtained for operating conditions of 20 volts 2 amps. The arc duration is of similar order to the arc recorded at 14 V 12 amps. The erosion pattern, however, is markedly different from the well defined pip and crater formation discussed in the previous paragraph. For these operating conditions the anode and cathode both appear to have material eroded in more places on the surface, while displaying material build-up in others. The short arc which occurs under these conditions is required to pass much less current than previously hence damage to the anode by colliding electrons is much less, with less material being transferred to the cathode. After the short arc stage most of the arc energy is dissipated in the cathode fall since the arc only attains a length of about .02 mm before extinction. Hence, for this latter stage cathode loss will predominate and some of the material deposited on the cathode due to the short arc may be transferred back.

This investigation of contact erosion due to an arc occurring under d.c. operating conditions has also effectively covered the conditions that can occur when the switch breaks an a.c. circuit.

i.e.   i.   High arc voltage (30 - 40 V) high current — arc which ignites at the beginning of a cycle.

ii.   Low arc voltage (12 - 15 V) high current — arc which ignites at the middle of a cycle.

iii.   Low current (2 amps), lower voltage (20 V) — arc which ignites towards the end of a cycle, i.e. prior to a zero.
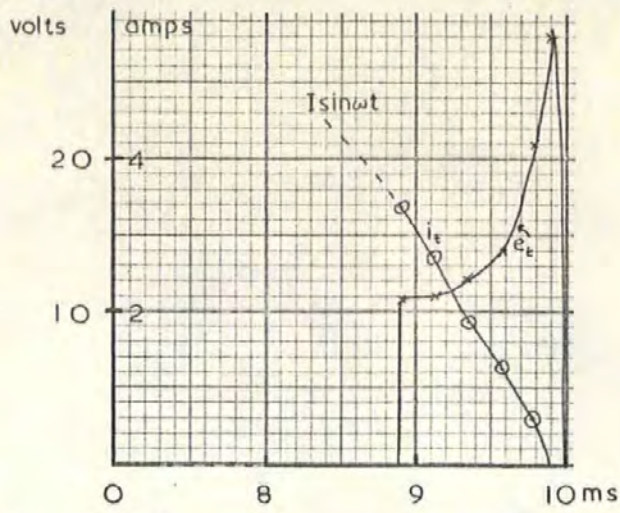
Fig.70a. Arc voltage and current
transients. Ignition 1.1ms
prior to an a.c. zero. Supply
voltage 340 volts peak, 50Hz,
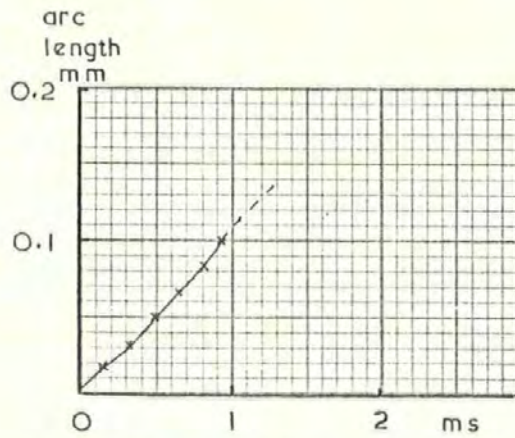load 10 amps peak resistive.

Fig.70b. Arc length/duration
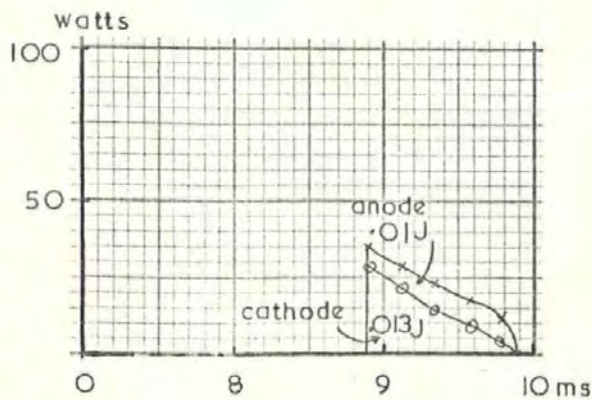obtained from the high
speed films record.

Fig.70c. Arc power curves. More energy is dissipated
in the cathode fall than the anode fall.

For one break operation on a.c. then it is possible to separate
out the various stages the arc goes through and interpret the
significance in terms of erosion.

The simplest way to do this is to consider in turn several
ignition points across the a.c. half cycle. The operating
conditions chosen were, resistive load of 10 amp (peak),
340 volts peak (240rms), 50 Hz.

4.8.2 Erosion due to the break arc : a.c. operating conditions

Case I   Ignition : 1.1m. seconds, prior to a zero

Circuit current at ignition $\hat{I}$ sin $(\omega t + \theta)$ = 3.1 Amps

Supply voltage   "   " $\hat{E}$ sin $(\omega t + \theta)$ = 105 volts

The oscillograph recordings for this operation are shown
in Fig.70a. The arc duration is 0.95ms and the high
speed film registers the maximum arc length achieved
as 0.10mm. The arc voltage is less than 16 volts for
the first 0.75ms of arc life, hence assuming the cathode
fall for silver of 8 volts, the anode fall will only
exceed the cathode fall for the last 0.20ms. The cathode
surface then will receive more energy from the arc than
the anode. This is seen in Fig.70c. from the arc power
curves, where the area under the power curve for the
cathode represents 57% ± 5% of the total. Since the arc
is short compared to the diameter of the electrodes, there
will be a negligible loss of energy or electrode material
to the surroundings.

From the knowledge gained from the previous section using
d.c. an estimate of the erosion processes occuring here
can now be made. The current at ignition is about 3 amps
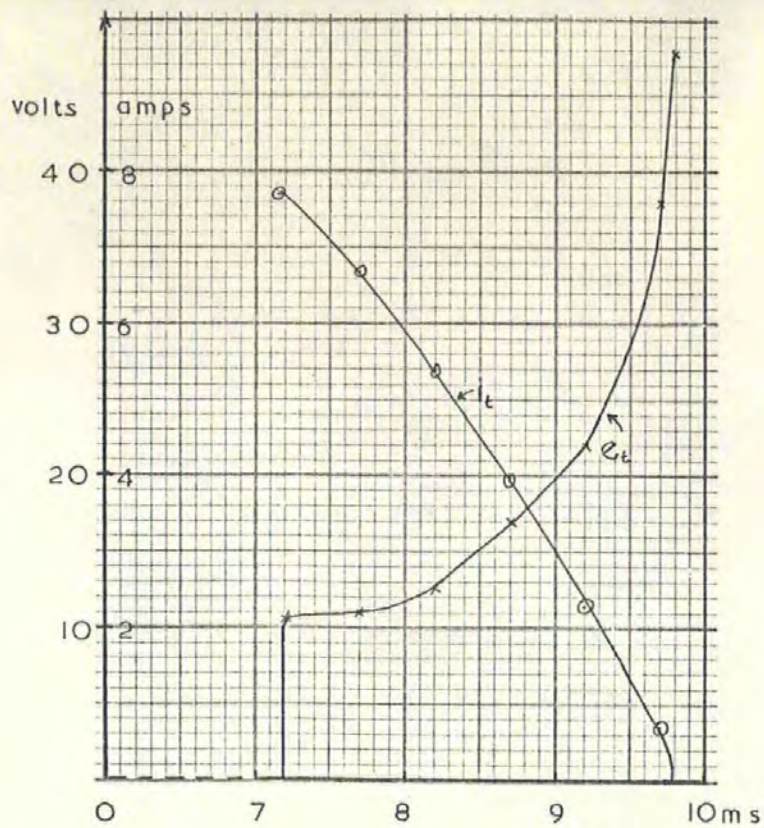so this will be the current the electrons constituting

Fig.71a. Arc voltage and current transients
Ignition 2.8 ms prior to an a.c.
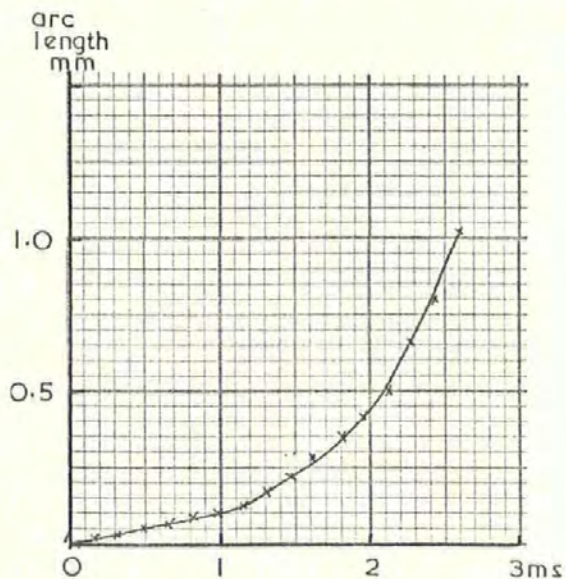zero. Operating conditions
viz. Fig.70a.

Fig.71b. Arc length/duration
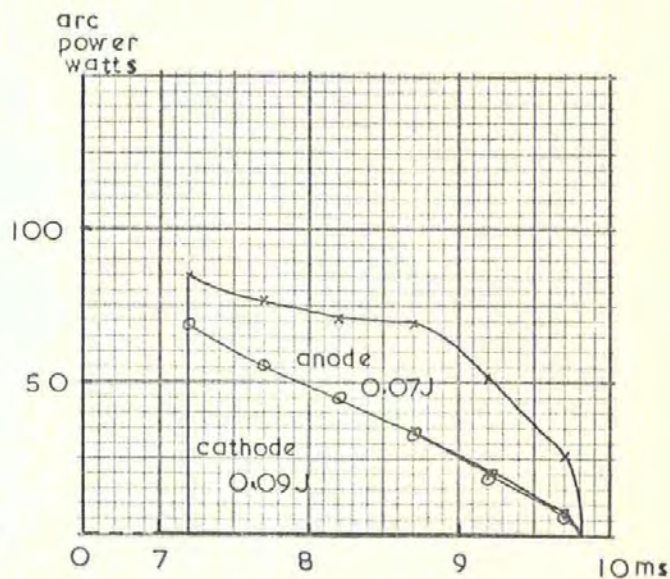obtained from
the high speed
films record.

Fig.71c. Arc power curves. More
energy is dissipated in
the cathode fall than
the anode fall.

the initial short arc will carry as they bombard the anode directly.
The damage caused by the short arc should just exceed that which
occured due to the short arc in the 20v 2 amp situation on d.c.
However, the arc duration here is much longer compared to the
former case (0.9ms as to 0.2ms) hence the erosion from the cathode
will exceed that which occured previously. During the last 0.15ms
when the anode fall exceeds the cathode fall, the arc power has
fallen to a low value so there will be little erosion of the anode
due to the long arc.

The erosion pattern then is thought to be some erosion and build
up of material from both contacts, however net movement of material
is likely to be cathode to anode. This is summarized in Fig.76a for
the relevant part of the a.c. cycle.

Case II   Ignition : 2.9ms prior to a zero.

Circuit current at ignition $\hat{I} \sin (wt + \theta)$ = 8 amps

Supply voltage   "   " $\hat{E} \sin (wt + \theta)$ = 269V.

The oscillograph recordings for this operation are shown in Fig.71a.
The arc duration is 2.6ms and the high speed film registers the
maximum arc length as 1mm (Fig.72b).

The arc voltage exceeds 16v after about 1.3msecs, the arc length at
this point is about 0.2mm (Fig.71b). Hence the cathode fall is greater
for the first 1.3msecs and the anode fall greater for the last
1.3msecs. However since the current has a higher value for the time
that the cathode fall is greater (drops from 8amps to 5 amps) more
energy will be dissipated in the cathode fall overall. (56% compared
to 44% in the anode fall). There is also some energy dissipated
in the arc column, however for an arc of this duration and length
this is small <.005 joules, and also since the arc length is still
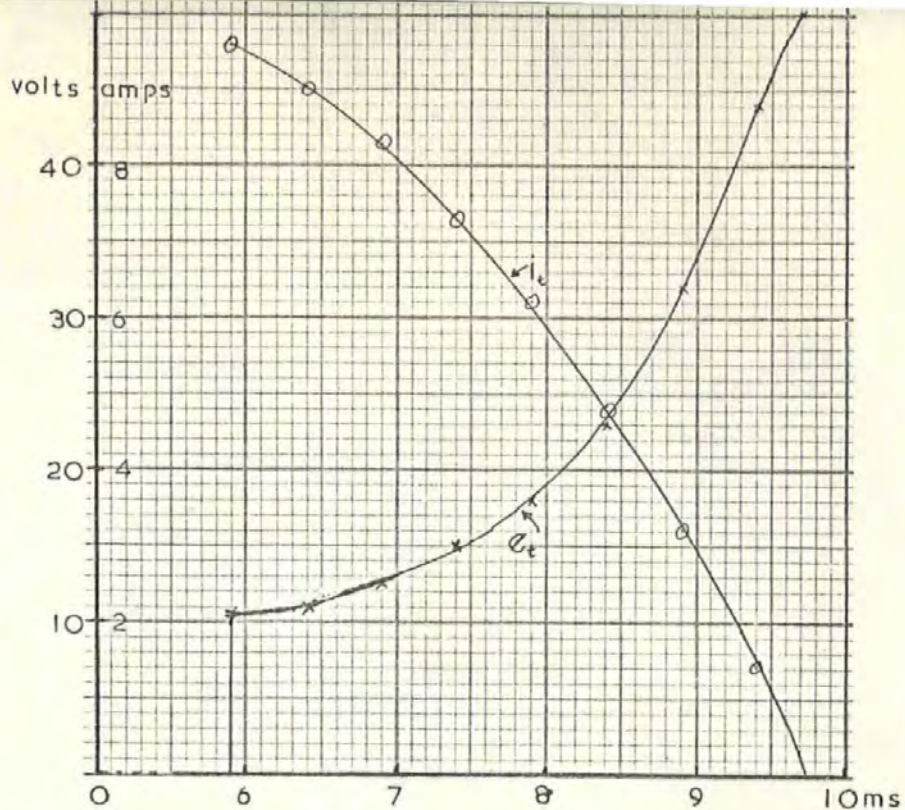small compared to the contact diameter there is no appreciable

Fig.72a. Arc voltage and current transients. Ignition
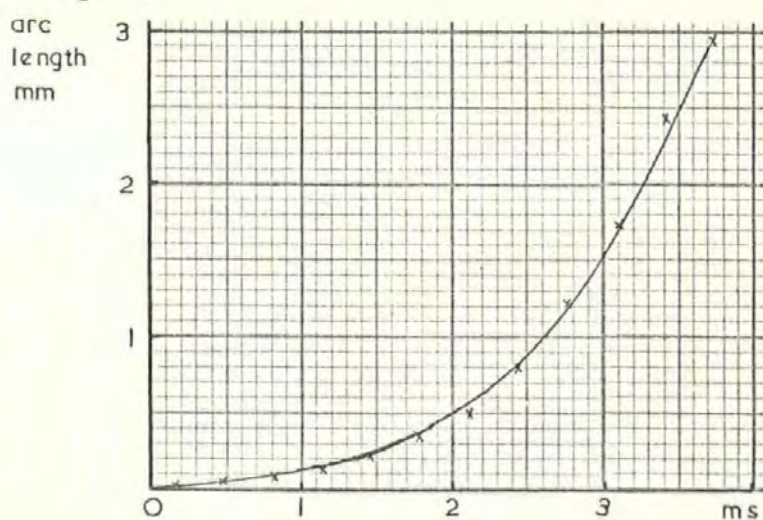4.1ms prior to an a.c. zero. Operating conditions
in Fig. 70a.

Fig.72b. Arc lengths/duration obtained from the high speed
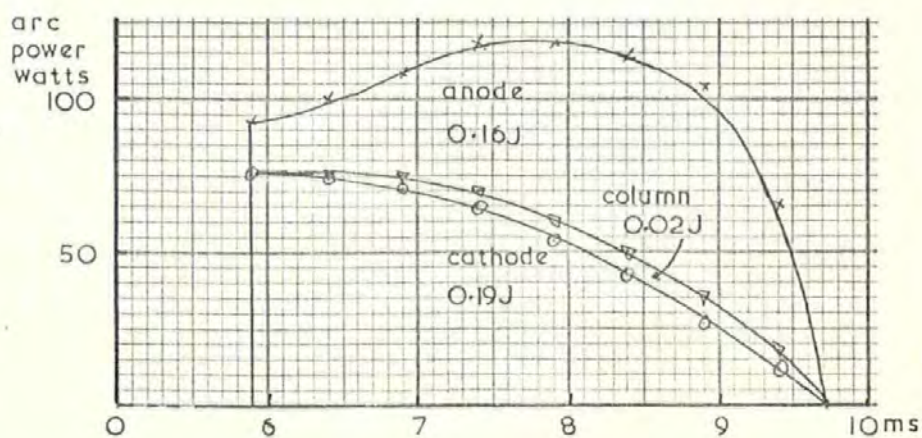film record.

Fig.72c. Arc power curves. More energy is dissipated in
the cathode fall than the anode fall.

material or energy loss to the surroundings. The erosion will be similar in form to that occuring in Case I, but of greater magnitude i.e. short arc initially (8 amps carried by electrons) then erosion from the cathode predominently. For the last millisecond there is more power dissipated in the anode fall than the cathode fall. However since the current is low by this time, overall there is more energy dissipated at the cathode as Fig.72c shows. The net transfer pattern will still be cathode to anode for arcs igniting in this region, with both surfaces having local areas of erosion and build up.

Case III   Ignition : 4.1ms prior to zero

Circuit current at ignition 9.7amps

Supply voltage at ignition 329volts.

Oscillograph recordings for this operation Fig.72a.

The arc voltage is seen to exceed 16v. after 1.6ms, since the total arc duration is 3.8ms, the time span for which the anode fall is greater than the cathode fall is 2.2ms. However the cathode fall is greater during the time of higher current values, hence the energy dissipated at the cathode still exceeds that dissipated at the anode as Fig.72c shows. The arc length reaches 3mm before extinguishing for this operating condition, Fig.72b, so the arc column will account for some of the total energy dissipated. Since for three quarters of the arc duration, the arc length is less than 1.5mm, it can still be considered that most of the energy dissipated in the column finds its way to the electrodes as opposed to the surroundings. Assuming the energy dissipated in the column divides equally between the cathode and anode, the difference between the energy received by each electrode can be seen to be decreasing i.e. 54% to the cathode, 46% to the anode.

The erosion pattern for this operating point will consist of material
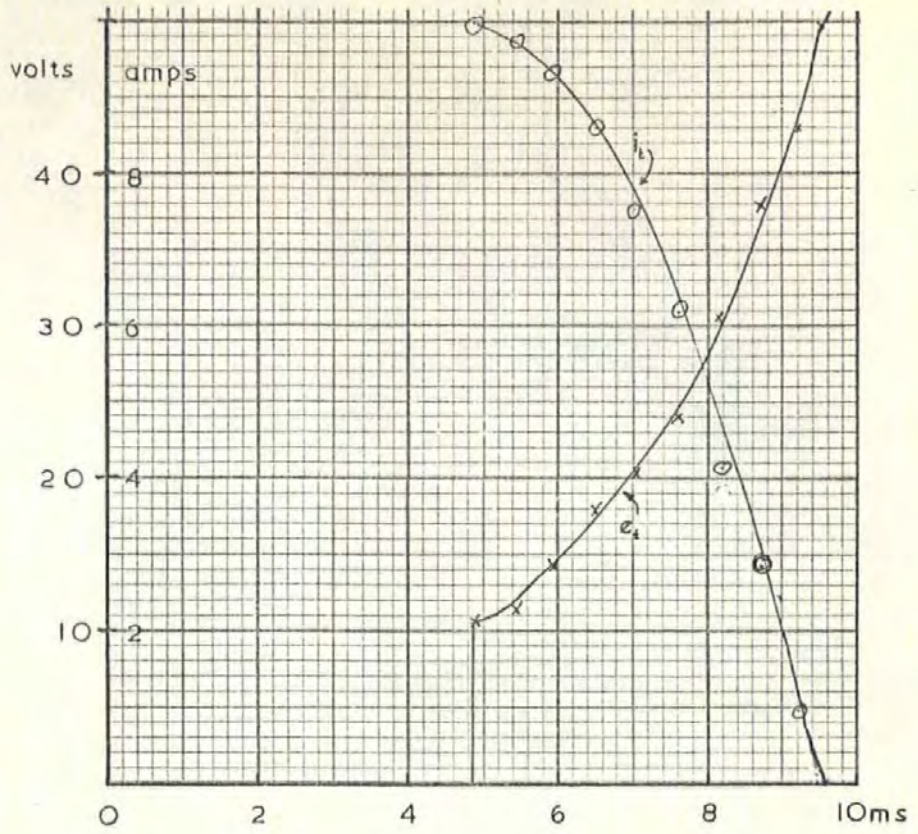
Fig.73a.   Arc voltage and current transients.   Ignition 5.1ms
           prior to an a.c. zero.   Operating conditions as Fig.70a.
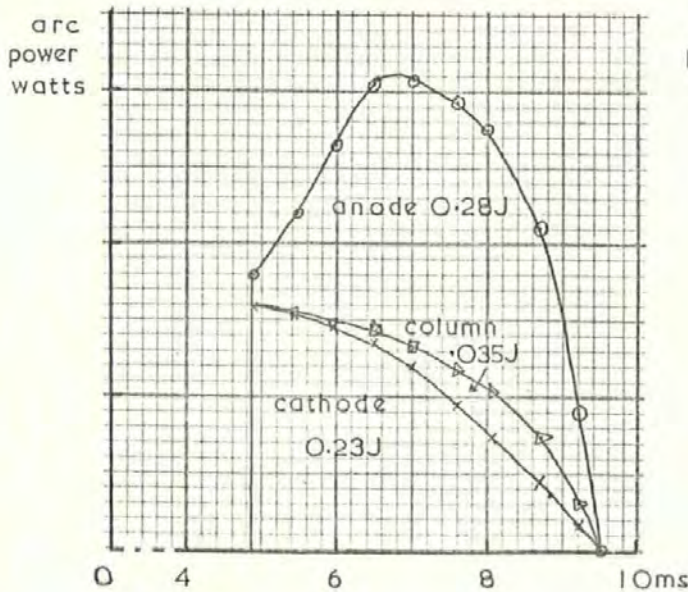

Fig.73b.   Arc power curves.   More energy
           is dissipated in the anode
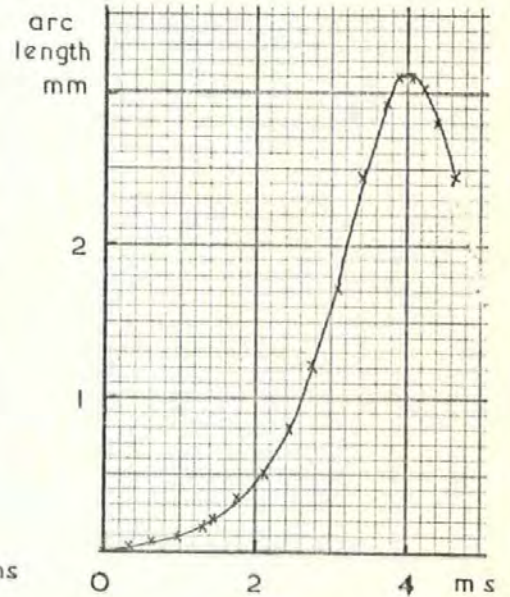   fall than the cathode fall.

Fig.73c.   Arc length/duration
           obtained from the
           high speed film record

- 172 -

going in both directions with both contacts losing and gaining material
with the possibility of there being a small net loss by the cathode.

The high-speed film plots of an arc length for the switch being used
to produce this particular set of experimental data shows that the
maximum contact separation achieved is 3.15mm. The switch was deliberately
set with a large operating stroke to produce typical data over the working
range of the switch including the extremities of operation. Normally
the maximum separation of the contacts is 2 - 2.5mm.

For the next ignition point considered, the arc length will peak and
then decrease as the contacts oscillate.

Case IV   Ignition : 5.1ms prior to zero

           Circuit current at ignition 10.0amps.

           Supply voltage at ignition 339volts.

Oscillograph recordings for this operation Fig.73a.

The total arc duration is 4.6ms and the arc voltage exceeds 16v. after
1.6ms, hence for 3ms the anode fall will be in excess of the cathode
fall. Fig.73c shows how the power dissipation in the anode fall quickly
rises during this first 1.6ms to exceed the dissipation at the cathode.
If the total eargy dissipated in the column is divided equally between
anode and cathode, the anode received 52% of the total arc energy.
The balance has now changed with the anode receiving more energy in
preference to the cathode.

The erosion pattern resulting from this operating point will consist
of material going in both directions with the possibility that there
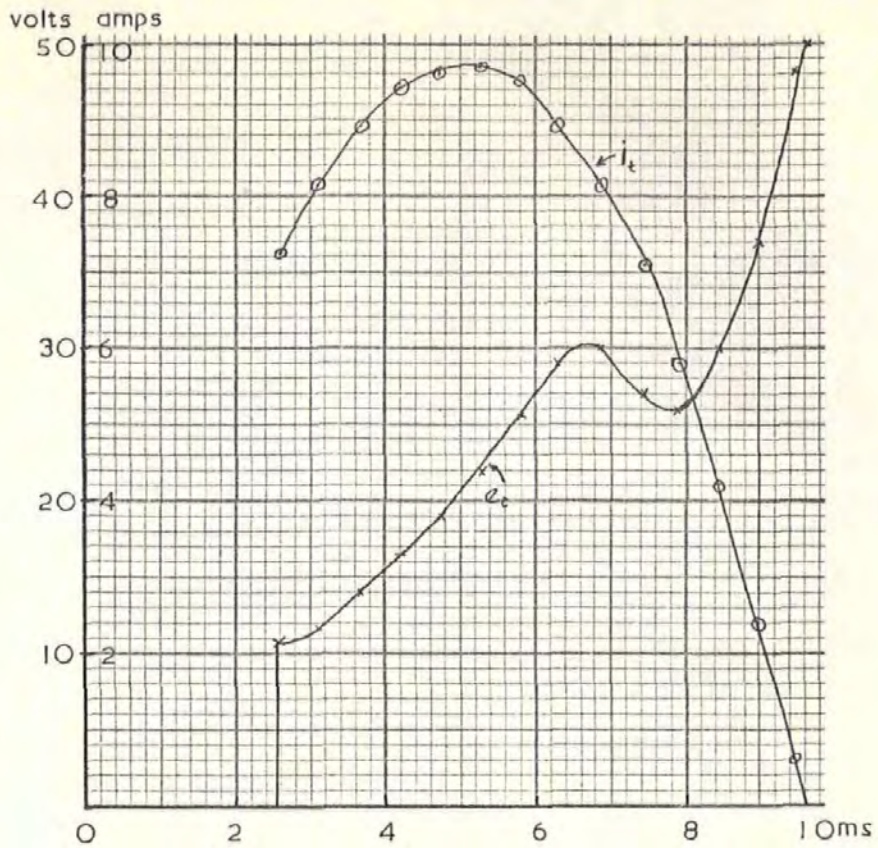will be a net loss by the anode.

Fig. 74a. Arc voltage and current transients. Ignition 7.4ms. prior to an a.c. zero. Operating conditions as Fig.70a.
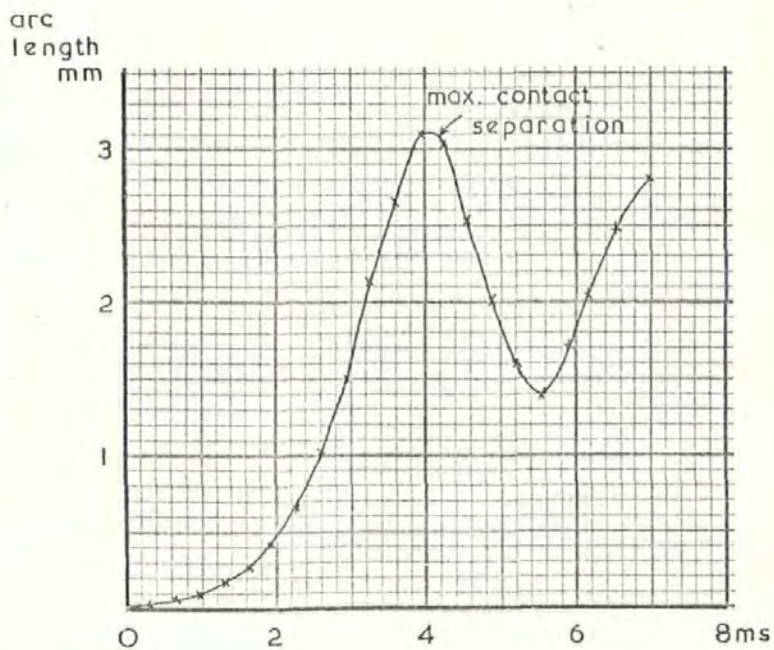

Fig.74b. Arc length/duration obtained from the high speed film record.

Some of the energy dissipated in the column of the arc will be lost to the surroundings though this amount will be small since the arc length is still less than the contact diameter. Also the contribution by the arc column to the total energy dissipated is only 5%.

Case V   Ignition : 7.4ms prior to zero

          Current at ignition 7.3amps.

          Supply voltage at ignition 247volts.

Oscillograph readings for this operation Fig.74a.

The total arc duration is 7ms, and the arc voltage exceeds 16v after 1.6ms. At this point the arc current is 4.4amps and has not yet reached its peak, hence the anode fall will have considerably more power dissipated in it since the high arc current coincides with the region of maximum arc length. The distribution of the energy as shown in Fig.74c is   anode fall   : 54% ± 5%

          Column   : 11% ± 5%

          Cathode fall : 35% ± 5%

The erosion characteristic here will be one where transfer from anode to cathode dominates due to the increased energy dissipation in the anode fall.

Case VI   Ignition : 1.3msec.

           Circuit current at ignition 3.9amps

           Supply voltage at ignition 135volts.

Oscillograph recordings for this operation Fig.75a.

Total arc duration is 8.5ms., 7ms. of which the anode fall is greater than the cathode fall. Distribution of energy is:

           Anode fall   : 53%

           Column   : 16%
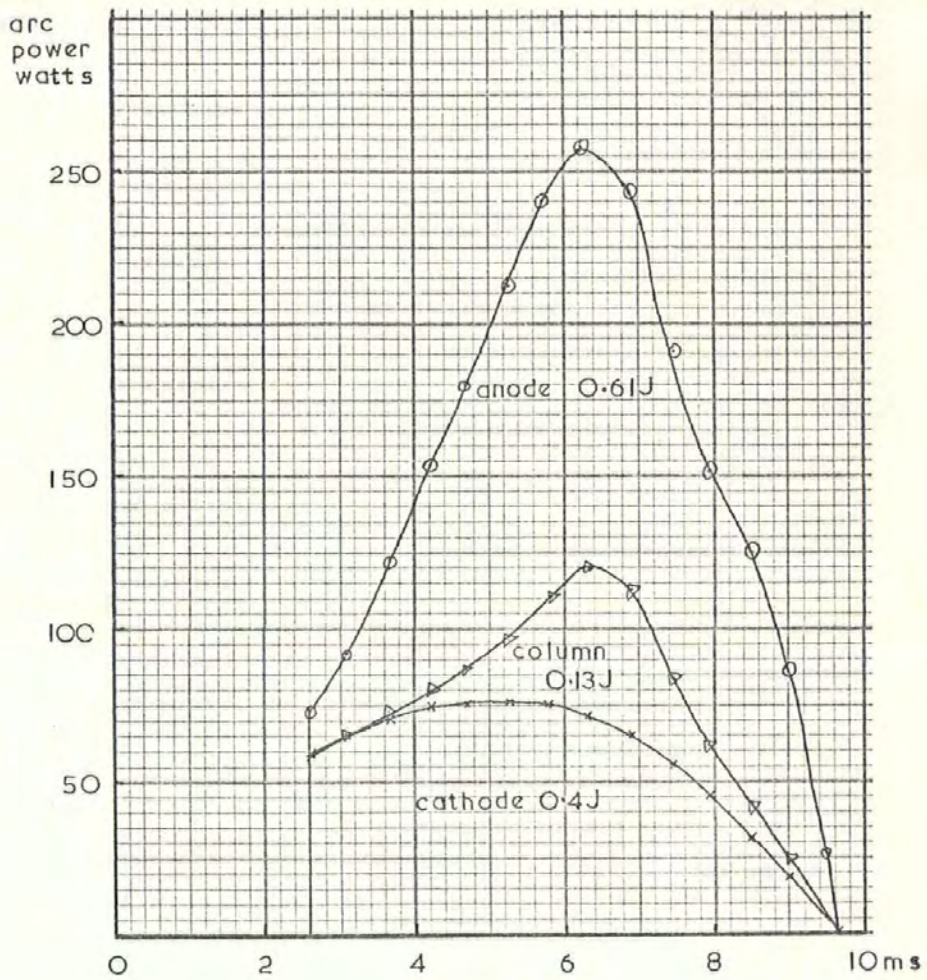
           Cathode fall : 31%

Fig.74c. Arc power curves. More energy is dissipated in the anode fall than the cathode fall.

The anode receives 22% more energy than the cathode, compared to 19%

more in the previous case considered. The energy in the column has

increased by about 50% compared to the previous set of results and most

of this energy appears to have come from the cathode. Dividing this

column energy equally produces 61% at the anode, 39% at the cathode.

This is complete reversal of the conditions existing in the first case

considered when the cathode fall contains 57% of the energy and the

anode 43%.

The erosion here then will be predominantly for the anode, resulting

in a transfer of material to the cathode.

These six case studies have produced a complete picture of the erosion

mechanisms resulting from different ignition points on the a.c. cycle.

This is summarised in Fig.76a. showing the half cycle divided into areas

of preferential erosion from the anode or cathode. This information

is presented quantitatively in Fig.76b. as a plot of the energy

dissipated in the various regions of the arc against ignition point on

the a.c. cycle. The crossover point on this graph represents the

region in the vicinity of which the erosion from each contact will be

about the same i.e. no net transfer.

In Section 4.7.1 a value was calculated for the average energy/operation

using the graphs of arc energy/ignition point. Similar values can be

calculated here for:-

        i. The average energy in the anode fall/operation = 0.33 Joules

       ii. The average energy in the cathode fall/operation = 0.24Joules

     iii. The average energy in the column/operation = .08 Joules
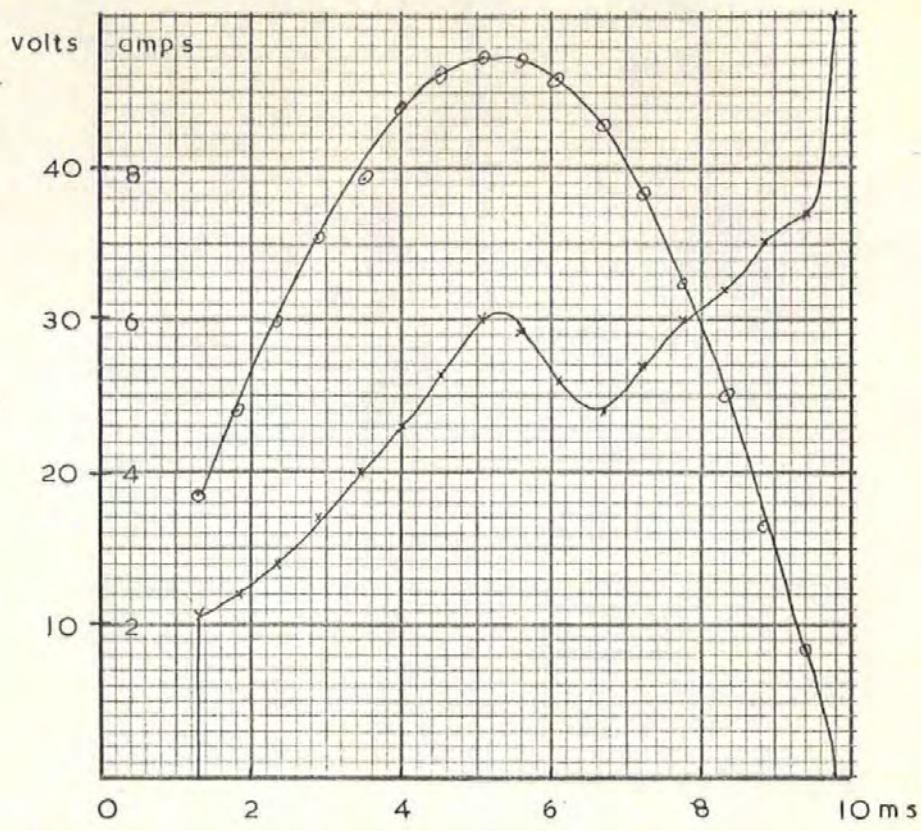
Fig.75a.   Arc voltage and current transients.   Ignition 8.7ms
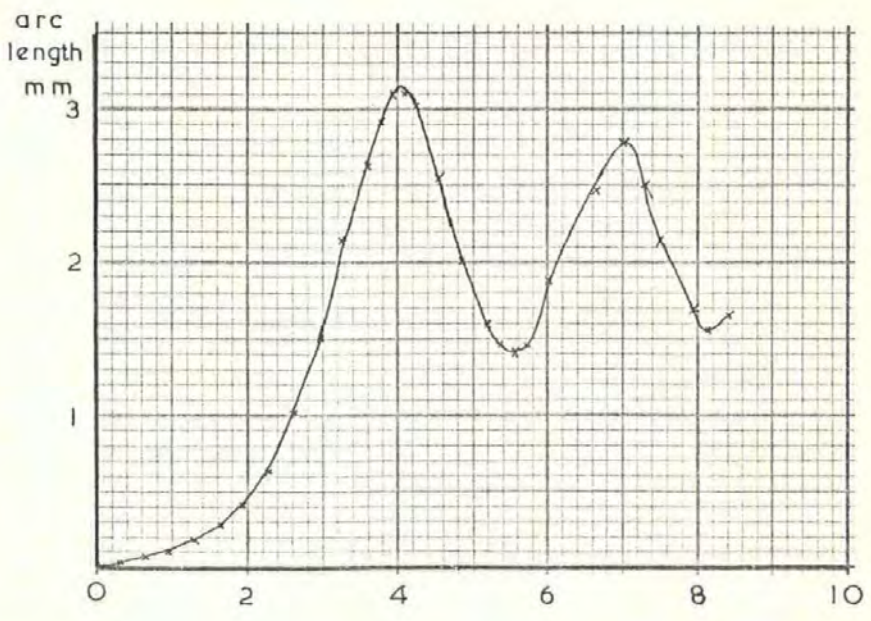   prior to an a.c. zero.   Operating conditiions as Fig.70a.

Fig.75b.   Arc length/duration obtained from the high speed
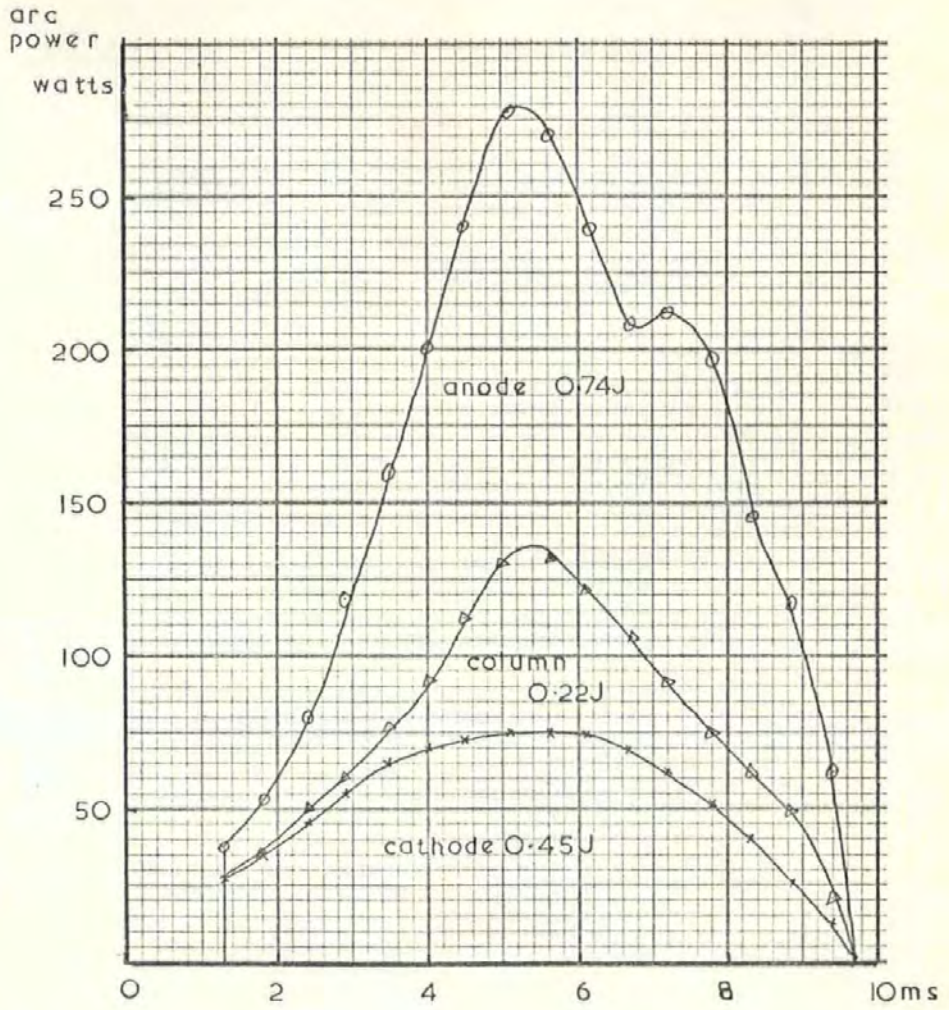   film record.

Fig.75c. Arc power curves. More energy is dissipated in
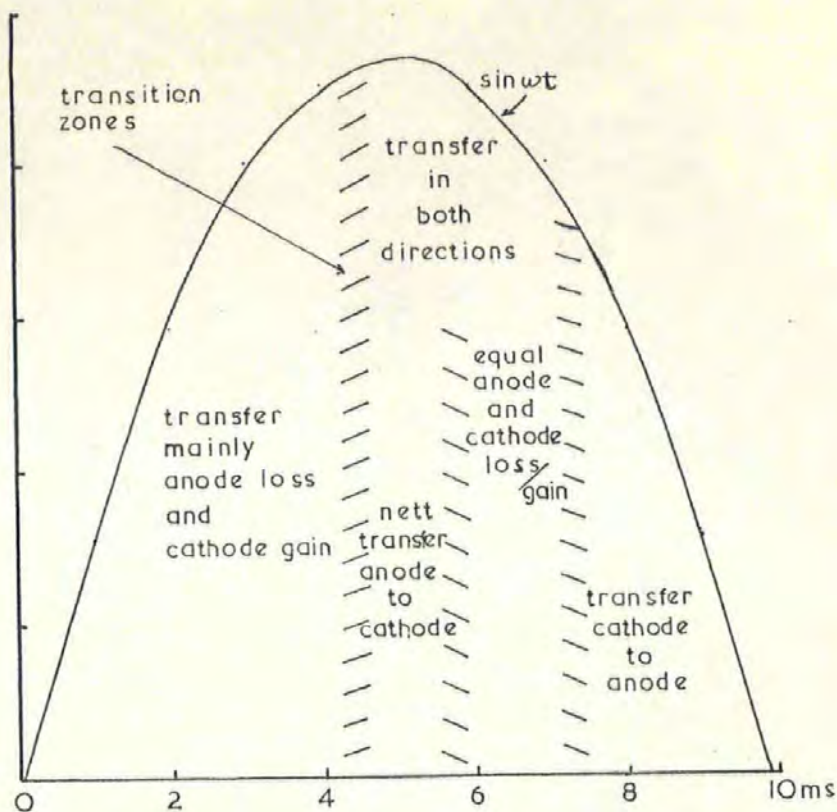the anode fall than the cathode fall.

Fig.76a. Schematic representation of how the direction of the electrode erosion is related to the ignition point on the a.c. cycle.
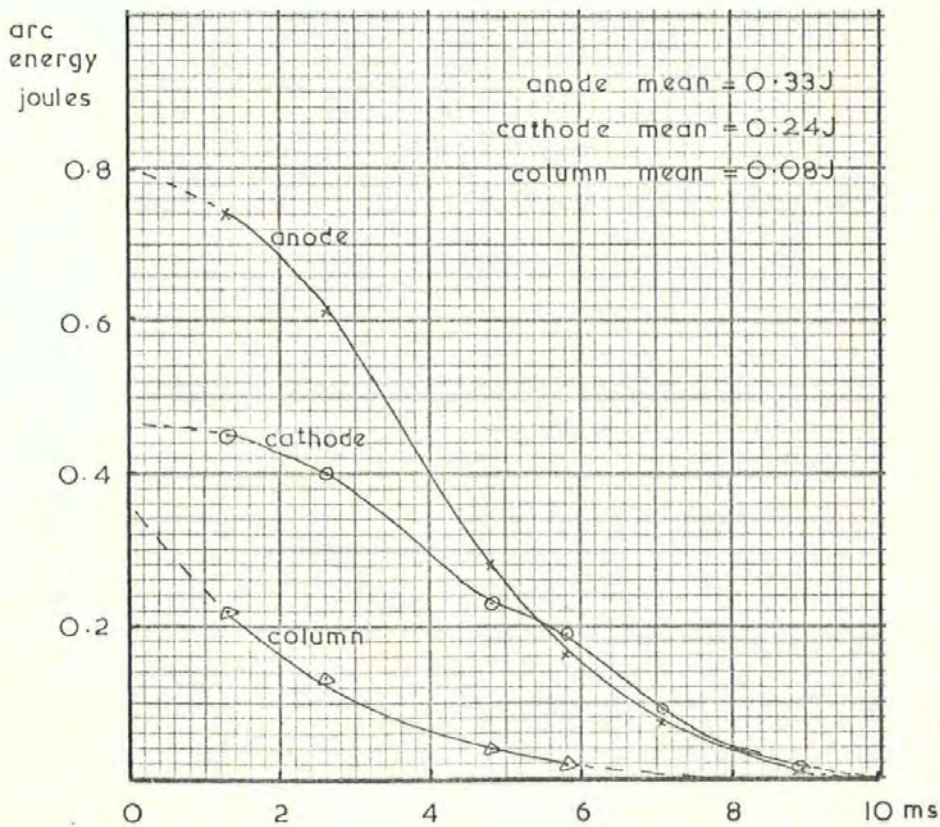

Fig.76b. Graph showing how the energy dissipated in the anode fall, arc column and cathode fall varies with ignition point.

Over 100 operations for example, assuming the column energy to be divided equally between the electrodes, 37 joules would be dissipated at the anode 28 joules at the cathode. Hence for multiple operation the anode received 30% more energy than the cathode.

Operating on full wave rectified a.c., it would be expected that the anode surface would suffer more erosion than the cathode, with a net transfer of material from anode to cathode.

This postulation concerning erosion due to the switching of full wave rectified a.c. has been made on the basis of the experimental results obtained using d.c. An attempt will be made now to corroborate these predictions with more experimental data.

A sample of 50 switches was used and particular switches were set to perform 100, 150, 200 operations etc. up to 500 operations in increments of 50. Between 6 and 12 voltage and current transients were recorded for each switch, so as to obtain sufficient ignition points evenly distributed across the half cycle. The testing current was 10 amps peak, supply voltage was 340v peak, full wave rectified 50Hz to produce a zero every 10ms. The full wave rectified supply enabled the polarity of the contacts to remain the same throughout the tests.

After the number of operations was complete, the contacts were removed from the switch and examined under the S.E.M. and a surface profile was obtained using the talysurf. Some S.E.M. photographs and talysurf plots are shown in Figs. 77. The anode possesses the dominant feature of a crater on the contact surface, of diameter 0.5 mm and depth 0.02 mm for the 150 operation contact. Forming a rim around the crater are
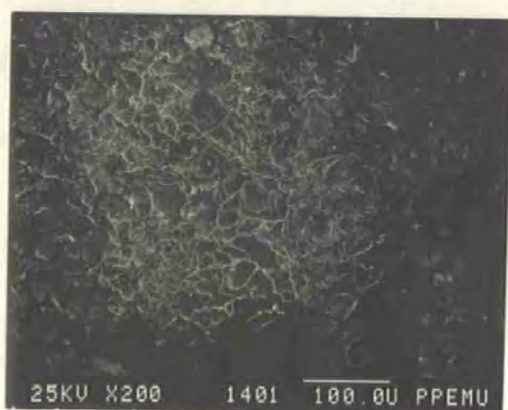
anode
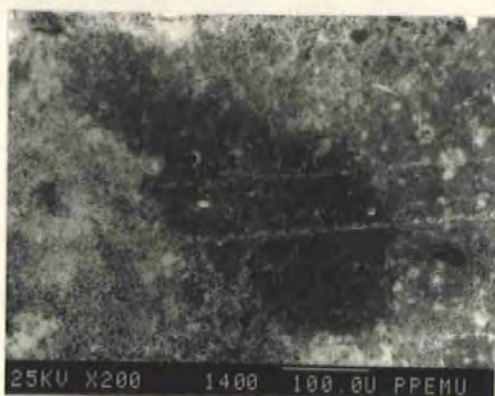
cathode

Fig.77a. S.E.M. photograph of the anode and cathode surfaces after 150 break operations. Operating conditions were 340volts peak, 50Hz, full wave rectified. Electrical load was 10amps peak, resistive.
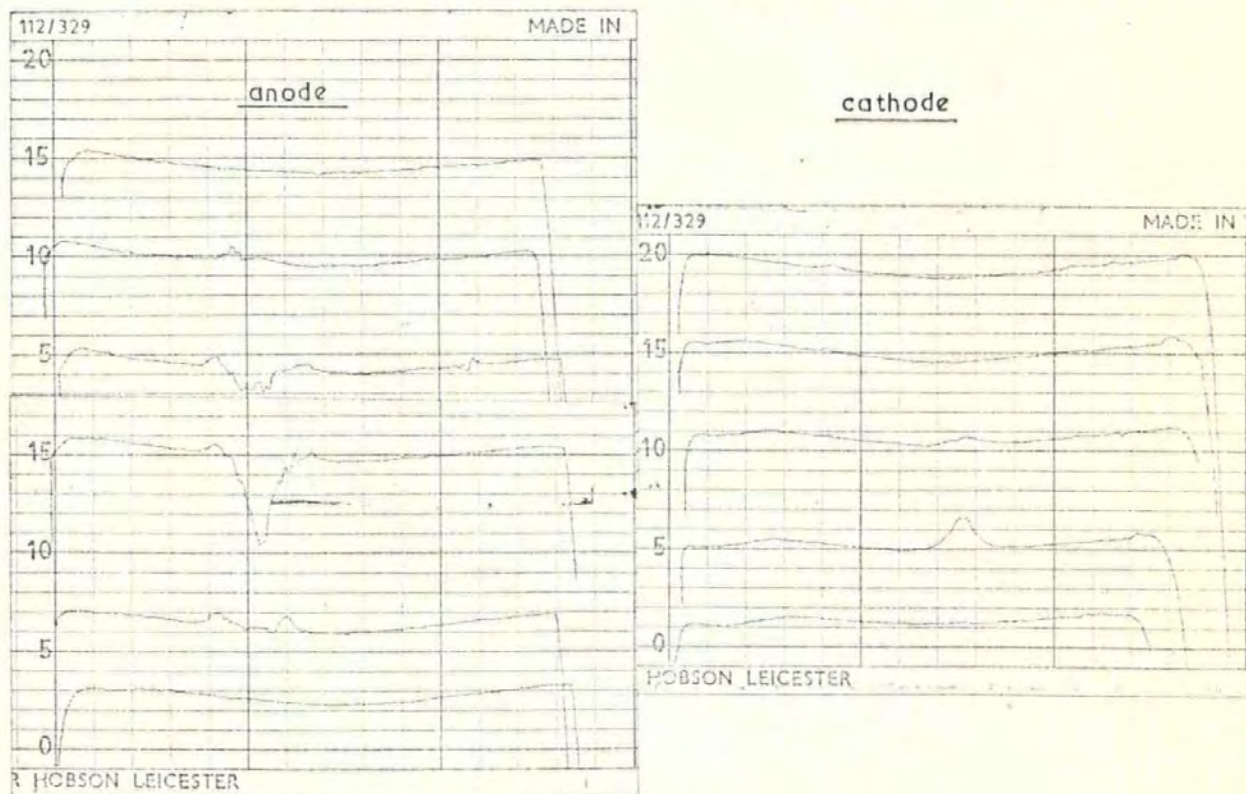
magnification: ↕ 500 X   0.2 mm between traces
←→ 20 X

Fig.77b. Talysurf profile traces of the electrode surfaces shown above.

Fig.78a.   Volume of material displaced on the anode surface against
total arc energy (= average energy per operation x number of
operations.

Fig.78b.   Volume of material displaced on the cathode surface against
total arc energy (= average energy per operation x number
of operations.

deposits of material which appear to have come from within the crater. The dominant feature of the cathode surface is a large build-up of material in one place, height ...mm, diameter....mm after 100 operations. Around the base 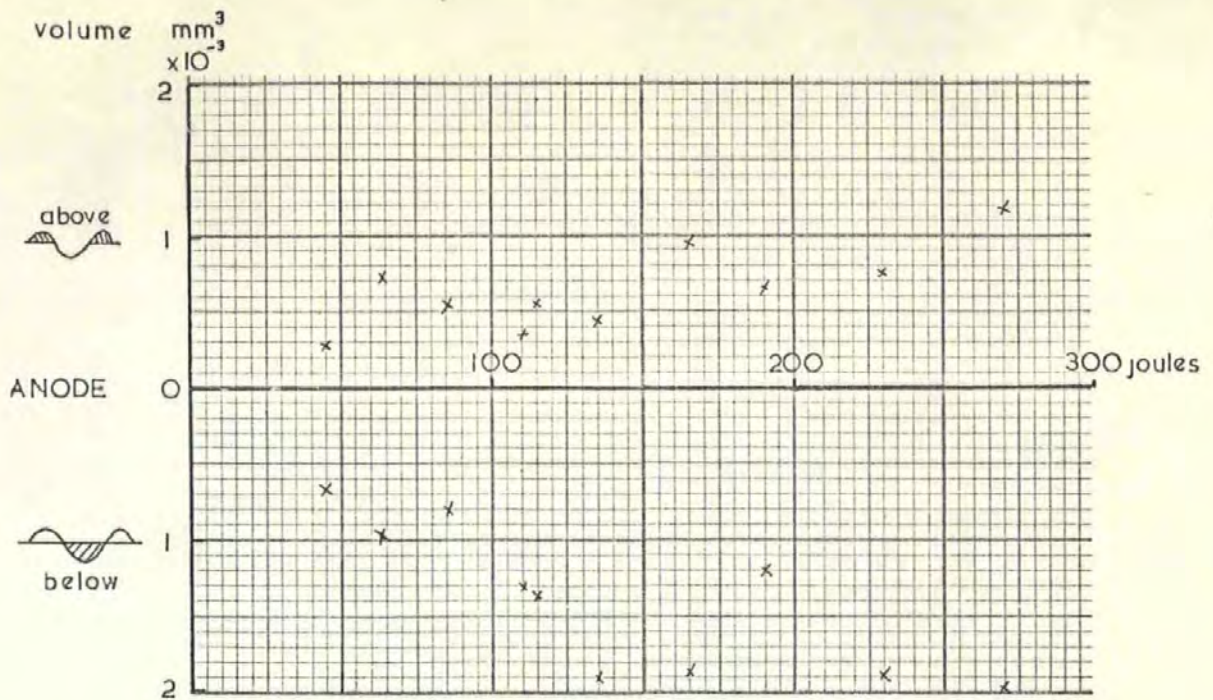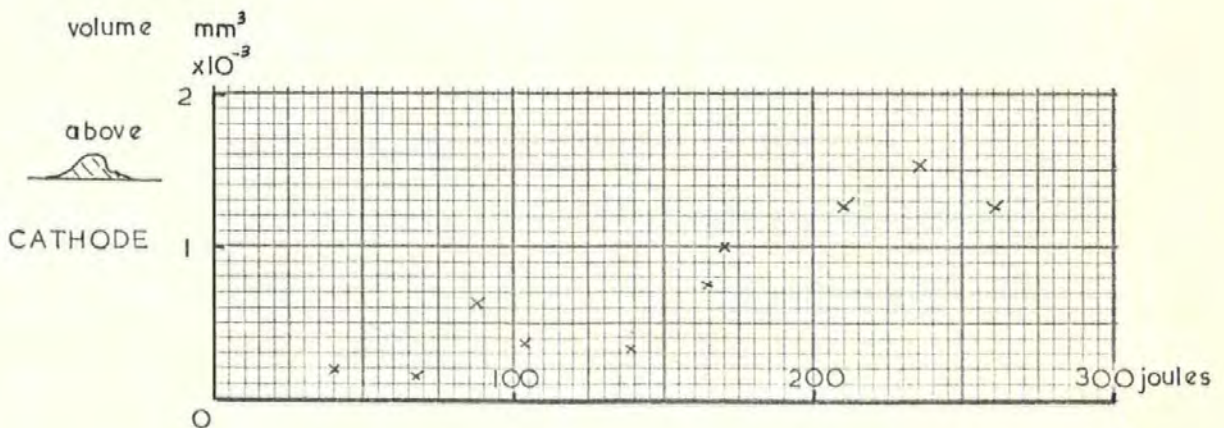of the protuberance are an abundance of small pits and spikes, too irregular to be measured as a volume displacement, but evidence of the erosion due to the energy dissipated in the cathode fall.

The results obtained over the whole experimental range are shown graphically in Fig.78. The anode erosion is presented in Fig.78a. as a plot of crater volume, and volume of material around the outer rim, against energy in joules. This energy represents the total energy dissipated between the contacts, and was obtained by multiplying the average total energy per operation by the number of operations. The sum of the volume of material around the anode crater rim, and the volume of material built up on the cathode, at any point, within the limits of the experimental measurements, is slightly less than the volume of the anode crater. The difference works out to be $0.5 \rightarrow 1 \times 10^{-6} \text{mm}^3$ per operation. This is an average value since material loss is more likely to occur when the arc ignites early on in the cycle, and the arc length is 2 - 3mm resulting in greater energy dissipation at the anode.

The erosion process under these operating conditions is evidently one of material transfer, anode to cathode, with a small amount of material loss occuring as a result of this transfer process mostly when the arc has a duration approaching that of a half cycle.
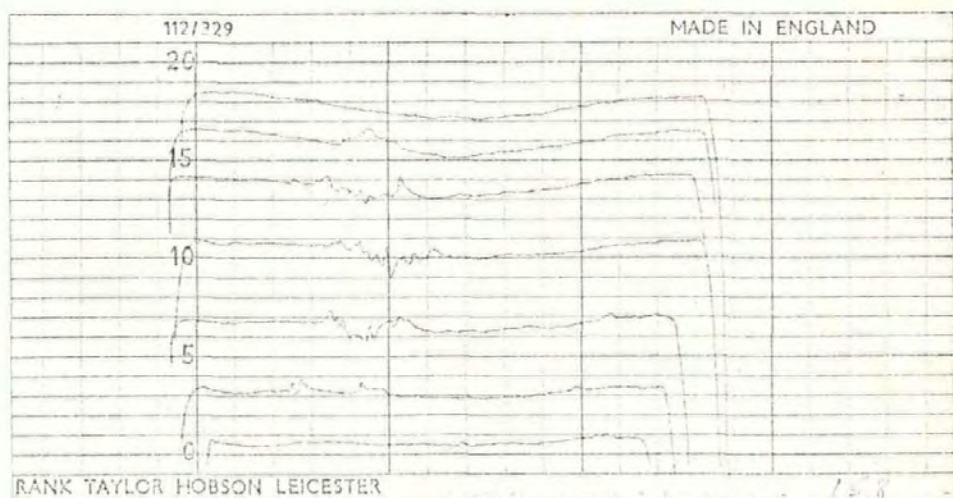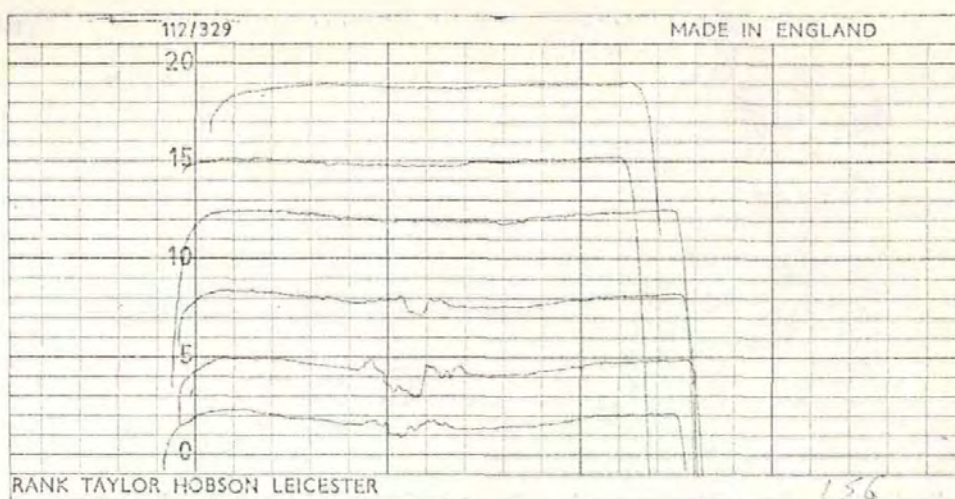
magn: ←→ 20 x, ↕ 500 x, 0.2 mm between traces

Figure 79. Talysurf profile traces of the electrode surfaces
after switching an a.c. load. (240Vrms, 50Hz,
10amp peak, resistive).

4.8.3 Erosion due to A.C. (Alternating Polarity)

When considering a.c. operation, not only is the ignition point on the half cycle a random event, but also the polarity of the contacts. The cumulative effects observed on full wave rectified a.c. will not be present in the same way. The actual material lost to the surroundings will be of the same order, since this only depends on the ignition point and the occurrence of transfer, and is not sensitive to the direction in which the transfer is taking place. The pip and crater formation observed on full wave rectified switching operations is unlikely to occur, since some of the material deposited on, say the cathode for one operation is just as likely to be transferred back on another subsequent operation when that same contact is the anode.

Another sample of switches was used to perform predetermined numbers of operations up to 1000 in increments of 100. Sufficient voltage and current oscillographs were recorded to obtain an even distribution of ignition points across the half cycle. The testing current used was 10amps peak again with the normal main supply voltage of 240Vrms (340 V pk.)

After the tests the contacts were removed for examination using the S.E.M. and Talysurf. Typical results are shown in Fig.79. The erosion pattern still appears in most cases with a singular crater formation. However, there is considerable material deposited either around the periphery of the crater or in some cases to one side of it. To enable the talysurf measurements to be presented graphically, the volume of the crater and surface build up were added together and halved to give a representative
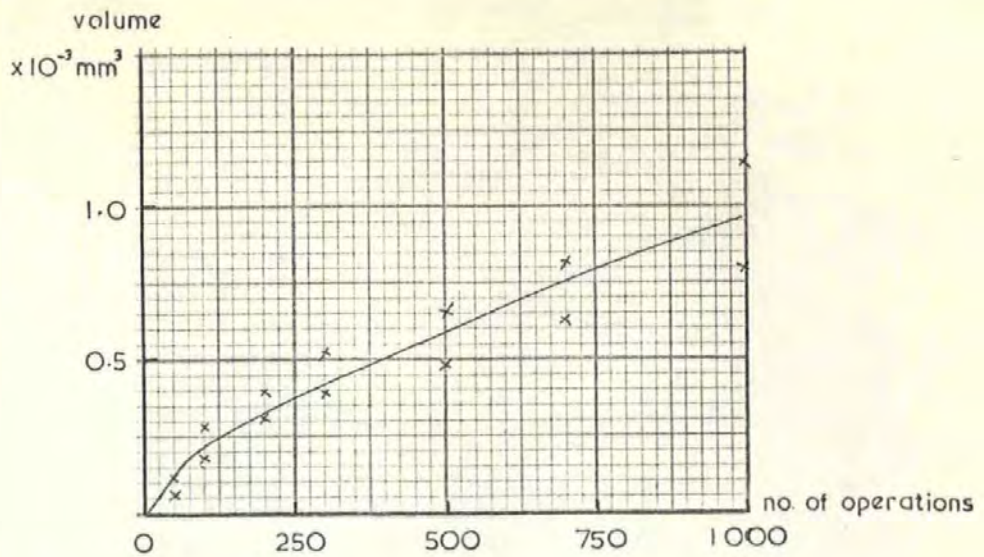
Fig.80. Material displaced on the electrode surface. Operating
conditions : 240Vrms, 50Hz, 10amps peak, resistive load.
Average total arc energy dissipated per operation is
0.7 joules. The points on the graph represent the spread
in the results obtained for different switches performing
the same number of operations.

Fig.81. Material displaced on the electrode surface for switch
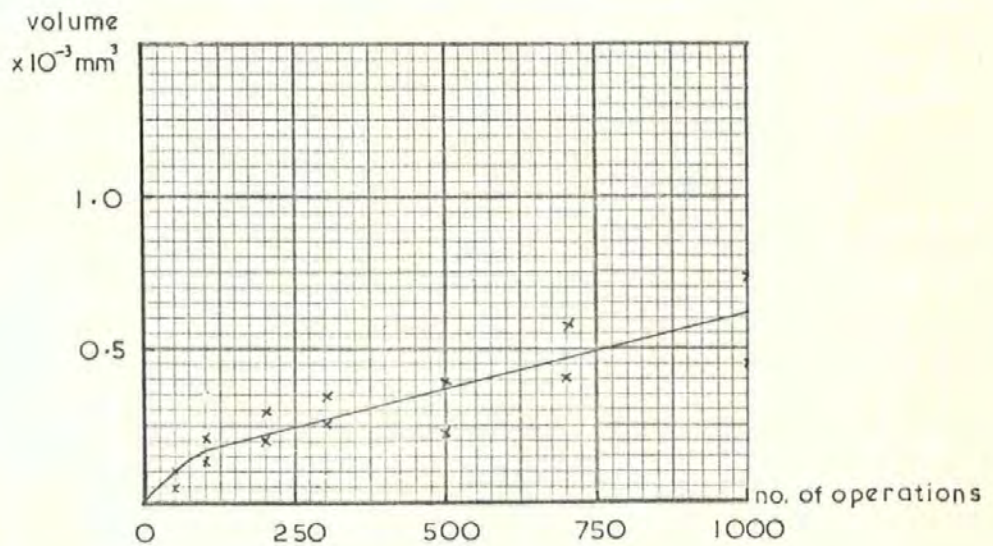with backstop inserted. Operating conditions : 240Vrms,
50Hz, 10amps peak resistive load. Average total arc
energy dissipated per operation is 0.45 joules. The points
on the graph represent the spread in the results obtained
for different switches performing the same number of
operations.

value of the amount of material displaced. The volume is plotted against the total number of operations in Fig.80.

From the Talysurf measurements it appeared that the contacts which had performed higher numbers of operations had a build up of material on the surface in excess of the volume of the crater. Fig. 85 shows photographs of sections through contacts after performing large numbers of operations. One of the things revealed by the sections is that the material deposited on the surface is not always solid throughout, but sometimes contains small cavities of trapped gas. Hewitt (15) also demonstrated that silver was capable of absorbing oxygen when in the molten state, introducing a volume change.

The experimental measurements of erosion performed on full wave rectified a.c. indicate that the anode surface is the one which has the most damage, with the formation of a crater. The cathode generally acts as the recipient of most of the material eroded from the anode. For normal a.c. then, with random polarity changes most of the 'damage' occurs to an electrode surface when it is the anode. Since the talysurf traces indicate a cumulative growth of the material build up (cathode) and crater volume (anode), it appears that every time an electrode is the anode, the arc erodes from the same previous arcing site, and every time it is the cathode, it received material in the same preferential location. This would explain why on a.c. there is sometimes a build up of material to one side of the crater.

Slade (16) has stated that the arc roots have preferential sites on each electrode, when switching a.c., resulting in complementary pip

and crater formation on both surfaces. The experimental

conditions here are different to those reported by Slade, whose

measurements were based on make and break operations, using a

'creep type' switch i.e. slow opening velocity characteristic

(typically 0.4×10^{-3}m/s) resulting in longer average arcing

time.

The measurements obtained for this work on a.c. show that

material transfer is taking place in both directions dependent

upon polarity, and the significant cause of erosion over many

operations is the cumulative effect of the anode end of the arc

eroding material from the same location each time.

4.8.4 Erosion of switch with modified opening characteristics

In Section 4.7.1 it was demonstrated that by reducing the travel

of the moving contact, the total arc energy could be reduced.

The effect of this reduction in energy on the erosion of the

contacts will now be investigated.

There are two immediately obvious effects of restricting the

travel of the contact.

    i. Anode fall is less likely to exceed the cathode fall,

        and if it does it will not be by so much as observed

        previously.

    ii. Less voltage will be dropped across the arc column

        due to the decrease in arc length.

As on previous tests a sample of switches was put through specified

numbers of operations up to 500. Full wave rectified supply was

used again, at 10amps peak current, so that the effect on the anode
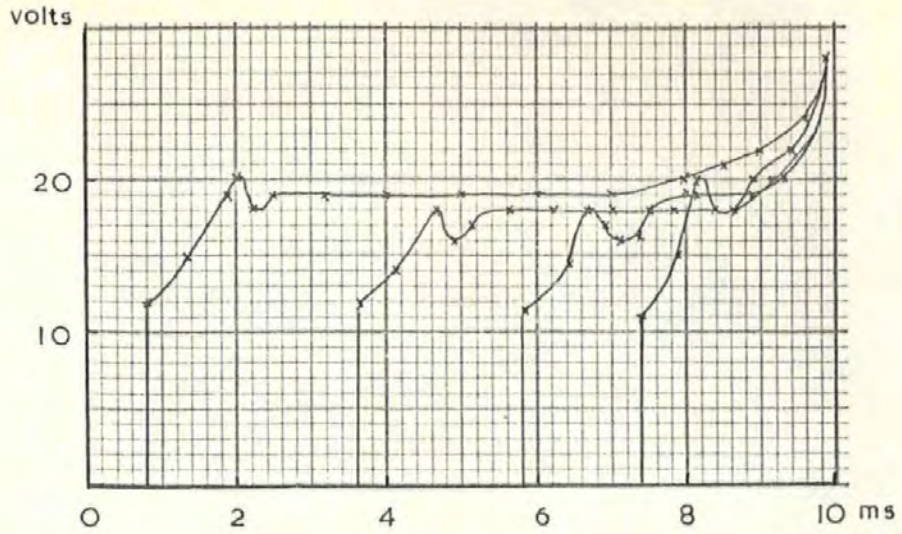
Fig.82a. Arc voltage transients occuring for switch with
          backstop inserted. Operating conditions : 240Vrms,
          50Hz, 10amps peak resistive load.
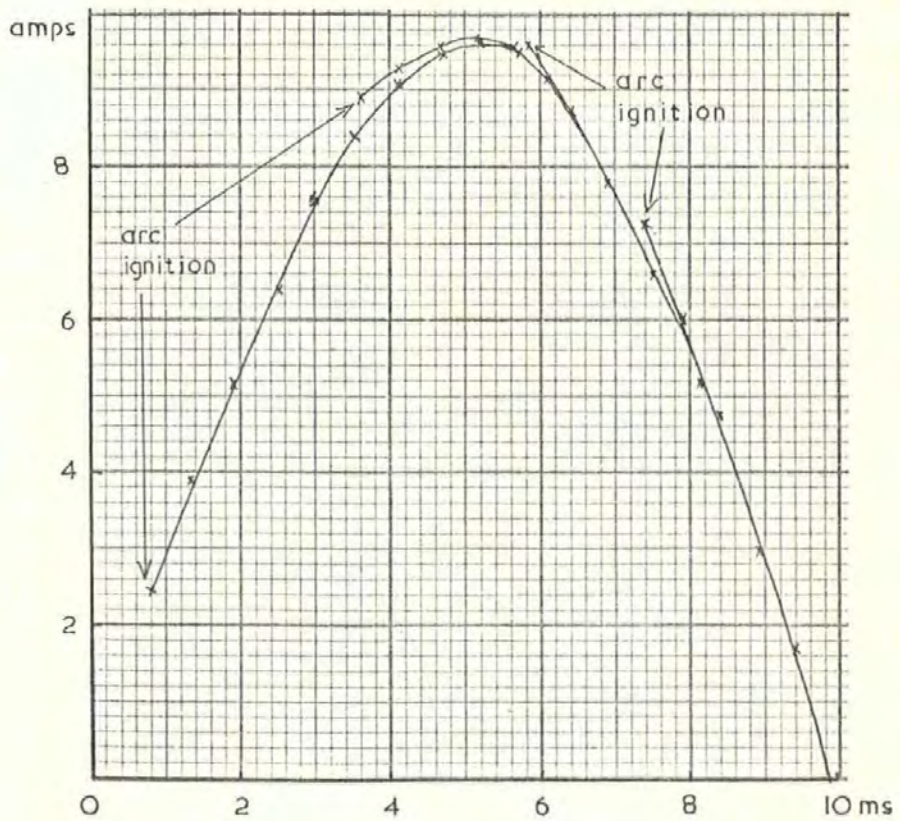

Fig.82b. Arc current transients corresponding to the
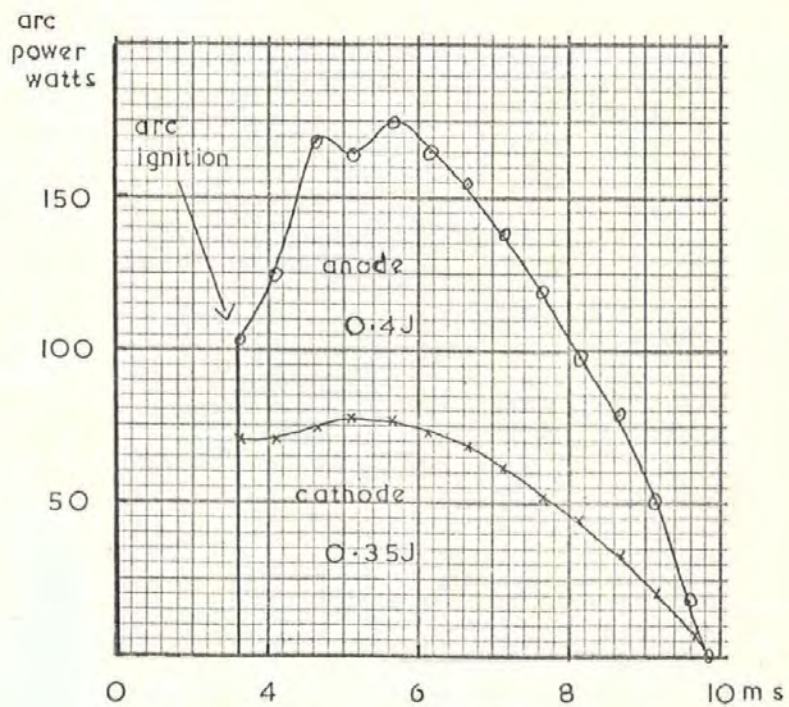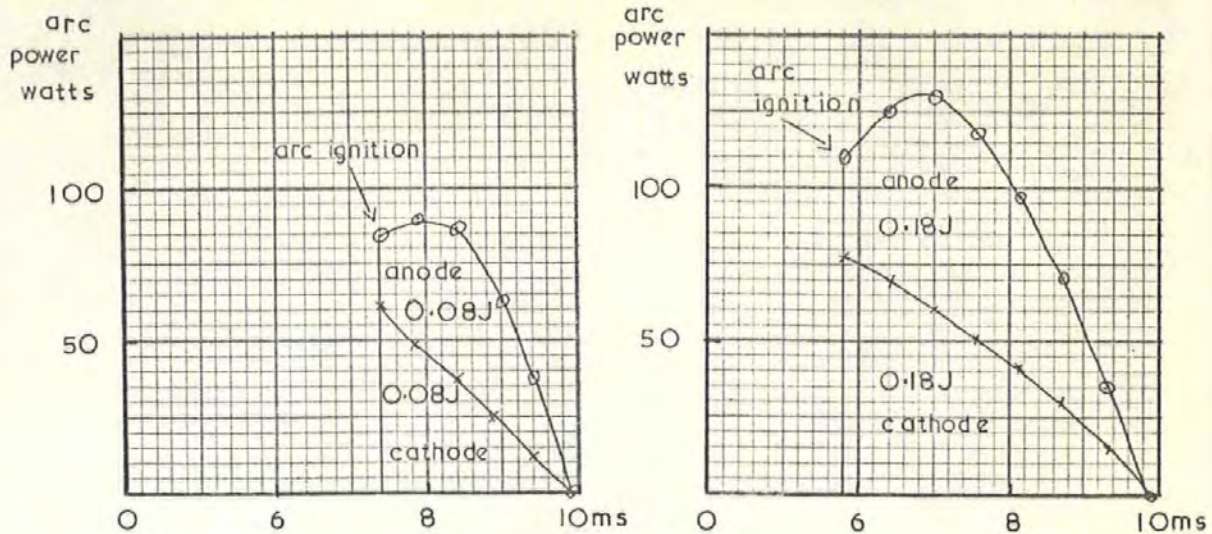   voltage transients shown above.

Fig.82c. Arc power curves for switch with backstop.
Ignition points correspond to those of Fig.82a.

and cathode, of reducing the arc length, could be observed.

Typical oscillographic recordings of the arc voltage and current are shown in Fig. 82 for four ignition points across the cycle. Typical arc power curves for the anode and cathode falls are shown in Figs. 82c & 82d. The voltage drop across the column in these results is less than half a volt so it has been ignored for the purposes of calculating the arc energy distribution. Fig.83 shows how the energy dissipated in the anode and cathode falls varies with ignition point on the cycle. For arc ignition 4 ms or less prior to a zero the energy dissipated in the anode and cathode falls is the same. For ignition points earlier in the cycle than this the energy dissipated in the anode fall becomes progressively greater than that dissipated in the cathode fall. For the ignition point of 9.2ms prior to zero the energy in the anode fall exceeds that in the cathode fall by about 0.2 joules.

The ignition point is a random occurrence again hence the average value of energy for a large number of operations can be calculated as before. For the anode fall the average is 0.3 Joules/operation, compared with 0.37 joules previously including half the energy dissipated in the column. The energy dissipated at the cathode is less by the amount previously added in from the column.

These average values do not demonstrate the significance of the energy reduction achieved. It was shown in the previous section that the maximum damage is inflicted to the anode surface as a result of early ignition by the arc. The reduction in energy at these earlier ignition points by using the backstop is appreciable, in some cases up to 35%.
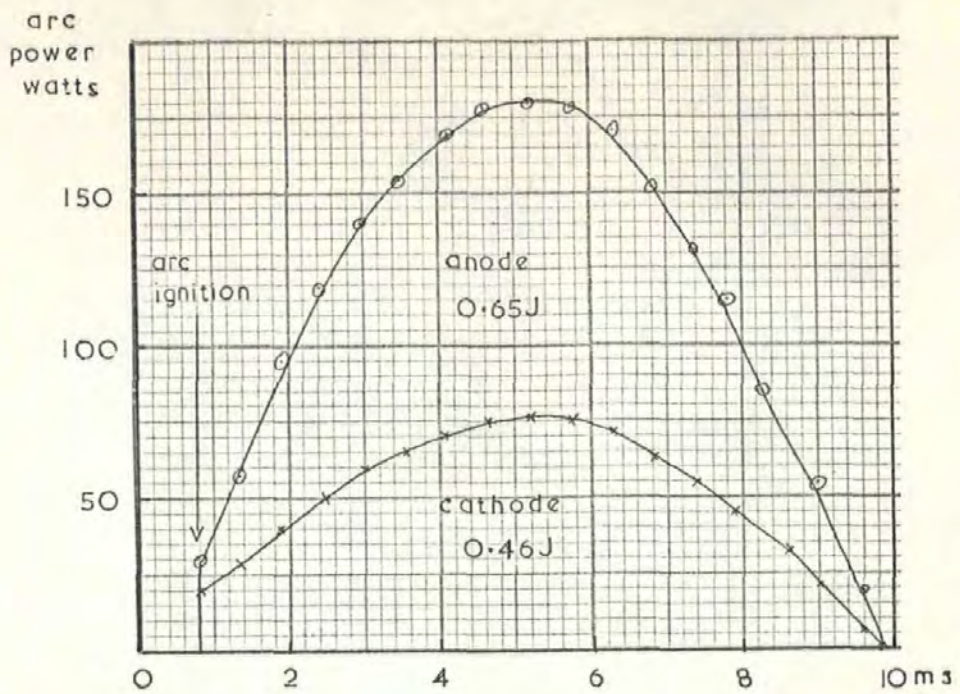
Fig.82d. Arc power curve for switch with backstop.
          Ignition point corresponds to that shown in Fig.82a.
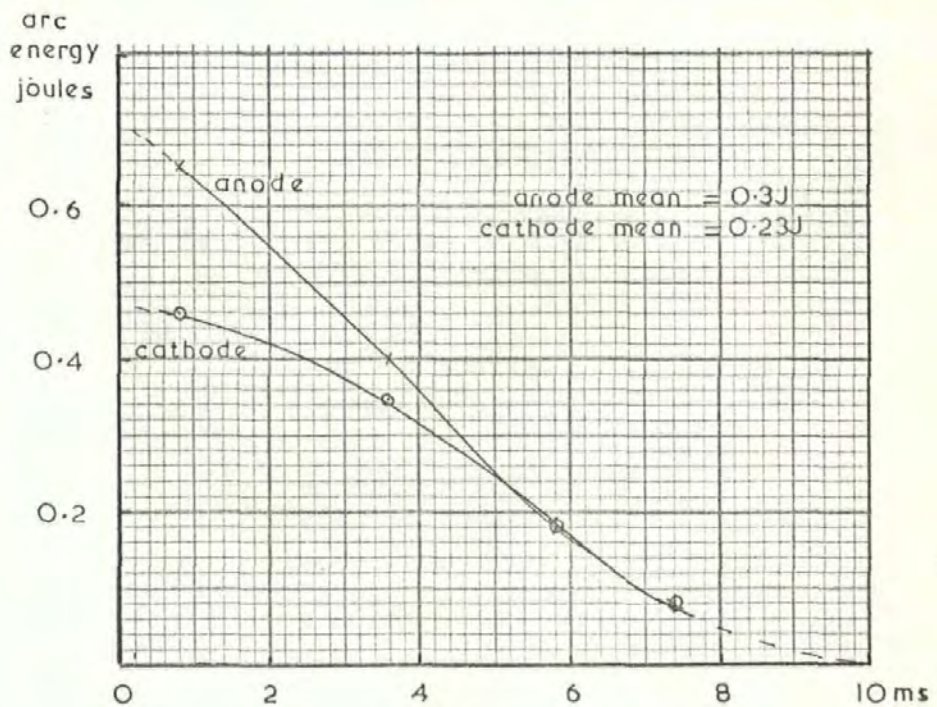
Fig.83. Graph showing how the energy dissipated in the anode and
         cathode falls varies with ignition points for a switch
         with a backstop inserted.
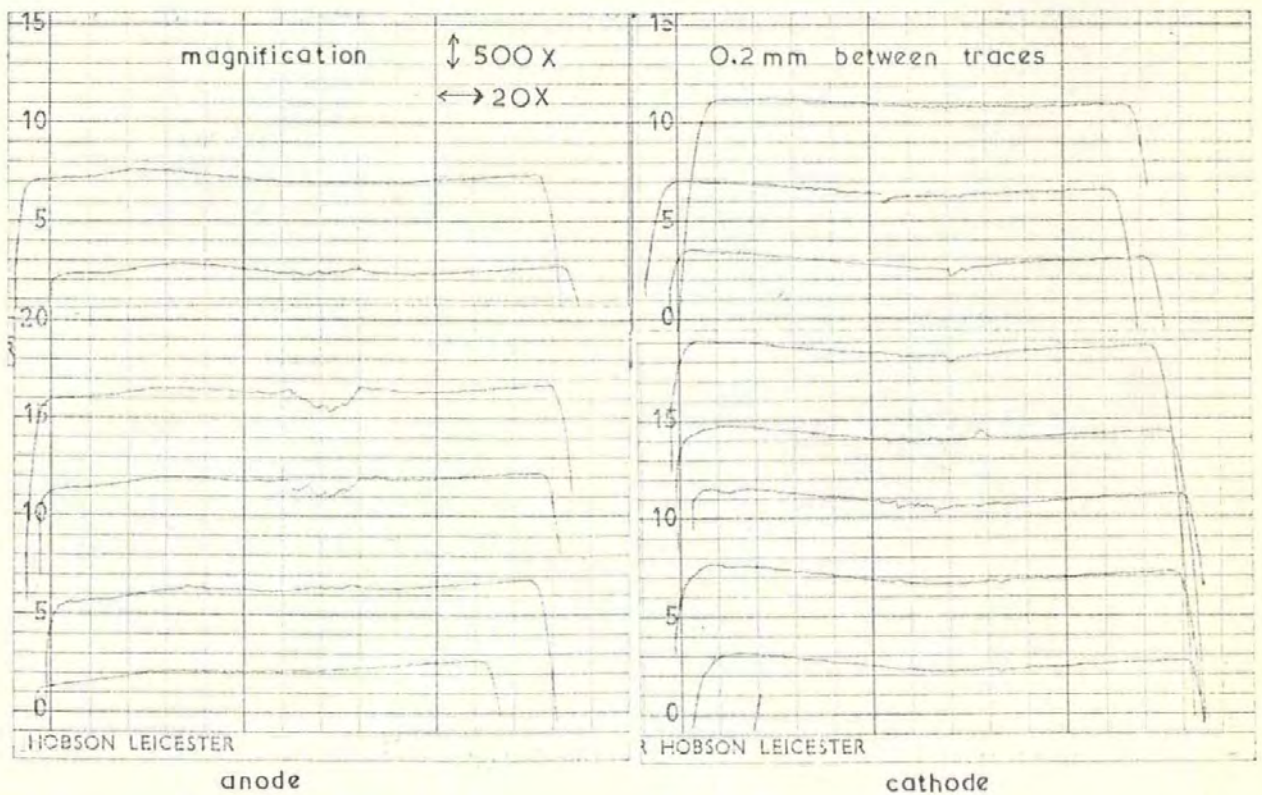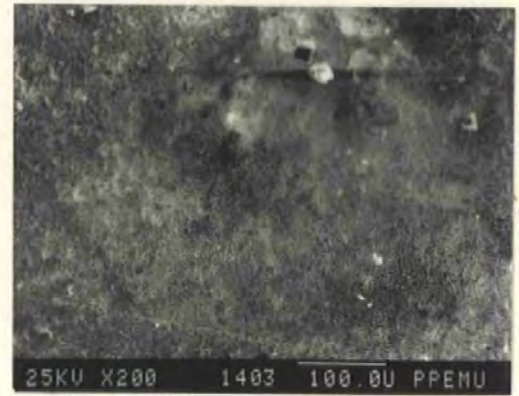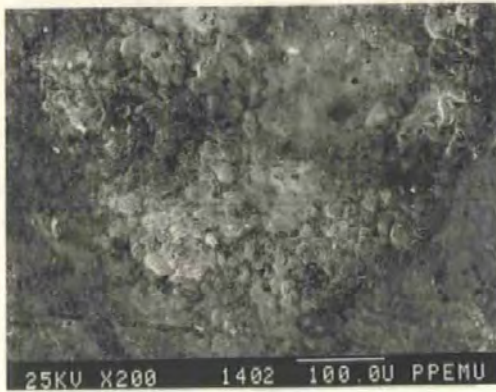
Fig.84. S.E.M. photographs and talysurf profile traces for the electrode surfaces of a switch with a backstop fitted. Results were obtained after 100 operations on 240Vrms, 50Hz, full wave rectified, 10amps peak, resistive load.

Specimen Talysurf traces and S.E.M. photographs are shown in Fig.84.
The anode is still characterised by a crater with material deposited in
the form of a rim. The cathode surface also displays a small crater in
its surface, but this is suppressed by a build up of material to one
side of it. The change to the cathode is much less prominent than that
occurring to the anode, and after 100 operations very little change on
the cathode surface was detectable at all. This supports a statement
made by Capp that increased energy input to the cathode is a result of
energy being thermally conducted from the column, since the arc
column at this arc length (typically 0.2mm) has negligible energy
dissipated in it.

The rate of growth of the anode crater for these switches with the
backstop is about 3.6 x 10^{-6}mm^3 per joule of energy dissipated by the
whole arc. This compares with about 7 x 10^{-6}mm^3 per joule for the
normal switch on full wave rectified a.c.

To conclude this section a set of measurements was made of the contact
erosion which occurred when switches fitted with a backstop were
operated on an a.c. supply voltage and a resistive load of 10amps.
Operating conditions were exactly the same as those specified in section
4.11.2, and the data was collected and plotted in the same way. The
results are shown in Fig.81 and can be compared directly with those of
Fig.80 for the normal production switch. The rate of erosion for the
un-modified switches is 0.7 x 10^{-6}mm^3 per operation, and for the switches
with the backstop fitted is 0.4 x 10^{-6}mm^3 per operation. It would seem
that this reduction in contact erosion could be a direct result of the
energy dissipation of the arc being reduced by the insertion of the
backstop. The reduction is 0.7 joules/operation to 0.45 joules/operation
using the average values calculated after many operations.

The measurements of weld strength between the switch contacts are contained in Appendix I. This work on welding is not in anyway an exhaustive study of this particular aspect of switch performance. It was undertaken because in the past Ranco have found that switch contacts have been prone to stick or weld in, without any apparent reason. On this basis it was decided to see if any correlation could be obtained between the number of break operations performed by the switch and the strength of the weld occurring between the contacts at the make operations. Since arc energy and erosion at break have been clearly defined, it may be possible to relate any sudden increase in the weld strength to the amount of energy previously dissipated at the contacts or the amount of erosion that has taken place. Although the results in Appendix I are not conclusive it is felt that they do provide a sufficient basis or starting point for future work to be done of a more detailed nature, in this area of switch performance.

REFERENCES - CHAPTER FOUR

1. J.M. Harris, G.R. Riley, R.C. Brunel.
    Summary Report on the Development of Improved Control Switches.
    Report to Control Division of Ranco Inc. by Battelle,
    Columbus Labs. Feb. 1972.

2. S.G. Eskin.
    'Effect of Contact Opening Speed on Arc Energy in a.c. Switching'
    Report of Engineering Dept., Edison General Electric Appliance Co.
    Inc., Chicago.

3. J.F. Tibolla.
    Private Communication, Nov. 1977.

4. W. Hanka.
    'Chance of Misfit in Assembly'.
    Product Engineering. May, 1959.

5. M.R. Hopkins and R.H. Jones.
    'Transient, Bridges and Micro-arcs in Low Voltage Electrical
     Contacts'.
    Holm Seminar on Electric Contacts, 1972.

6. A. Erk and H. Finke.
    'Behaviour of Contact Materials in Bouncing Electrical Contacts'
    E.T.Z. A (1965). Heft. 9, p. 297.

7. P.G. Slade.
    'Current Interruption in Low Voltage Circuits'.
    Holm Seminar on Electric Contacts. 1968.

8. R. Holm.
    Electric Contacts, Theory and Application.
    Fourth Edition, Springer-Verlag, 1967.

9. M. Sato, M. Hijikata and I. Morimoto.
    'Characteristics of the Arc breaking a Non-indicative Circuit in Air'.
    Trans. Jap. Int. Metals No. 2, March 1974.

10. A. Takahachi and K. Miyachi.
    'Arc Termination Current on Breaking Contacts'.
    Holm Seminar on Electric Contacts, 1975.

11. M. Sato.
    'Studies on Silver based Electrical Contact Materials'.
    Trans. Nat. Res. Inst. for Metals. Japan. Vol. 18, No. 2, 1975.

12. B. Capp.
    'Power Balance in Electrode Dominated Arcs'.
    J. Physics. O. Appl. Phys., Vol. 5, 1972.

13. D.J. Dickson and A. Von Engel.
    'Resolving the Electrode Fall Spaces of Electric Arcs'.
    Proc. of the Royal Society A. Vol. 300, 1966.

14. G.A. Farrall.
    'Arcing Phenomena at Electrical Contacts.'
    Holm Seminar on Electric Contacts, 1969.

15. B.L. Hewitt.
    'Erosion of Silver-Palladium alloys in different gases'.
    Thesis - Univ. of London, May 1974.

16. P.G. Slade and F.A. Holmes.
    'Pip and Crater Formation during Interruption of Alternating
    Current'.
    Int. Conf. on Electric Contact Phenomena. Japan 1976.

CHAPTER FIVE

CONCLUSIONS

5.1 Review

This research work has evaluated the operation and performance of snap-action switches produced for use in thermostatic controls operating on 240 V. r.m.s., 50 Hz. Results from initial experimental work indicated that the events occurring during a switching operation comprised three areas for investigations. These were defined as the mechanical performance, electrical performance and contact phenomena. As the experimental work progressed it was clear that an understanding of how the switch mechanism characteristics influenced both the electrical and contact performance was required. It was anticipated that this would lead to the emergence of design criteria that would produce an overall optimum performance characteristic for the switch that could be used as a basis for future designs.

Accordingly a detailed analysis of the switch mechanism performance was the first objective of the project. This knowledge was then used to aid interpreting the results obtained for the electrical character-istics of the switch. The information from these two areas of investigation was subsequently applied to a study of the contact performance with a view to reducing the rate of erosion of the contacts.

5.2 Switch Mechanism Performance

The results from the high speed films of the switch contacts closing and opening are detailed in Sections 4.3.1 and 4.3.2, in the form of contact separation versus time graphs. Switches set to the same operating stroke produce similar opening and closing loci. Variations in the mechanical performance over the prescribed lifetime (200,000

operations) are minimal, , with 12-15% being a typical worst case difference on the separation or time scales of the loci. Typical closing times from the instant of toggle were found to be 2.85 ms for a switch with an operating stroke of .020" (0.53 mm). After first impact the moving contact oscillates or rolls about its final rest position for 1-2 ms. Typical opening times, to the point of maximum separation (1.6 mm) were found to be 2.6 ms for the same operating stroke. After reaching the point of maximum separation the moving contact oscillates about its final rest position, with an initial amplitude of 0.6 mm, which decays to zero over 30-50 ms. The frequency of the oscillation is about 400 Hz, but increasing with time. An equation to describe the type of motion was deduced as

$$\text{Contact separation} = h \left[1 - e^{-\alpha t} \cos(\omega_s t)^n \right]$$

where h is the final separation of the contacts at rest

$\alpha = \dfrac{1}{\tau}$ where τ is the time constant of the oscillation decay

ω_s is the angular frequency of the contact oscillation

n takes into account the decreasing period of the oscillations

The values of these constants are the same for switches set to the same operating stroke.

5.3 Electrical Performance

Arcing as a result of contacts bouncing apart after first impact was observed on the electrical transient recorders (4.4.2). Typical bounce arc times were in the range 0.1-0.2 ms. Although no physical separation was visible from the high speed films, the bouncing occurs during the rolling motion of the contacts after impact. The erosion pattern which resulted from the bouncing arc was found to lie along the axis of roll (Fig. 29). Talysurf measurements of the contact surface after multiple make operations showed the erosion characteristic to be one

of material transfer anode to cathode with pip and crater formation (Figs. 32 and 33).

Measurements of the erosion after arc break operations on 40V, 8A d.c. (Fig. 30) indicated that surface degradation and movement of contact material was greater by several orders of magnitude than that which occurred due to contact bounce.

Having identified the main source of contact erosion, i.e. the break arc, much of the experimental work was then concentrated in this area, in order to more completely define the characteristics of this arc. The relationship between the maximum arc length attained, between separating contacts, before extinction and the values of circuit parameters, i.e. supply voltage and load current, was shown to conform to the equation:- arc length $\ell = K(E - E_m - \frac{E}{I} . I_m)^{\frac{3}{2}} . I^{\frac{1}{2}}$

for d.c. operating conditions, 20-80V supply, 1-10A resistive load, where K is constant of value 4×10^{-6} for silver cadmium oxide contacts (Ag.CdO 85/15).

This equation and the equation for the contact separation locus enabled two equations to be developed to relate the instantaneous values of the arc voltage and current to the circuit parameters and switch mechanism characteristics for d.c operating conditions.

Arc voltage $e_t = E_m + \left[E - E_m - \frac{E}{I} . I_m \right]^{-\frac{1}{2}} . \frac{h}{k} \left[1 - e^{-\alpha t} \cos(\omega_s t)^n \right]$

Arc current $i_t = I - \frac{I}{E} . E_m - \left[E - E_m - \frac{E}{I} . I_m \right]^{-\frac{1}{2}} . \frac{I}{E} . \frac{h}{K} \left[1 - e^{-\alpha t} \cos(\omega_s t)^n \right]$

The product of e_t and i_t gives the instantaneous arc power. Good agreement was shown between the experimentally measured values and those obtained using these two equations (Fig. 39). The area under the graphs of arc power against arc duration gives the total arc energy

dissipated in the arc for these d.c. operating conditions, i.e.

$$\int_0^T e_t \cdot i_t \cdot dt \text{ where T is the arc duration (Fig. 40).}$$

Hence after a known number of operations the total energy dissipated between the contacts was calculated.

For a.c. operating conditions, typically 240V, 50 Hz, 1-12 amps resistive or inductive load, the equation to define the arc voltages was shown to be

$$e_t = E_m + \left[\frac{h \ (1 - e^{-\alpha t} \cos \ (\omega_s t)^n)}{K \ (\hat{I} \sin \ (\omega t + \theta))^{\frac{1}{2}}} \right]^{\frac{2}{3}}$$

where θ represents the ignition point of the arc relative to the preceding a.c. zero (Section 4.7). The arc current was shown to deviate by less than 10% from the value of the circuit current i.e. $\hat{I} \sin (\omega t + \theta)$, hence to a first approximation the arc power and therefore the arc energy was found from the product of e_t and $\hat{I} \sin (\omega t + \theta)$. (Fig. 45 and 46, Section 4.7.1)

From these graphs the dependence of the arc energy on the ignition point relative to the a.c. zeros was demonstrated. Since there is no control over the arc ignition point, i.e. it is a random event, it was shown that a meaningful value for the average arc energy per operation could be calculated for a large number of operations (e.g. more than 100). Hence the total arc energy dissipated between the contacts is obtainable from the product of this average value and the number of operations performed.

5.4 Contact Erosion

Measurements of the contact erosion after switching a d.c. resistive load (Section 4.8.1) showed that the amount of material displaced or removed from the contact surface was dependent upon the total energy dissipated in the arc. The direction of the net material transfer also appeared to depend on the energy dissipated in the arc, e.g. as the circuit current was changed, there was a reversal in the direction of the net material transfer:-

40V 4A (.035J/operation) transfer cathode to anode

40V 12A (0.196J/operation) transfer anode to cathode

Further to this it was suggested that the relative amounts of the arc energy that are absorbed by the anode and cathode depend upon the rate of growth of the arc and the length it achieves prior to extinction.   This was related to the relative magnitudes of the anode and cathode fall voltages.   The former was assumed to increase with increasing arc length, as shown by Capp (1), whereas the cathode fall voltage remains constant for the duration of the arc. Net transfer from cathode to anode usually occurs when the anode fall voltage is less than the cathode fall voltage for the duration of the arc.   Transfer anode to cathode occurs when the anode fall voltage exceeds that of the cathode fall.   A transition or crossover region occurs when at the extinction of the arc the energy received by the anode and cathode is equal.   For these switches the values of the circuit parameters when this occurs are 40V, 8A d.c. (Figs. 60 and 61).

When circuit conditions and mechanism characteristics are such that cathode loss is dominant (40V, 4A), it is sufficient to consider the erosion process from the cathode as being dependent upon the total

charge passed in the arc, since the cathode fall voltage is constant.

i.e.   Erosion α Arc energy

Arc energy $= V_c \times q$

α q since V_c is constant

When anode loss is the dominant feature it is not sufficient to consider only the arc charge since the anode fall voltage is now a significant part of the total arc voltage drop and varies with the length of the arc, thus the arc energy is the significant constraint. Since the maximum contact gap achieved by these switches (usually less than 2 mm) is less than the contact diameter (4 mm) the energy dissipated in the arc column is considered to be absorbed by the contacts. The error introduced by this assumption is small since the amount of energy in the arc column is only 3% of the total for operating conditions of 40V, 12A.

As a result of these conclusions from the measurements made using d.c. circuits, the following comments are made regarding the experimental results obtained for a.c. circuits (Section 4.8.2):-
For any one particular operation the erosion characteristic may be anode to cathode, cathode to anode or no net transfer, depending upon where on the a.c. cycle the switch contacts open and the arc ignites. For the purposes of identifying the contact erosion the a.c. cycle is divided into three parts:-

(1) Arcs igniting 7 ms or more after a zero (Fig. 71);
the cathode fall is greater than the anode fall for most
of the arc duration. More energy is therefore dissipated
at the cathode than the anode and net transfer of material
occurs from cathode to anode.

(2) Arcs igniting between 5.5 and 7 ms after a zero; due to the opening characteristic of the switch the arc energy is equally divided between the anode and cathode, and therefore material transfer occurs in both directions.

(3) Arcs igniting up to 5 ms after a zero; the anode fall is greater than the cathode fall for a large proportion of the arc duration, since the contacts open to the point of maximum separation and then oscillate about this distance during the arc lifetime. Erosion is predominantly anode to cathode since the anode receives more energy than the cathode.

Multiple operation on full wave rectified a.c. produces a crater formation on the anode and a pip on the cathode. This is in agreement with the 'average' values obtained for the energy dissipated at the anode and cathode respectively, after many operations, taking into account the varying ignition point, i.e. anode 0.33J/operation, cathode 0.24J/operation at 240V, 10A, 50 Hz, full wave rectified. Also when arc ignition occurs early in the cycle more material is involved in the transfer process anode to cathode than where the arc ignites later in the cycle and the net transfer direction is cathode to anode. This is due to the greater arc lengths achieved after early ignition and the relatively higher arc energies that ensue. For these greater arc lengths some of the contact material involved in the transfer process is lost to the ambient surroundings. (Fig. 78).

For switches operating on a.c. when the polarity of the contacts

regularly reverses, the Talysurf measurements have shown that both contacts have a crater formation with a build up of material to one side of the crater. It seems that most damage or erosion occurs whenever a contact is the anode and early ignition of the arc occurs relative to the a.c. cycle. Pip and crater formation may then occur due to the arc occurring at a same previous arcing site, as suggested by Slade (2), and material being deposited at the same preferential location on the cathode.

5.5 Improvements to Switch Performance

A reduction in the rate at which the switch contacts erode was obtained by reducing the energy dissipated in the arc at any one operation. This was achieved using a normal production switch with an adjustable backstop inserted under the moving contact to restrict the maximum contact separation. This effectively limits the length of the arc for its duration and therefore the arc voltage is held at a lower value. As a result the arc energy is reduced (Figs. 53 and 54). The contact gap used to obtain the results was 0.2 mm. The rate of growth of the anode crater for full wave rectified a.c. was reduced from 7×10^{-6} mm^3/joule to 3.6×10^{-6} mm^3/joule of total arc energy. On a.c. the rate of material displacement was reduced from 0.7×10^{-6} mm^3/operation to 0.4×10^{-6} mm^3/operation (Figs. 80 and 81). The corresponding decrease in total average arc energy was 0.7 J to 0.45 J per operation for 240 V r.m.s., 50 Hz, 10A peak.

The results have shown that for the arc energy and therefore the contact erosion to be a minimum, the maximum contact separation must be limited to a value of 0.2 mm, which is not practically viable due to the possibility of electrical breakdown or accidental shorting of the contacts. A realistic solution for switch improvement is to reduce
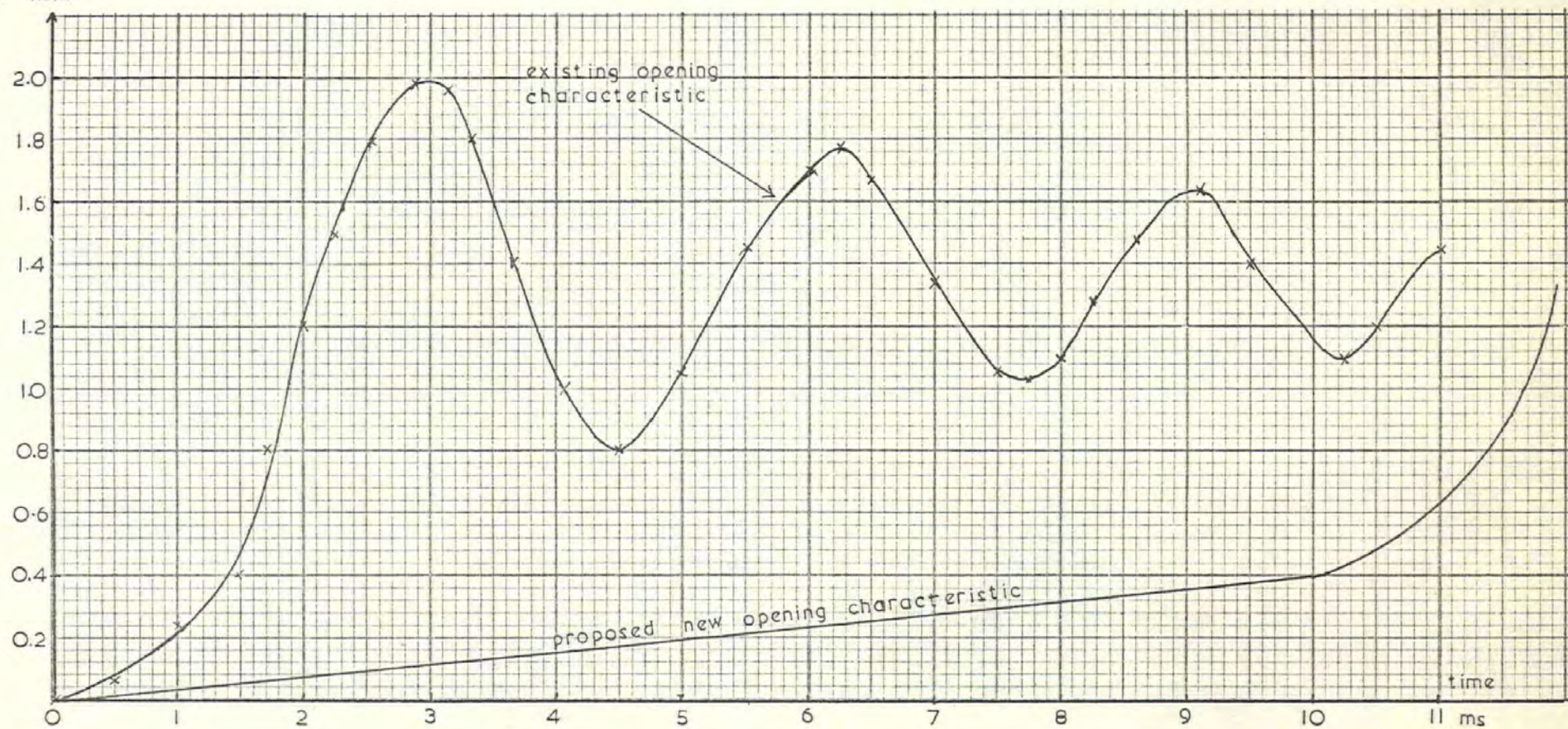
Fig. 84. Proposed opening characteristic to reduce the contact erosion of the snap action switch. The opening locus of an existing switch is shown for comparison.

the initial rate of acceleration of the contacts so that for the arc duration the contact separation is maintained at a sufficiently low value. After the arc extinguishes the contacts continue to separate until the required separation is reached. The switches tested in this study had an acceleration rate which produced a velocity of 200-1000 mm/sec after about 1 ms, and the contacts usually maintained a separation of 2-2.5 mm after 2.5 ms. It is considered that an opening velocity of 40-50 mm/sec for the first 10 ms would achieve the required results. This would produce a contact separation of 0.4-0.5 mm after 10 ms, the maximum duration of any arc. After 10 ms the contact can continue to open to any desired gap. A possible improved opening locus is shown in Fig. 84 with an existing mechanism characteristic for comparison.

This method of optimising the switch opening characteristic provides one way of improving the performance of the switch and increasing the life expectancy of the contacts. On the basis of this optimised design, future work could be undertaken to arrive at a smaller size of contact which will still perform the required 200,000 operations. The resulting reduction in the amount of silver used for each contact will then provide an economic saving in the material cost of each switch.

The main objectives of this research have been realised, and it is felt that the results and recommendations provide a basis for further experimental and theoretical research.

magn: 570 x

Fig.85. Sections through the electrodes after 100 000 operations.
Depletion of Cadmium oxide is apparent near the surface, with
areas of resolidified silver. Bubbles of gas also appear to
be trapped in the surface layers of resolidified material.

APPENDIX I

Weld Strength Testing

Introduction

The relation between energy dissipated in the break arc and erosion of the contact surfaces has been demonstrated in Chapter 4. In this section the strength of the weld occurring when the contacts close an electric circuit has been investigated. The intention has not been to exhaustively explore the mechanisms which contribute to contacts welding, but to try and observe whether the progressive erosion by the break arc results in any increase in the weld strength at subsequent make operations. It may be possible to ascertain whether there is likely to be any beneficial decrease, in the rate of rise of the weld strength, due to a decrease in the energy dissipation in the arc at break.

Surface degradation as a result of arcing after many operations has been shown to take the form of progressive growth of surface irregularities i.e. small craters and protrusions distributed over the surface. It has also been shown by Kossowsky et al (1), Shen et al (2) that erosion of the surface is accompanied by depletion of cadmium oxide in areas of prolonged arcing, leaving large areas of silver. Section 4.11.2 referred to sections through contacts revealing gas bubbles trapped within resolidified contact material. These photographs are shown in Fig. 85. Besides these visible gaps within the contact surface, areas depleted of cadmium oxide are apparent in the surface layers with large areas of resolidified silver. Koepke et al (3) have reported that silver contacts are prone to produce stronger welds than silver cadmium oxide contacts which were found to have a consistent weld resisting tendency. Hence, areas of cadmium oxide free silver are undesirable if a reliable

resistance to welding is to be maintained.

The weld strength resulting from a make operation will be related
to two parameters:-

1.   Bounce time i.e. Does a larger bounce time (hence greater
     energy dissipation) produce stronger welds?

2.   Number of operations: i.e. Does the cumulative energy
     dissipation due to the break arc result in an increase in the
     weld strength at subsequent make operations?

Experimental Work

A 240volt 50Hz supply was used and the switches were set up on the
recycling rig to switch a 10amp (peak) resistive load. Before commencing
the recycling tests, the switch on test was made to perform one make
operation closing a load of 36amps d.c.   This is the duty required to
meet B.S. 5.4.24 part I applicable to these switches. The bounce time
for this make operation was recorded and then the current was switched
off at another point in the circuit. The strength of the weld due to
one make operation was then measured.

The switch was then allowed to recycle the 10amp a.c. load up to a
certain number of operations after which one make operation was performed
again at 36amp d.c. The bounce time and weld strength were both
recorded and the recycling process recommenced. This procedure continued
until the nominal life of the switch had been exceeded (i.e. 200 000
operations).

The results from these measurements are presented graphically in Fig.86.
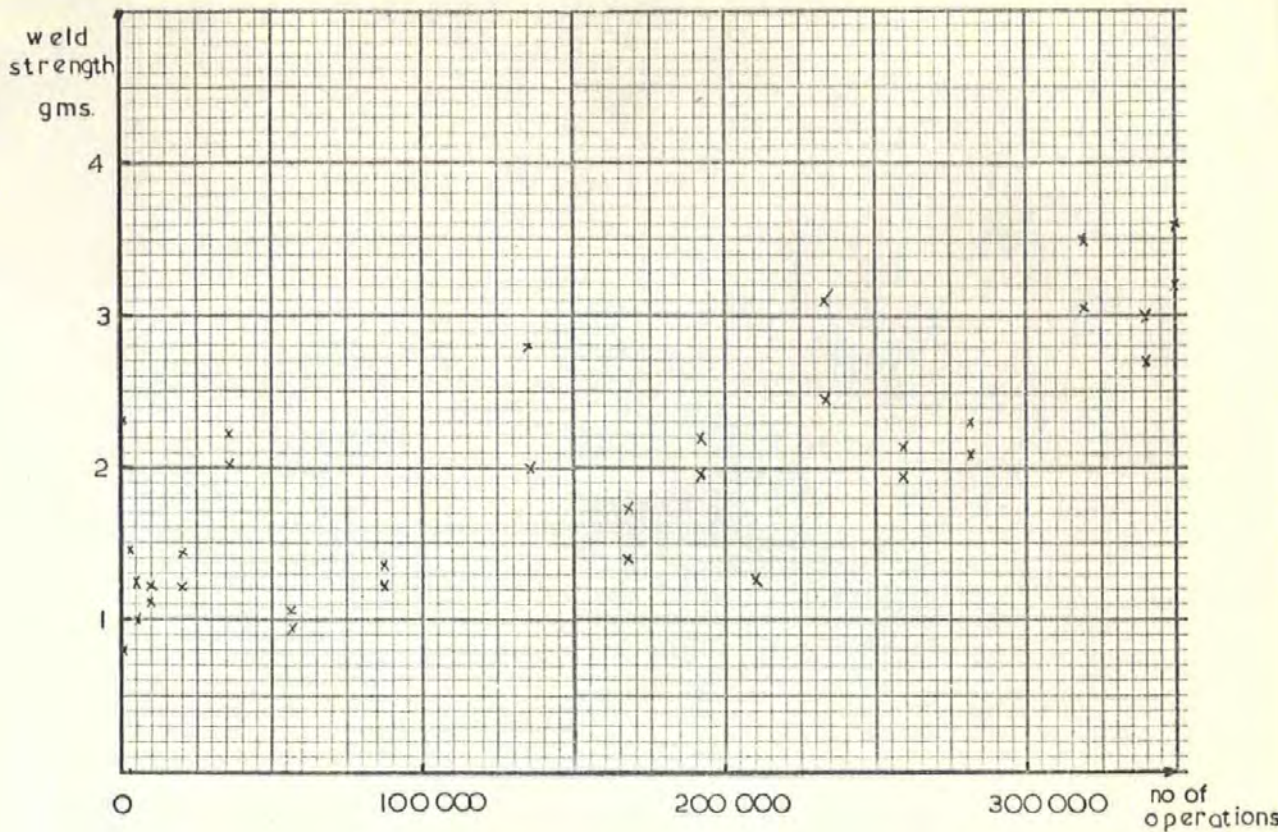Fig.86a shows a plot of weld strength against number of operations.

Fig.86a. Weld strength/number of operations. A small increase in the weld strength occurs as the number of operations performed increases.
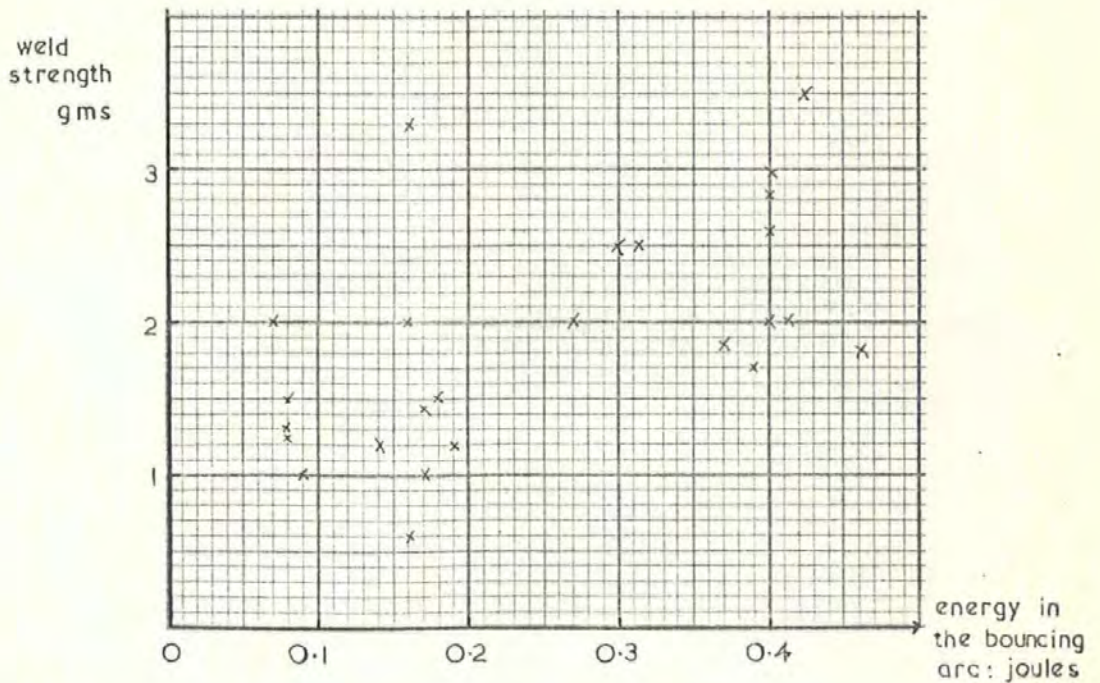

Fig.86b. Weld strength/energy in arc which occurs due to contact bounce. The weld strength is generally stronger for the bounces with the larger energies dissipated.

Since the average energy/operation is known from the oscillograph recordings, this is also a plot of weld strength/energy dissipated in the break arc. Fig.86b comprises the results obtained from the oscillographic recordings of the make operations at 36amps d.c. and is a plot of weld strength/energy dissipated during bouncing by the arc. Essentially it is a comparison of the different weld strengths produced by bounce times of differing durations.

As previously reported by Holm & Erk & Finke (4), there is a large spread in the results for weld strength plotted in Fig.86a. The amount of scatter in the results is approaching the values of the weld strength themselves. However, the graph shows a definite positive slope i.e. weld strengths increase as the number of operations completed by the switch increases, and the mean value of the weld strength can be described by the equation:-

$$\text{Weld strength(W) gms} = 1 + 7 \times 10^{-6}.n$$

which is the equation of the straight line drawn through the points Where n is a positive integer defining the number of operations. Fig.86a is typical of the results obtained with many other switches tested under the same operating conditions, after a few operations all the switches produced a weld of strength 1gm ±0.5.grms.

Fig.86b is a result of the fact that for every make operation the bounce time changes slightly. For the switch used to produce these results, the bounce time is seen to vary between 0.1 and 0.4 msecs. over about 300 000 operations. Again there is a large degree of scatter with a slight rising trend in the results i.e. a longer bounce time produces a stronger weld.
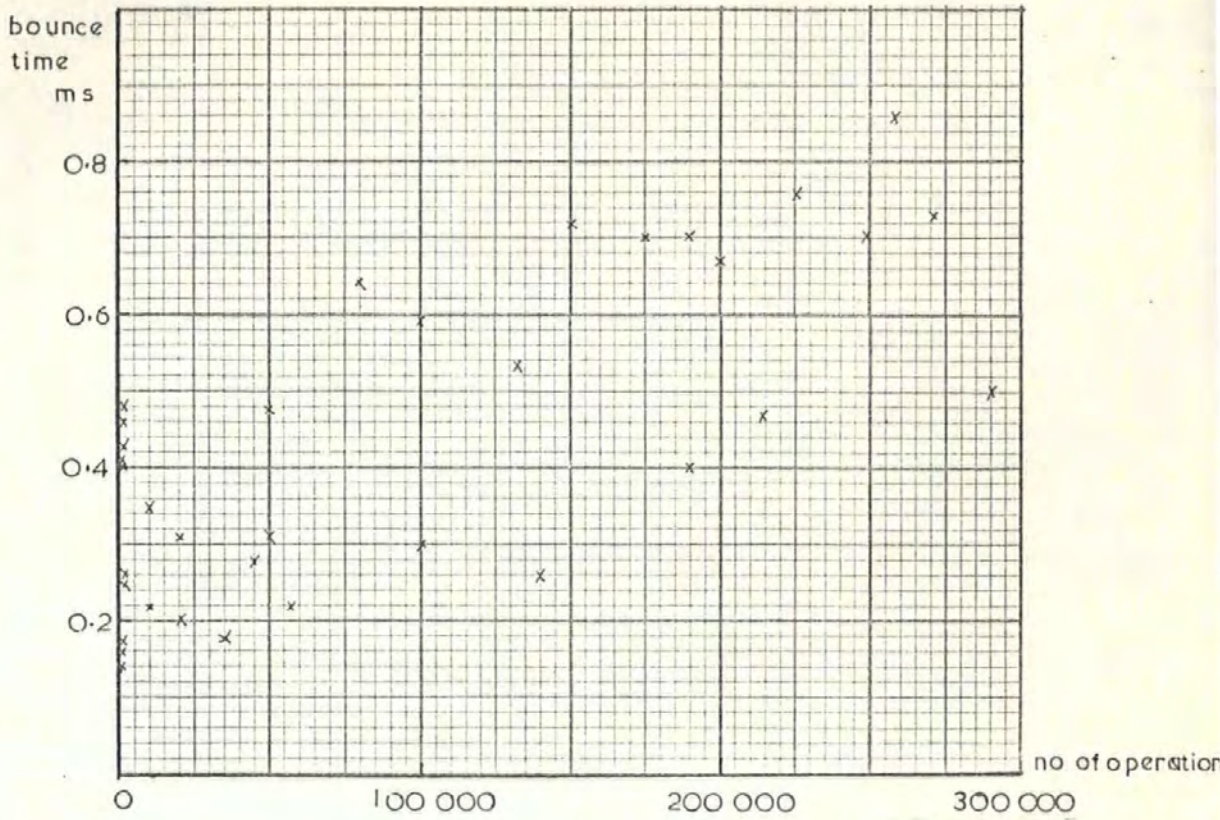
Fig.86c. Bounce Time/number of operations. Bounce times have much variation, but the higher bounce times occur after the larger numbers of operations.

A plot of bounce time against number of operations is shown in Fig.86c. Again there is a large degree of scatter, but there appears to be a tendency for longer bounce times to occur more regularly after a large number of operations (e.g. 100 000). The work at the beginning of Chapter 4 has showed that there is no sign of mechanism fatigue manifested in the switch closing characteristics. Since the only other variable is the contact surface it seems that the surface irregularities produced may have the effect of causing the contacts to take longer coming to rest after impact, with more transient separations occurring.

Of the three graphs drawn in Fig.86, graph (a) of weld strength against number of operations has the most correlation. This seems to indicate that the weld strength is more influenced by the surface condition of the contact than the duration of the bounce occurring during the process of establishing contact. Hence the rate of increase of weld strength will also benefit from a reduction in the erosion caused by the break arc. Reducing the rate of growth of pits and protrusions on the contact surface will also reduce the probability of mechanical interlock contributing appreciably to the value of the weld strength.

REFERENCES   -   APPENDIX I

1.   R. Kossowsky and P.G. Slade.
     'Arcing and the Microstructure and Morphology of Ag Cd O Contacts'.
     Holm Seminar on Electric Contact Phenomena, 1972.

2.   Yuan Shou Shen and R.H. Krock.
     'A Study of the Erosion Modes of Ag Cd O Contact Material'.
     Paris Symposium on Electrical Contact Phenomena, 1974.

3.   B.G. Koepke and R.I. George.
     'Welding of Medium Energy Electric Contacts'.
     Holm Seminar on Electric Contact Phenomena, 1972.

4.   A. Erk and H. Finke.
     'Behaviour of Different Contact Materials for Bouncing Contacts'.
     Heft, 9, 297. E.T.Z.-A (1965).